

*Gravitational Waves:
A Revolution in the Way
We Study the Universe*



Irene Di Palma

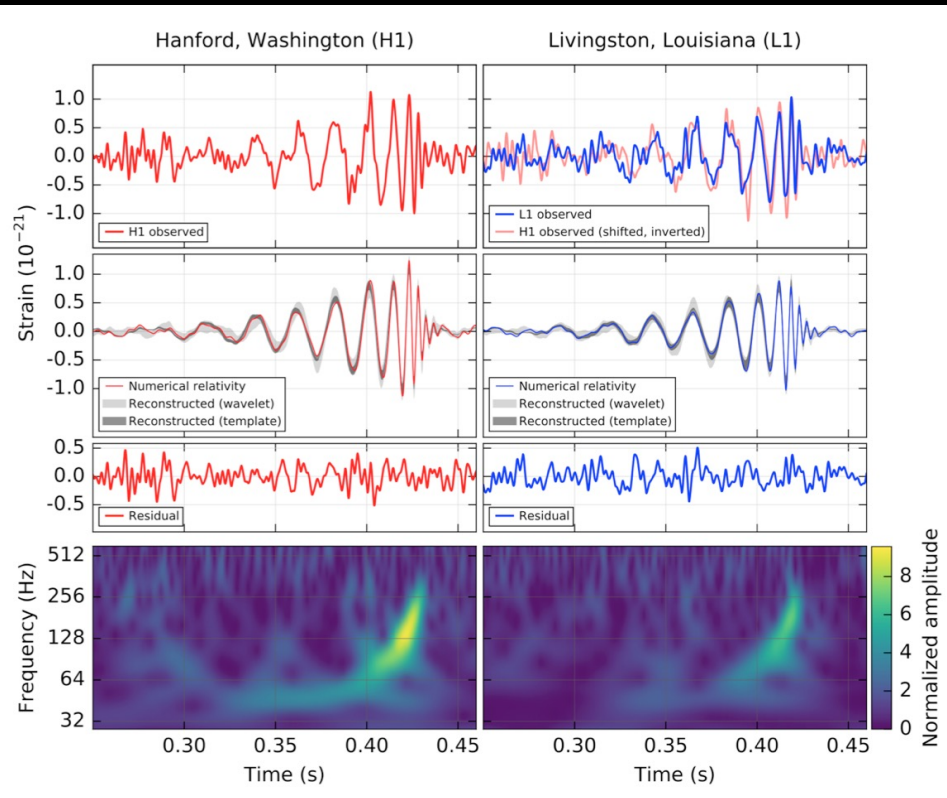
Sapienza University
of Rome and INFN
Irene.DiPalma@uniroma1.it



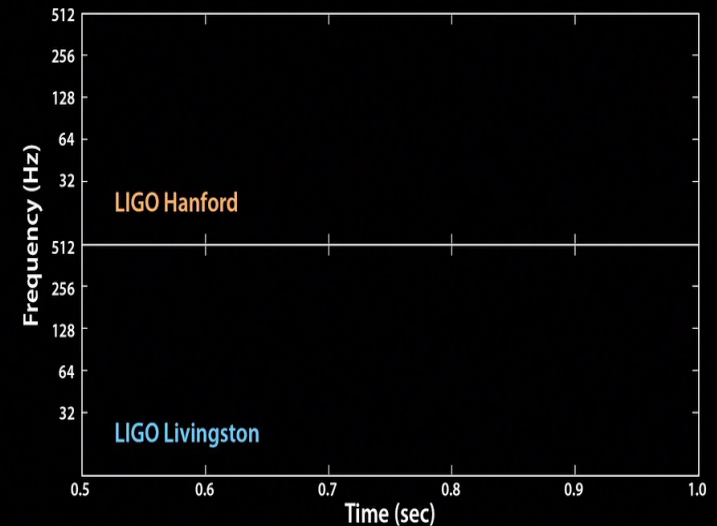
Outline

- **Einstein and the General Relativity**
- **Basic Analysis Concepts**
- **Gravitational Wave Detectors**
- **Some of the most interesting discoveries so far**

GW150914: The First Binary Black Hole Merger



Andy Bohn, François Hébert, and William Throwe, SXS Collaboration



Abbott, et al. ,LIGO Scientific Collaboration and Virgo Collaboration, "Observation of Gravitational Waves from a Binary Black Hole Merger" [Phys. Rev. Lett. 116, 061102 \(2016\)](#)



Gravitational wave science

The **Study of gravitational waves** is at the *frontiers of science* in at least four different fields:

- **General Relativity (GR)** – physics at the extremes: strong (non-linear) gravity, relativistic velocities
- **Astrophysics of compact sources** – neutron stars, black holes, the big bang – the most energetic processes in the universe
- **Interferometric gravitational wave detectors** – the most precise measuring devices ever built
- **GW data analysis** – the *optimal* extraction of the weakest signals possible out of noisy data.



Einstein's view of gravity: The General Theory of Relativity

- Starting in 1915, Albert Einstein began the development of a new theory of gravity.
- The basic idea is that gravity is not a force, but rather a manifestation of the curvature of space-time.
- Space and time aren't just a simple backdrop to the world, but have properties of their own. In particular, they can be “curved”, which means that matter can be prevented by the properties of space-time from moving uniformly in a straight line.
- Space-time curvature is caused by mass.

Thus, **General Relativity embodies the idea of gravity, and even “explains” it.**

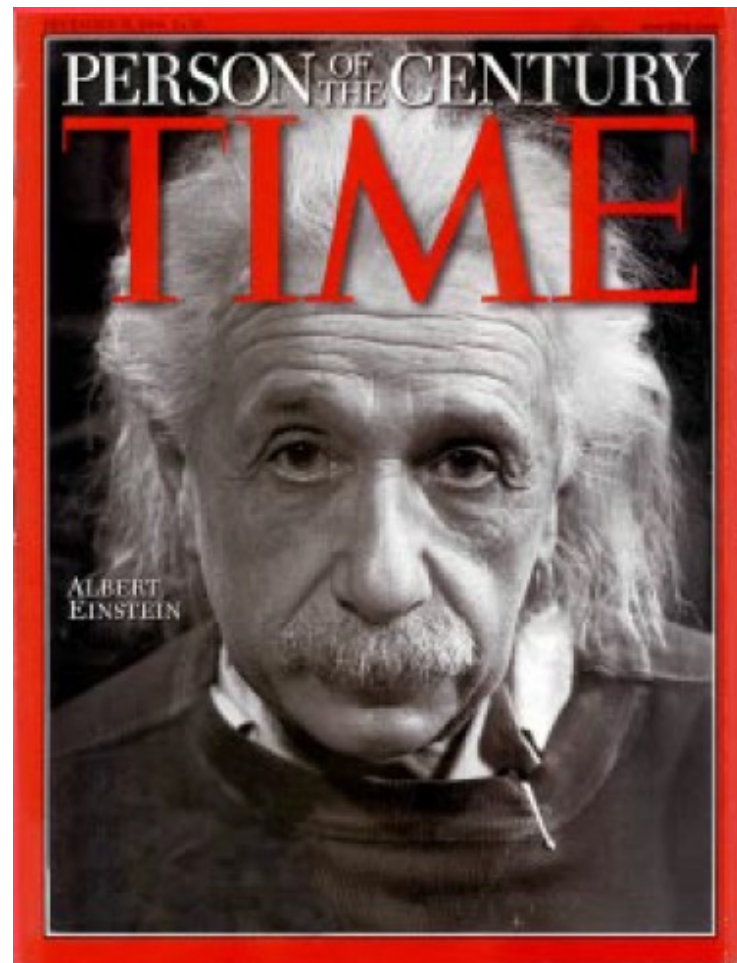
Einstein and relativity

It all starts with Einstein!

- Special relativity (1906)
 - Distances in space and time change between observers moving relative to one another, but the space-time interval remains invariant:

$$ds^2 = dx^2 + dy^2 + dz^2 - c^2 dt^2$$
 - space + time \rightarrow 4D space-time geometry
 - Energy and momentum form a 4D vector with invariant (rest) mass:

$$(m_0 c^2)^2 = E^2 - (pc)^2 \quad (\text{or } E = mc^2)$$



Space-time geometry

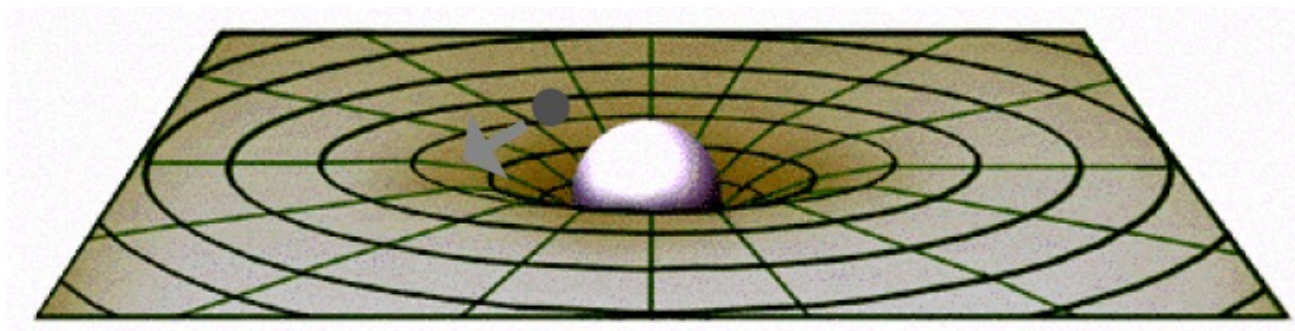
Relativity and space-time geometry:

- Discards concept of absolute motion; instead treats only relative motion between systems
- Space and time no longer viewed as separate; rather as four dimensional space-time
- Gravity described as a warpage (curving) of space-time, not a force acting at a distance



Warped space-time: Einstein's General Relativity (1916)

- A geometric theory of gravity
 - Gravitational acceleration depends only on the geometry of the space that the “test mass” occupies, not any properties of the test mass itself
 - For gravity (as opposed to all other forces), motion (acceleration) depends only on location, not mass
- Image space as a stretched rubber sheet.
- A mass on the surface will cause a deformation
- Another mass dropped onto the sheet will roll toward that mass
- Einstein theorized that smaller masses travel toward larger masses, not because they are “attracted” by a mysterious force, but because the smaller objects travel through space that is warped by the larger object.



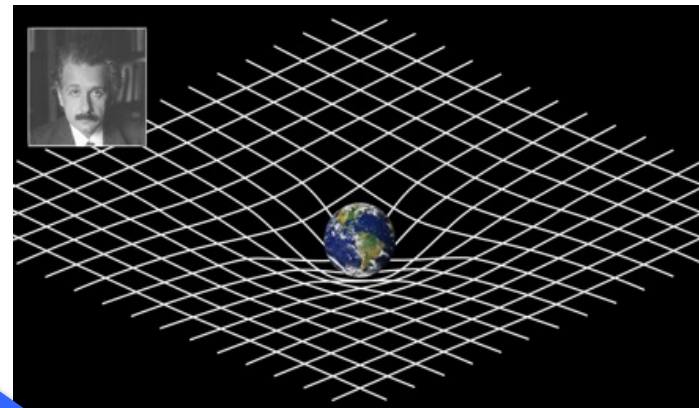
General Relativity and Gravitational Waves

Einstein field tensor

Stress-energy-momentum tensor

General
Relativity:
Einstein Field
Equations

$$G_{\mu\nu} = \frac{8\pi G}{c^4} T_{\mu\nu}$$



Weak field approximation

space-time is slightly
perturbed from flat space-
time:

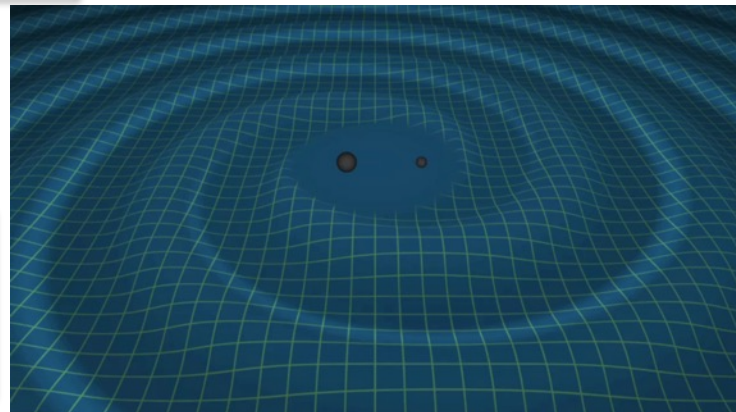
$$g_{\mu\nu} \approx \eta_{\mu\nu} + h_{\mu\nu}$$

Free Space:
 $T_{\mu\nu} = 0$

$\sim 10^{-43}$

Wave equation for $h_{\mu\nu}$!

$$\left(\nabla^2 - \frac{1}{c^2} \frac{\partial^2}{\partial t^2} \right) h_{\mu\nu} = 0$$



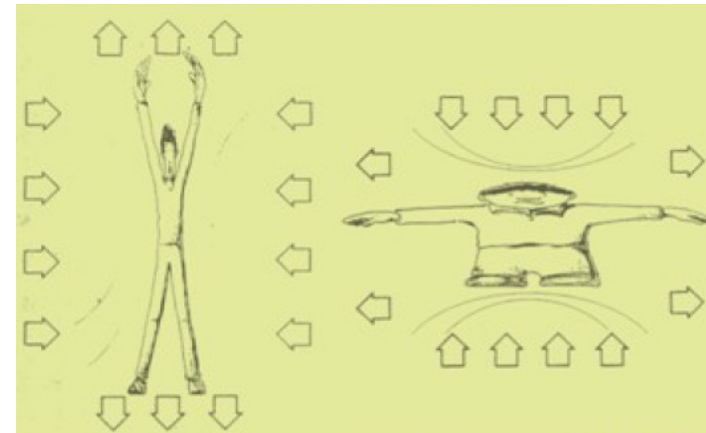
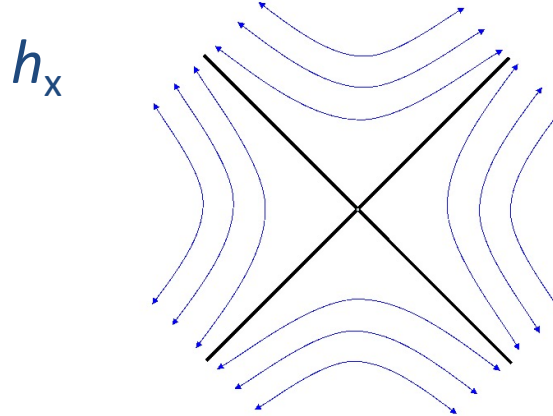
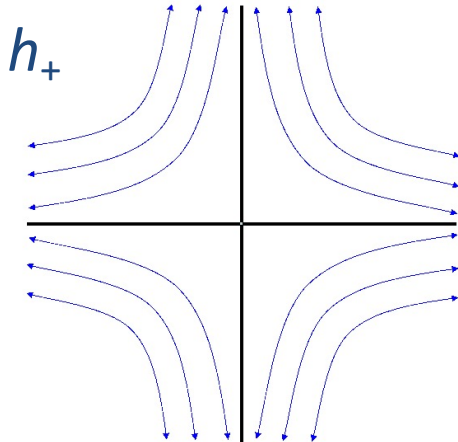
Gravitational Waves

Solution for an outward propagating wave in z-direction:

$$h(t, z) = h_{\mu\nu} e^{i(\omega t - kz)} = h_+(t - z/c) + h_\times(t - z/c)$$

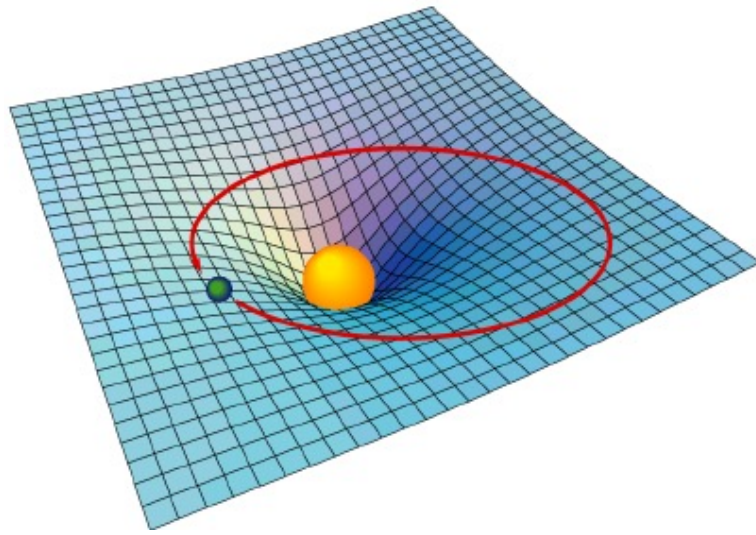
$$h_{\mu\nu} = \begin{pmatrix} 0 & 0 & 0 & 0 \\ 0 & h_+ & h_\times & 0 \\ 0 & h_\times & -h_+ & 0 \\ 0 & 0 & 0 & 0 \end{pmatrix}$$

Physically, h is a *strain*: $\Delta L/L$



General relativity (1916)

- Space-time warps in response to the presence of matter, energy, motion.
- Motion of matter is determined by space-time curvature.
- For gravity (as opposed to all other forces), motion (acceleration) depends only on location, not mass.
- 16 coupled non-linear differential equations; analytical solutions in only the simplest of cases (spherical symmetry, static, etc).





Metric perturbation h

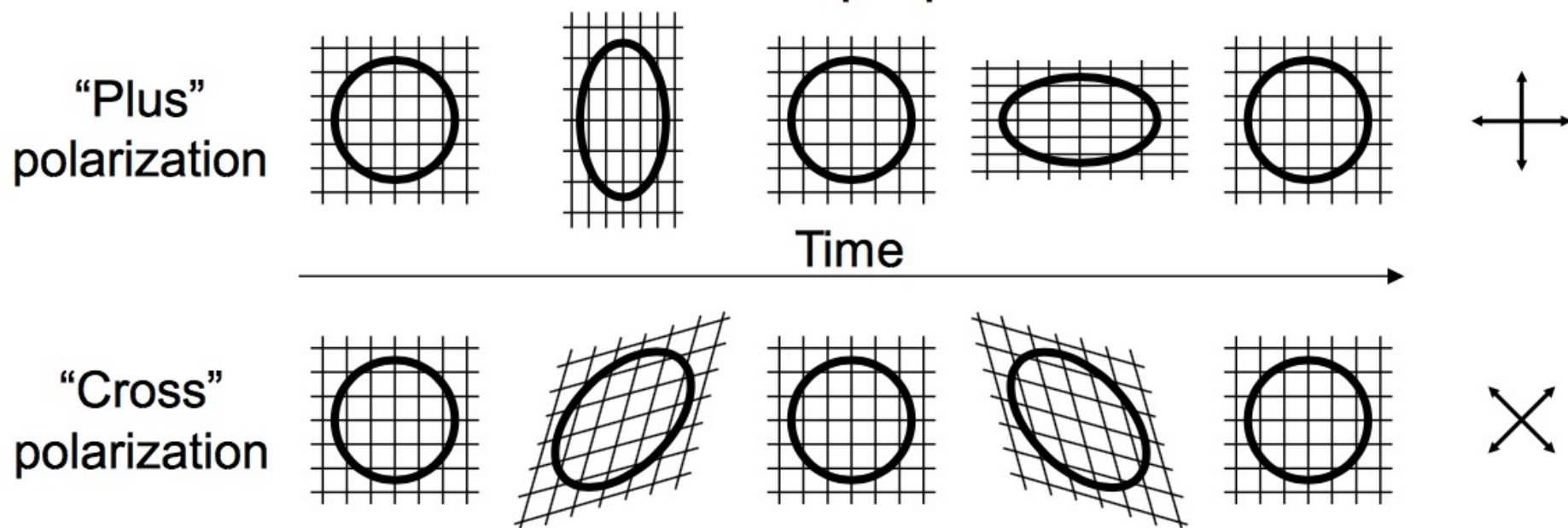
- In the weak-field limit ($h \ll 1$), Einstein's field equations can be linearized.
- In the “transverse traceless” (TT) gauge, they become a wave eqn for h (no matter sources):

$$\left(\nabla^2 - \frac{1}{c^2} \frac{\partial^2}{\partial t^2} \right) h_{\mu\nu} = 0$$

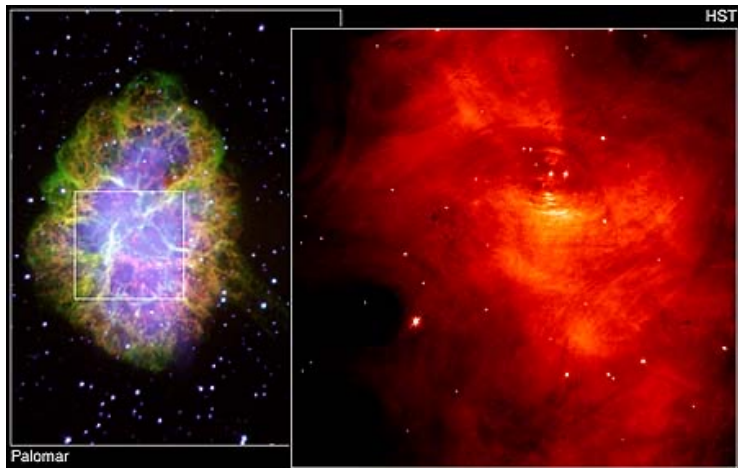
- The metric perturbation is interpreted as a gravitational wave amplitude, travelling at the speed of light.
- Gravitational wave metric perturbations stretch and squeeze the space they pass through (strain amplitude).

Gravitational waves

Gravitational waves are **deformations of space** itself, stretching it first in one direction, then in the perpendicular direction.



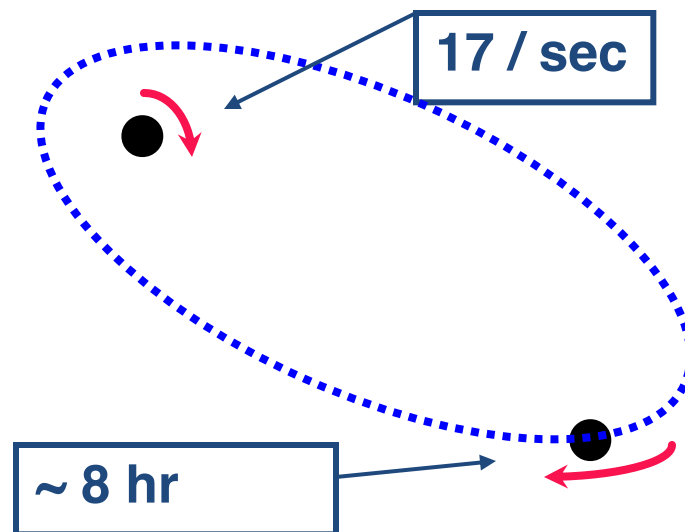
Hulse-Taylor binary pulsar



Neutron Binary System

PSR 1913 + 16 -- Timing of pulsars

- A rapidly spinning pulsar (neutron star beaming EM radiation at us 17 x / sec)
- Orbiting around an ordinary star with 8 hour period
- Only 7 kpc away
- Discovered in 1975, orbital parameters measured continuously over 25 years!



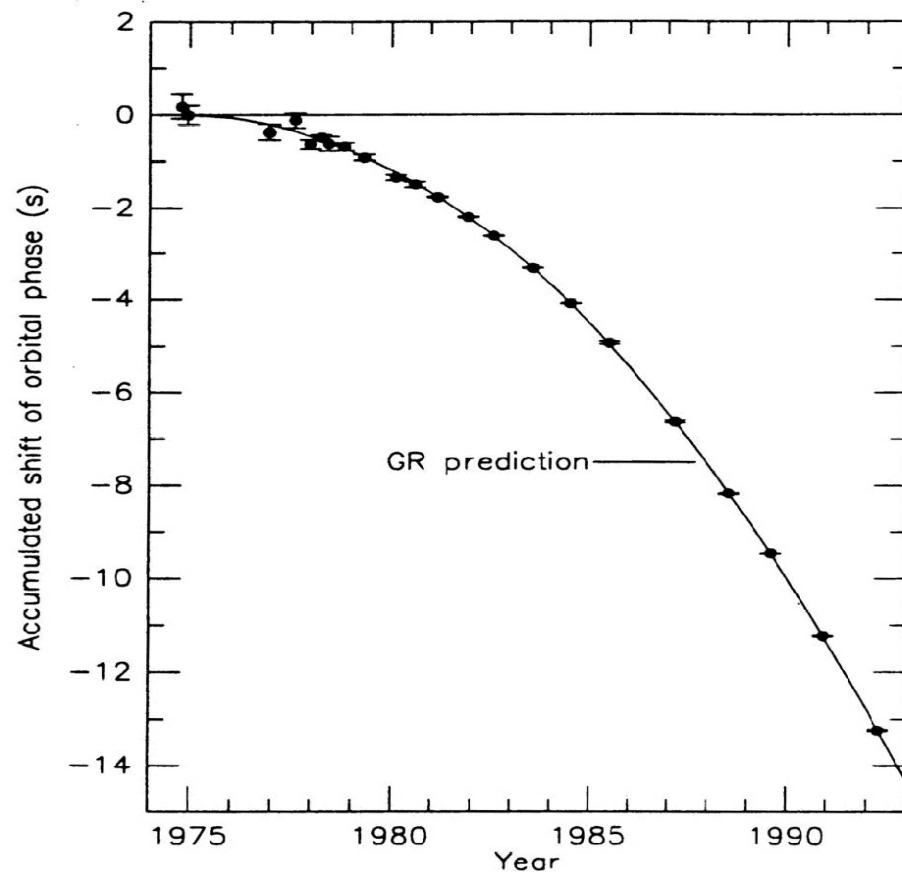


GWs from Hulse-Taylor binary



emission of gravitational waves by compact binary system

- Period speeds up 14 sec from 1975-94
- Measured to ~50 msec accuracy
- Deviation grows quadratically with time
- Merger in about 300M years
(\ll age of universe!)
- shortening of period \Leftarrow orbital energy loss
- Compact system:
negligible loss from friction, material flow
- Beautiful agreement with GR prediction
- GW emission will be strongest near the end:
 - Coalescence of neutron stars!
- Nobel Prize, 1993



Outline

- **Einstein and the General Relativity**
- **Basic Analysis Concepts**
- **Gravitational Wave Detectors**
- **Some of the most interesting discoveries so far**

Basic Analysis Concepts

The output of a gravitational wave detector is a time series $s(t)$ that includes instrument noise $n(t)$ and the response to the gravitational wave signal $h(t)$:

$$s(t) = F^+(t)h_+(t) + F^\times(t)h_\times(t) + n(t).$$

The instrument response is a convolution of the antenna patterns F^+ , F^\times with the two gravitational wave polarizations h_+ , h_\times .

The information contained in the time series is usually represented in the Fourier domain as a strain amplitude spectral density, $h(f)$. This quantity is defined in terms of the power spectral density $S_s(f) = \tilde{s}^*(f)\tilde{s}(f)$ of the Fourier transform of the time series

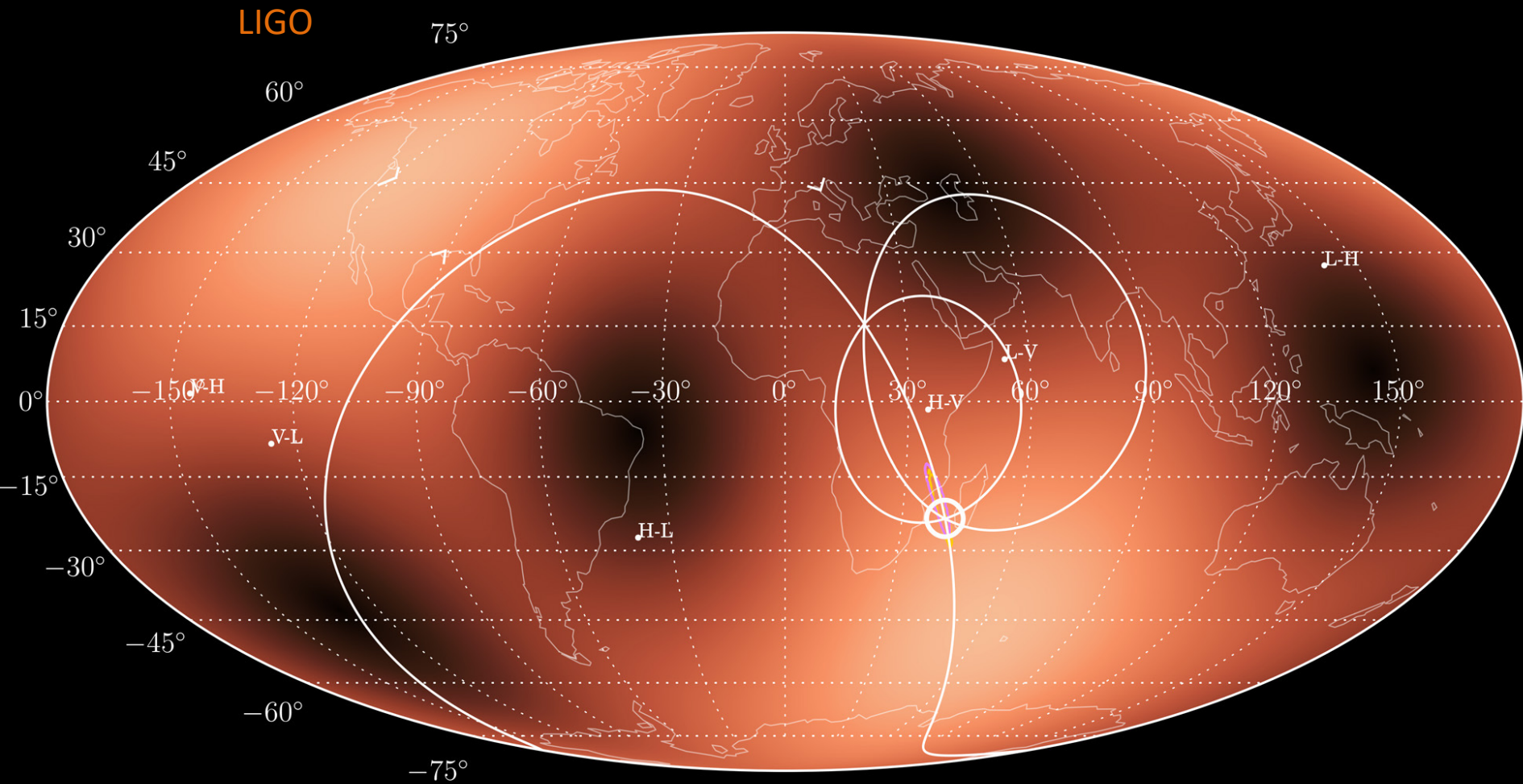
$$\tilde{s}(f) = \int_{-\infty}^{\infty} e^{-2\pi ift} s(t) dt.$$

A commonly used quantity for sensitivity curves is the square root of the PSD or the amplitude spectral density

$$\sqrt{S_s(f)} = h_n(f)f^{-1/2}$$

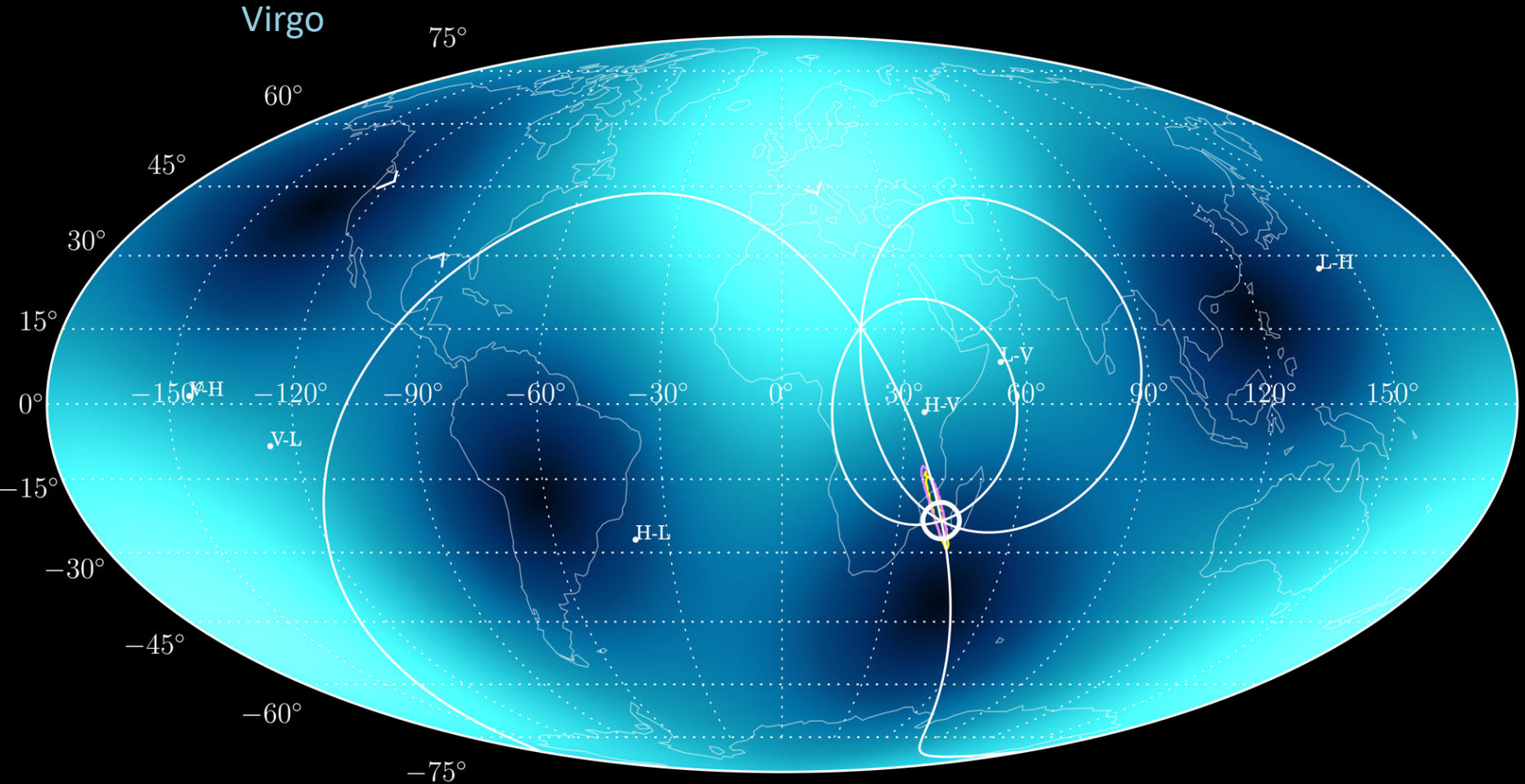


LIGO Antenna Patterns

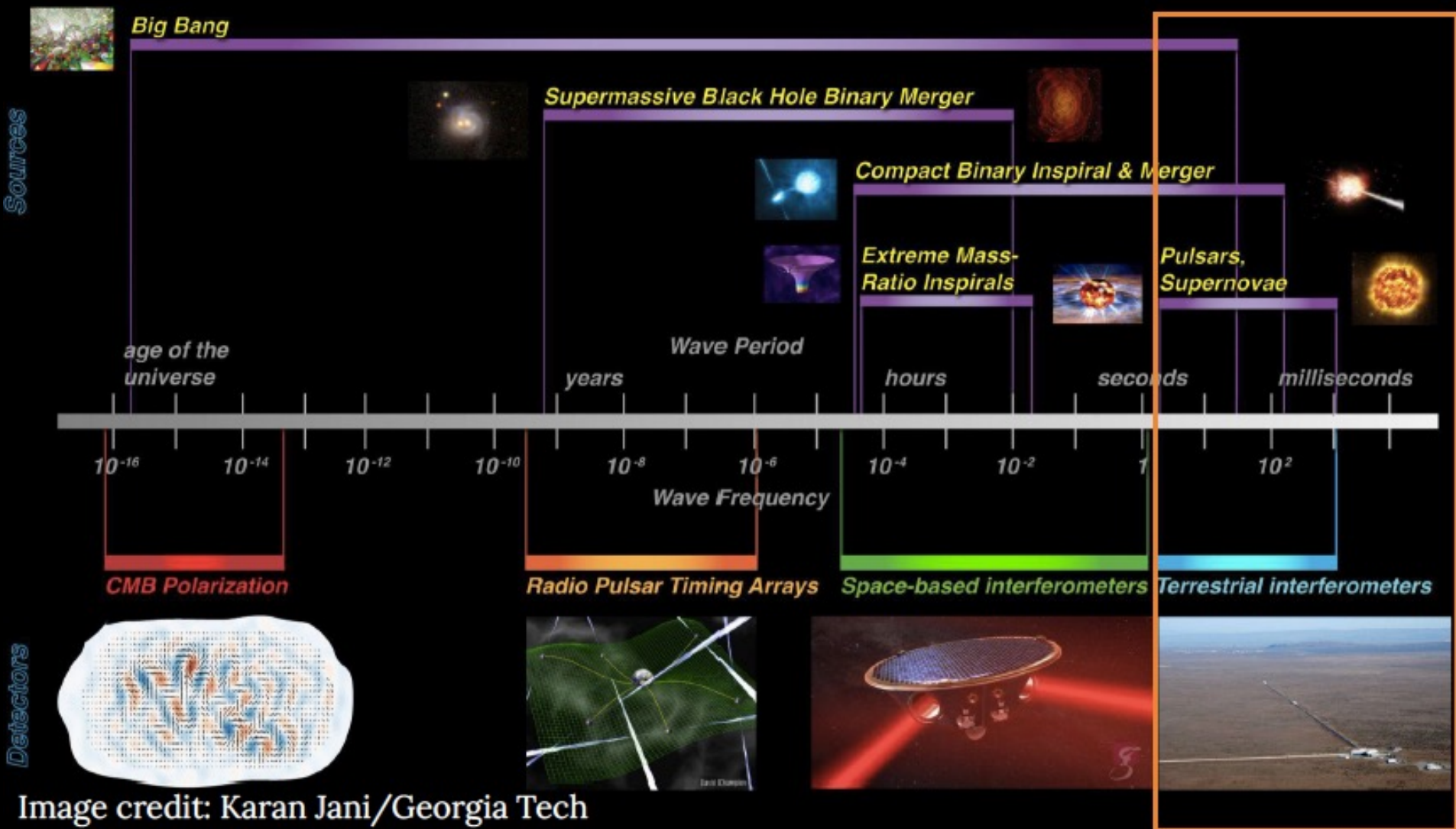




Virgo Antenna Patterns



The Gravitational-Wave Spectrum



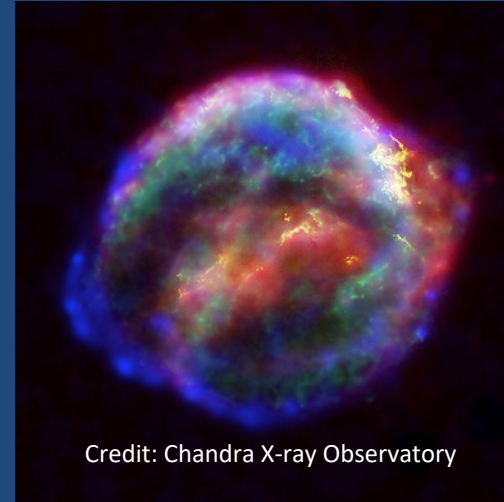
The Astrophysical Gravitational-Wave Source Catalog



Coalescing Binary Systems

- Black hole – black hole
- Black hole – neutron star
- Neutron star – neutron star
- modeled waveform

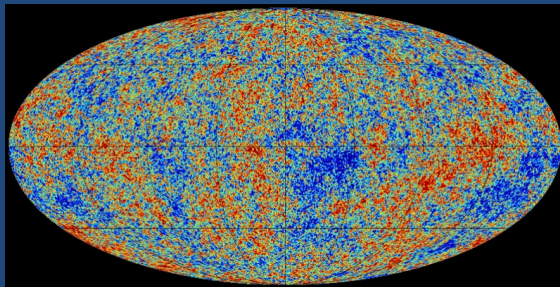
Credit: Bohn, Hébert, Throwe, SXS



Transient 'Burst' Sources

- asymmetric core collapse supernovae
- cosmic strings
- ???
- Unmodeled waveform

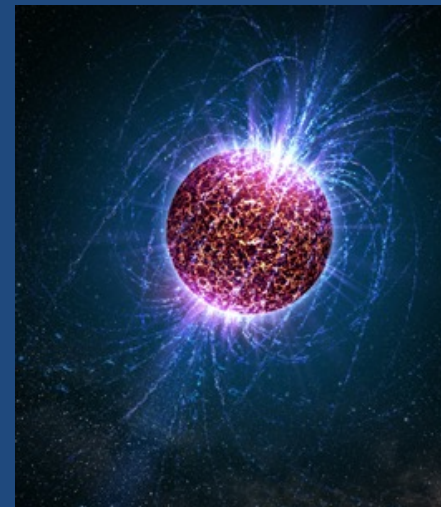
Credit: Chandra X-ray Observatory



Cosmic GW Background

- residue of the Big Bang
- probes back to $< 10^{-15}$ s
- stochastic, incoherent background
- Difficult (impossible?) for LIGO-Virgo to detect

Credit: Planck Collaboration



Continuous Sources

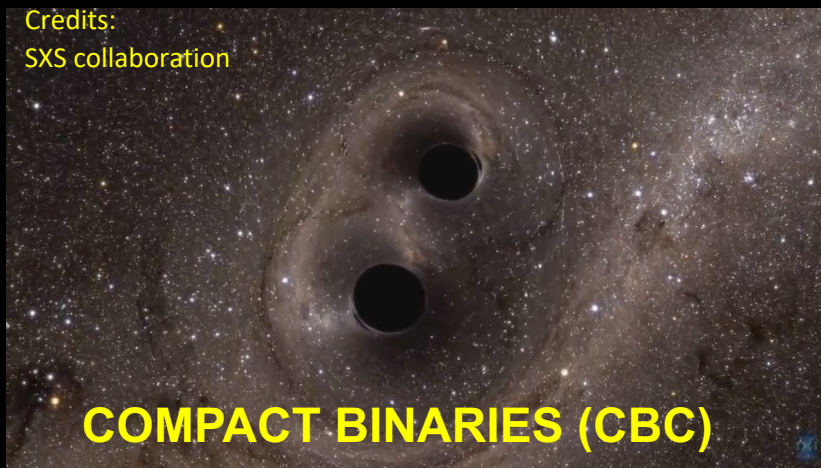
- Spinning neutron stars
- monotone waveform

Credit: Casey Reed, Penn State

Gravitational Wave Targets

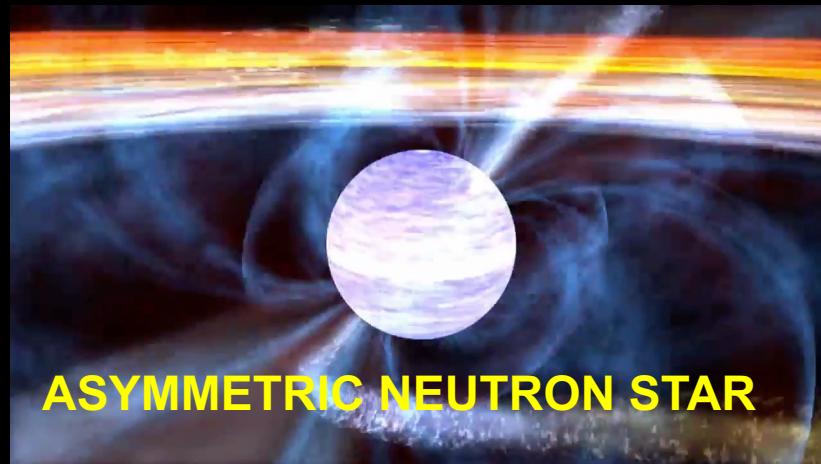
TRANSIENT

Credits:
SXS collaboration



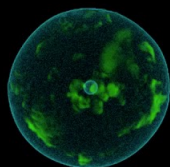
COMPACT BINARIES (CBC)

PERSISTENT



ASYMMETRIC NEUTRON STAR

**MATCHED
FILTER**



BURSTS: Core collapse Supernovae



STOCHASTIC BACKGROUND

UNMODELED



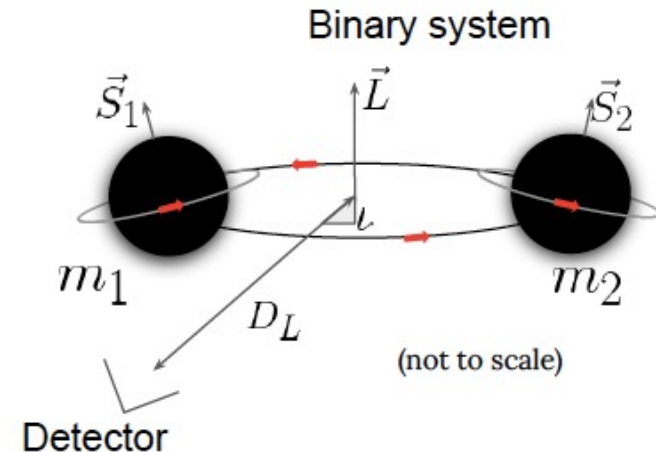
The Matched Filter is the best linear approach to extract a signal of known shape when it is embedded in a stationary Gaussian noise

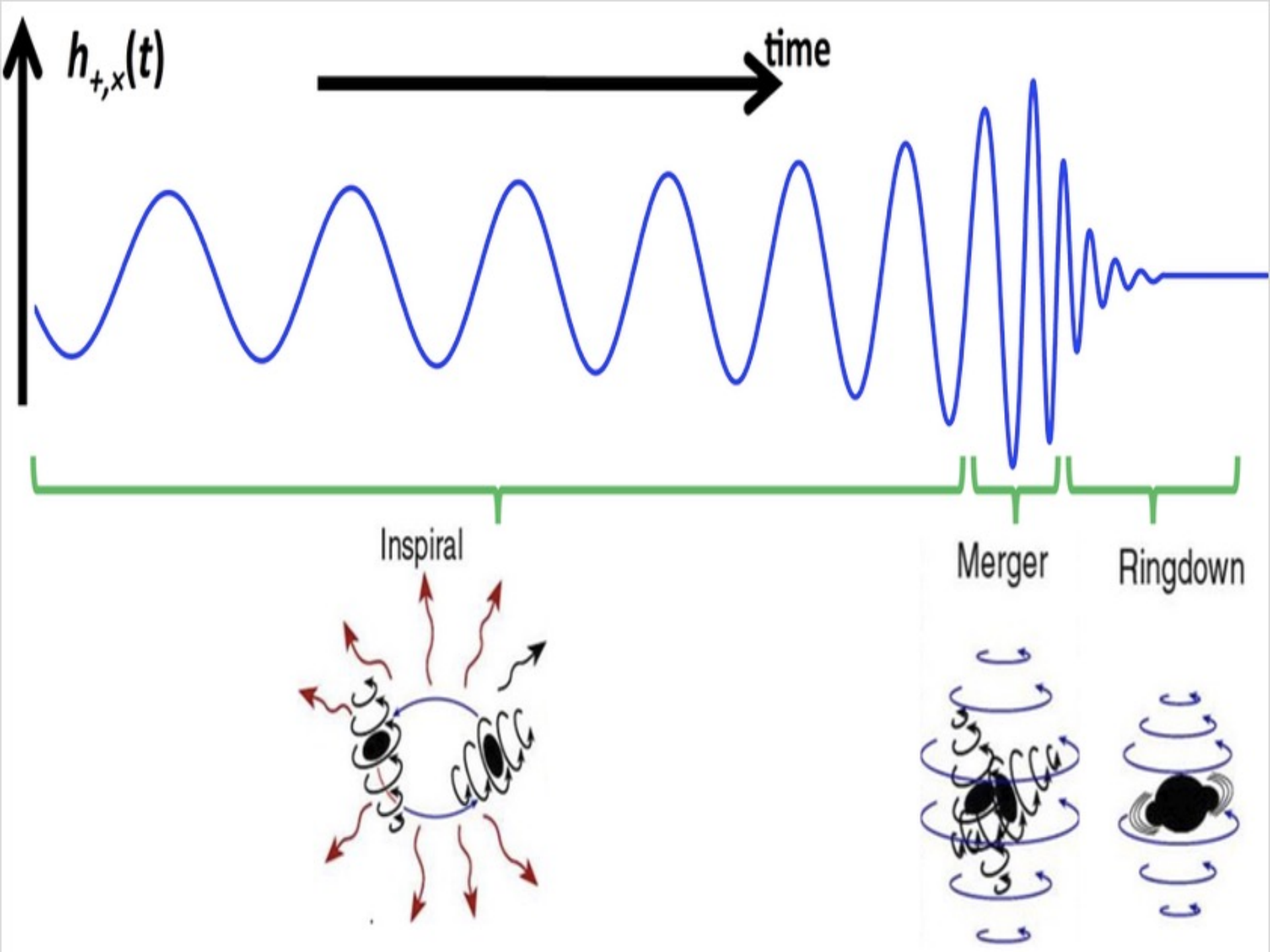
Modelling colliding black holes

What will the signals from these systems look like in the data?

The signal from a binary system made up of black holes will be described by fifteen parameters

- Intrinsic parameters:
 - Component Masses: m_1 m_2
 - Component spins in each direction: s_{1x} s_{1y} s_{1z} s_{2x} s_{2y} s_{2z}
- Extrinsic Parameters:
 - Location: Right Ascension and Declination
 - Inclination angle between line of sight and orbital plane, i
 - Polarisation angle,
 - Phase at coalescence
 - Luminosity distance, D_L
 - Time of coalescence

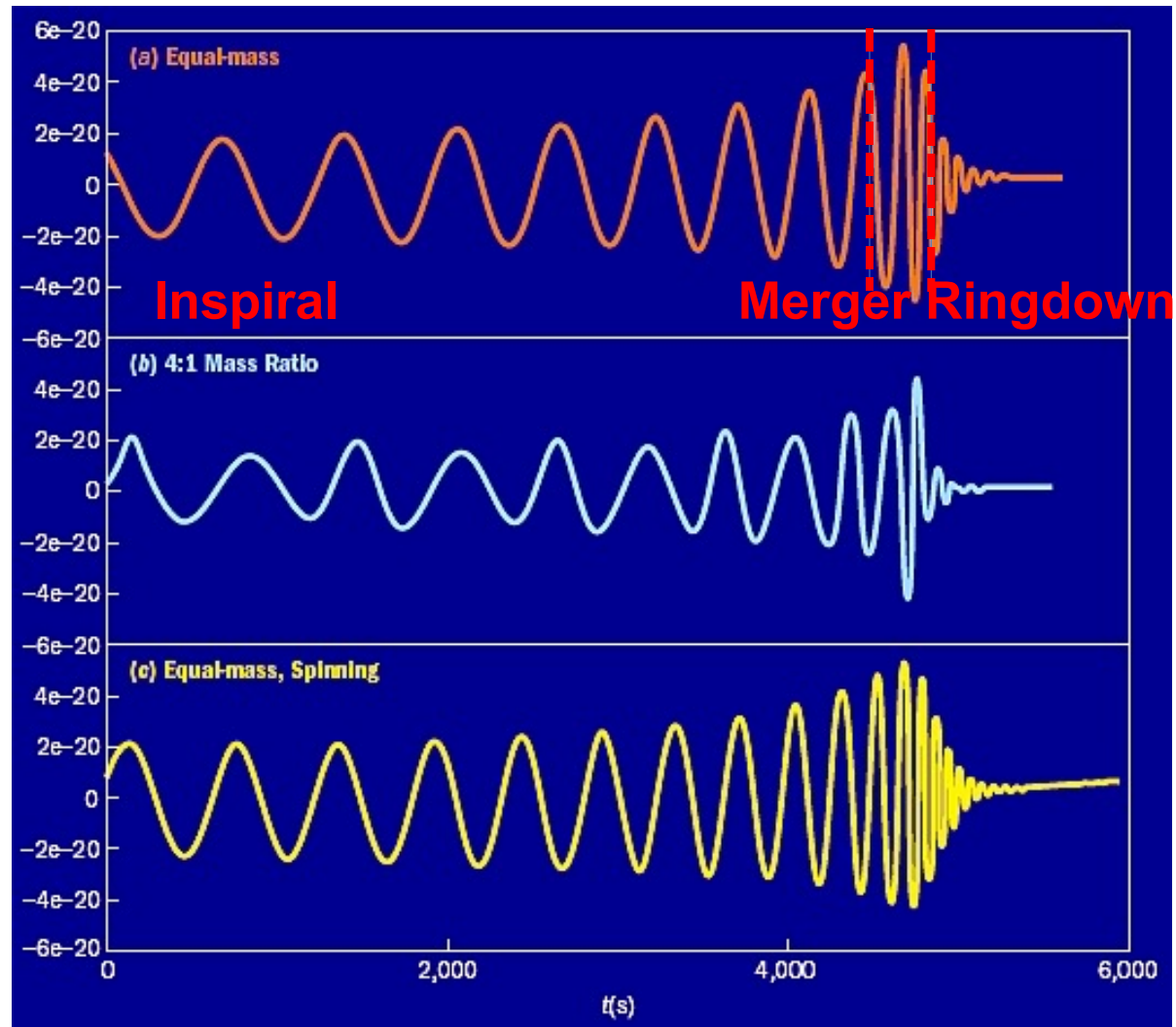






Extracting Astrophysical Parameters from GW Waveforms

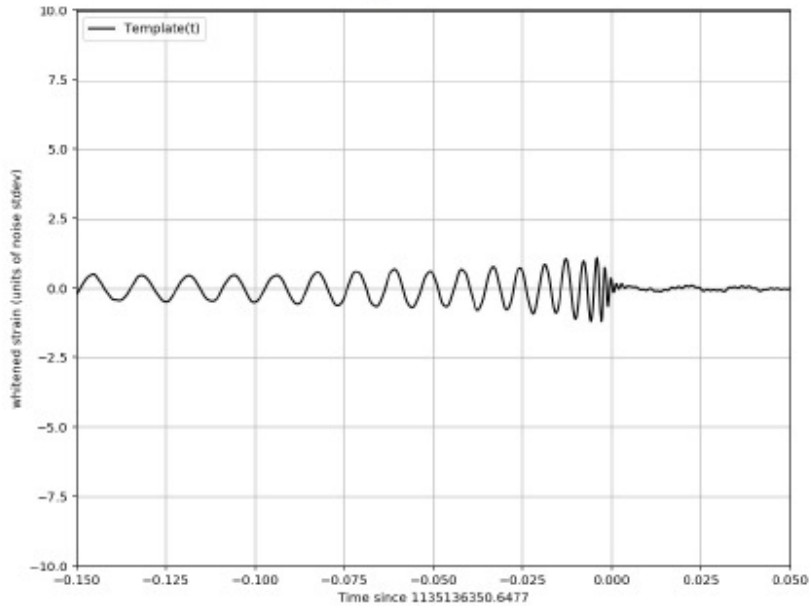
- Compact object parameters encoded in the waveforms:
 - Constituent masses, constituent spins, sky location, luminosity distance, orbital inclination, time of arrival
- Intrinsic degeneracies make parameter estimation difficult!
 - E.g., luminosity distance vs. inclination angle
- The SNR of the waveform matters
 - often buried in detector noise; lower SNR obscures parameter estimation



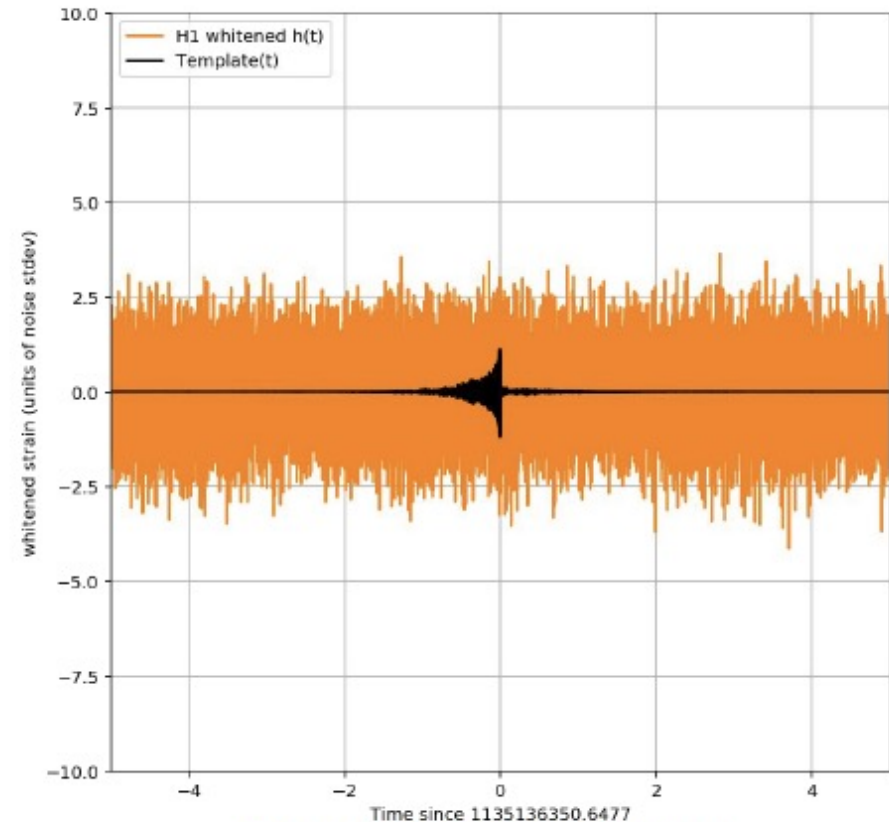
LIGO Scientific Collaboration and Virgo Collaboration, "Parameter estimation for compact binary coalescence signals with the first generation gravitational wave detector network" [Phys. Rev. D 88\(2013\) 062001](#)

Detection problem

We know what the signal looks like



But it is buried in detector noise



Adapted from GWOSC tutorial

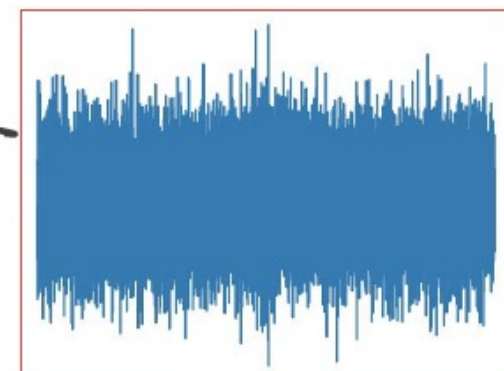
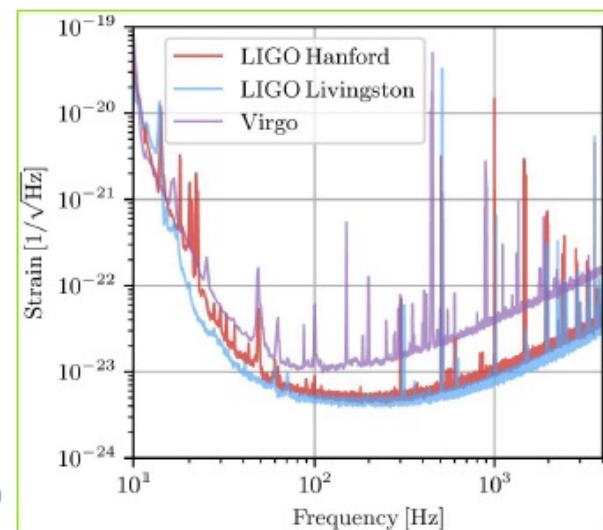
Matched filter

Optimal for signals:

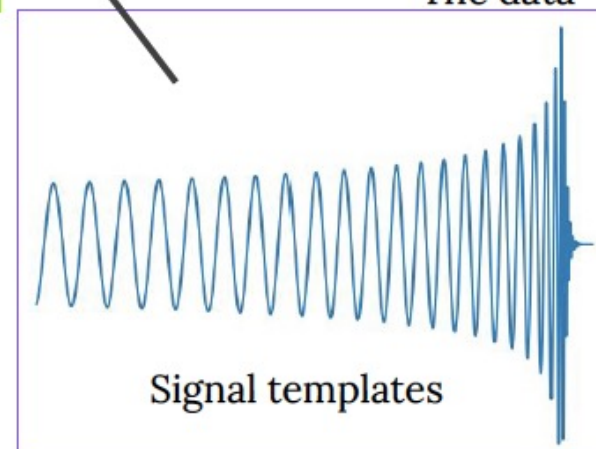
- in stationary Gaussian noise
- with known PSD

(Wainstein and Zubakov, 1962)

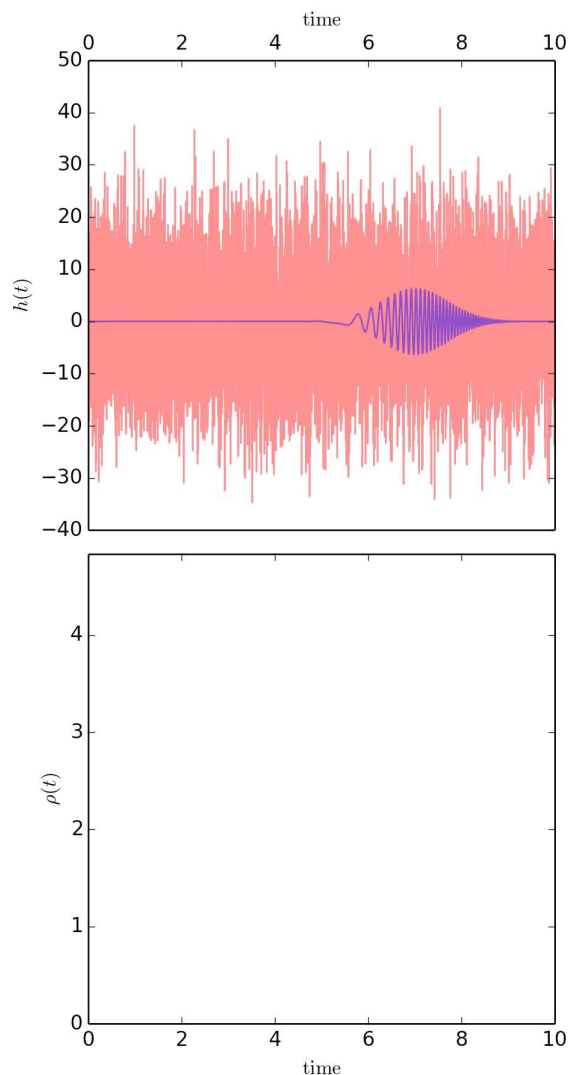
$$(s|h) = 4\Re \int_0^\infty \frac{s(f) \tilde{h}^*(f)}{S_h(f)} df$$



The data



Assessing Statistical Significance: Modeled Search



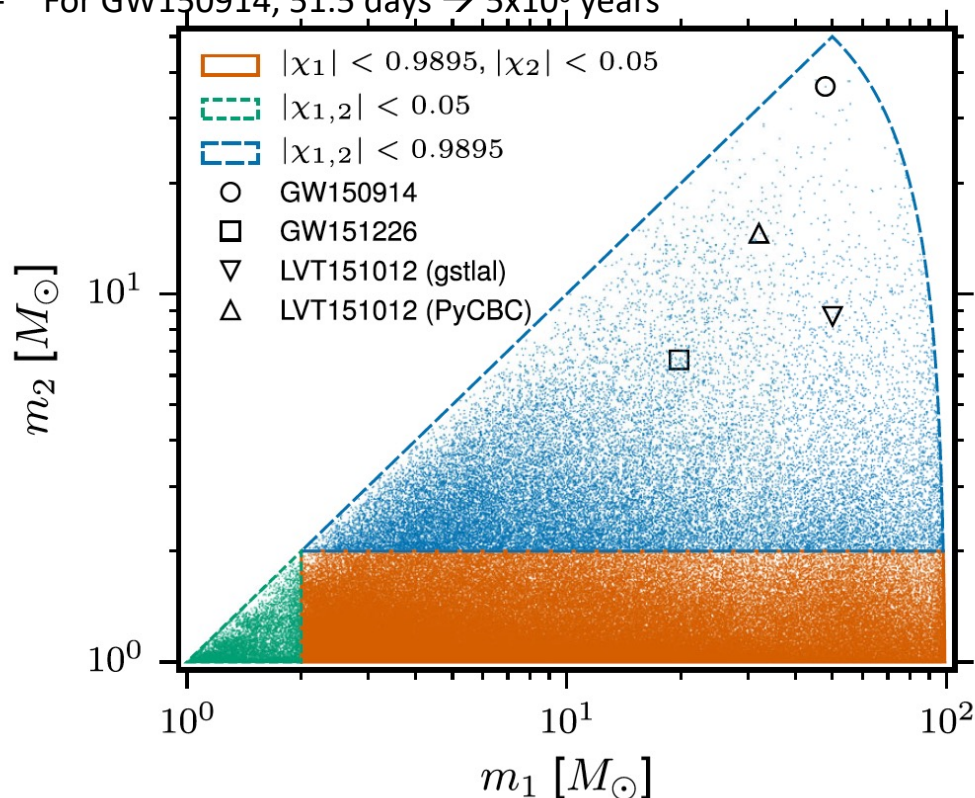
Simulation: Reed Essick, LIGO MIT

- Matched filter search: X-correlation of L1, H1 data streams

$$\rho = \frac{\langle s|h \rangle}{\sqrt{\langle h|h \rangle}}$$

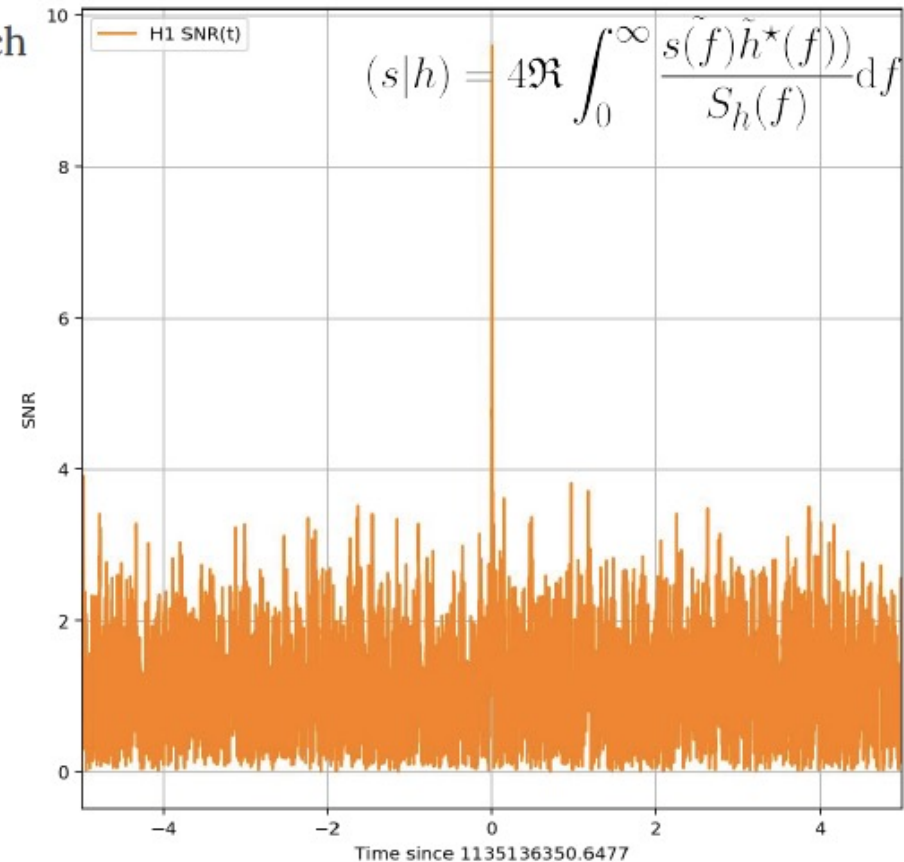
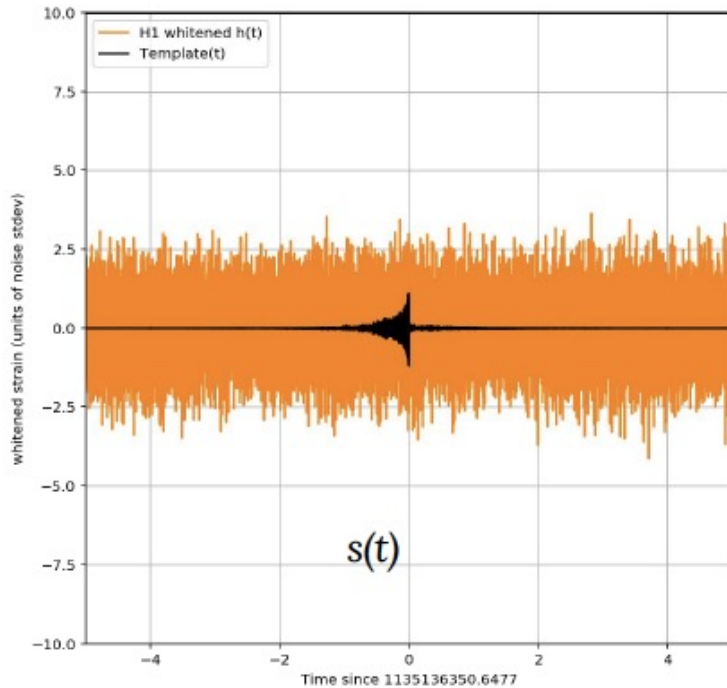
$$\langle a|b \rangle = 4\text{Re} \int_{f_{\text{low}}}^{f_{\text{high}}} \frac{\tilde{a}(f)\tilde{b}(f)}{S_n(f)} df$$

- Background computed from time-shifting coincident data in 100 ms steps
 - For GW150914, 51.5 days $\rightarrow 5 \times 10^6$ years



SNR time series

We end up obtaining a time series of SNR values for each template. The peaks in this time series are triggers



Modelling the Waveforms

Matched filtering relies on knowing the shape of the signal.

For CBC waveforms we can model the signals with **template waveforms**.

We construct **template banks** of waveforms that vary over the intrinsic parameters.

4D template banks - $\{m_1, m_2, s_{1z}, s_{2z}\}$

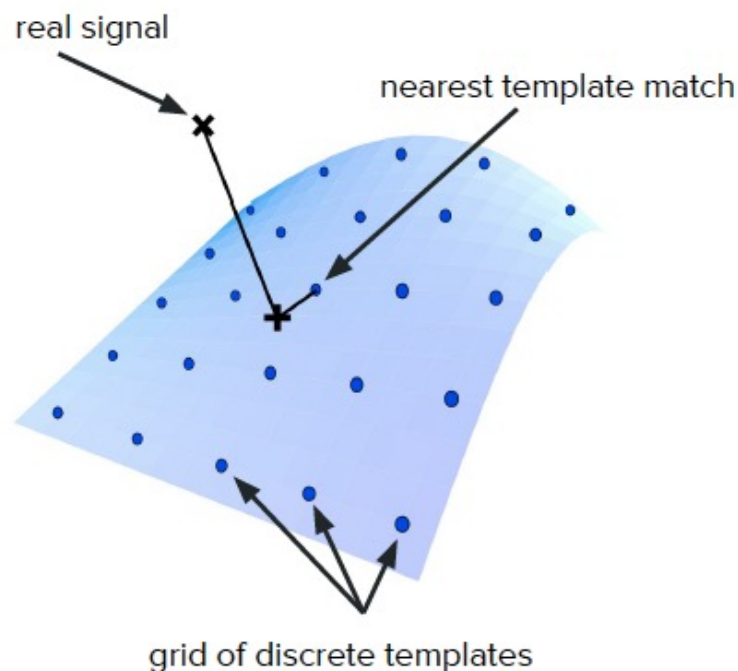


image credit: [arXiv:gr-qc/9511032](https://arxiv.org/abs/gr-qc/9511032)

How many templates do we need?

If the signal perfectly matches the template we will have an optimal SNR.

Any **mismatch causes an SNR loss.**

Construct banks with a dense grid of templates such that any signal will be close enough to the nearest template.

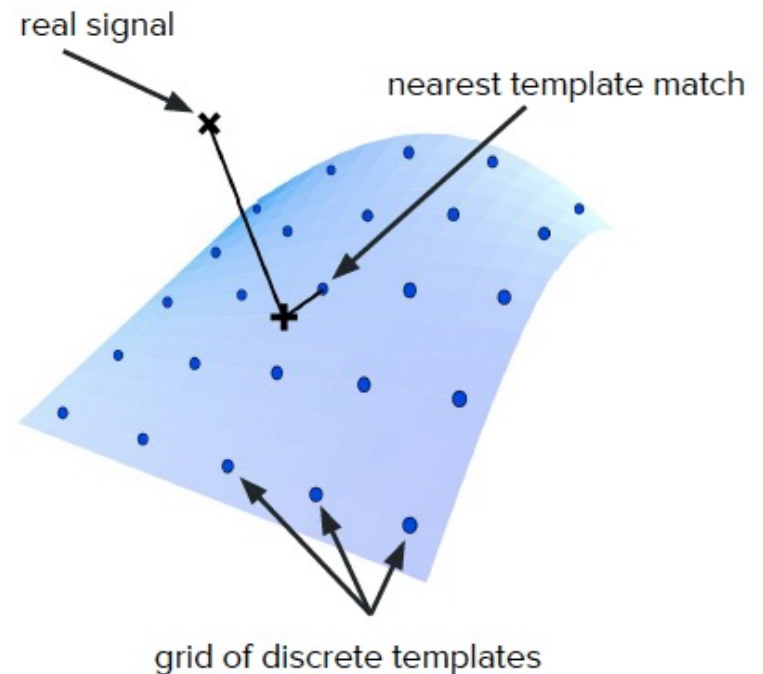


image credit: [arXiv:gr-qc/9511032](https://arxiv.org/abs/gr-qc/9511032)

$$N_{\text{templates}} \sim \mathcal{O}(10^5 - 10^6)$$

Which waveforms do we use?

As mentioned earlier, the parameters with most impact on the signal waveform are the masses and aligned spins of the components

We place templates within the bank randomly, but only if the match ($h|h$) between templates is below a specific threshold.

This means that we end up with a bank which should match well to any signal within this parameter space

The template on the right has been used for the PyCBC-Broad search for many recent publications, and contains ~400k templates

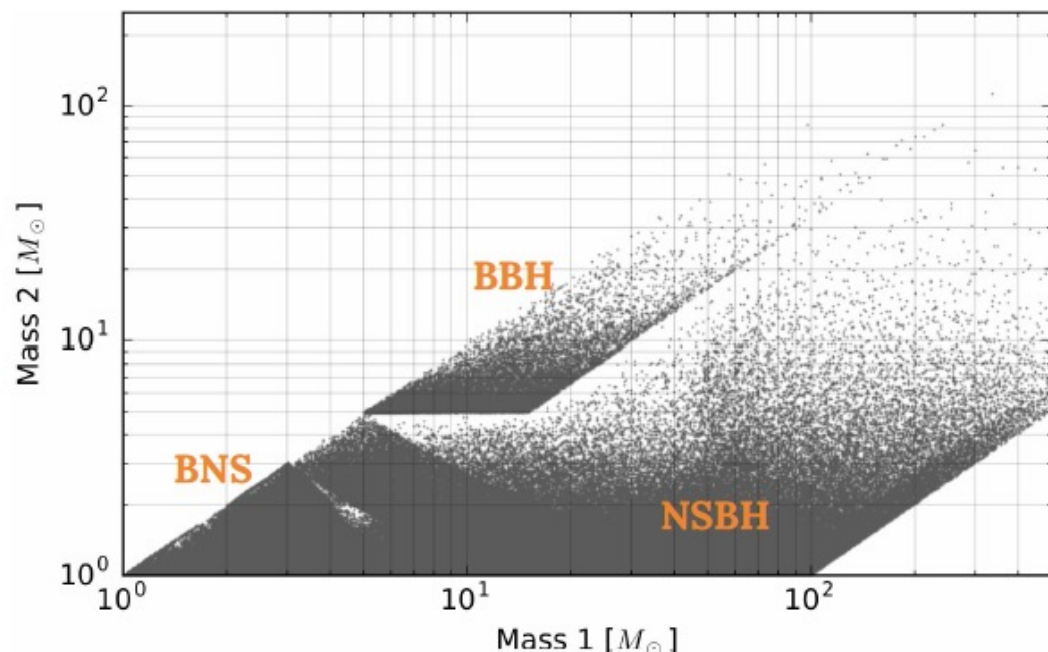


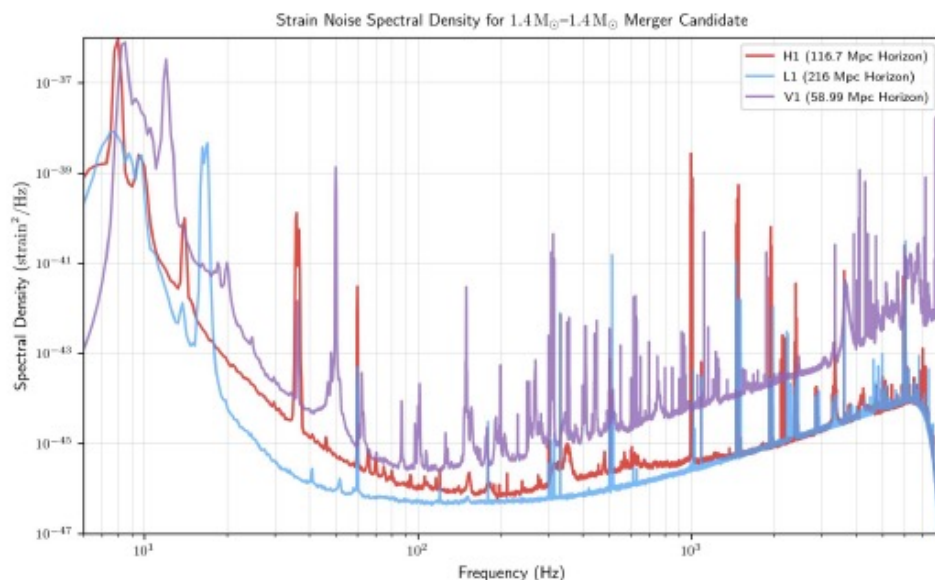
Image credit: Dal Canton and Harry (2017)



Revisiting our assumptions – non-stationarity

Noise properties can vary over **long timescales**.

We must continuously track the noise properties and update our estimate of the PSD.



LIGO and Virgo PSD for O3.

This is a **snapshot of the PSD** for about 1 hour of O3 data, but at another time the PSD could be different.

Non-stationarity

The detector sensitivity is not constant, this can happen rapidly or slowly.

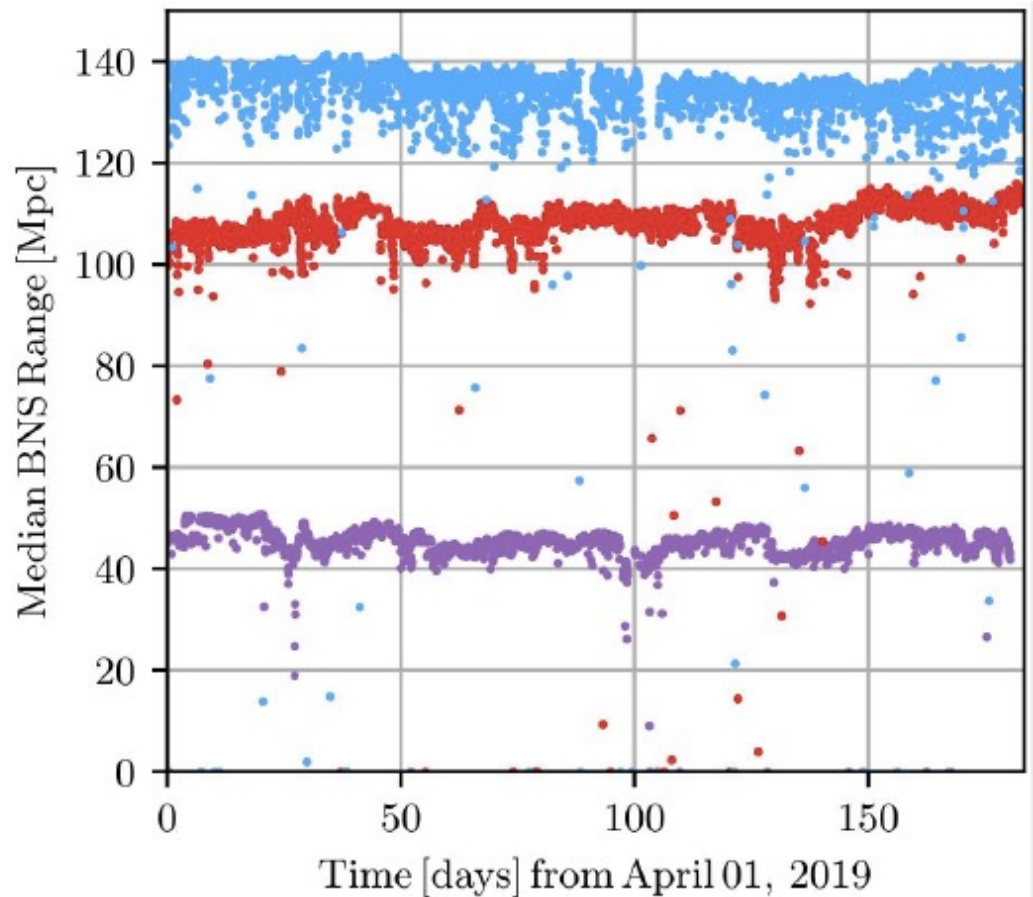
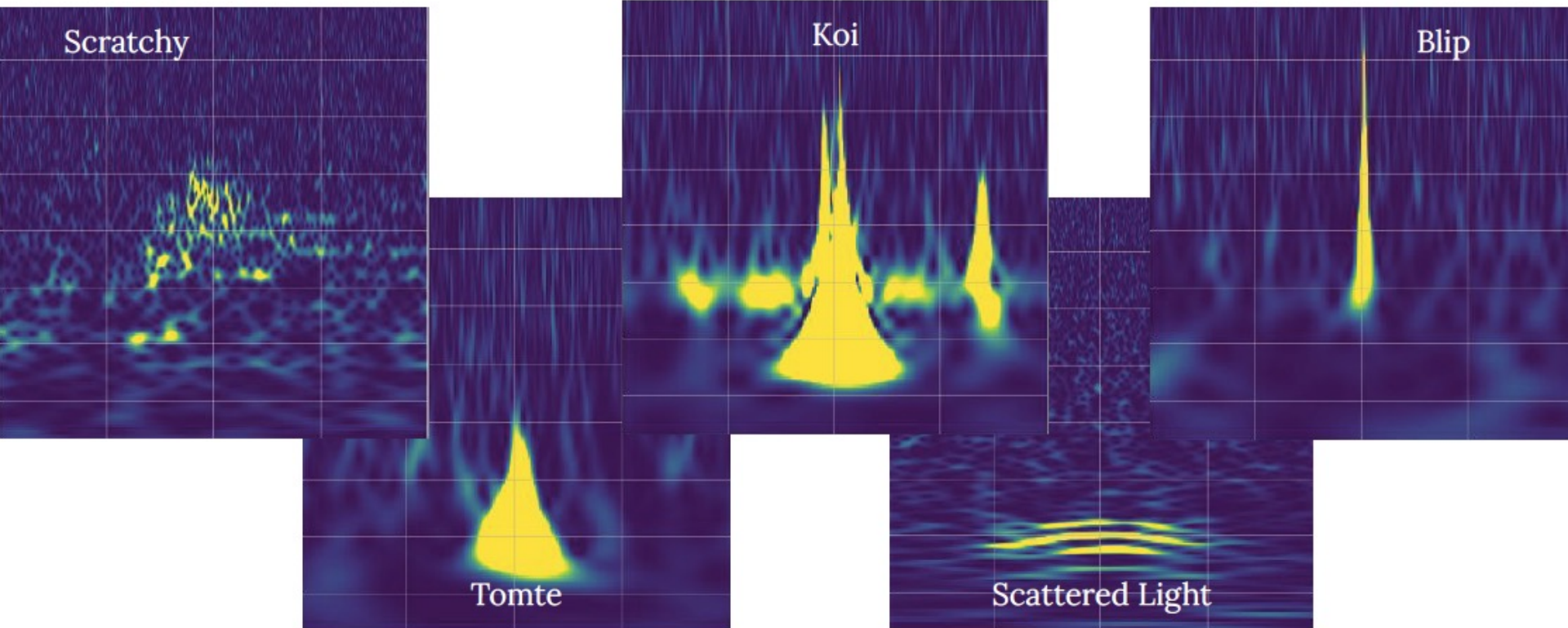


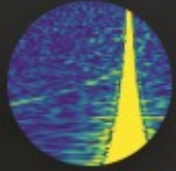
Image from Abbott et al (2020) GWTC-2 2010.14527


Non-Gaussian glitches

Gravity Spy: <https://www.zooniverse.org/projects/zooniverse/gravity-spy>

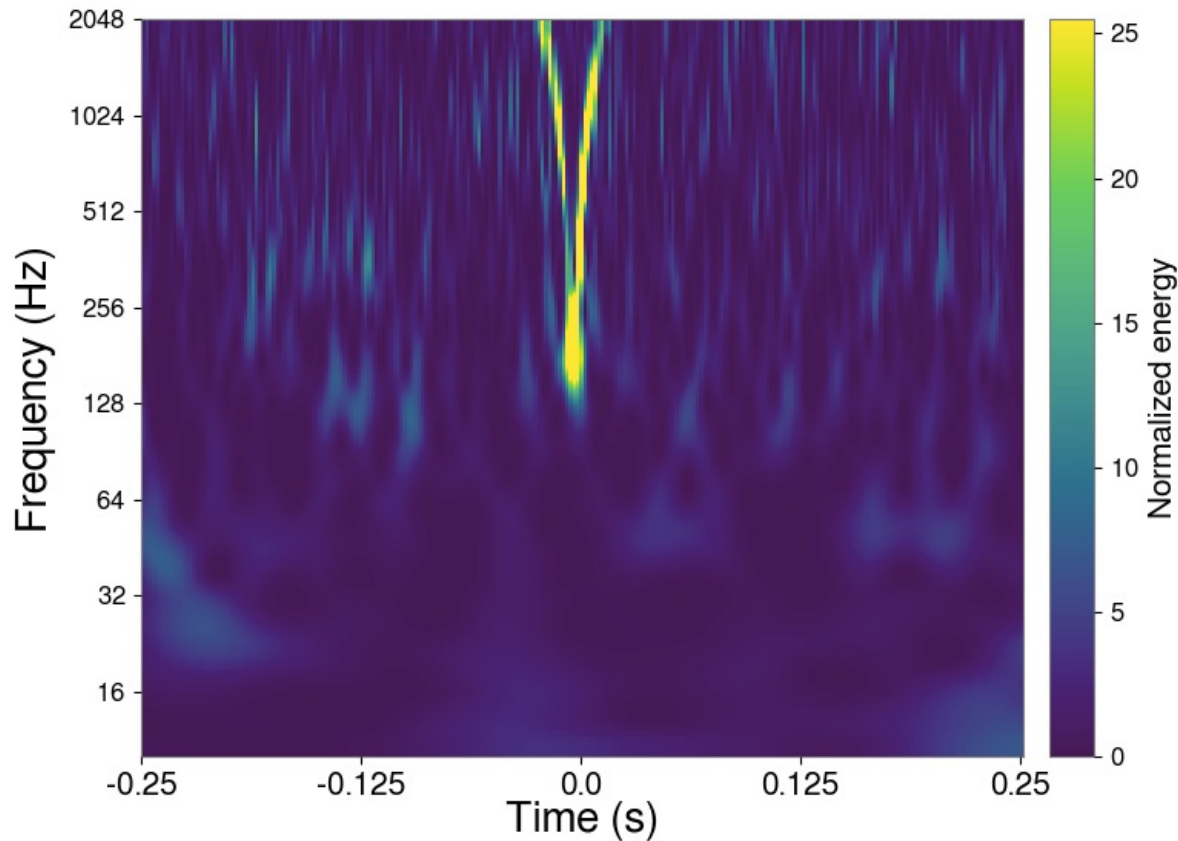


Glitch classification



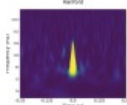
Gravity Spy 

Hanford - O3

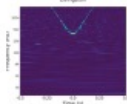


TASK

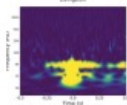
TUTORIAL




Blip



Whistle



None of the Above

Showing 3 of 3  Clear filters

Done & Talk

Done

Outline

- **Einstein and the General Relativity**
- **Basic Analysis Concepts**
- **Gravitational Wave Detectors**
- **Some of the most interesting discoveries so far**

A black and white portrait of a man with dark, curly hair and round glasses. He is wearing a light-colored shirt with thin vertical stripes. He is looking slightly to the left of the camera with a neutral expression. The background is blurred, showing what appears to be a bookshelf.

-
- The diagram illustrates a laser interferometer system for seismic measurements. A LASER beam enters from the right and passes through a POKEL EFFECT PHASE SHIFT MODULATOR. The beam then splits at a BEAM SPLITTER into two paths. One path goes through a POKEL EFFECT PHASE SHIFTER and a MULTIPLE PASS ARM (containing a SPHERICAL MIRROR and a HORIZONTAL SEISMOMETER) before being reflected back to the beam splitter. The other path goes through a HORIZONTAL SEISMOMETER and a MULTIPLE PASS ARM (containing a SPHERICAL MIRROR and a HORIZONTAL SEISMOMETER) before being reflected back to the beam splitter. The beams recombine at the beam splitter and pass through a PHOTO DETECTOR. The output of the photo detector is sent to an OSCILLATOR, which provides a reference signal to a CORRELATOR. The CORRELATOR also receives input from a LOW-PASS FILTER and a HIGH-PASS FILTER. The LOW-PASS FILTER receives input from a SLOW CONTROLLER and a HORIZONTAL SEISMOMETER. The HIGH-PASS FILTER receives input from a HORIZONTAL SEISMOMETER. The output of the CORRELATOR is sent to TO RECORDERS AND SIGNAL PROCESSING EQUIPMENT.



LIGO



Drever

LIGO Chronology

idea to realization ~ 15 years



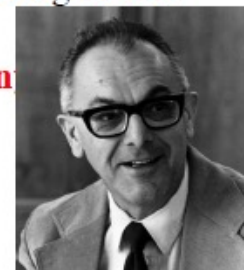
Weiss

1970s	Feasibility studies and early work on laser interferometer gravitational-wave detectors
1979	National Science Foundation (NSF) funds Caltech and MIT for laser interferometer R&D
1984	Development of multiple pendulum Advanced LIGO Concept
1989 December	Construction proposal for LIGO submitted to the NSF (\$365M as of 2002)
1990 May	National Science Board approves LIGO construction proposal
1994 July	Groundbreaking at Hanford site
1999	LIGO Scientific Collaboration White Paper on a Advanced LIGO interferometer concept
2000 October	Achieved "first lock" on Hanford 2-km interferometer in power-recycled configuration
2002 August	First scientific operation of all three interferometers in S1 run
2003	Proposal for Advanced LIGO to the NSF (\$205 NSF + \$30 UK+German)
2004 October	Approval by NSB of Advanced LIGO
2005 November	Start of initial LIGO Science run, S5, with design sensitivity
2008 April	Advanced LIGO Project start
2009 July	Science run ("S6") starts with enhanced initial detectors
2014 May	Advanced LIGO Livingston first two-hour lock
2015 March	Advanced LIGO all interferometers accepted
2015 September	Advanced LIGO observation run 1 scheduled

Initial LIGO events

Advanced LIGO events

R&D of aLIGO using iLIGO facility



Vogt



Thorn



Executive
producer &
consultant of
movie
"Interstellar"

Real size R&D for the real detection

Journey for the new astronomy

The Initial and Enhanced GW detector network

- The **three Initial LIGO detectors** completed five science observation runs (S1-S5) from 2002-2007.
- **Virgo's VSR1** was conducted in 2007, jointly with **LIGO's S5, which operated at design sensitivity for 2 years.**
- Two **"Enhanced LIGO" detectors conducted S6** during 2009-2010, jointly with **Virgo VSR2 and (enhanced) VSR3.**
- Many different searches were done with these data, but **no gravitational wave signals were found**; upper limits are still above plausible expectations.
- **Two Advanced LIGO detectors** are now taking data since September 14th 2015.
- **The Advanced Virgo** started the data acquisition in August 2017, joining the second observation run of LIGO.



The Advanced GW Detector Network

Advanced LIGO
Hanford



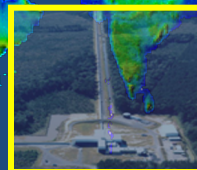
GEO600 (HF)



Advanced
Virgo



Advanced LIGO
Livingston



LIGO-India



KAGRA

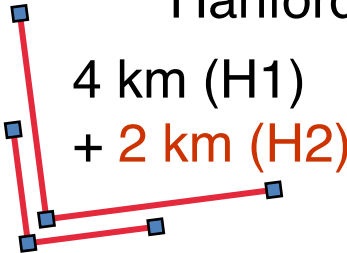


LIGO: Laser Interferometer Gravitational-wave Observatory



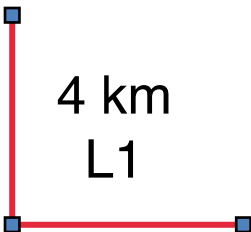
LHO

Hanford, WA



4 km (H1)

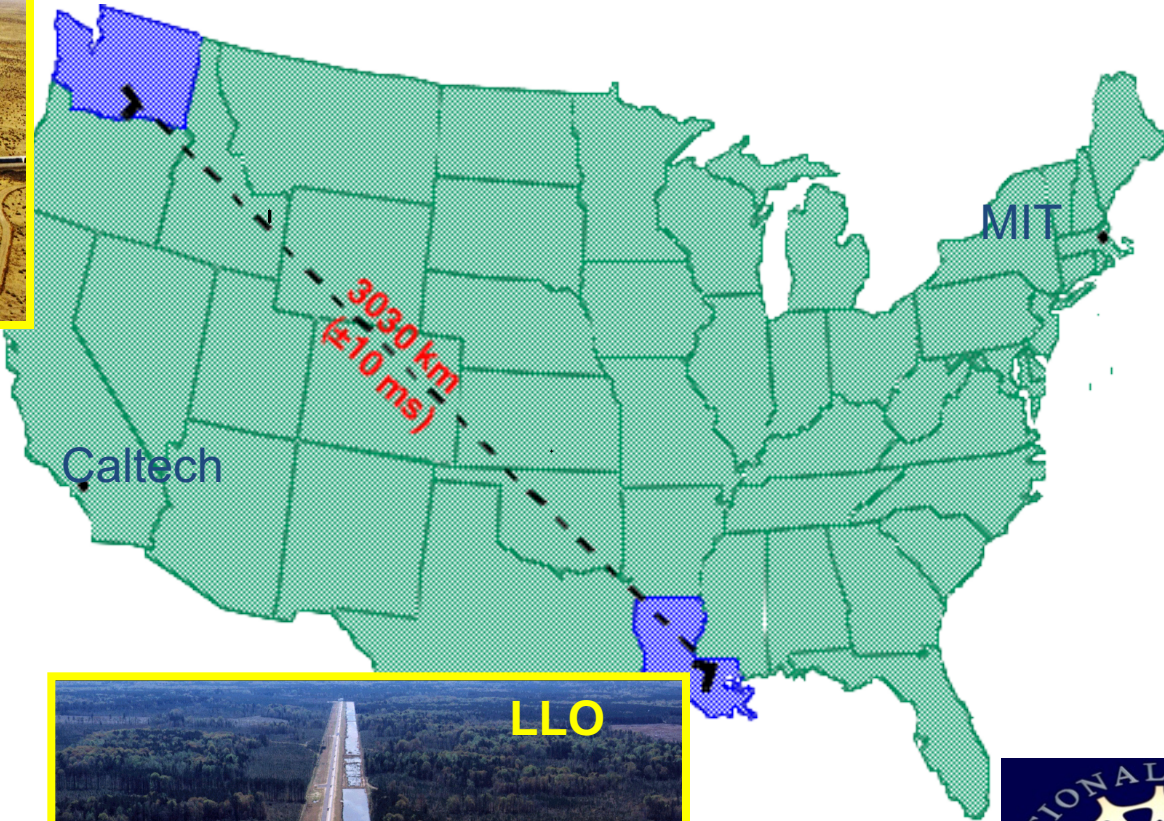
+ 2 km (H2)



4 km

L1

Livingston, LA



LLO





Despite a few difficulties, science runs started in 2002.



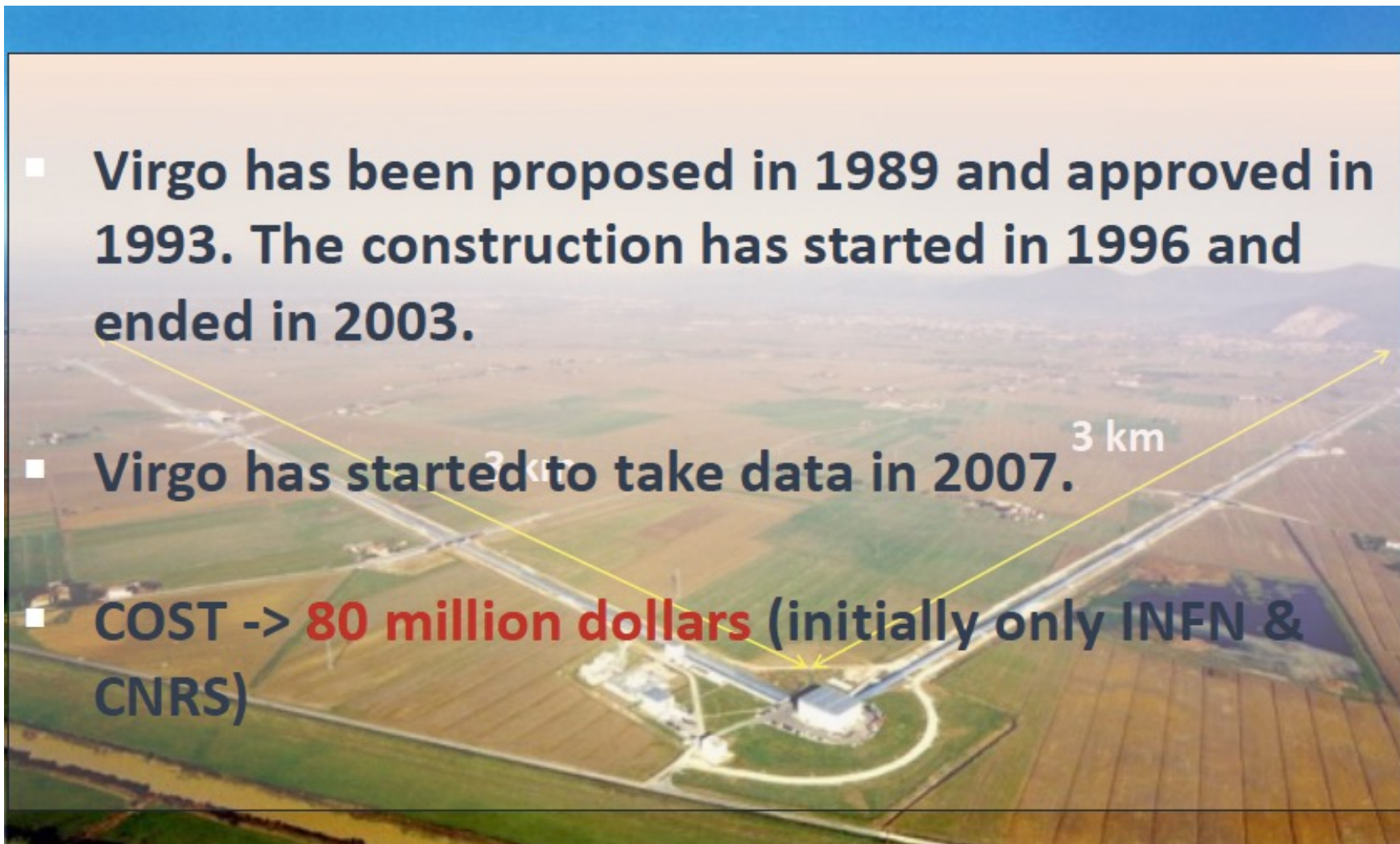


Virgo Interferometer



Virgo Interferometer

- Virgo has been proposed in 1989 and approved in 1993. The construction has started in 1996 and ended in 2003.
- Virgo has started to take data in 2007.
- COST -> **80 million dollars** (initially only INFN & CNRS)

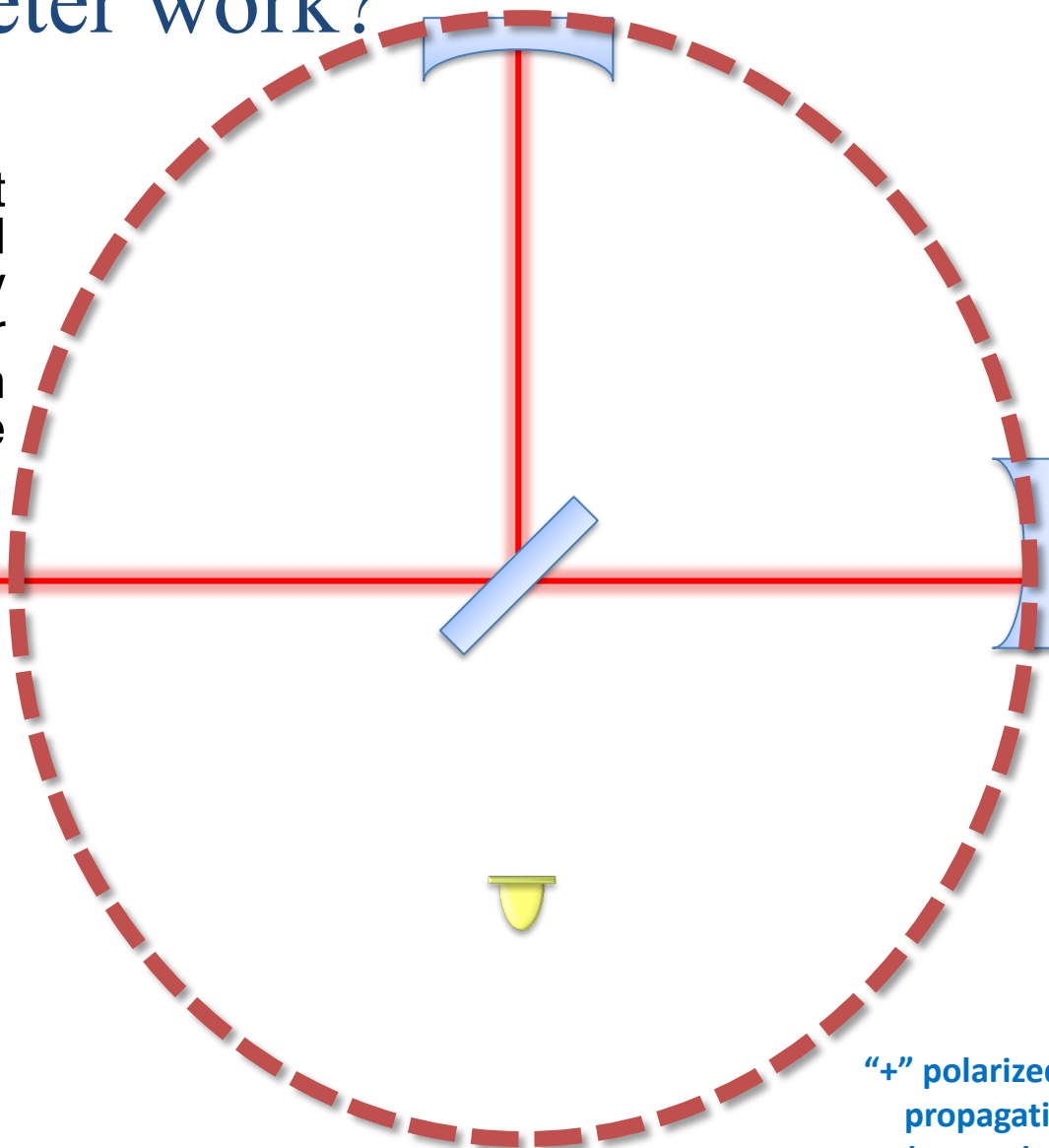




How does an interferometer work?

- Gravitational waves twist the space-time and during their crossing they produce a positive or negative separation among the two free masses.

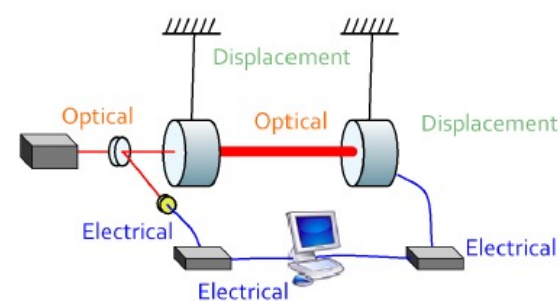
Laser



“+” polarized GW
propagating
orthogonal to the
screen

$$h = \frac{\Delta L}{L}$$

Optics



Low optical loss mirror
Low optical loss coating
Mirror precise polishing
Long baseline optics
optical recycling

Low mech. loss substrate
Low mech. loss coating
High rigidity optics supports

**Interferometer
control**

multiple pendulum suspension
monolithic suspensions
vibration isolation
high vacuum environment

Actuators
Low noise position sensors
Low noise accelerometers
Active vibration isolation

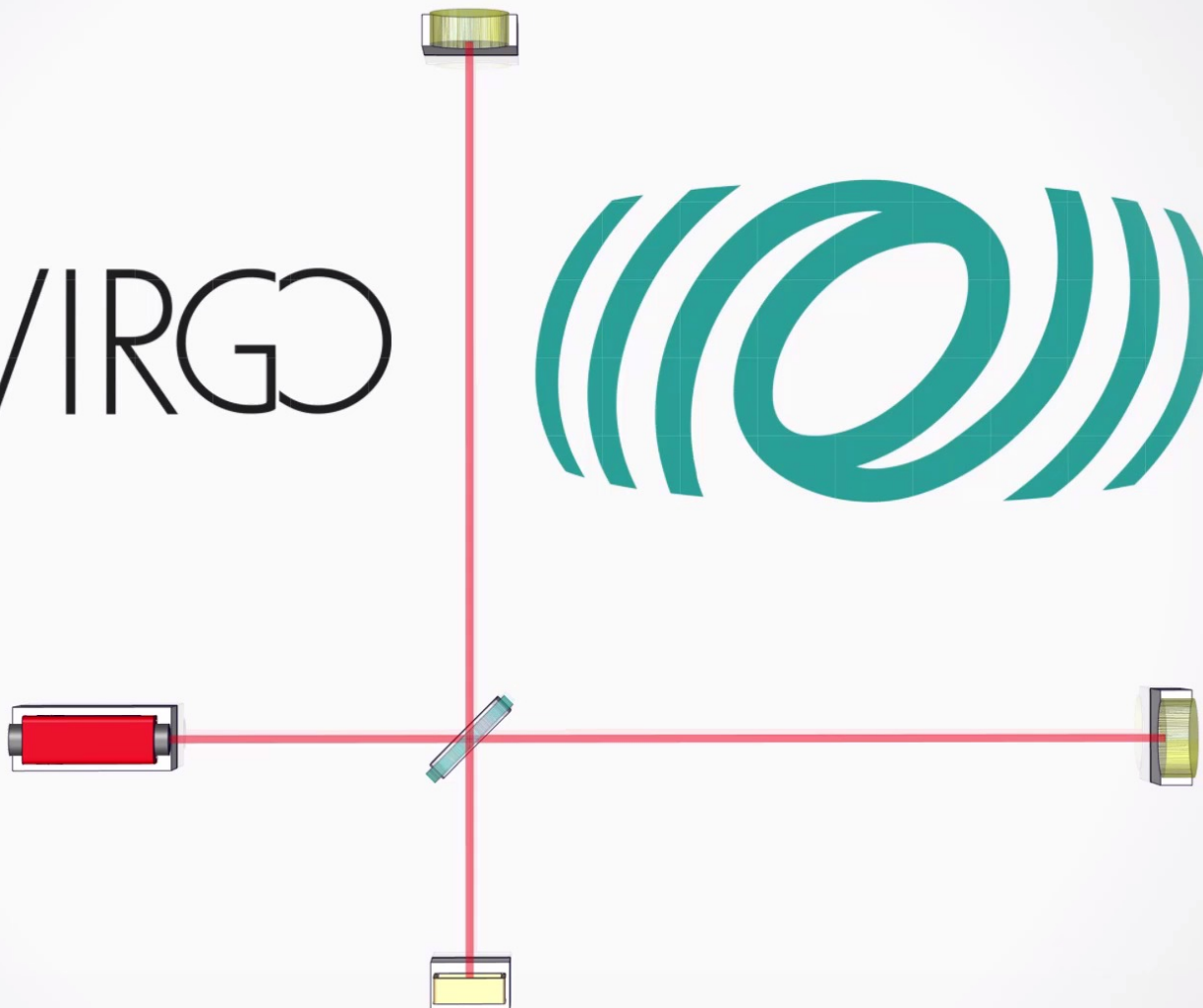
Modulation Crystal
Photodetector
High power stable laser
Modulation/Demod.
Quantum Optics

RF modulation
Analog high speed ctrl
Analog front end
Real time digital cont
User interface
Data acquisition
Data archive
Computing

Electronics

Mechanics

VIRGO

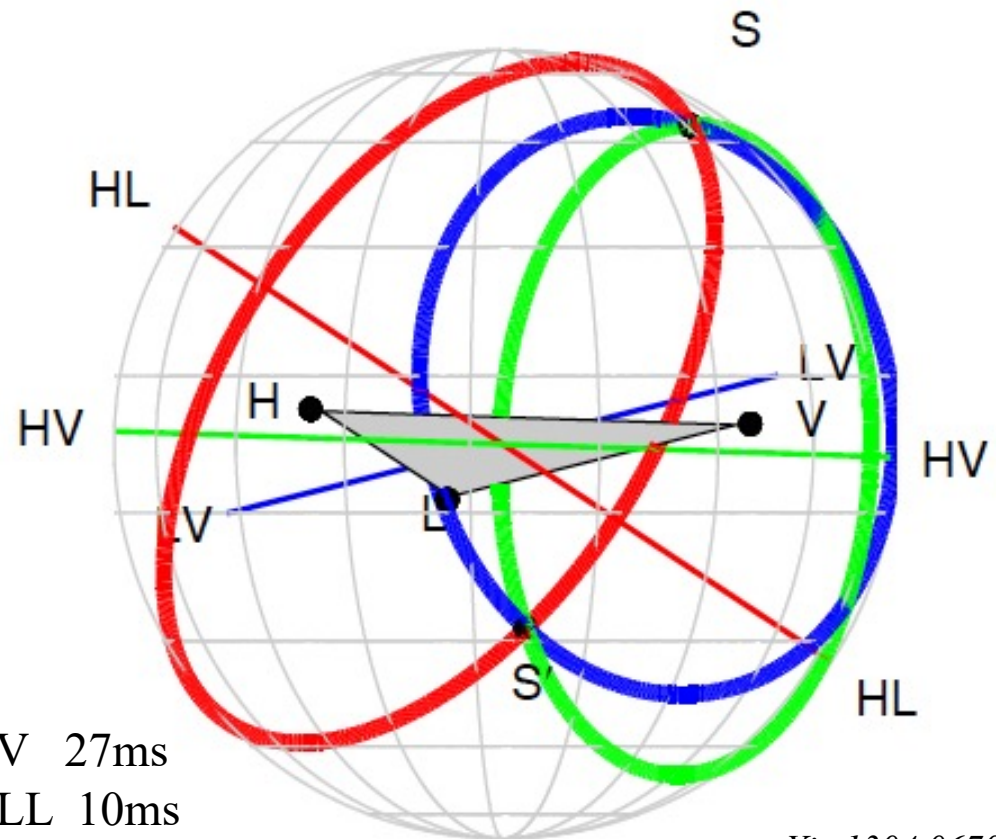


Sky localization: triangulation



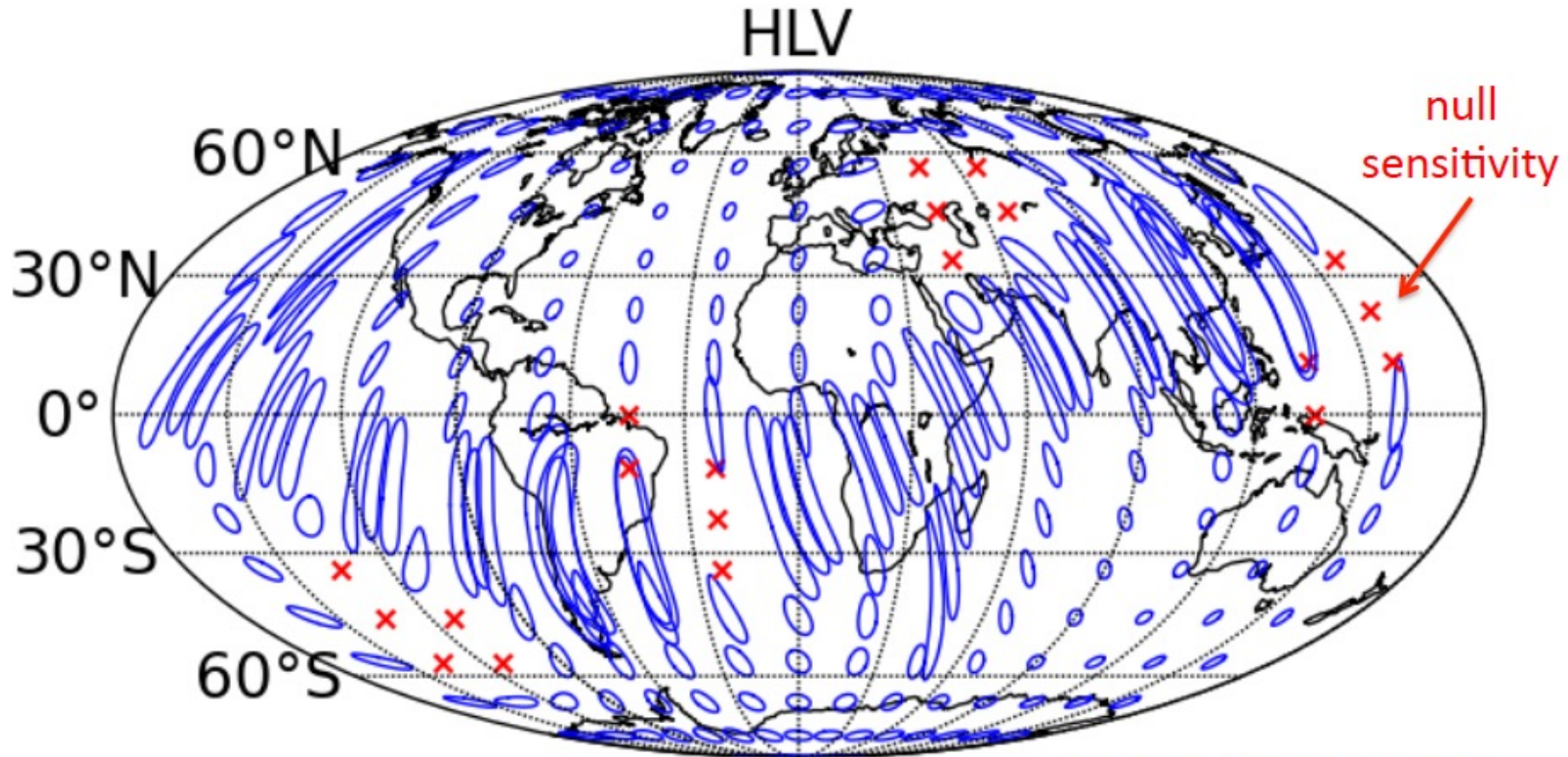
- A pair of detectors localizes to a ring on the sky.
- Width of rings depends upon timing accuracy and distance between detectors.
- More widely spaced detectors improves localization

$LH \leftrightarrow V$ 27ms
 $LH \leftrightarrow LL$ 10ms



arXiv 1304.0670

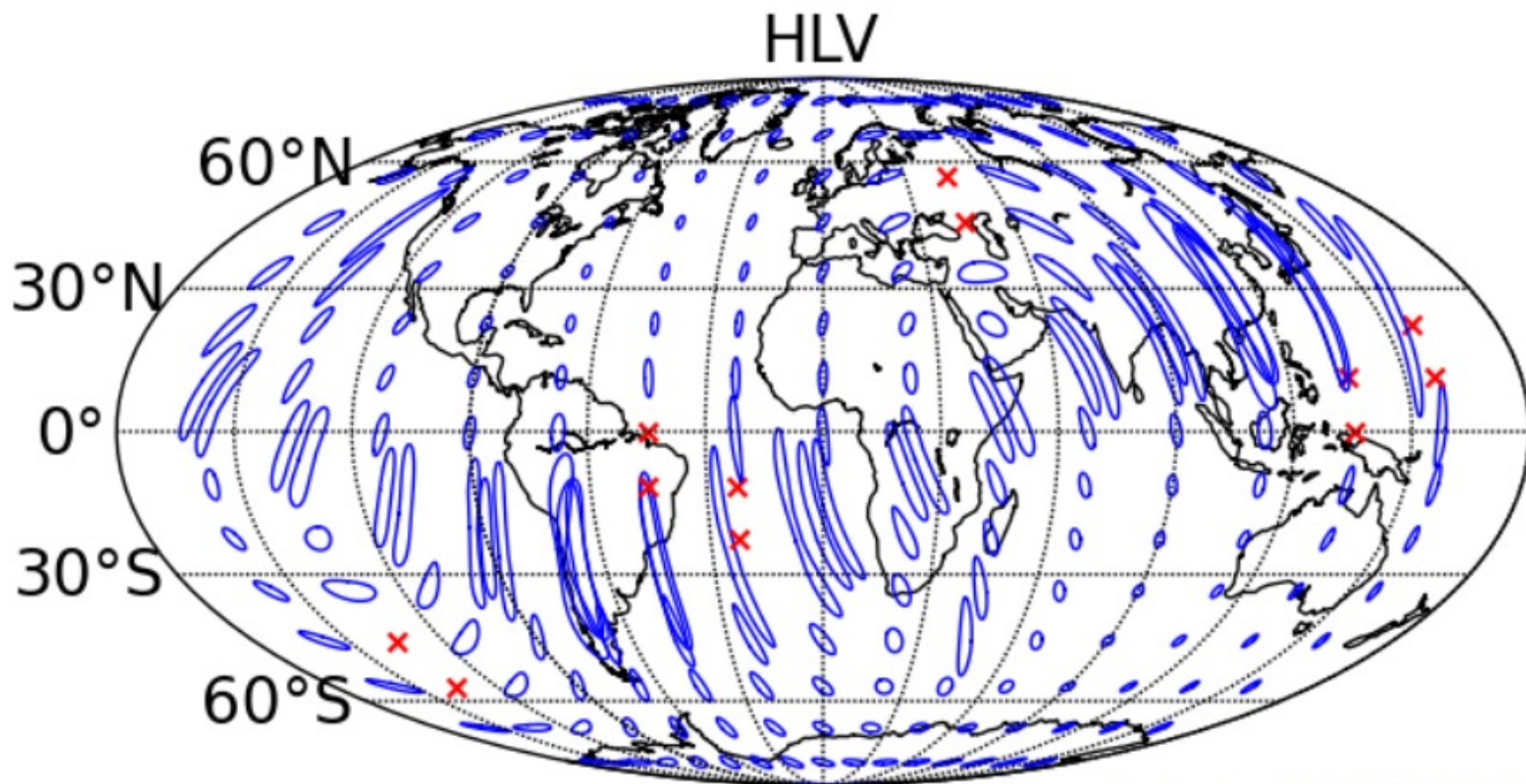
Sky localization – 2015



Aasi et al. 1304.0670

Localization expected for a BNS system at 80 Mpc by the HLV network. The ellipses show 90% confidence localization areas and the red crosses regions of the sky where the signal would not be confidently detected.

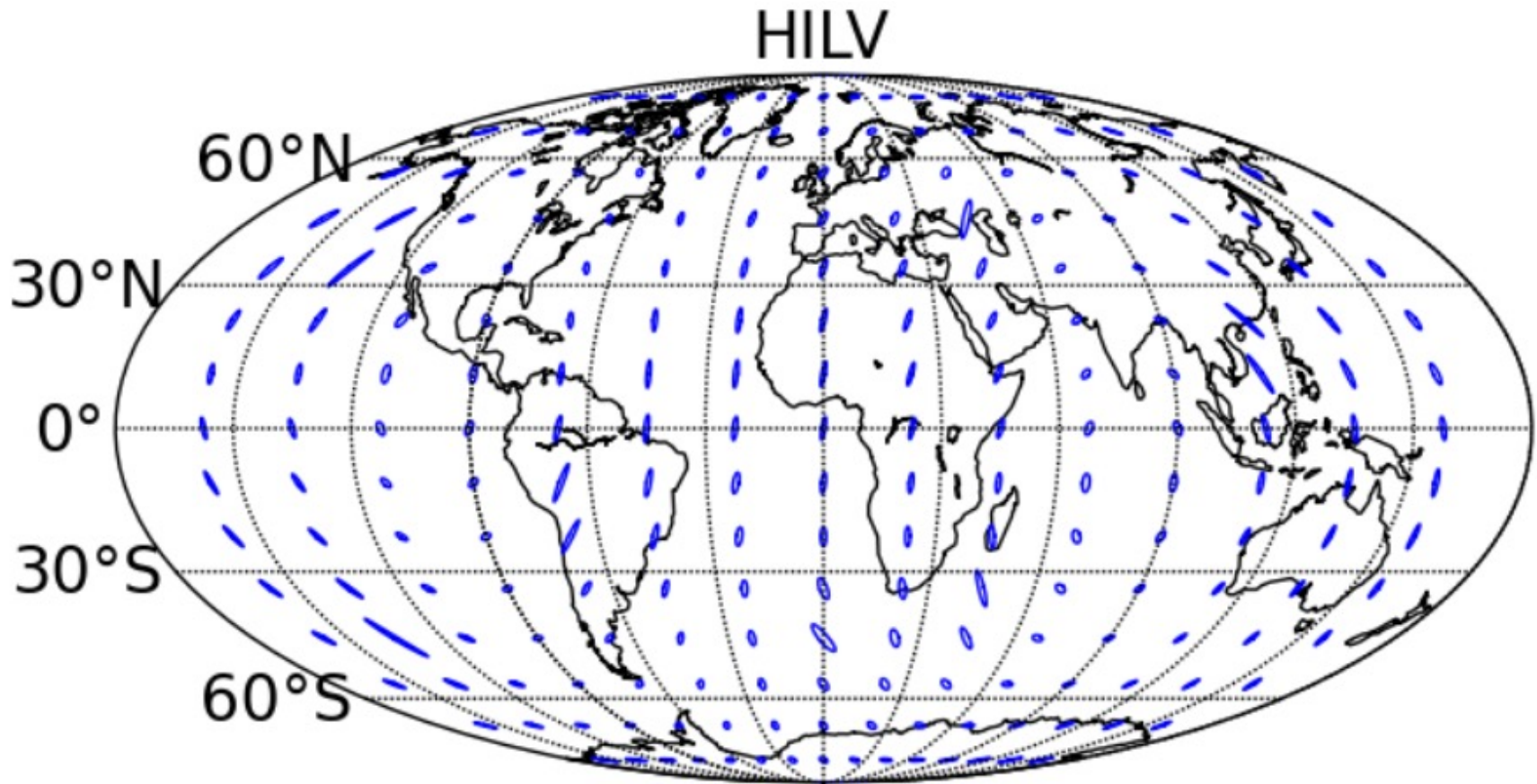
Sky localization – 2019+ (design)



Aasi et al. 1304.0670

Localization expected for a BNS system at 160 Mpc by the HLV network. The ellipses show 90% confidence localization areas and the red crosses regions of the sky where the signal would not be confidently detected.

Sky localization – 2022+ (LIGO-India)



Aasi et al. 1304.0670

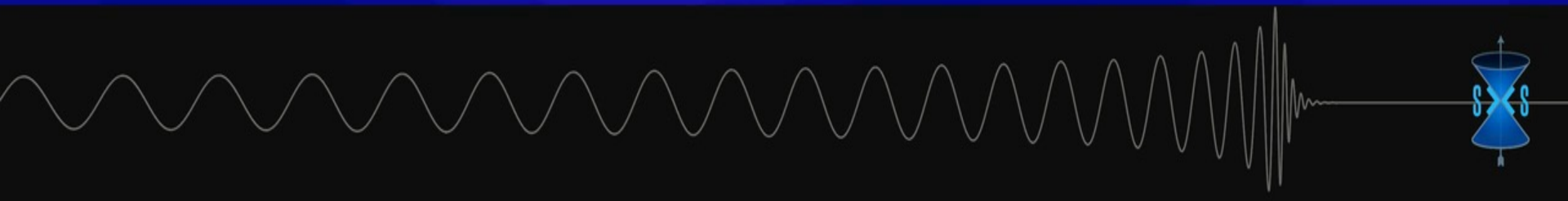
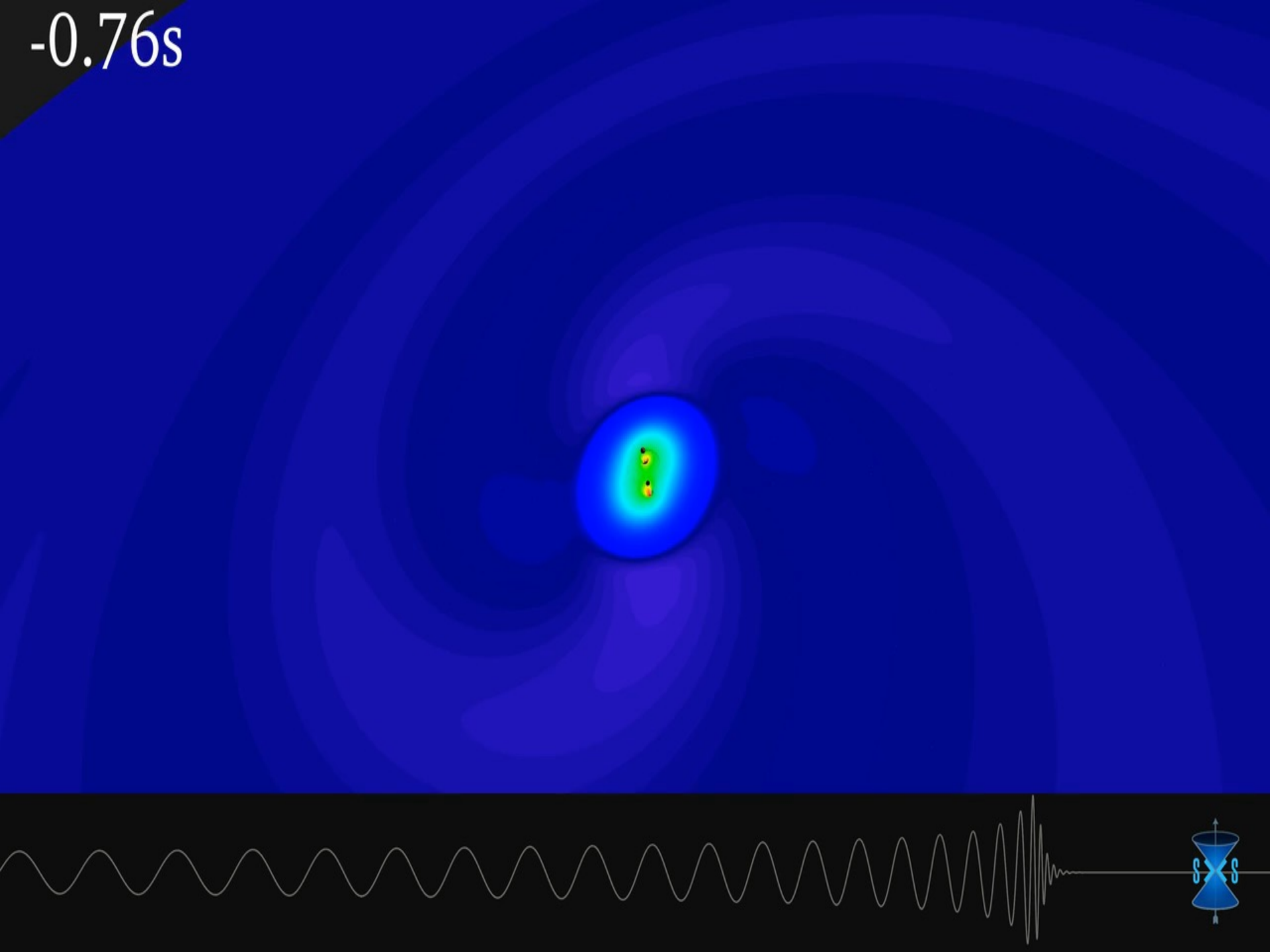
Localization expected for a BNS system at 160 Mpc by all detectors at final design sensitivity. The inclusion of a fourth site in India provides good localization over the whole sky.

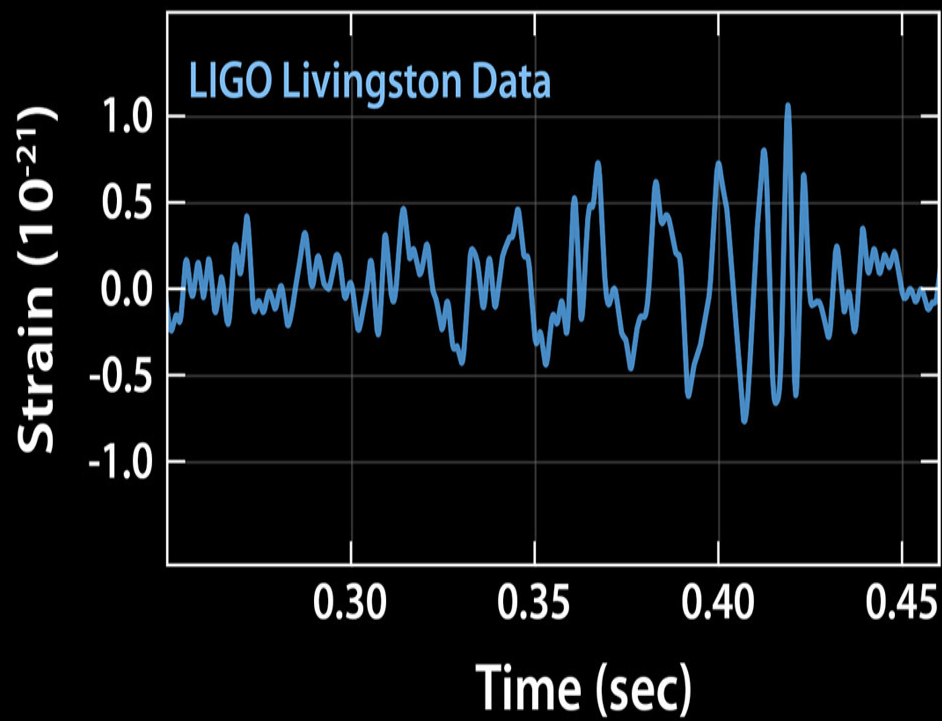
LIGO-KAGRA network qualitatively similar. (Fairhurst 2011)

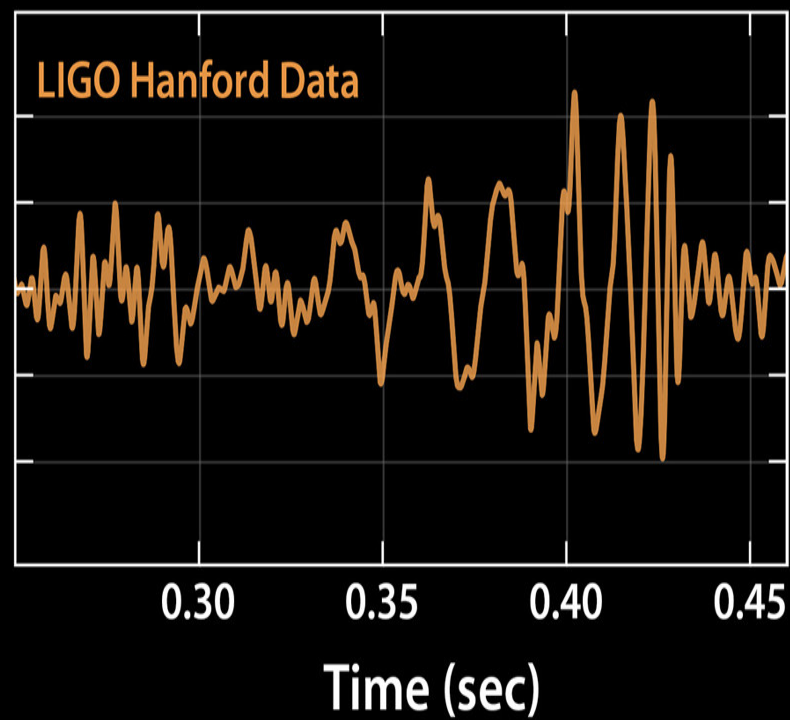
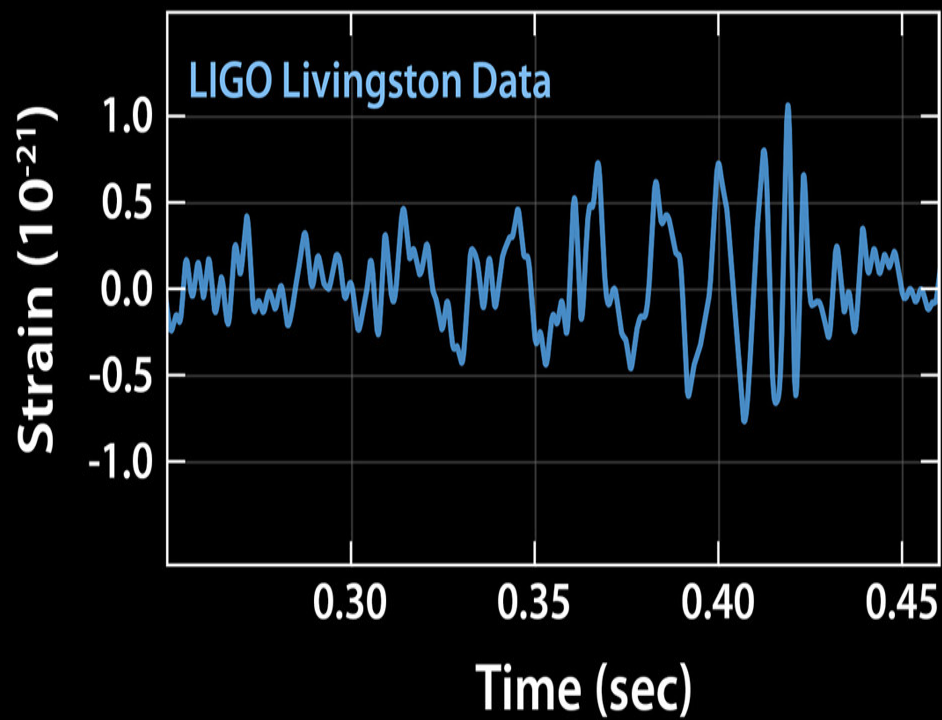
Outline

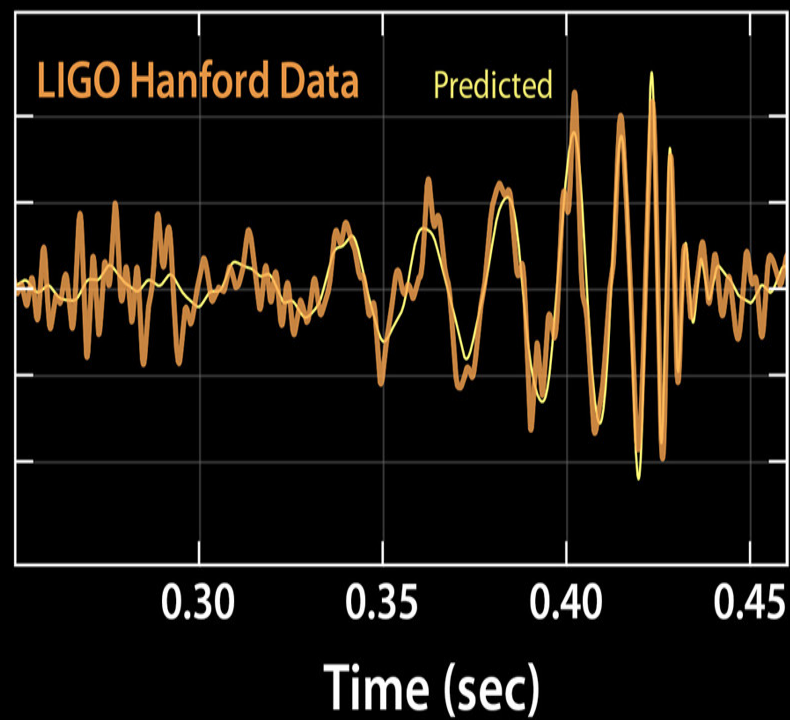
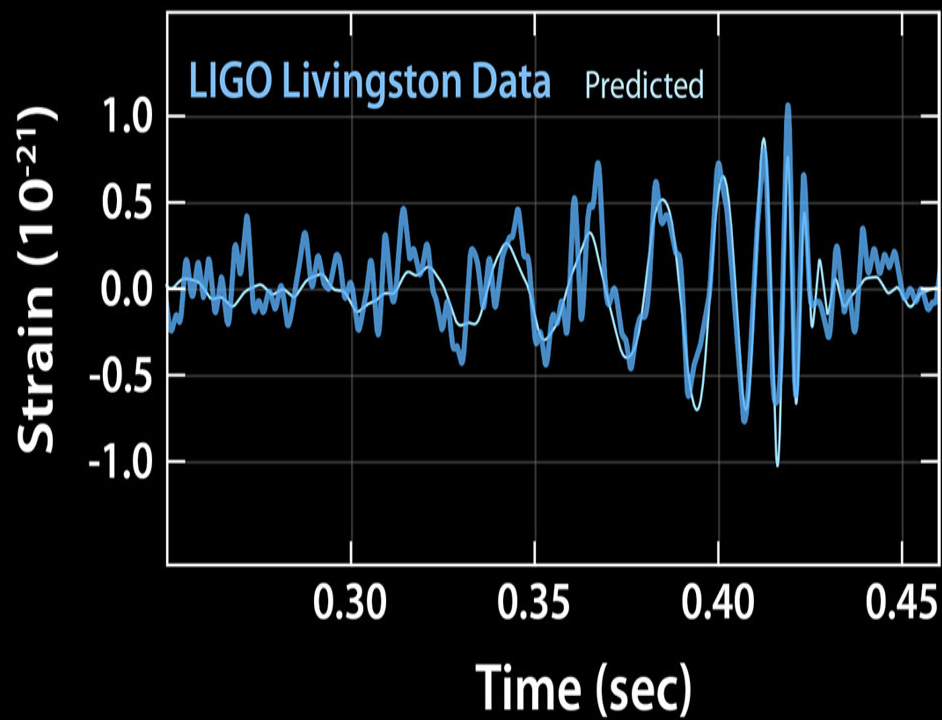
- **Einstein and the General Relativity**
- **Basic Analysis Concepts**
- **Gravitational Wave Detectors**
- **Some of the most interesting discoveries so far**

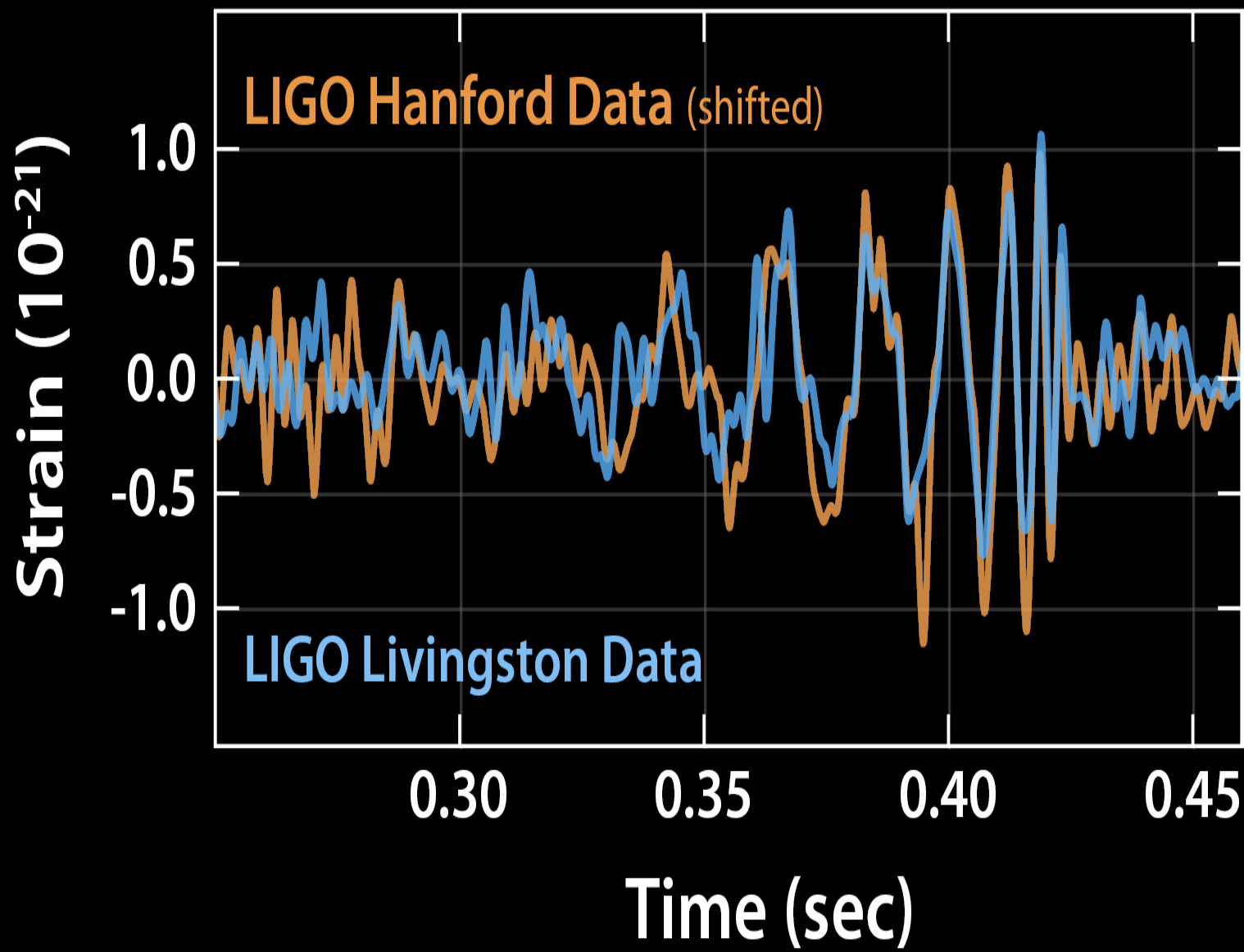
-0.76s

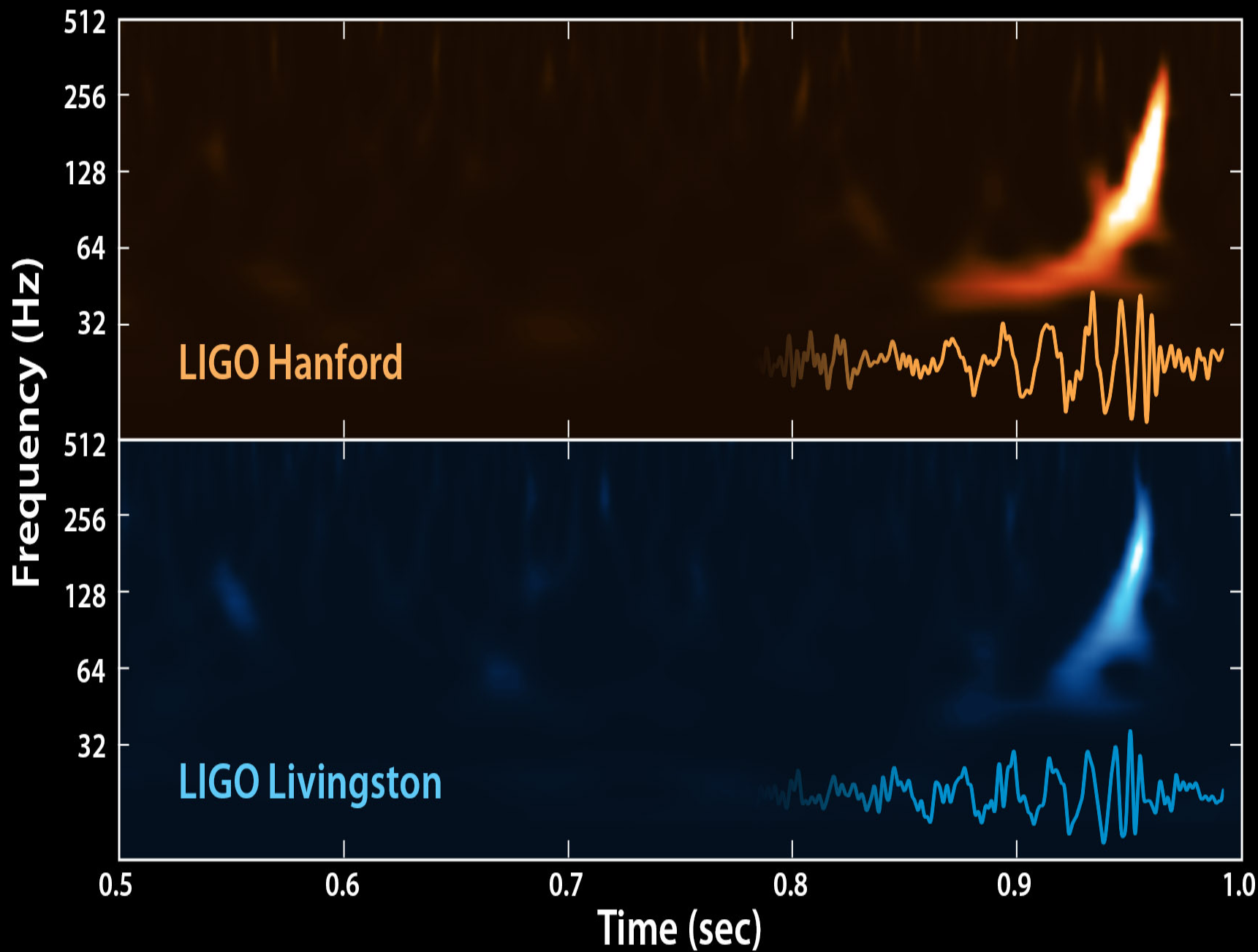


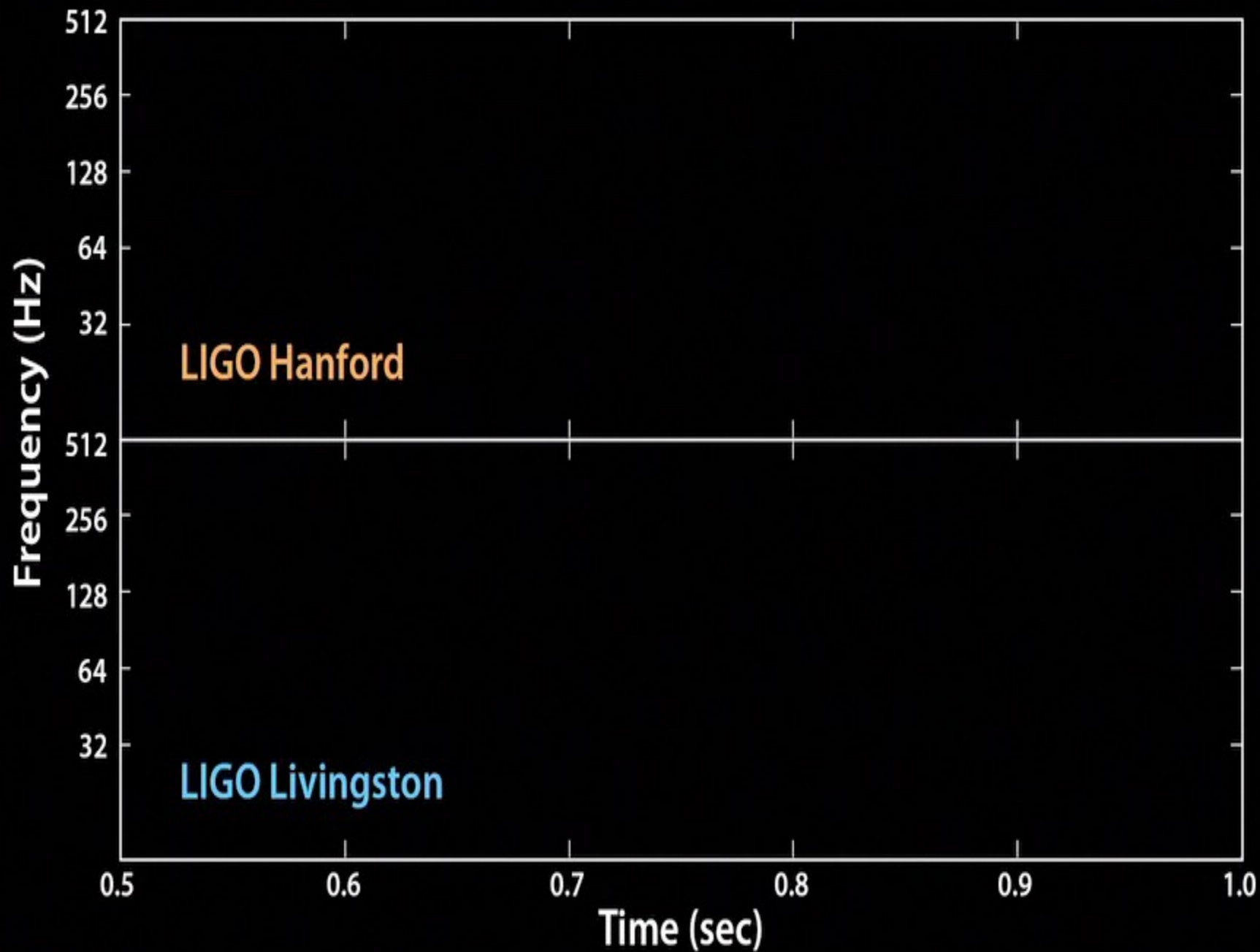


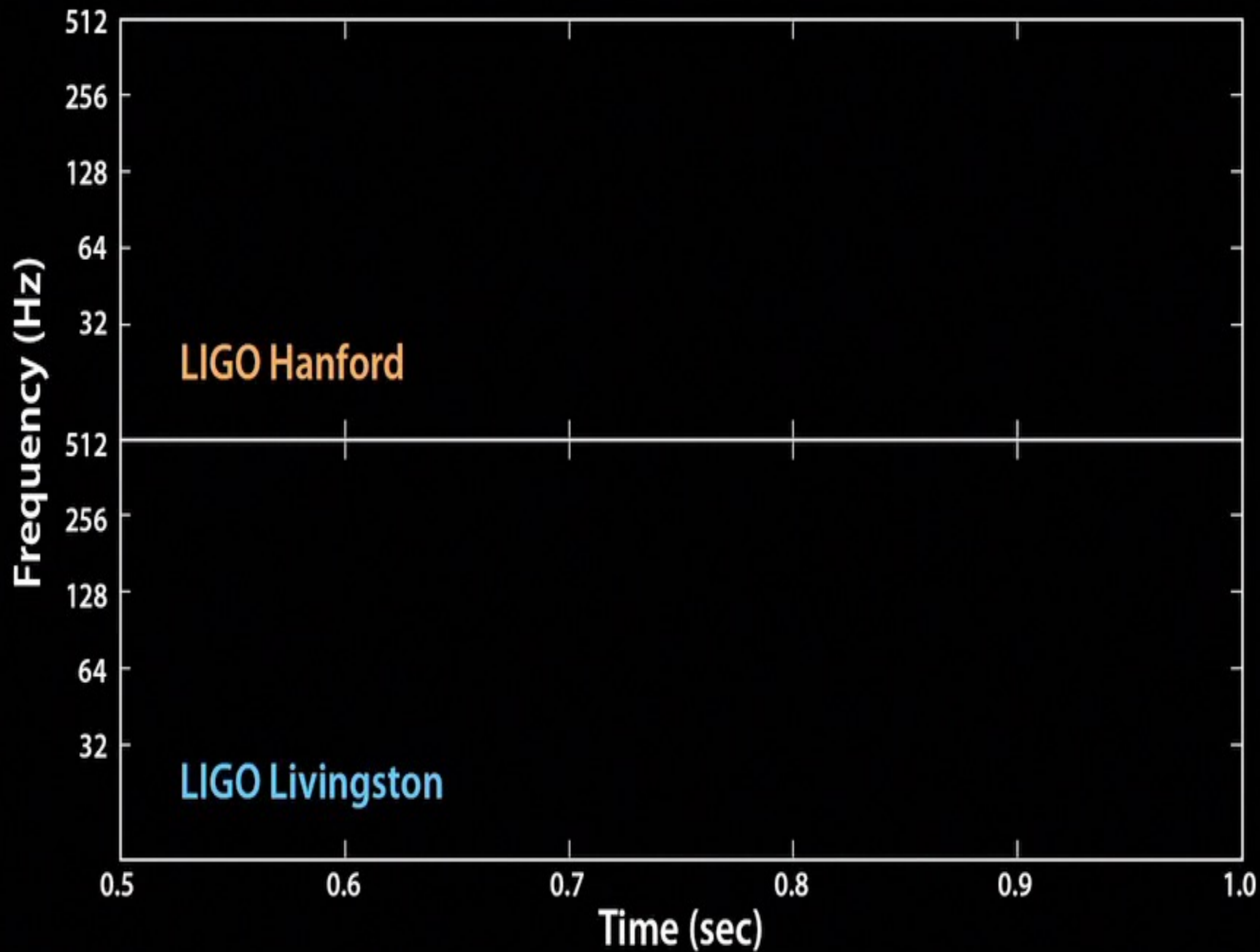












Ref: Phys. Rev. Lett. 116, 061102 (2016)

TABLE I. Source parameters for GW150914. We report median values with 90% credible intervals that include statistical errors, and systematic errors from averaging the results of different waveform models. Masses are given in the source frame, to convert to the detector frame multiply by $(1+z)$ [87]. The source redshift assumes standard cosmology [88].

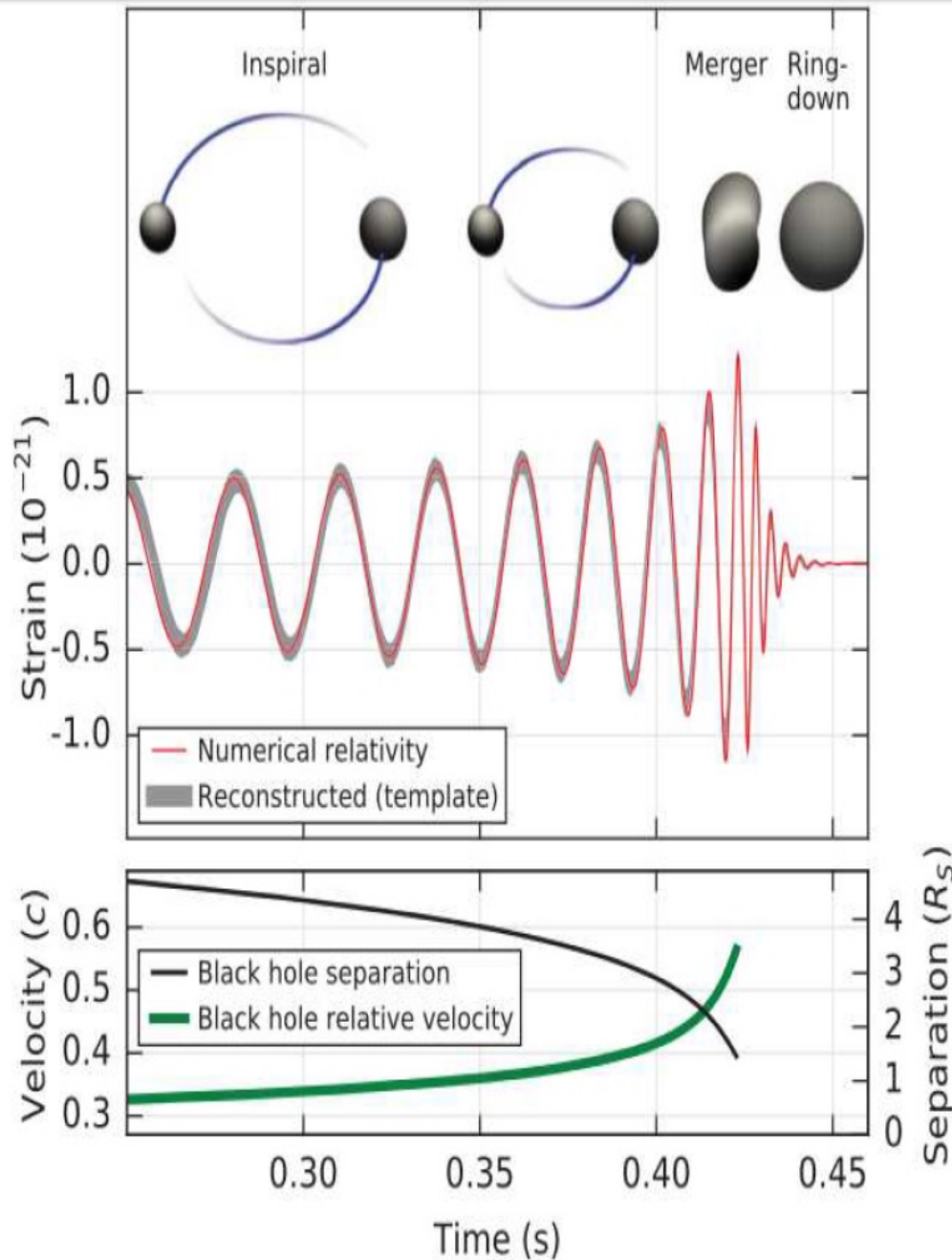
Primary black hole mass	$36^{+5}_{-4} M_{\odot}$
Secondary black hole mass	$29^{+4}_{-4} M_{\odot}$
Final black hole mass	$62^{+4}_{-4} M_{\odot}$
Final black hole spin	$0.67^{+0.05}_{-0.07}$
Luminosity distance	$410^{+160}_{-180} \text{ Mpc}$
Source redshift, z	$0.09^{+0.03}_{-0.04}$

The Keplerian effective black hole separation in unit of Schwarzschild radii

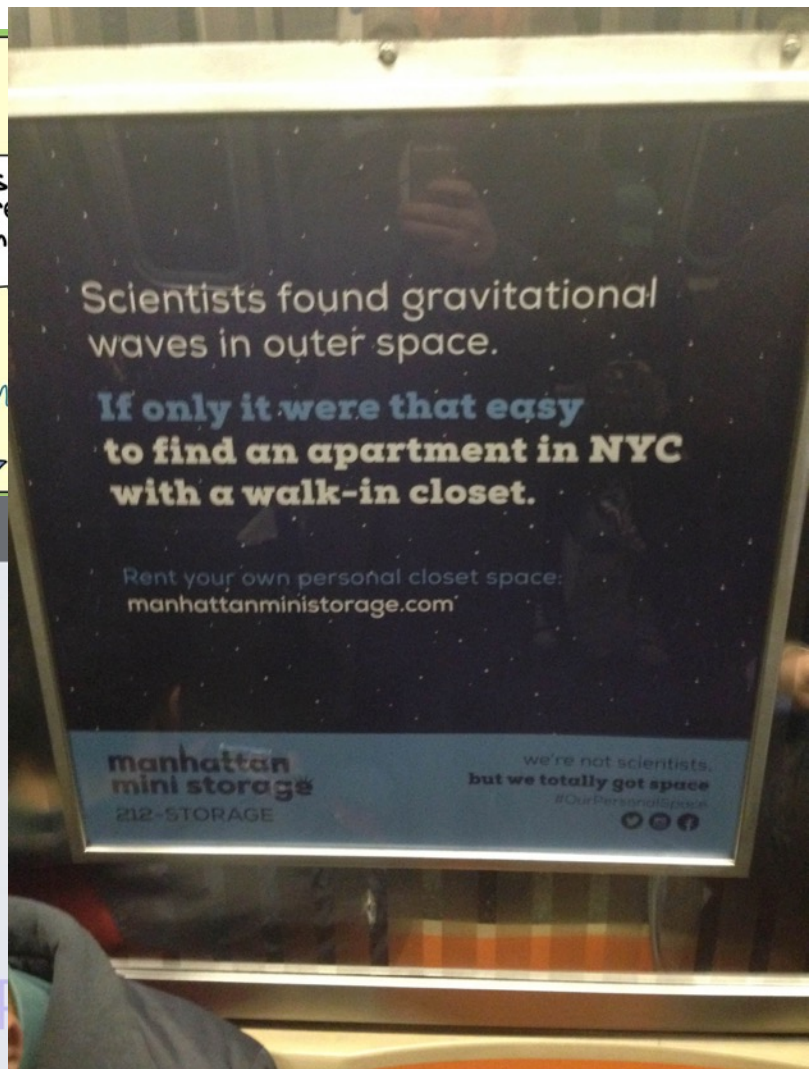
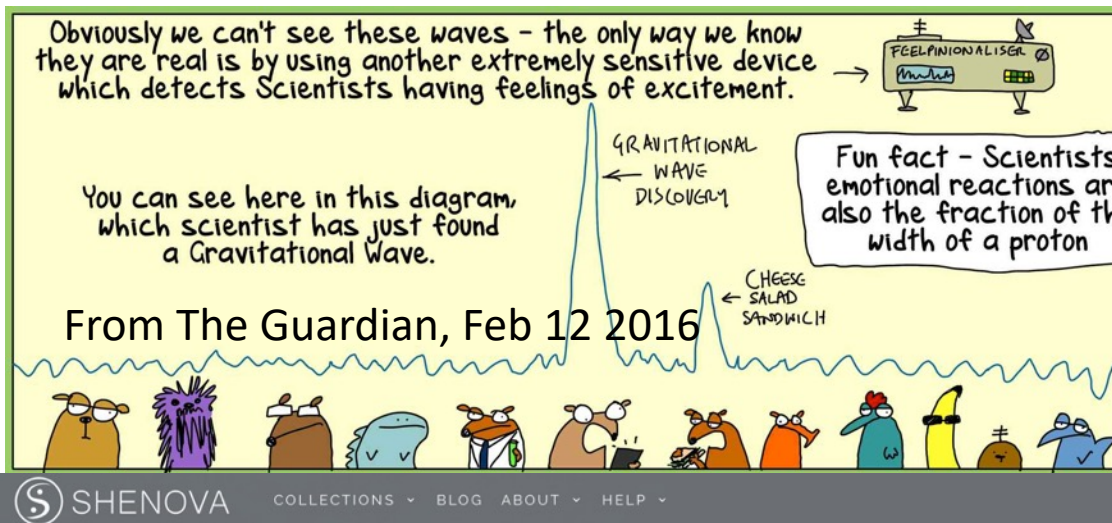
$$R_S = 2GM/c^2$$

and the effective relative velocity given by the post-Newtonian parameter

$$v/c = (GM\pi f/c^3)^{1/3}$$



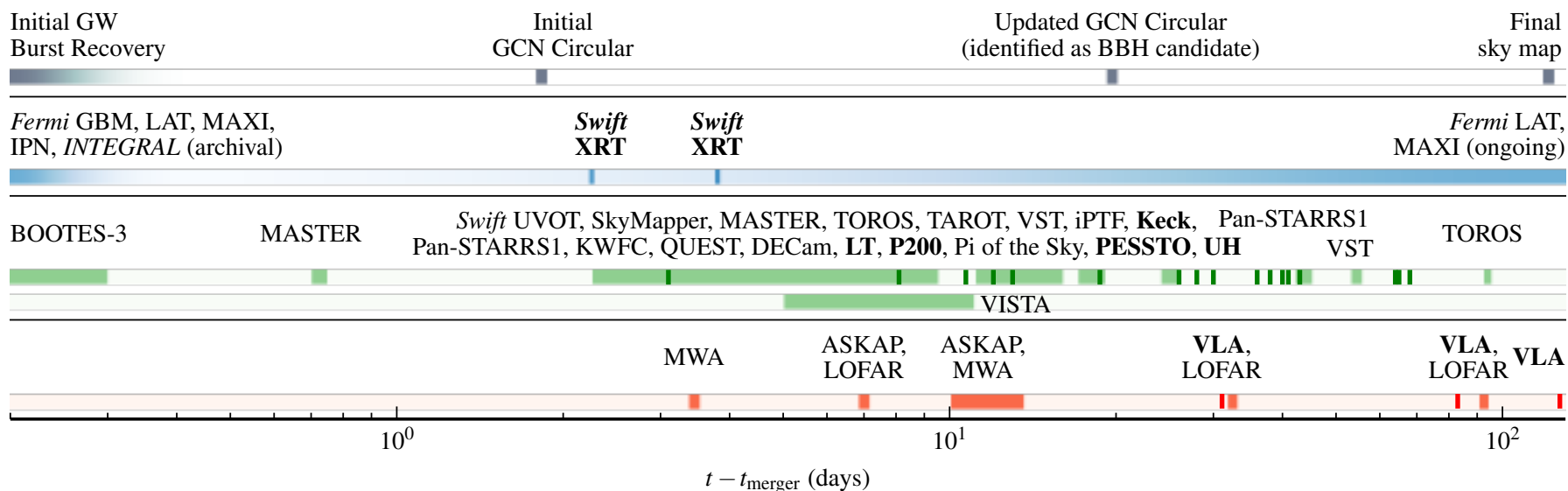
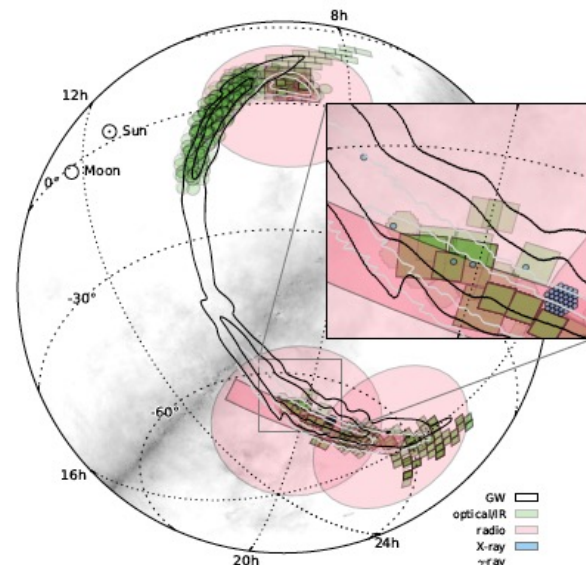
Gravitational Waves in Pop Culture



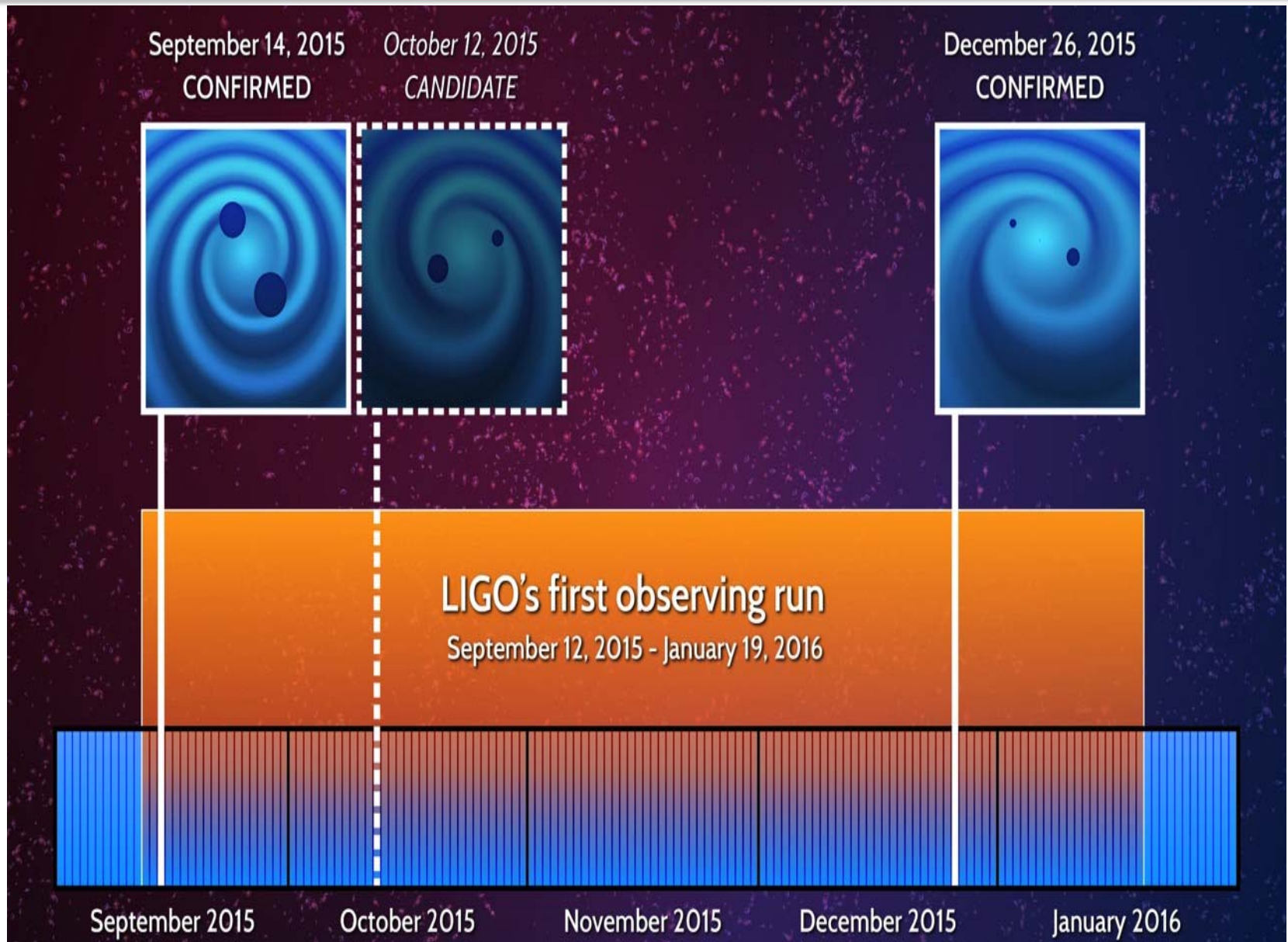
GW150914 EM Follow Up

- Follow-up observations reported by 25 teams via private Gamma-ray Coordinates Network (GCN) Circulars

Abbott, et al. ,LIGO Scientific Collaboration and Virgo Collaboration, "Localization and Broadband Follow-Up of the Gravitational-Wave Transient GW150914", Ap. J. Lett, 826:L13, 2016.

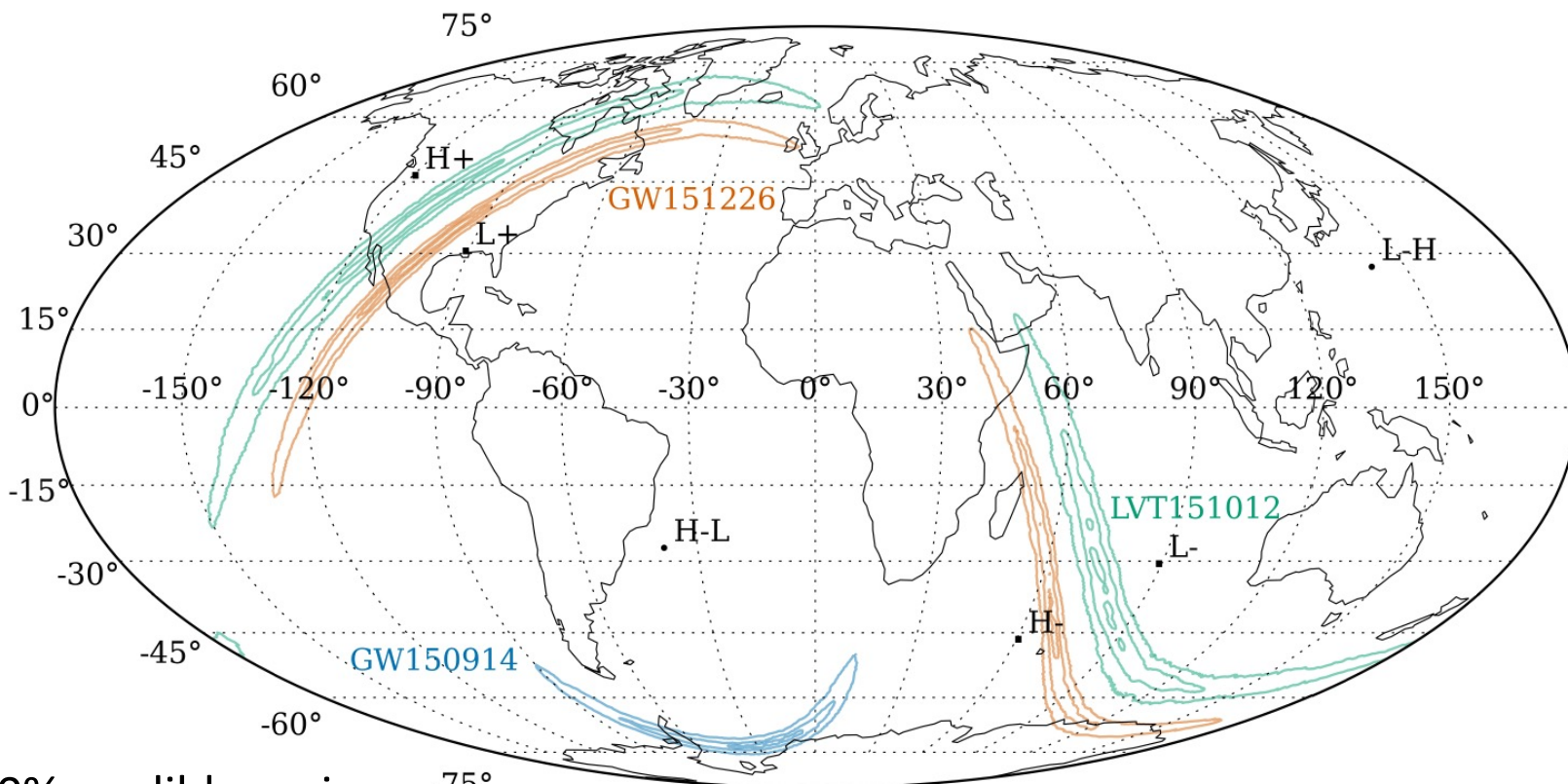


Events Observed during O1



Event Sky Location

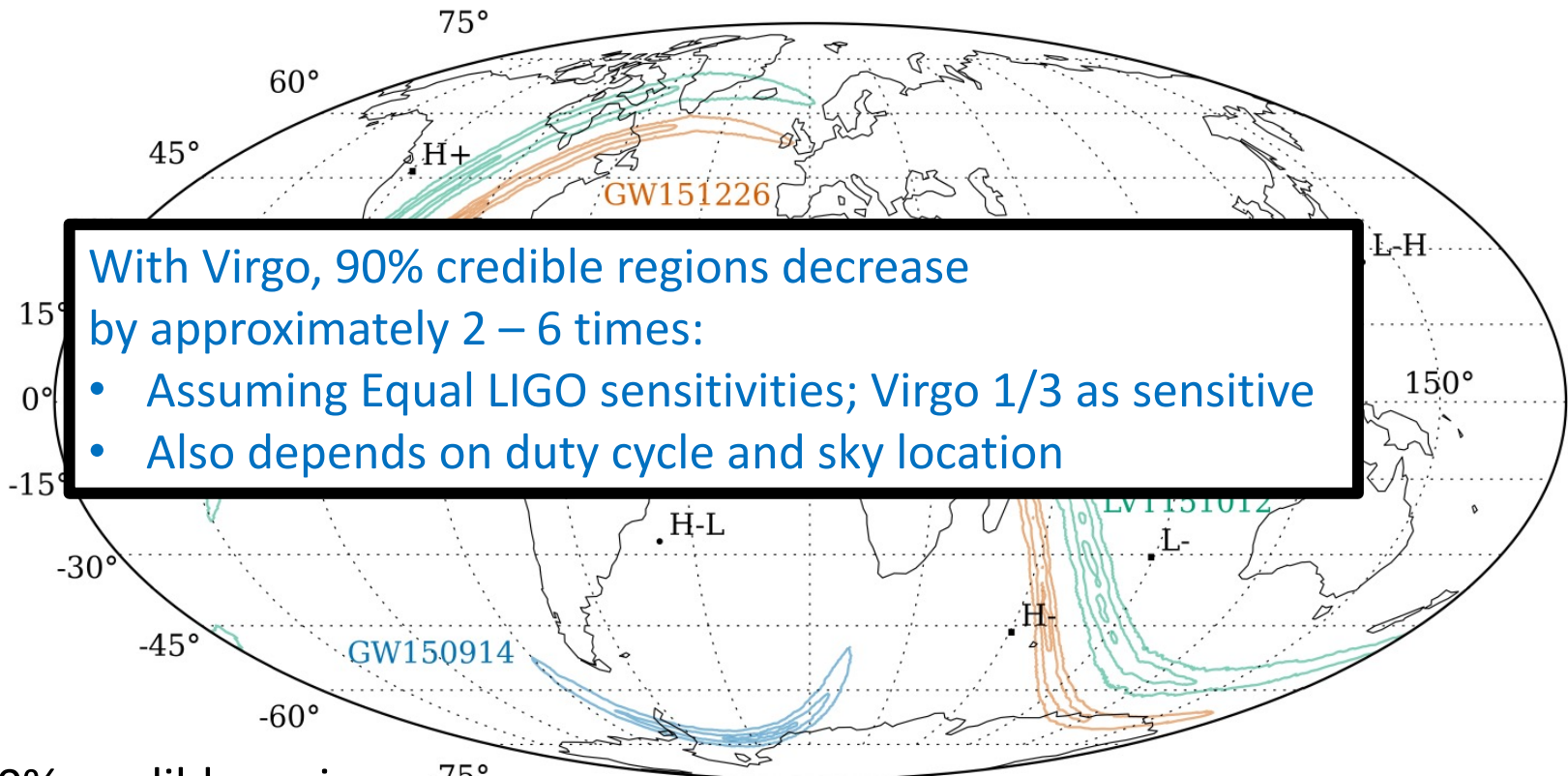
- With 2 detectors can only limit location to annulus on the sky
 - Preferential angles from interferometer antenna patterns



- 90% credible regions:
 - GW150914: 230 deg²
 - GW151226: 850 deg²
 - LVT151012: 1600 deg²
 - (GW170104: 1200 deg²)

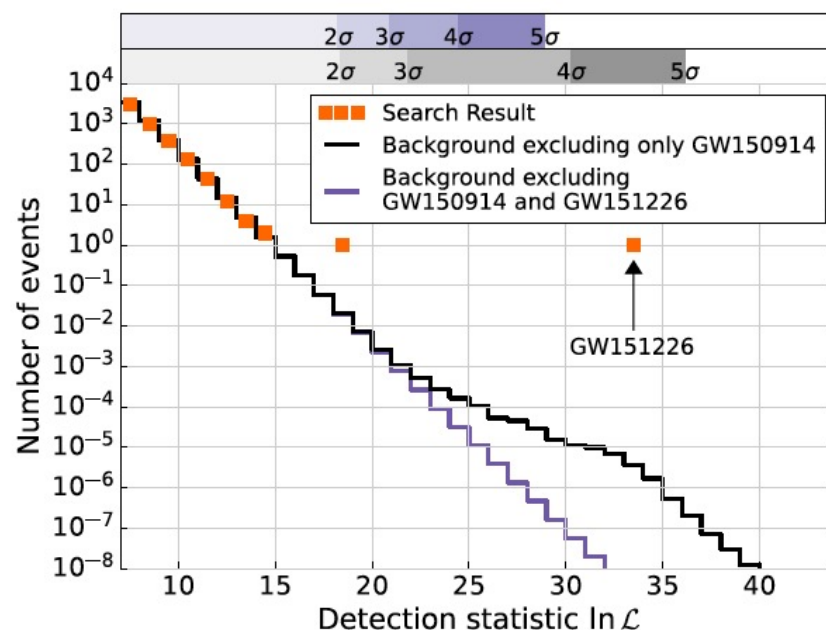
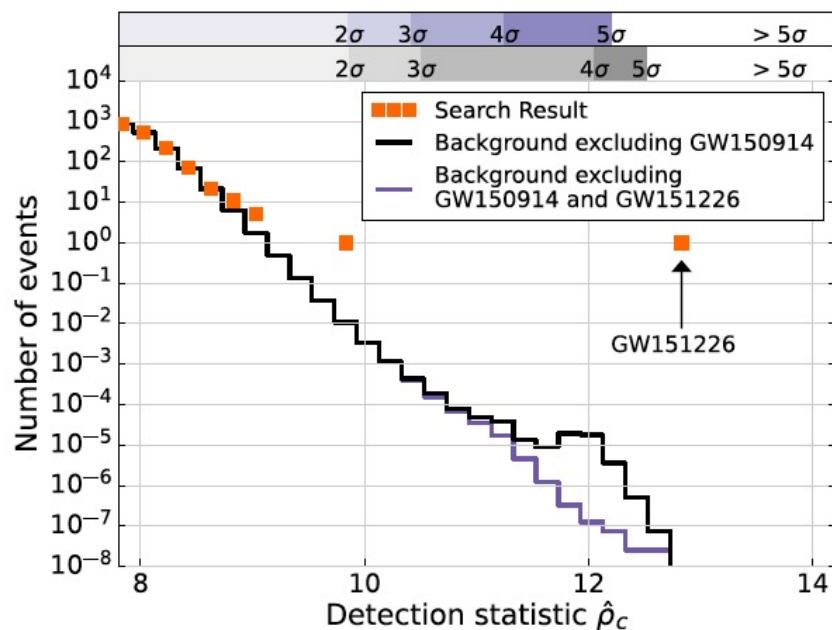
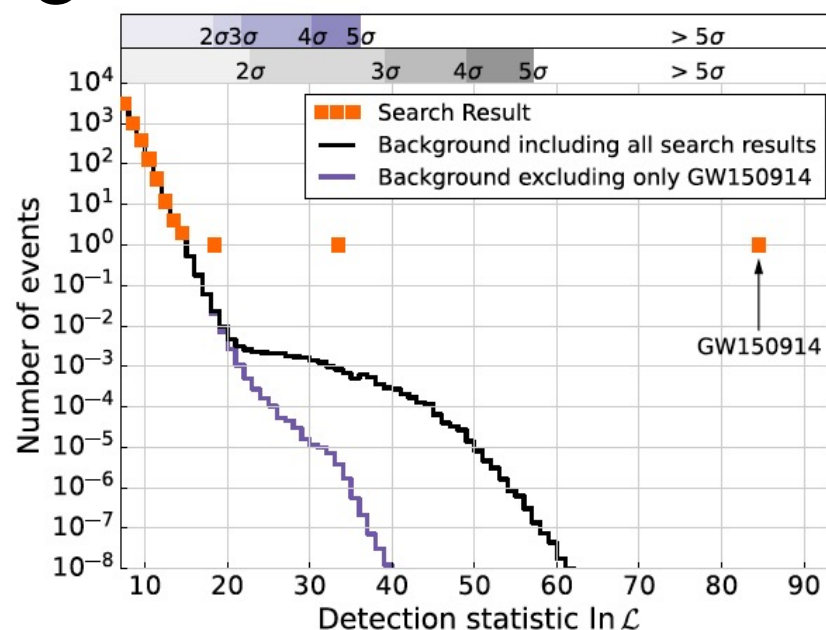
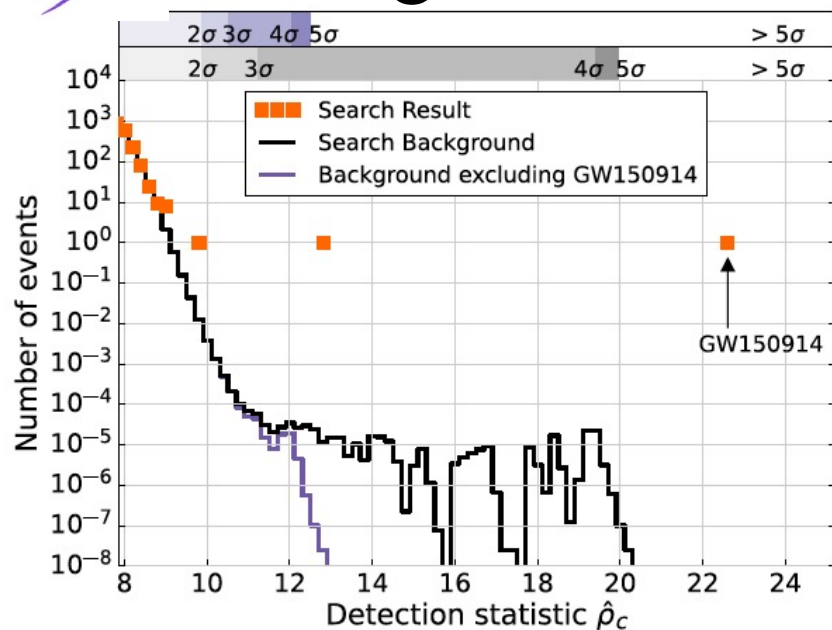
Event Sky Location

- With 2 detectors can only limit location to annulus on the sky
 - Preferential angles from interferometer antenna patterns



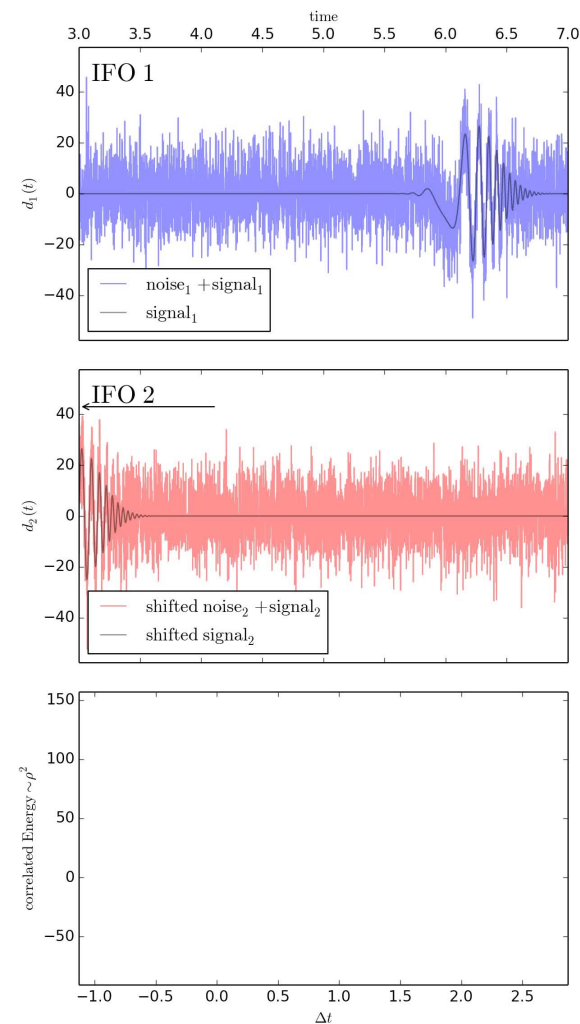
- 90% credible regions: -75°
 - GW150914: 230 deg²
 - GW151226: 850 deg²
 - LVT151012: 1600 deg²
 - (GW170104: 1200 deg²)

Assessing Statistical Significance: Modeled Search

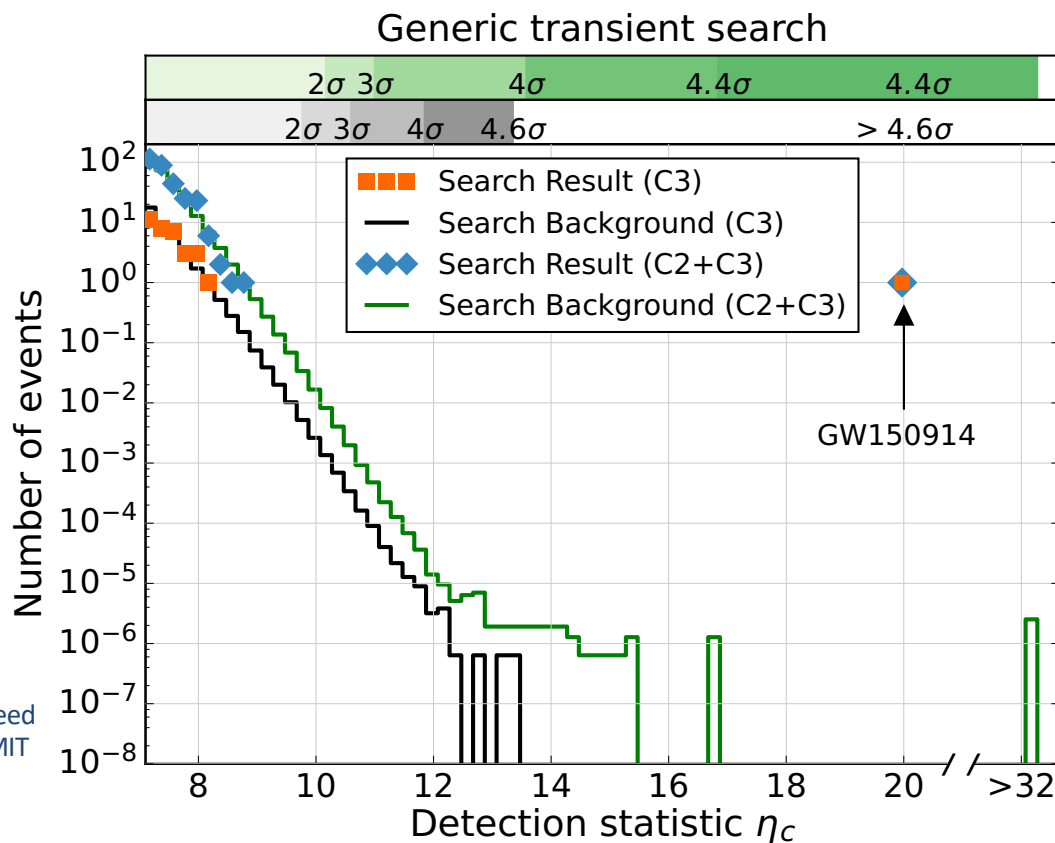


Assessing Statistical Significance: Unmodeled Search

- Pipelines look for excess power in time-frequency domain
 - e.g. wavelet basis
 - More sensitive to generic sources, but also to noise transients in the interferometers



Simulation: Reed
Essick, LIGO MIT



Extracting Astrophysical Parameters from Waveforms

- **Total Mass:** $M = m_1 + m_2$

- **Mass ratio:** $q = \frac{m_2}{m_1} \leq 1$

- **Chirp Mass:** $\mathcal{M} = \frac{(m_1 m_2)^{3/5}}{M^{1/5}}$

$$\mathcal{M} = \frac{c^3}{G} \left(\frac{5}{96} \pi^{-8/3} f^{-11/3} \dot{f} \right)^{3/5}$$

- **Black Hole Spins:**

$$a_{1,2} = \frac{c}{Gm_{1,2}^2} |S_{1,2}|$$

- **Spin component aligned with orbital angular momentum:**

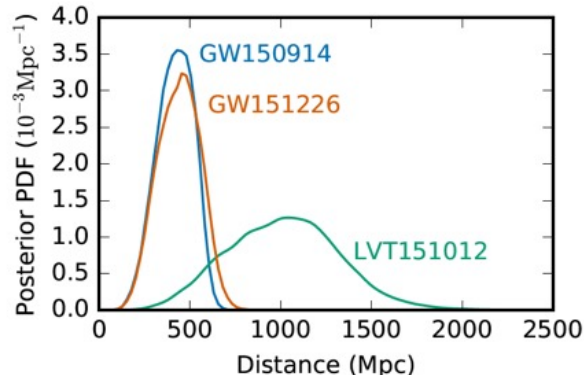
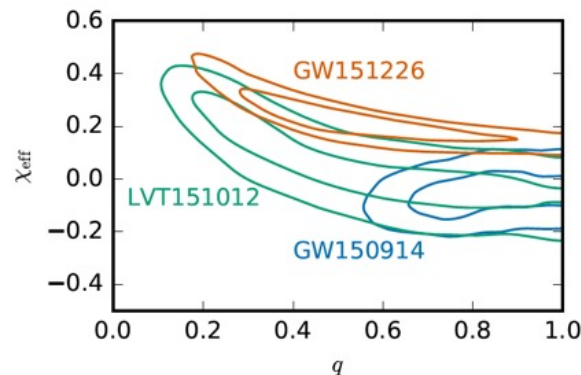
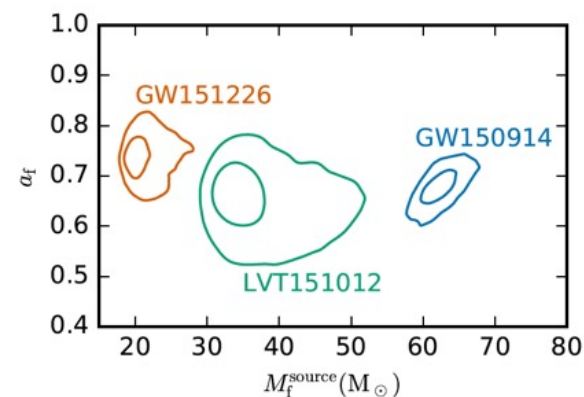
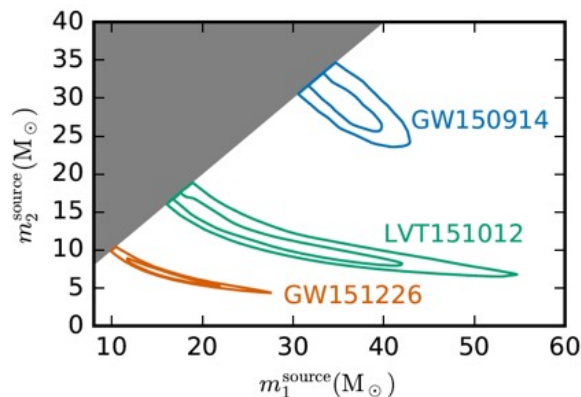
$$\chi_{1,2} = \frac{c}{Gm_{1,2}^2} S_{1,2} \cdot \hat{L}$$

- **Effective spin parameter:**

$$\chi_{\text{eff}} = \frac{m_1 \chi_1 + m_2 \chi_2}{M}$$

- **Luminosity Distance D_L**

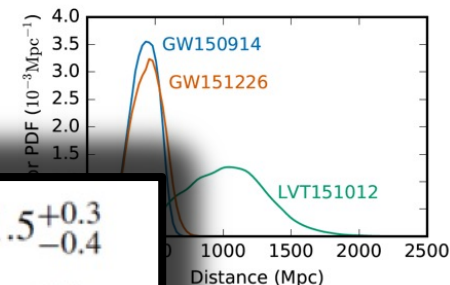
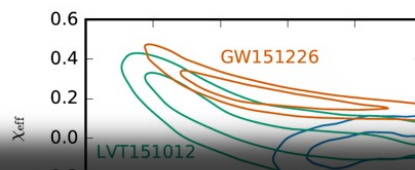
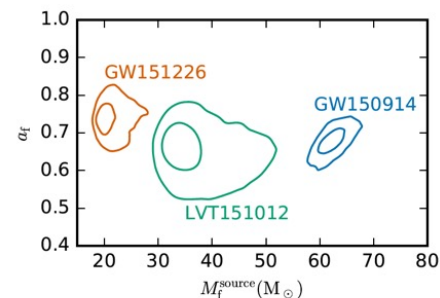
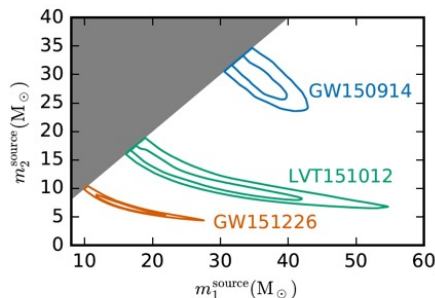
- Bayesian computation of posterior PDFs
 - Markov chain Monte Carlo
 - Nested Sampling



Abbott, et al., LIGO Scientific Collaboration and Virgo Collaboration, "Binary Black Hole Mergers in the first Advanced LIGO Observing Run", Phys. Rev. X 6, 041015 (2016).

Astrophysical Parameters of the Detected BBH Mergers

Event	GW150914	GW151226	LVT151012
Signal-to-noise ratio ρ	23.7	13.0	9.7
False alarm rate FAR/yr ⁻¹	$< 6.0 \times 10^{-7}$	$< 6.0 \times 10^{-7}$	0.37
p-value	7.5×10^{-8}	7.5×10^{-8}	0.045
Significance	$> 5.3\sigma$	$> 5.3\sigma$	1.7σ
Primary mass $m_1^{\text{source}}/M_\odot$	$36.2^{+5.2}_{-3.8}$	$14.2^{+8.3}_{-3.7}$	23^{+18}_{-6}
Secondary mass $m_2^{\text{source}}/M_\odot$	$29.1^{+3.7}_{-4.4}$	$7.5^{+2.3}_{-2.3}$	13^{+4}_{-5}
Chirp mass $\mathcal{M}^{\text{source}}/M_\odot$	$28.1^{+1.8}_{-1.5}$	$8.9^{+0.3}_{-0.2}$	$15.1^{+1.4}_{-1.1}$
Total mass $M^{\text{source}}/M_\odot$	$65.3^{+5.7}_{-4.7}$	$21.7^{+8.6}_{-3.9}$	38^{+24}_{-9}
Effective inspiral spin χ_{eff}	$-0.04^{+0.08}_{-0.08}$	$-0.14^{+0.09}_{-0.09}$	$-0.15^{+0.10}_{-0.10}$
Final mass $M_f^{\text{source}}/M_\odot$	$62.3^{+5.4}_{-4.4}$	$21.2^{+8.4}_{-3.9}$	37^{+24}_{-9}
Final spin a_f	$0.68^{+0.05}_{-0.06}$	$0.74^{+0.06}_{-0.06}$	$0.66^{+0.09}_{-0.10}$
Radiated energy $E_{\text{rad}}/(M_\odot c^2)$	$3.0^{+0.5}_{-0.4}$	$1.0^{+0.1}_{-0.2}$	$1.5^{+0.3}_{-0.4}$
Peak luminosity $\ell_{\text{peak}}/(\text{erg s}^{-1})$	$3.6^{+0.5}_{-0.4} \times 10^{56}$	$3.3^{+0.8}_{-1.6} \times 10^{56}$	$3.1^{+0.8}_{-1.8} \times 10^{56}$
Luminosity distance D_L/Mpc	420^{+150}_{-180}	440^{+180}_{-190}	1000^{+500}_{-500}
Source redshift z	$0.09^{+0.03}_{-0.04}$	$0.09^{+0.03}_{-0.04}$	$0.20^{+0.09}_{-0.09}$
Sky localization $\Delta\Omega/\text{deg}^2$	230	850	1600



Radiated energy

$$E_{\text{rad}}/(M_\odot c^2)$$

$$3.0^{+0.5}_{-0.4}$$

$$1.0^{+0.1}_{-0.2}$$

$$1.5^{+0.3}_{-0.4}$$

Peak luminosity

$$\ell_{\text{peak}}/(\text{erg s}^{-1})$$

$$3.6^{+0.5}_{-0.4} \times 10^{56}$$

$$3.3^{+0.8}_{-1.6} \times 10^{56}$$

$$3.1^{+0.8}_{-1.8} \times 10^{56}$$

Chirp mass \mathcal{M}

Total mass M

Final black hole mass M_f

Radiated energy E_{rad}

Peak luminosity ℓ_{peak}

Effective inspiral spin parameter χ_{eff}

Final black hole spin a_f

Luminosity distance D_L

Source redshift z

GW170104

$$31.2^{+8.4}_{-6.0} M_\odot$$

$$19.4^{+5.3}_{-5.9} M_\odot$$

$$21.1^{+2.4}_{-2.7} M_\odot$$

$$50.7^{+5.9}_{-5.0} M_\odot$$

$$48.7^{+5.7}_{-4.6} M_\odot$$

$$2.0^{+0.6}_{-0.7} M_\odot c^2$$

$$3.1^{+0.7}_{-1.3} \times 10^{56} \text{ erg s}^{-1}$$

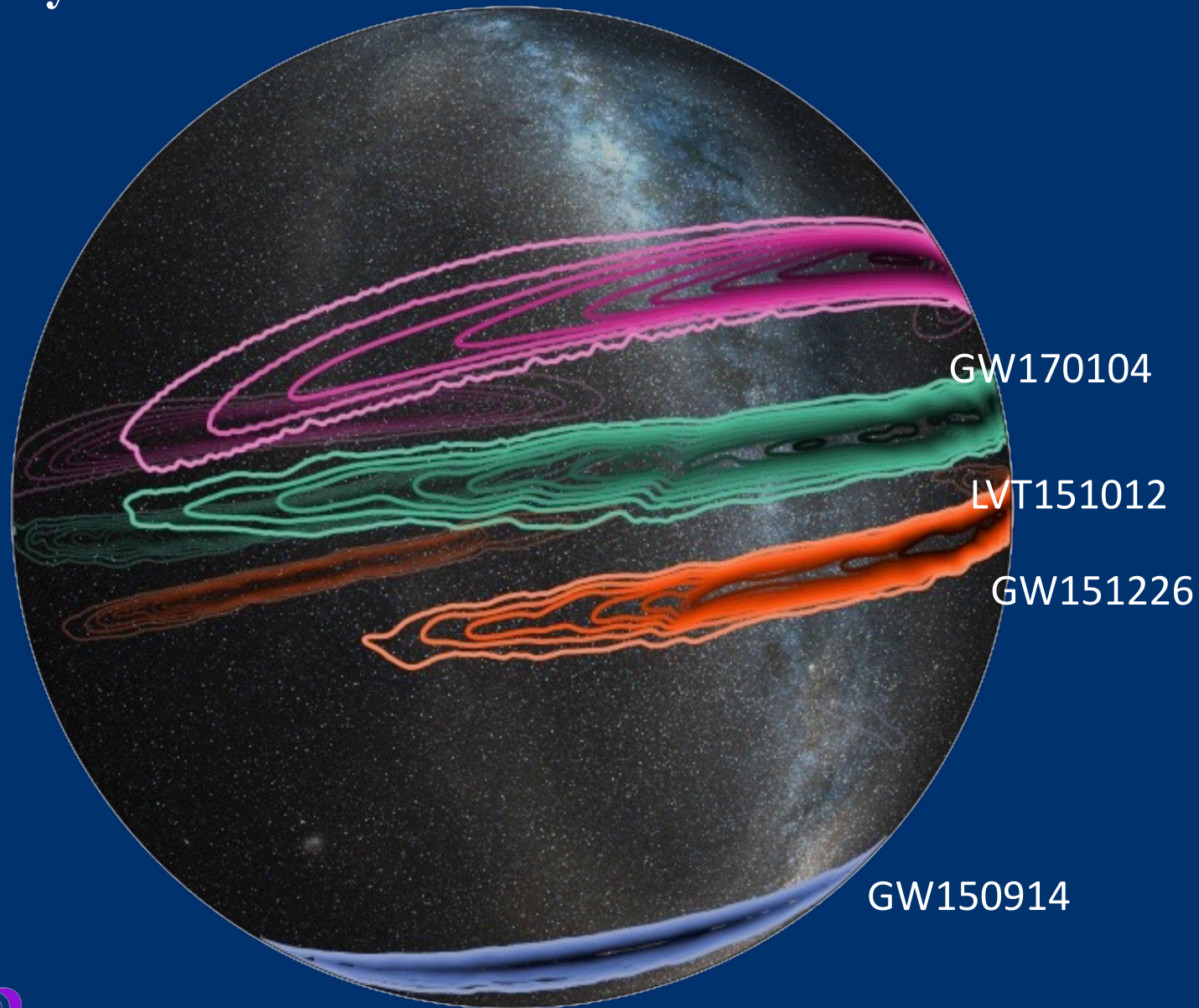
$$-0.12^{+0.21}_{-0.30}$$

$$0.64^{+0.09}_{-0.20}$$

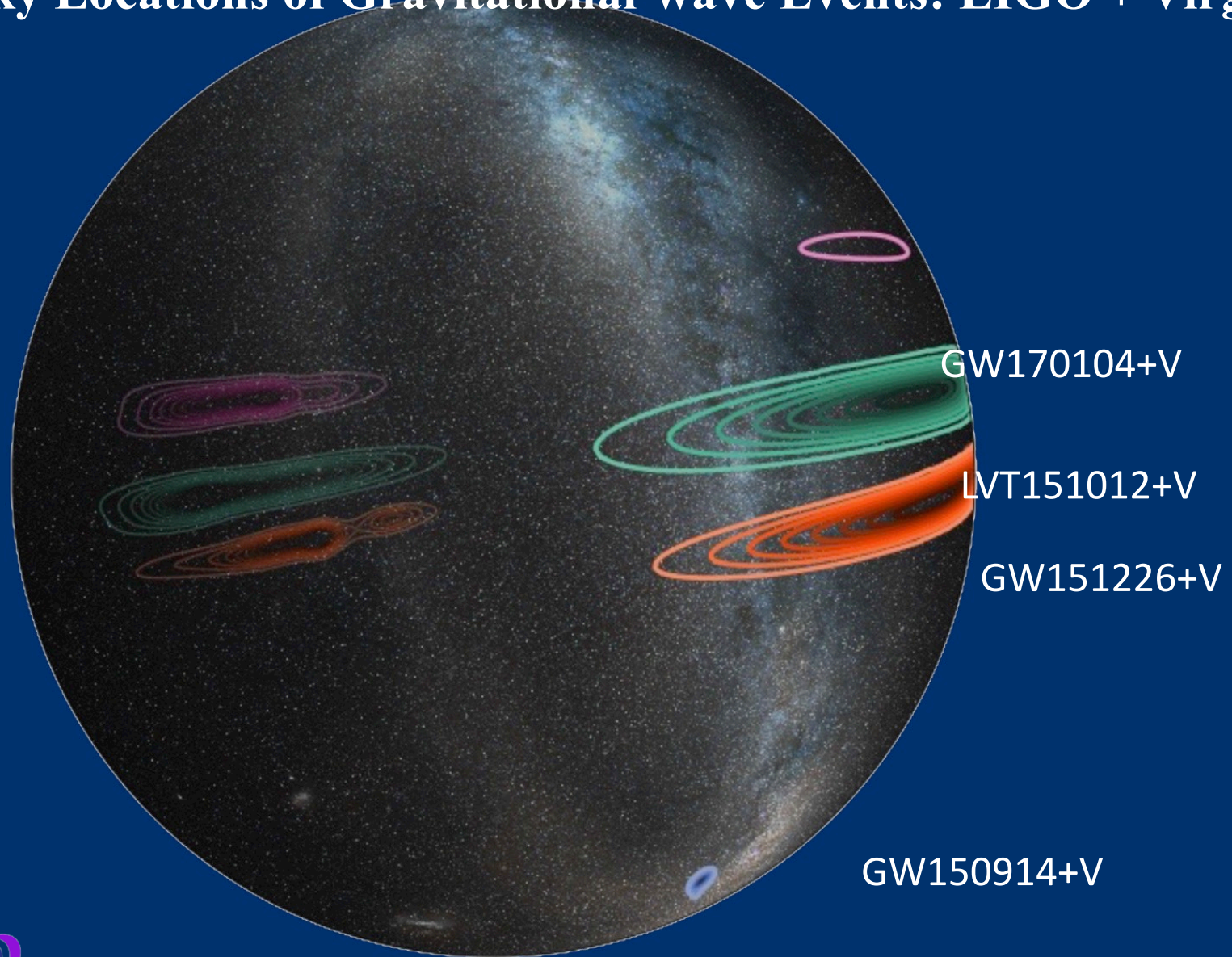
$$880^{+450}_{-390} \text{ Mpc}$$

$$0.18^{+0.08}_{-0.07}$$

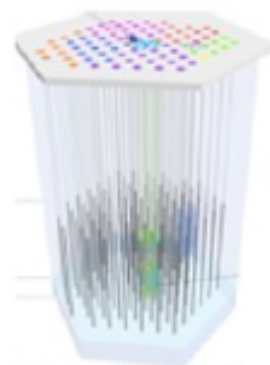
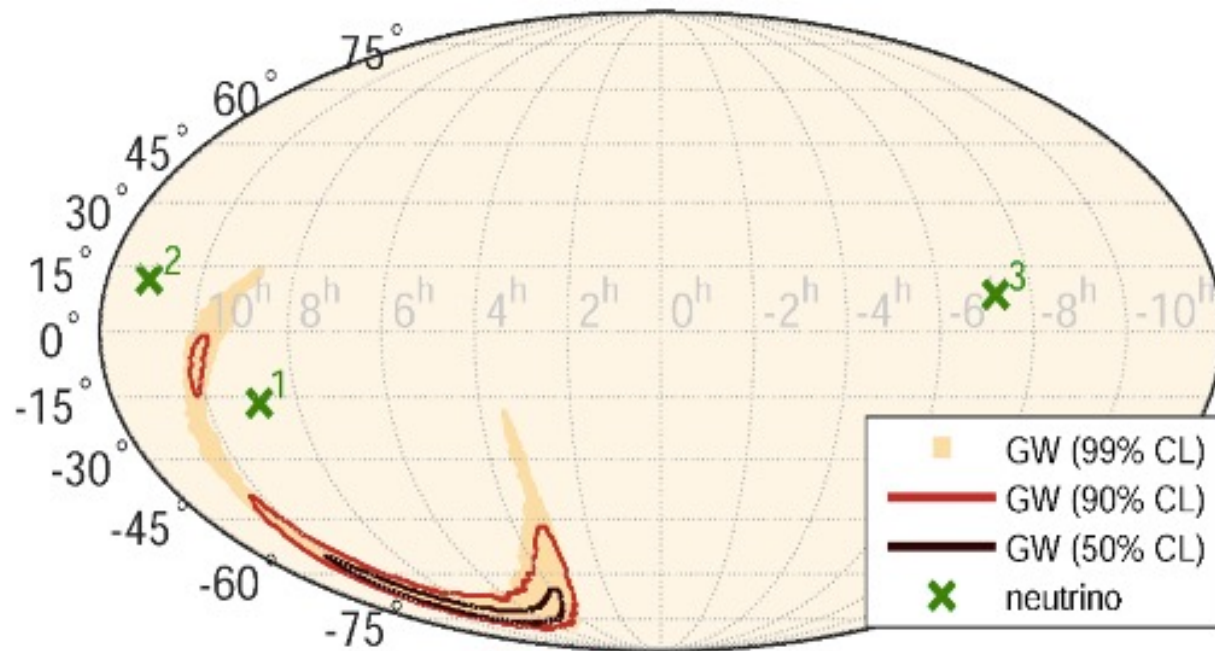
Sky Locations of Gravitational-wave Events: LIGO Only



Sky Locations of Gravitational-wave Events: LIGO + Virgo



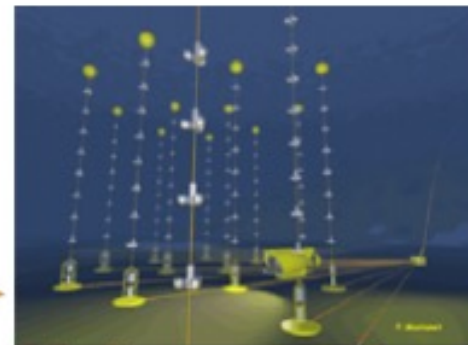
Previous search: GW150914



← IceCube

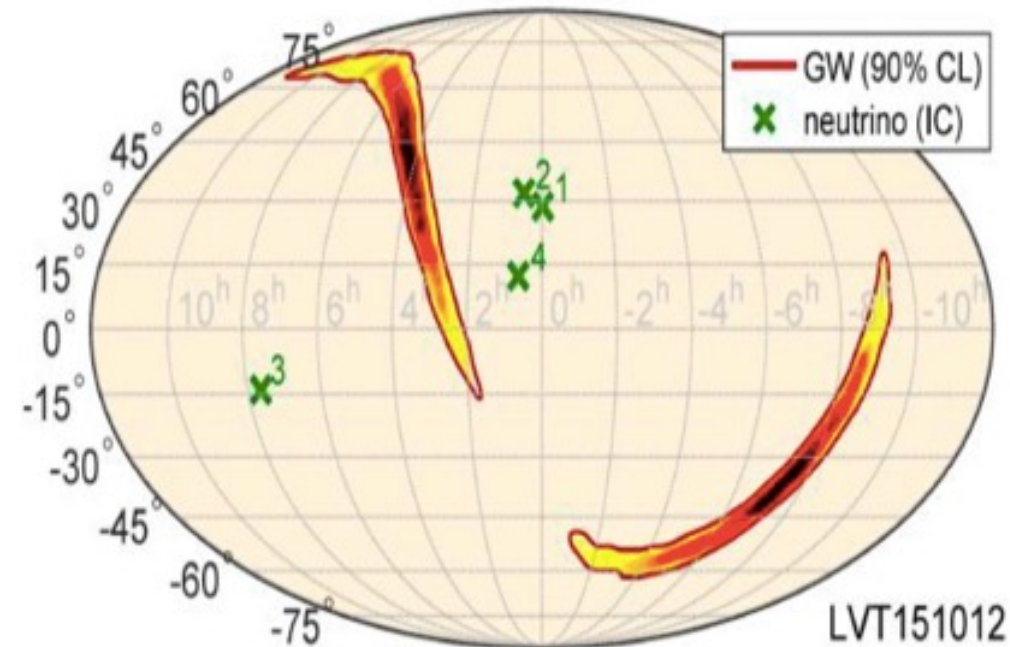
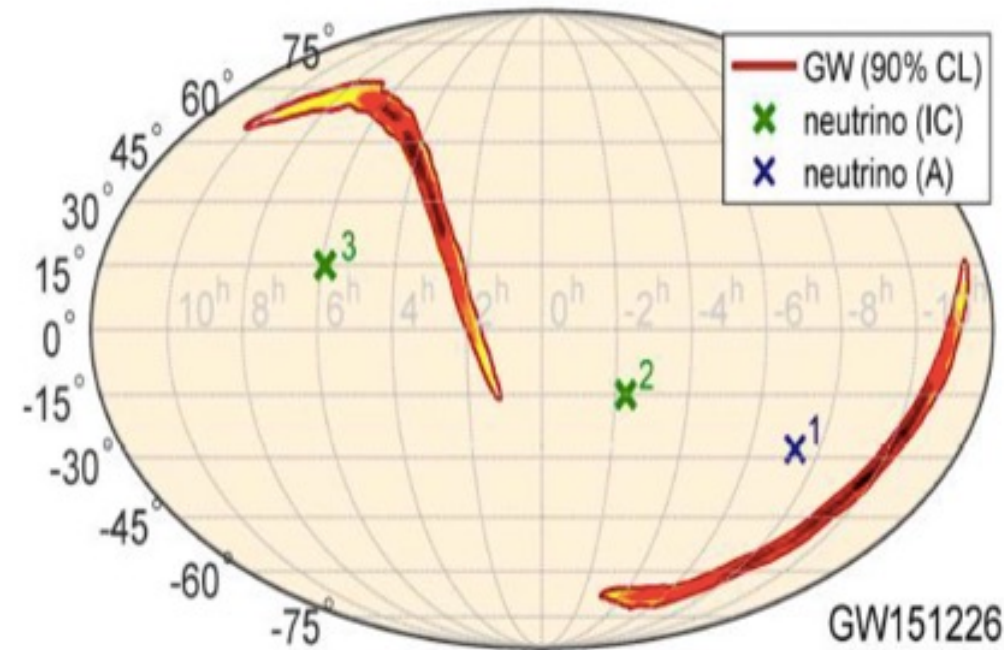
South Pole

ANTARES →



Mediterranean Sea

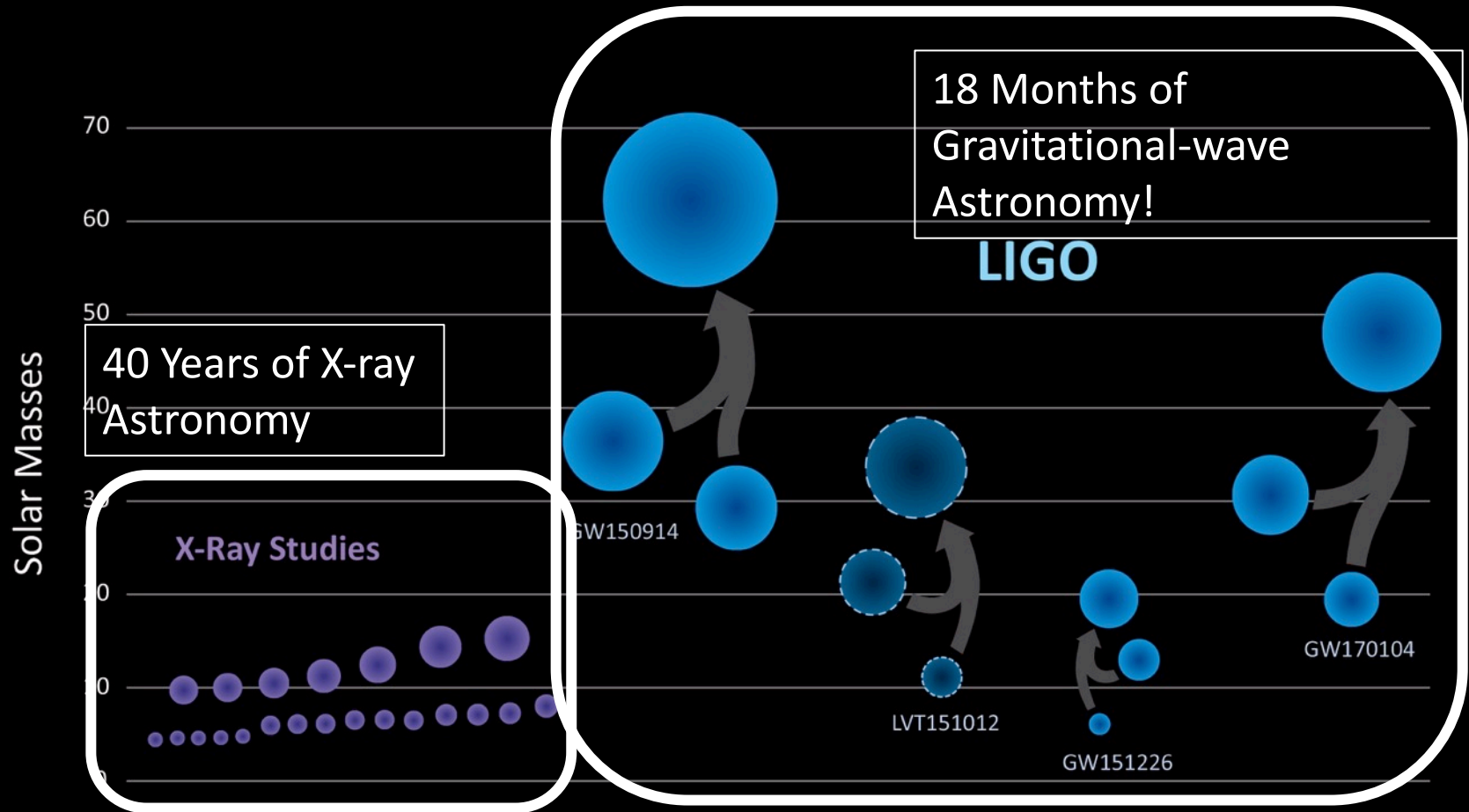
GW151226 & LVT151012



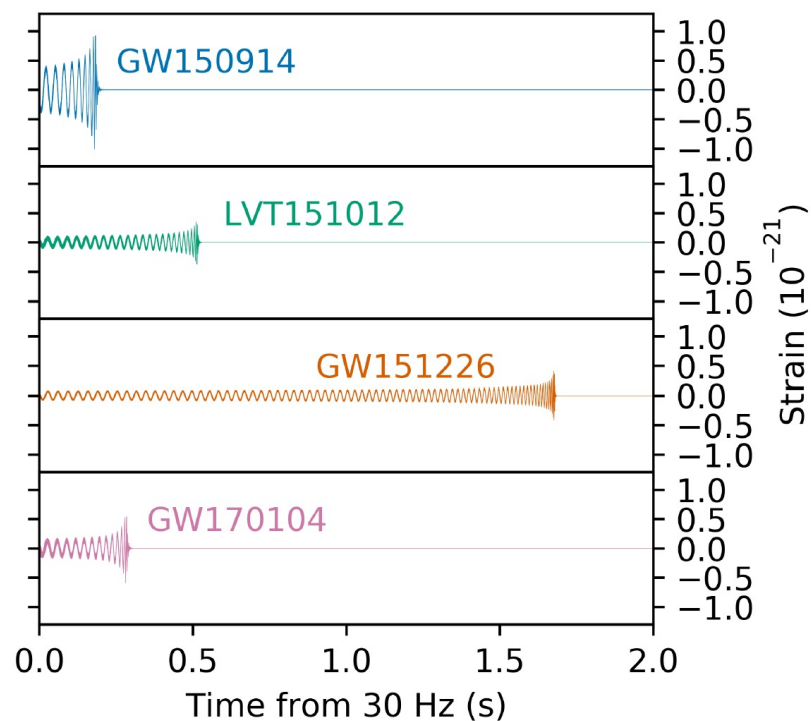
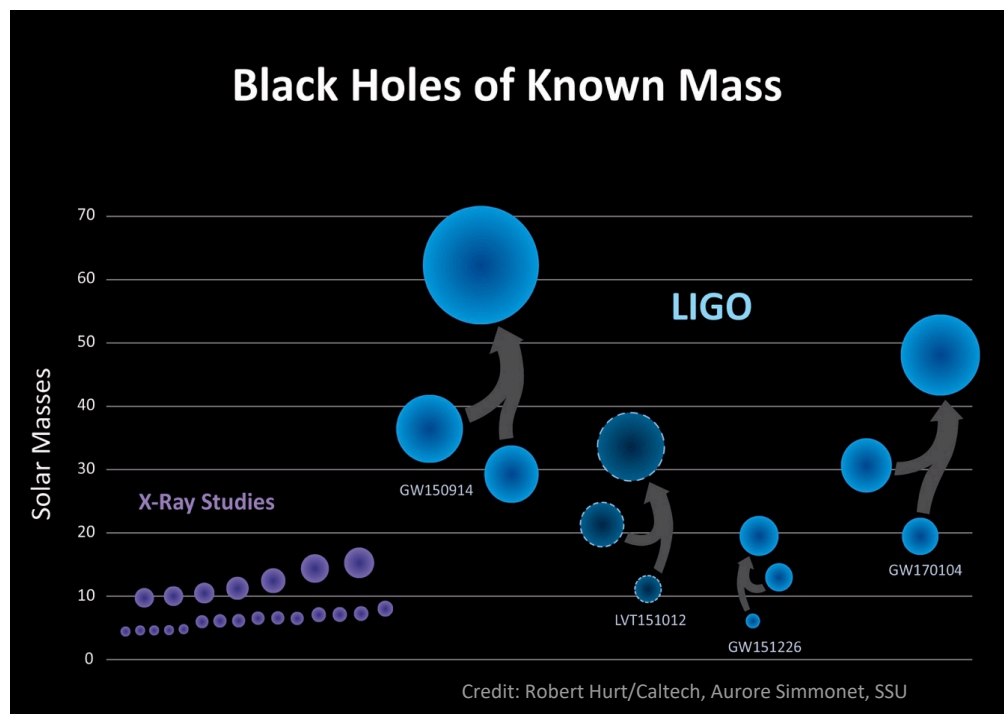
Event	#	Detector	ΔT [s]	RA [h]	Dec [°]	$\sigma_{\mu}^{\text{rec}}$ [°]	E_{μ}^{rec} [TeV]
GW151226	1	ANTARES	-387.3	16.7	-28.0	0.7	9
GW151226	2	IceCube	-290.9	21.7	-15.1	0.1	158
GW151226	3	IceCube	-22.5	5.9	14.9	0.7	6.3
LVT151012	1	IceCube	-423.3	24.0	28.7	3.5	0.38
LVT151012	2	IceCube	-410.0	0.5	32.0	1.1	0.45
LVT151012	3	IceCube	-89.8	7.7	-14.0	0.6	13.7
LVT151012	4	IceCube	147.0	0.6	12.3	0.3	0.35

The Black Hole Mass Menagerie

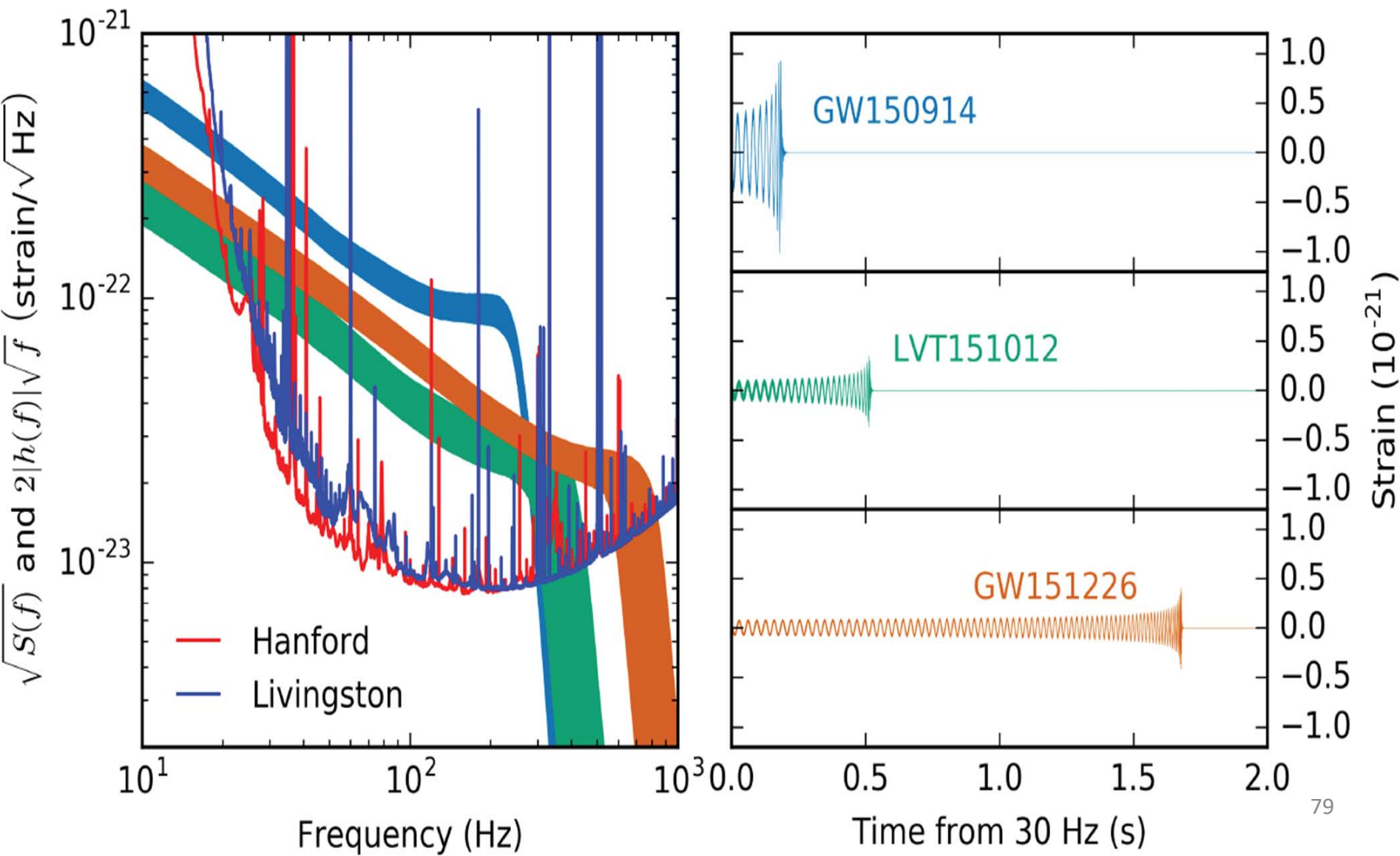
Black Holes of Known Mass



Black Holes Detected By LIGO



Frequency dependence of 3 events in O1 compared to the LIGO sensitivity



[LIGO'S **GRAVITATIONAL-WAVE** DETECTIONS]

[GW150914]

DISCOVERED:

14.09.2015

1.3 BILLION
LIGHT-YEARS
AWAY

62 SOLAR
MASSES

360 KILOMETRES IN
DIAMETER

[GW151226]

DISCOVERED:

26.12.2015

1.4 BILLION
LIGHT-YEARS
AWAY

21 SOLAR
MASSES

120 KILOMETRES IN
DIAMETER

[GW170104]

DISCOVERED:

04.01.2017

3 BILLION
LIGHT-YEARS
AWAY

49 SOLAR
MASSES

270 KILOMETRES IN
DIAMETER

1 BILLION
LIGHT YEARS

2 BILLION
LIGHT YEARS

3 BILLION
LIGHT YEARS

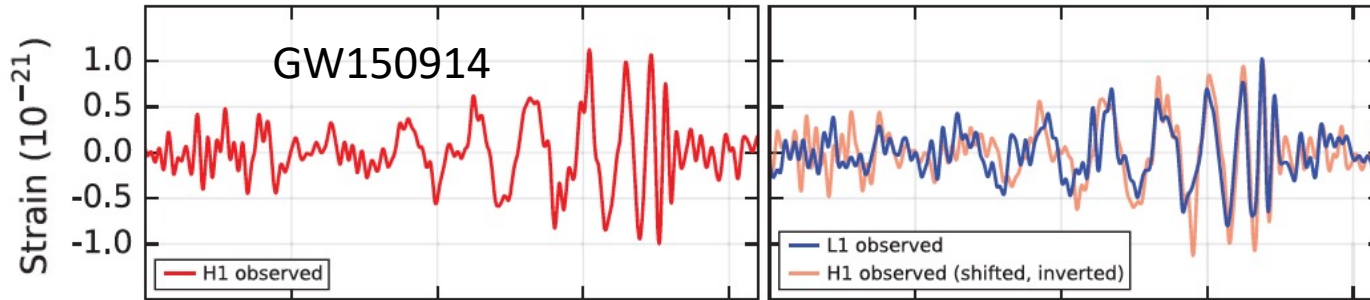
4 BILLION
LIGHT YEARS

YOU ARE
HERE

DID YOU KNOW ?

THE SOLAR MASS is
A STANDARD UNIT OF MASS
IN ASTRONOMY
IT IS EQUAL TO
THE MASS OF THE SUN
EQUAL TO APPROXIMATELY
 1.99×10^{30} KG

Black Holes Detected By LIGO



PRL **116**, 061102 (2016) **PHYSICAL REVIEW LETTERS** week ending 12 FEBRUARY 2016



Observation of Gravitational Waves from a Binary Black Hole Merger

B. P. Abbott *et al.**

(LIGO Scientific Collaboration and Virgo Collaboration)
(Received 21 January 2016; published 11 February 2016)

PRL **116**, 241103 (2016) **PHYSICAL REVIEW LETTERS** week ending 17 JUNE 2016



GW151226: Observation of Gravitational Waves from a 22-Solar-Mass Binary Black Hole Coalescence

B. P. Abbott *et al.**

(LIGO Scientific Collaboration and Virgo Collaboration)
(Received 31 May 2016; published 15 June 2016)

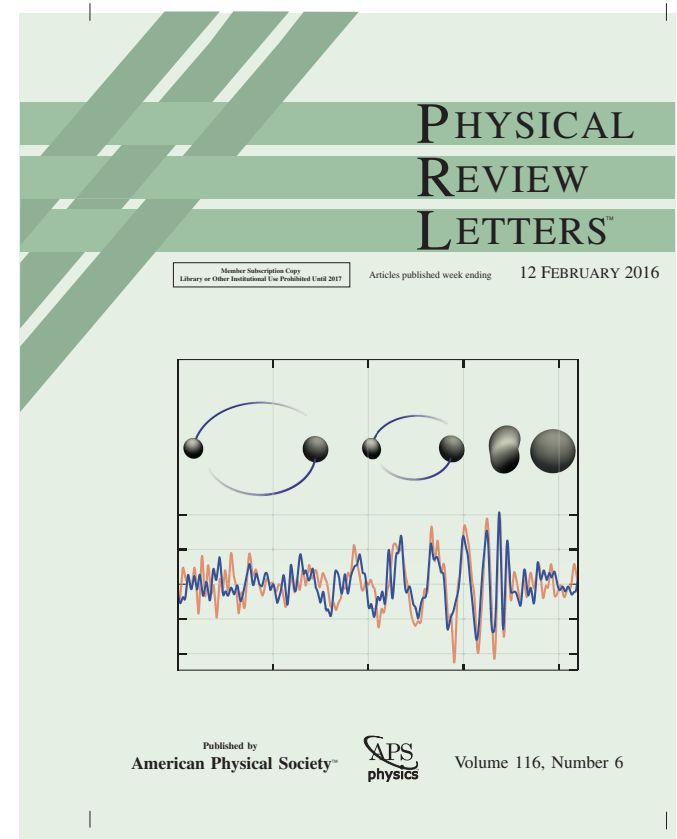
PRL **118**, 221101 (2017) **PHYSICAL REVIEW LETTERS** week ending 2 JUNE 2017



GW170104: Observation of a 50-Solar-Mass Binary Black Hole Coalescence at Redshift 0.2

B. P. Abbott *et al.**

(LIGO Scientific and Virgo Collaboration)
(Received 9 May 2017; published 1 June 2017)



Published by
American Physical Society™



Volume 116, Number 6

"For the greatest benefit to mankind"
Alfred Nobel



The Royal Swedish Academy of Sciences has decided to award the

2017 NOBEL PRIZE IN PHYSICS



Rainer Weiss
Barry C. Barish
Kip S. Thorne

"for decisive contributions to the LIGO detector and the observation of gravitational waves"

 Nobelprize.org



The 2017 winners of the @NobelPrize in Physics: @LIGO pioneers Rai Weiss, Kip Thorne and Barry Barish. Watch their lectures online at youtube.com/watch?v=scVyxV...

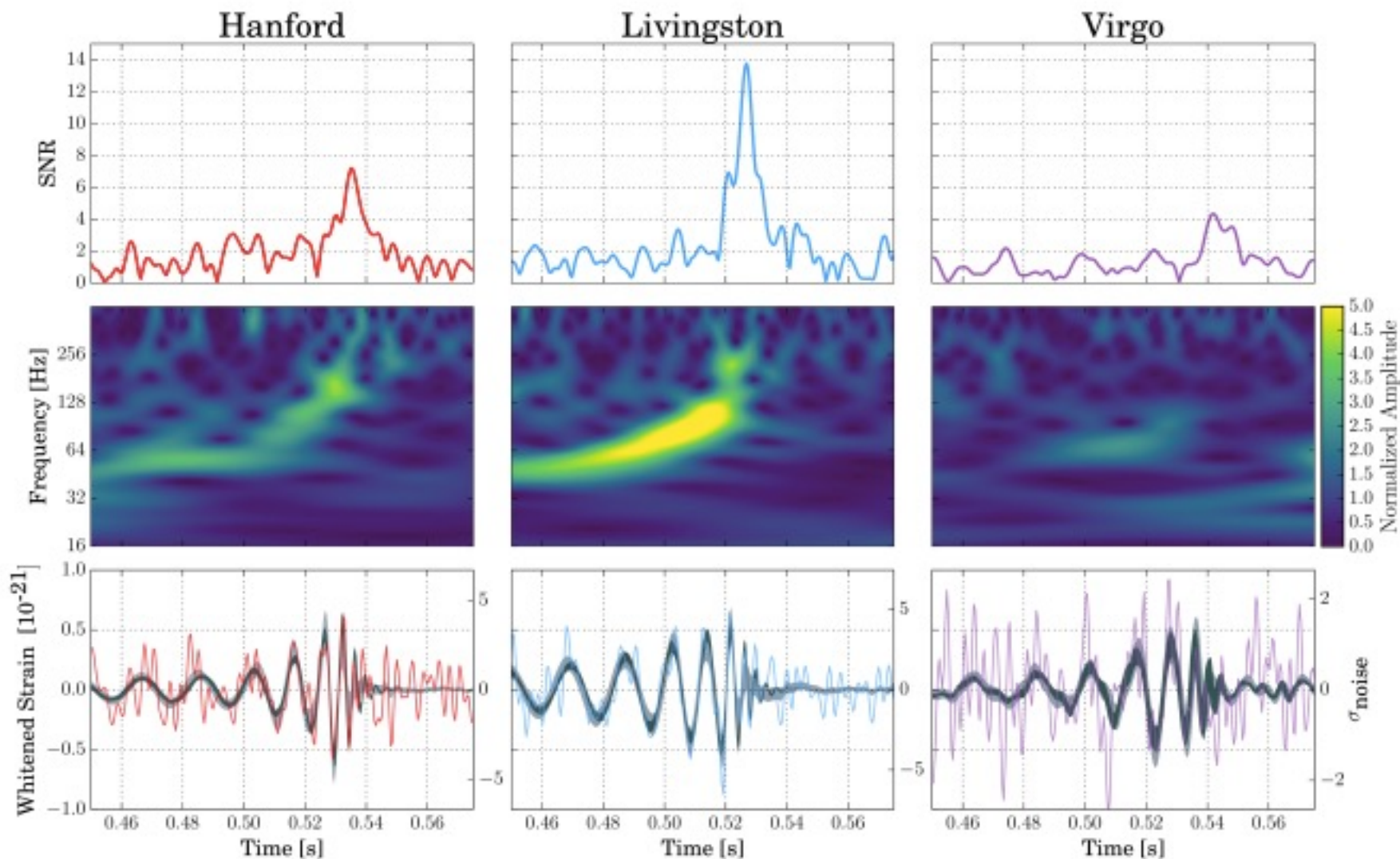


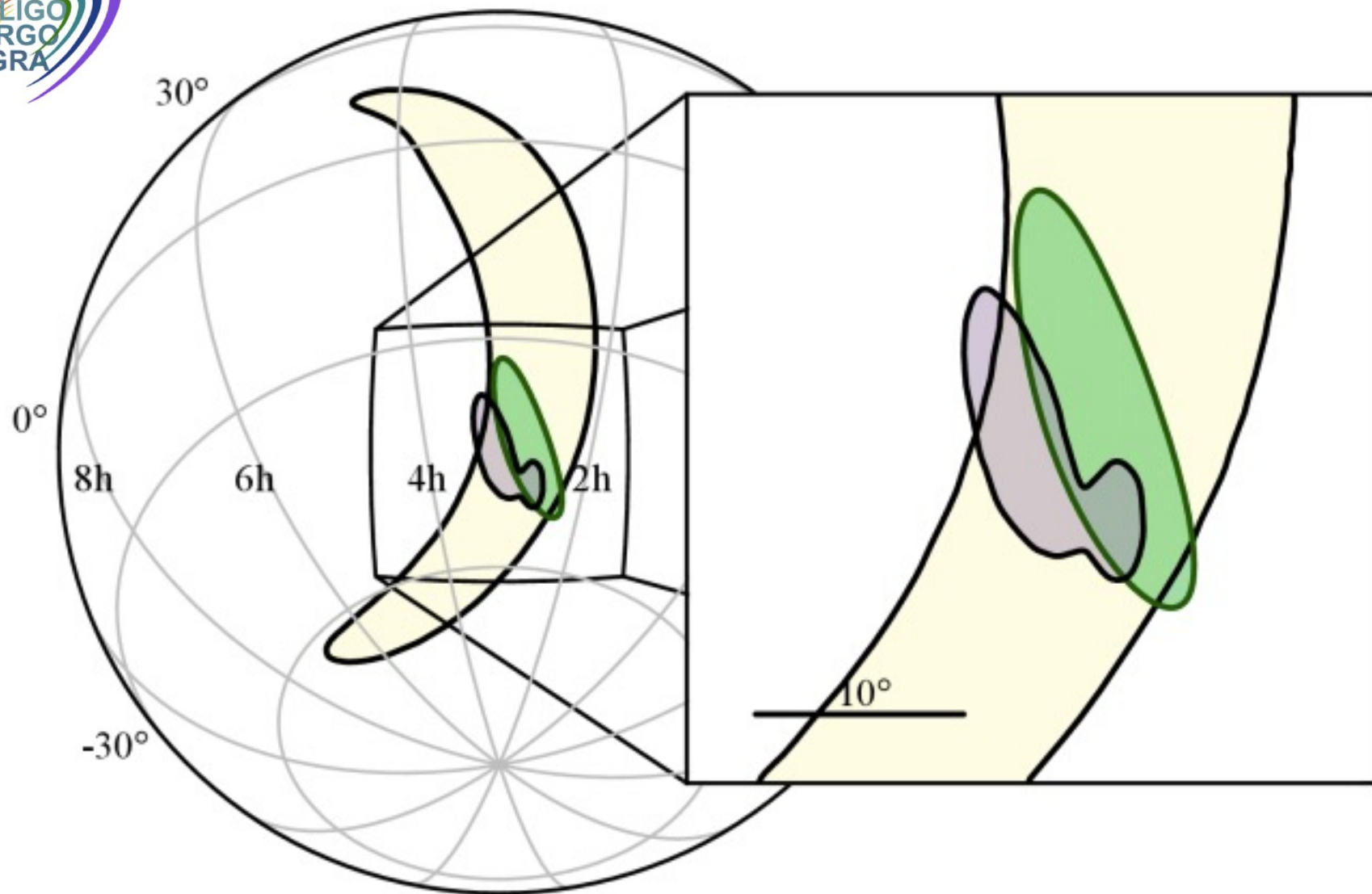
12:26 PM - 8 Dec 2017

92 Retweets 208 Likes

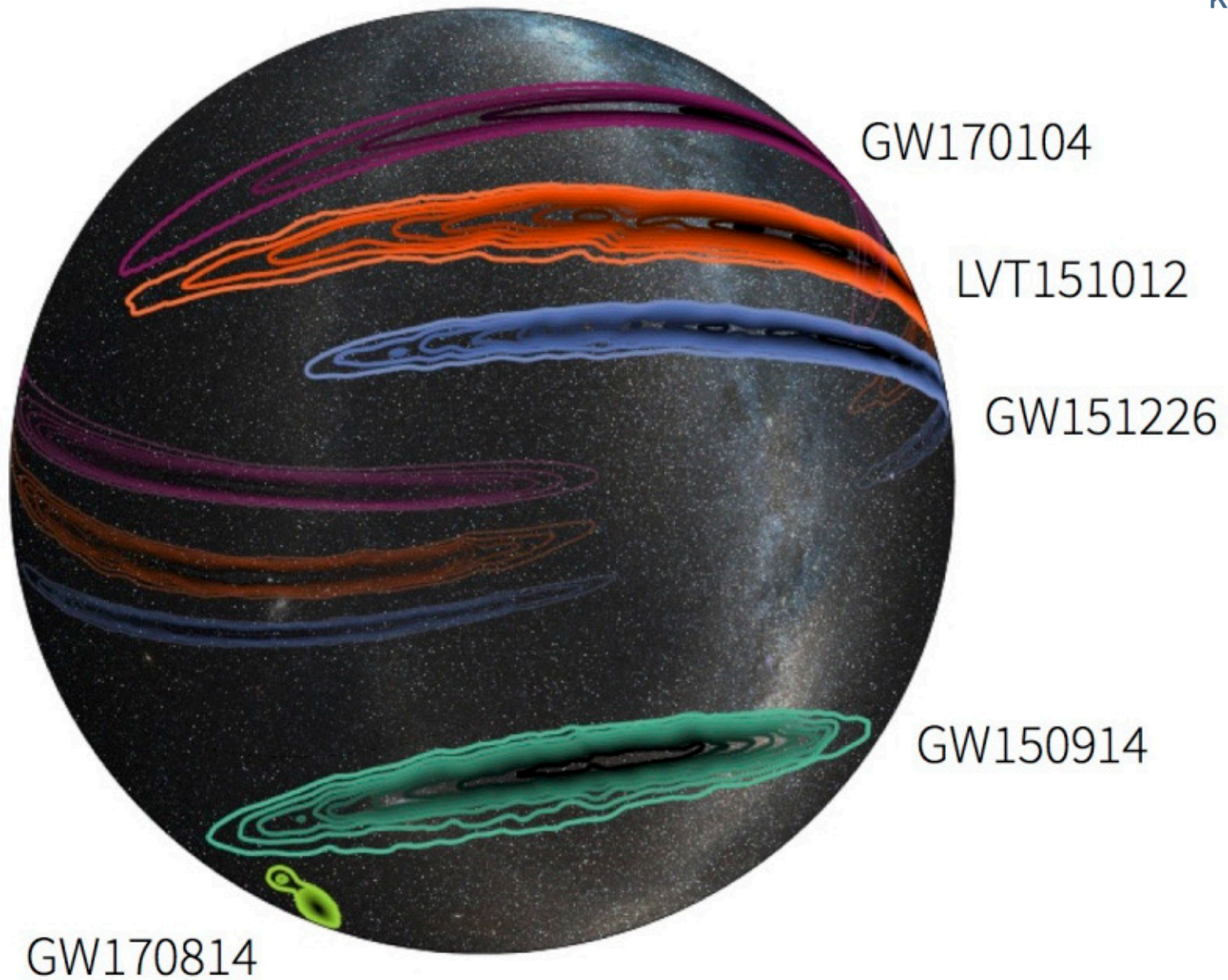
4 92 208

GW170814: First three-detector signal

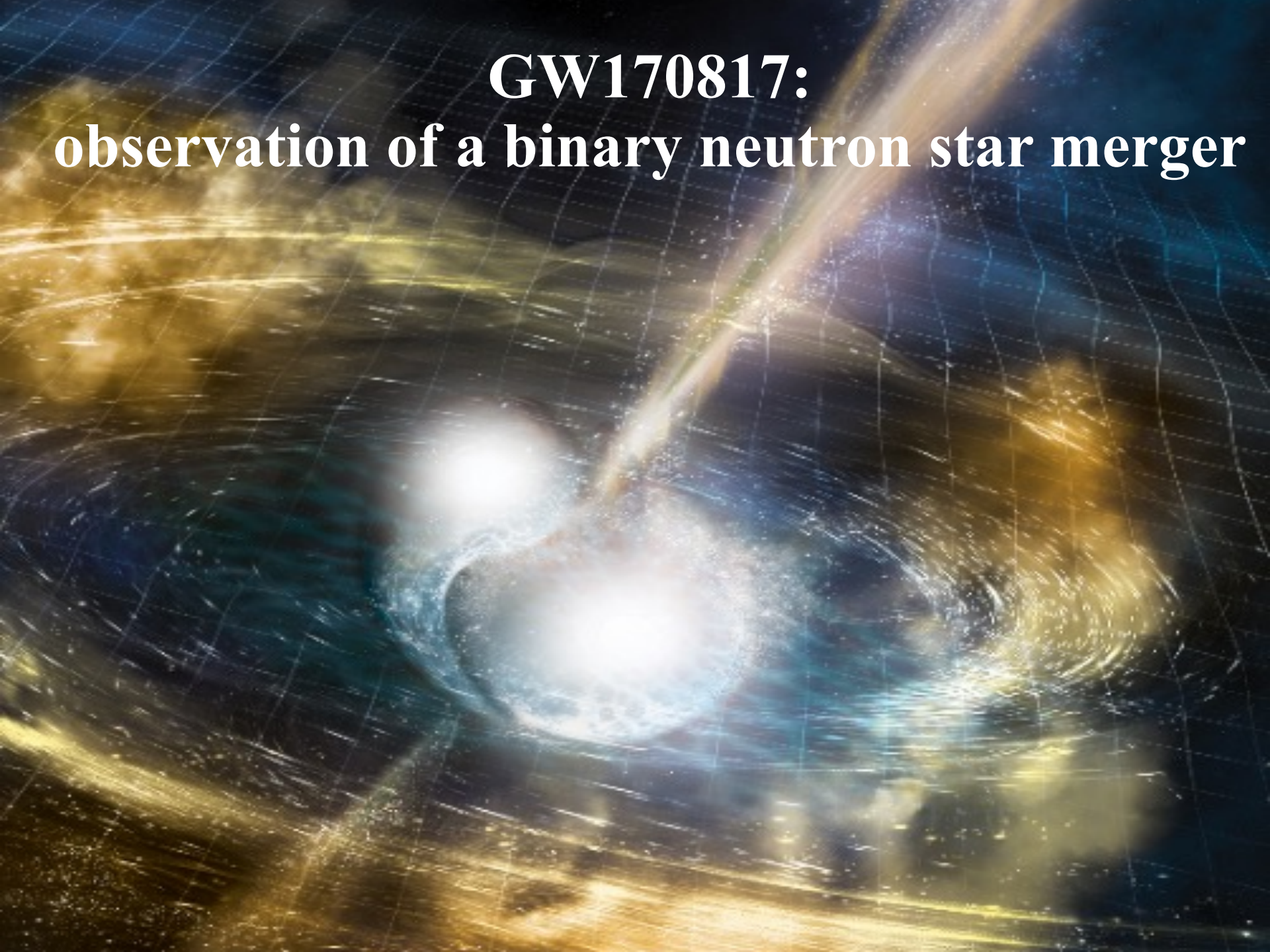




If we only had the two LIGO detectors, we'd have an uncertainty on the source's sky position of over 1000 square degrees (yellow), but adding in Virgo, we get this down to 60 square degrees (green). The purple map is the final localization from our full parameter estimation analysis. That's still pretty large by astronomical standards (the full Moon is about a quarter of a square degree), but a fantastic improvement!



GW170817: observation of a binary neutron star merger



GW170817: observation of a binary neutron star merger

FIRST COSMIC EVENT OBSERVED IN GRAVITATIONAL WAVES AND LIGHT

Colliding Neutron Stars Mark New Beginning of Discoveries

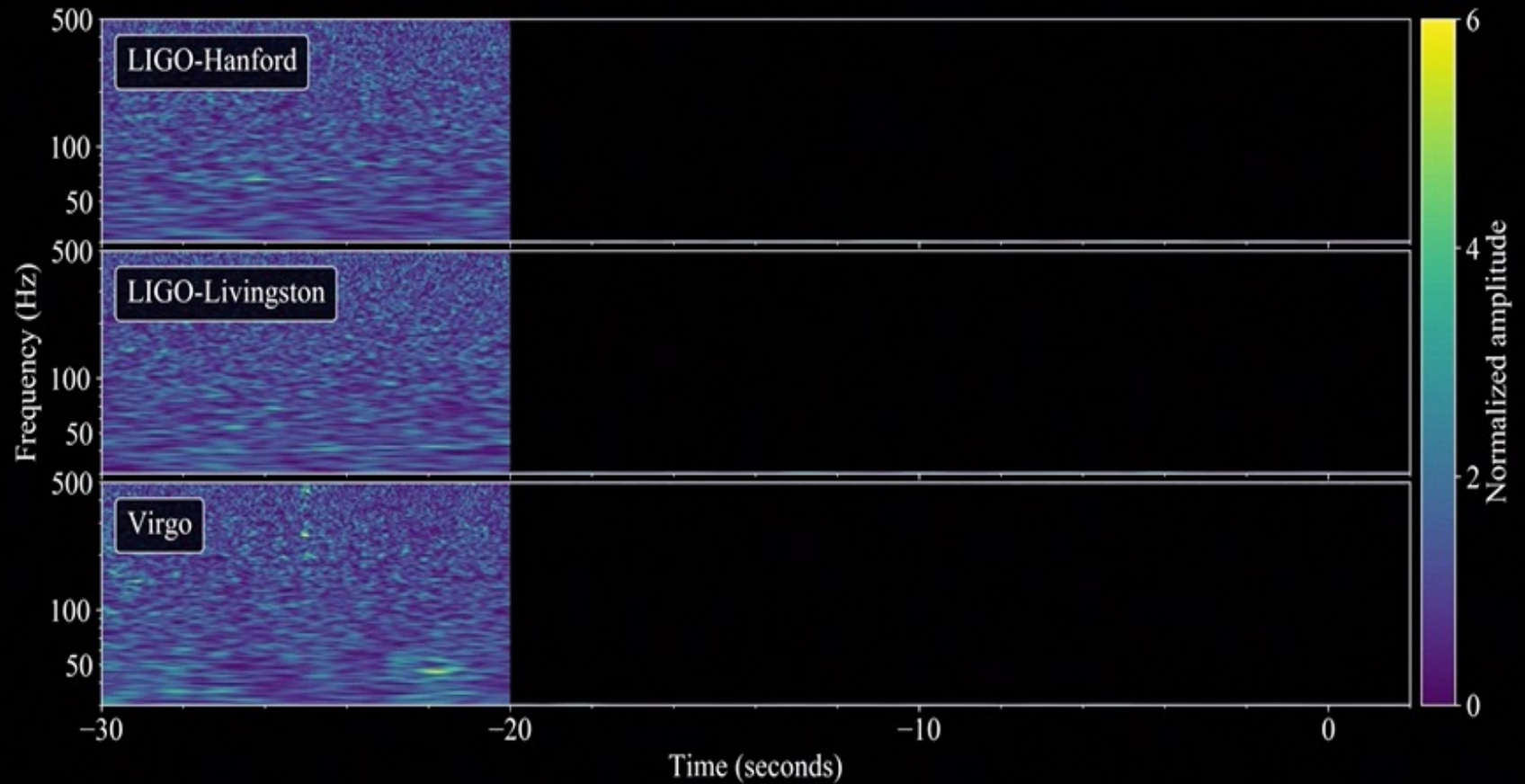
Collision creates light across the entire electromagnetic spectrum. Joint observations independently confirm Einstein's General Theory of Relativity, help measure the age of the Universe, and provide clues to the origins of heavy elements like gold and platinum

Gravitational wave lasted over 100 seconds

On August 17, 2017, 12:41 UTC, LIGO (US) and Virgo (Europe) detect gravitational waves from the merger of two neutron stars, each around 1.5 times the mass of our Sun. This is the first detection of spacetime ripples from neutron stars.

Within two seconds, NASA's Fermi Gamma-ray Space Telescope detects a short gamma-ray burst from a region of the sky overlapping the LIGO/Virgo position. Optical telescope observations pinpoint the origin of this signal to NGC 4993, a galaxy located 130 million light years distant.

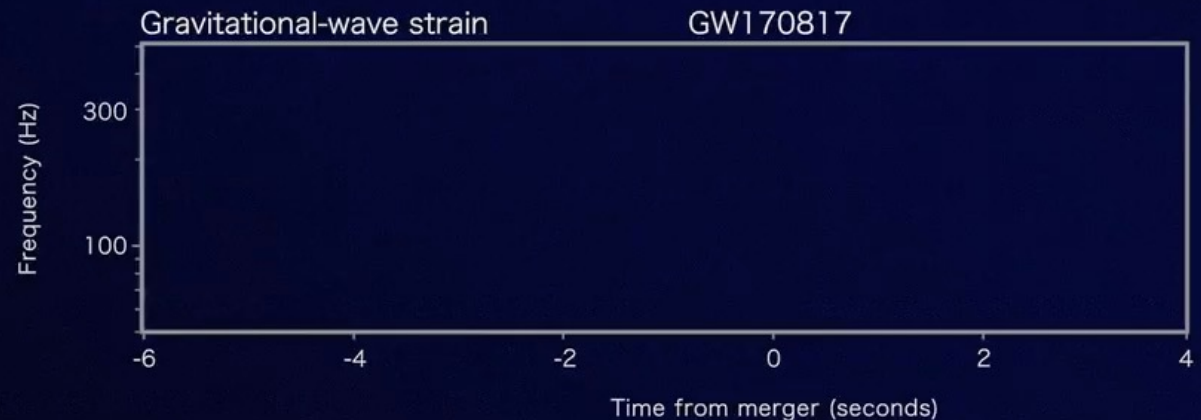
GW170817



Fermi detected a short gamma ray burst in coincidence with GW170817

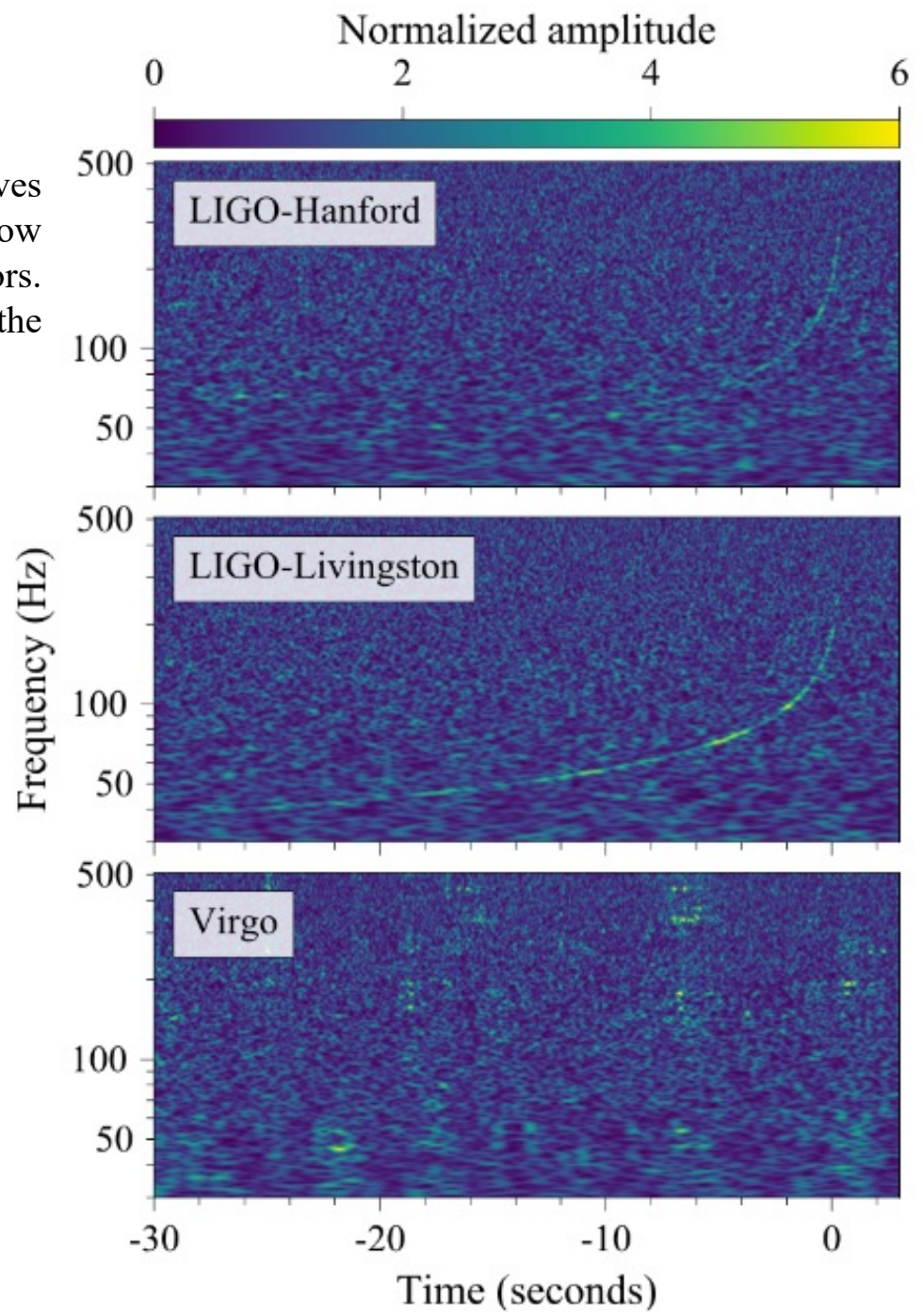
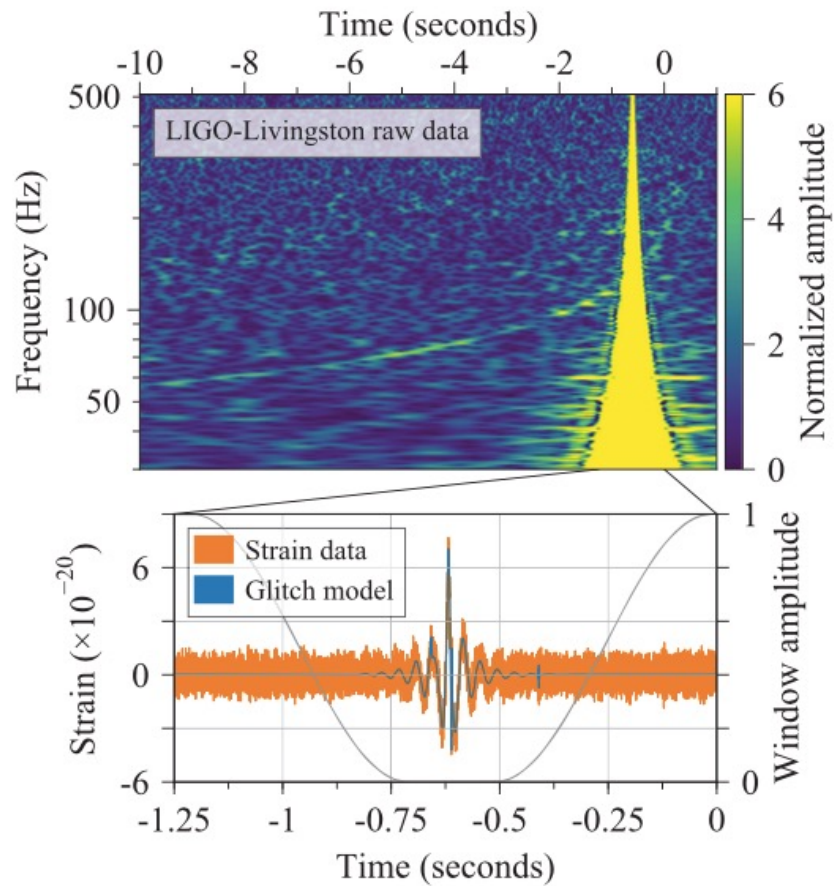


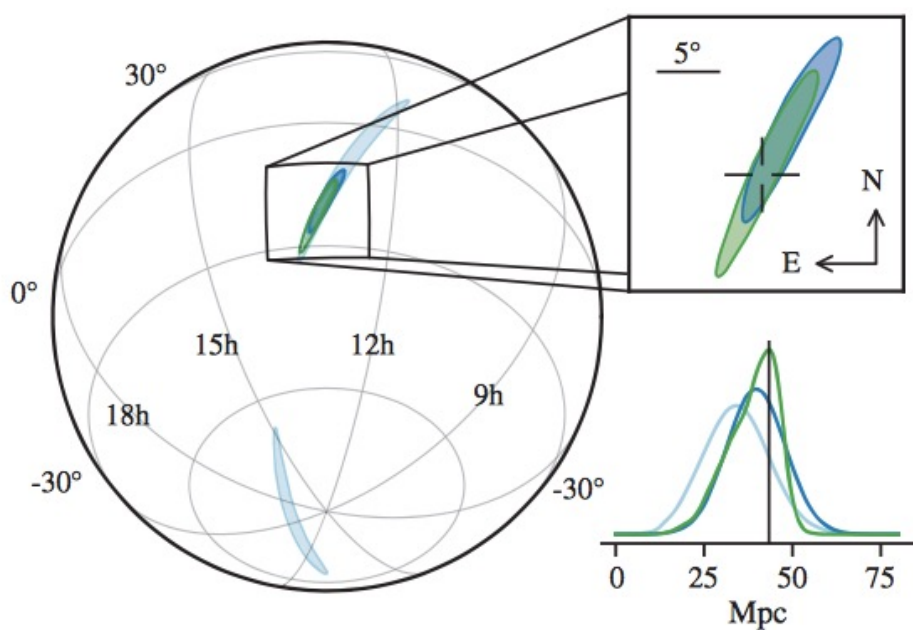
LIGO





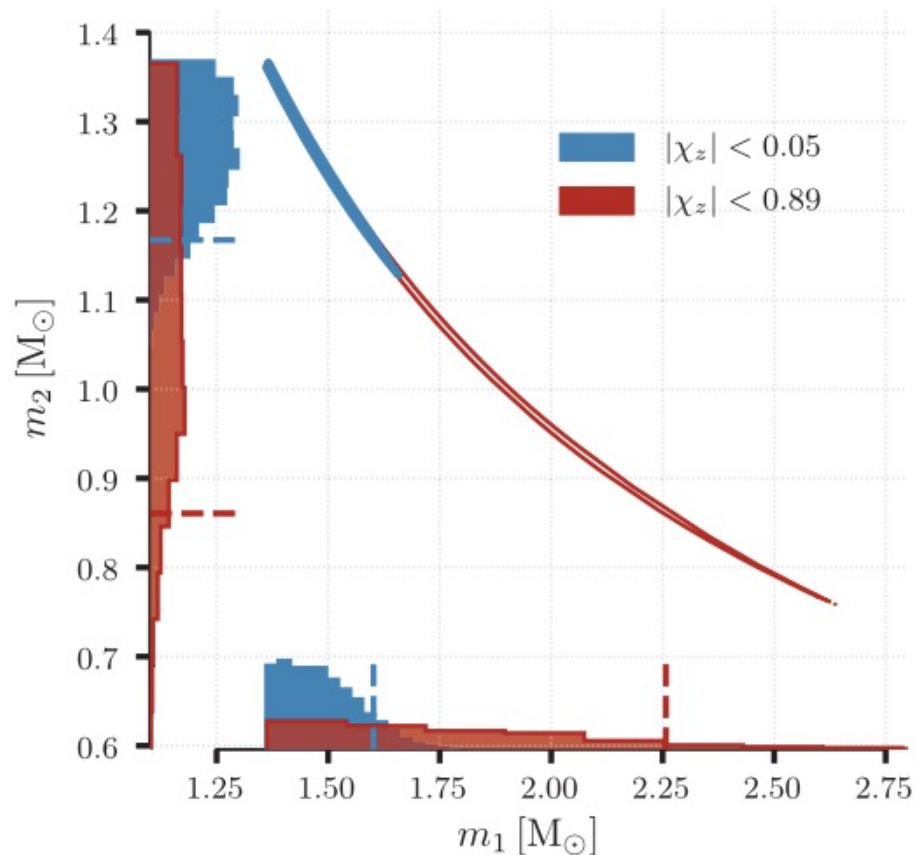
Shown here is a spectrogram of the gravitational waves as seen in the LIGO-Livingston detector. Here we show the spectrograms from all three LIGO-Virgo detectors. You can see the characteristic "chirp", when the frequency increases, of a binary merger.





Sky location reconstructed for GW170817 by a rapid localization algorithm from a Hanford-Livingston (190 deg^2 , light blue contours) and Hanford-Livingston-Virgo (31 deg^2 , dark blue contours) analysis. A higher latency Hanford-Livingston-Virgo analysis improved the localization (**28 deg^2** , green contours). In the top-right inset panel, the reticle marks the position of the apparent host galaxy NGC 4993.

Two dimensional posterior distribution for the component masses m_1 and m_2 in the rest frame of the source for the low-spin scenario ($|\chi| < 0.05$, blue) and the high-spin scenario ($|\chi| < 0.89$, red). The colored contours enclose 90% of the probability from the joint posterior probability density function for m_1 and m_2 .



GW170817: observation of a binary neutron star merger

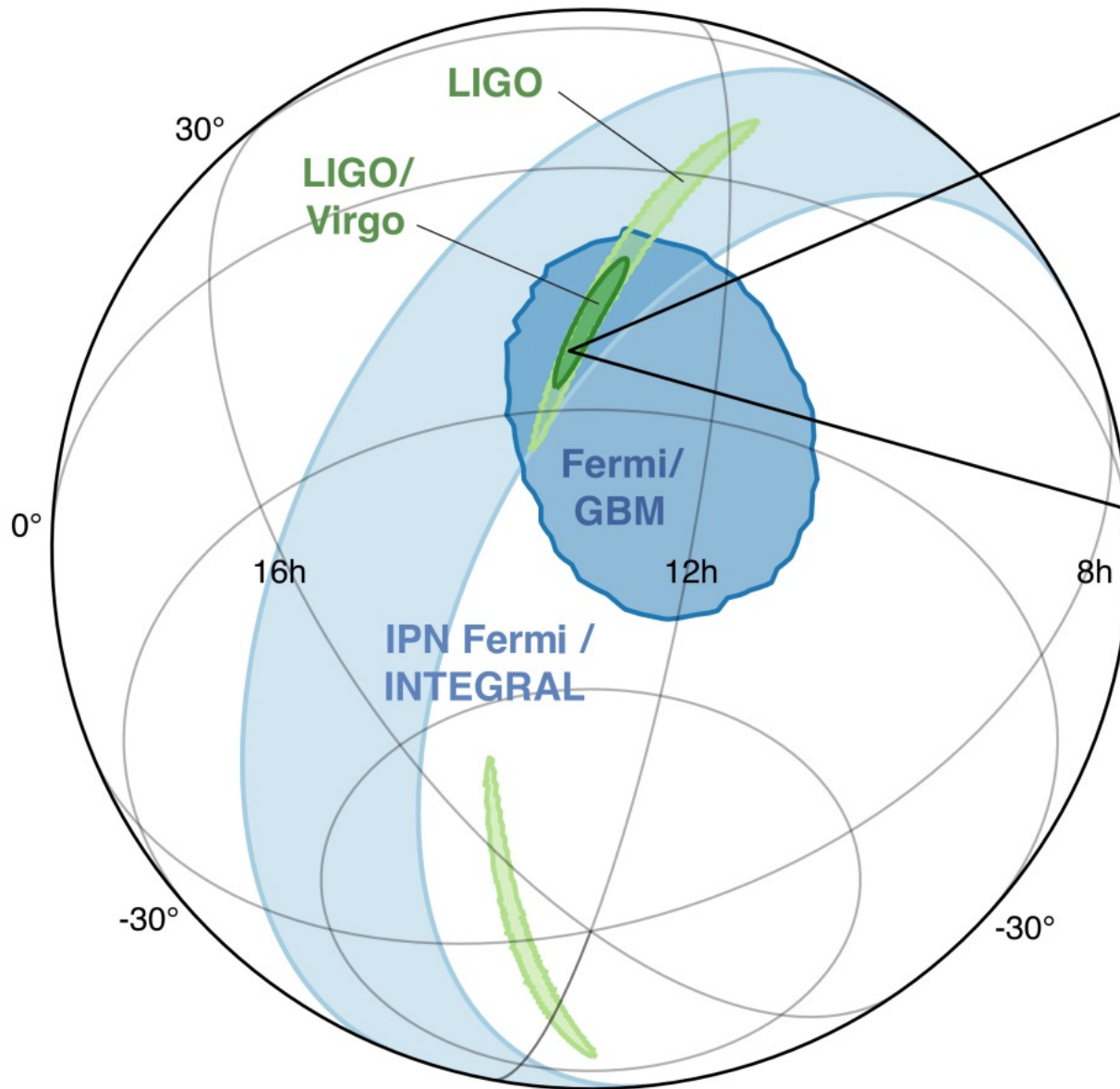
PRL **119**, 161101 (2017)

PHYSICAL REVIEW LETTERS

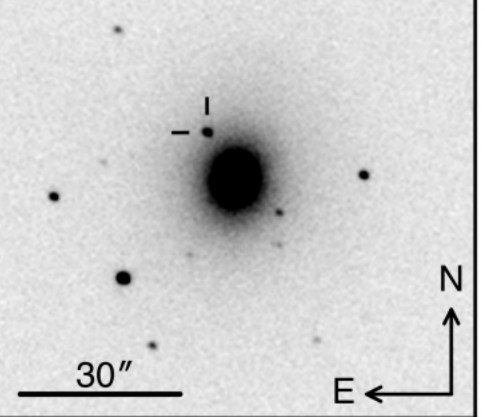
week ending
20 OCTOBER 2017

TABLE I. Source properties for GW170817: we give ranges encompassing the 90% credible intervals for different assumptions of the waveform model to bound systematic uncertainty. The mass values are quoted in the frame of the source, accounting for uncertainty in the source redshift.

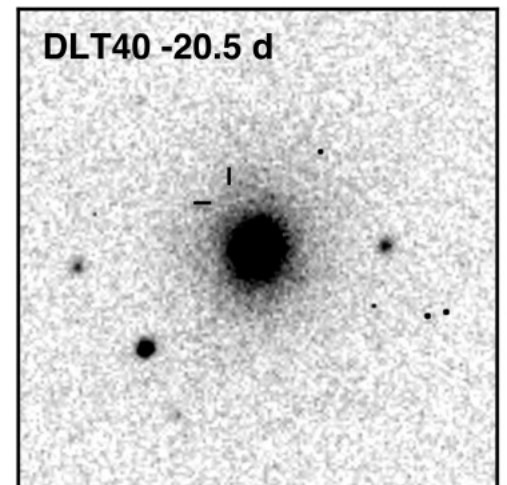
	Low-spin priors ($ \chi \leq 0.05$)	High-spin priors ($ \chi \leq 0.89$)
Primary mass m_1	1.36–1.60 M_\odot	1.36–2.26 M_\odot
Secondary mass m_2	1.17–1.36 M_\odot	0.86–1.36 M_\odot
Chirp mass \mathcal{M}	$1.188^{+0.004}_{-0.002} M_\odot$	$1.188^{+0.004}_{-0.002} M_\odot$
Mass ratio m_2/m_1	0.7–1.0	0.4–1.0
Total mass m_{tot}	$2.74^{+0.04}_{-0.01} M_\odot$	$2.82^{+0.47}_{-0.09} M_\odot$
Radiated energy E_{rad}	$> 0.025 M_\odot c^2$	$> 0.025 M_\odot c^2$
Luminosity distance D_L	40^{+8}_{-14} Mpc	40^{+8}_{-14} Mpc
Viewing angle Θ	$\leq 55^\circ$	$\leq 56^\circ$
Using NGC 4993 location	$\leq 28^\circ$	$\leq 28^\circ$
Combined dimensionless tidal deformability $\tilde{\Lambda}$	≤ 800	≤ 700
Dimensionless tidal deformability $\Lambda(1.4M_\odot)$	≤ 800	≤ 1400

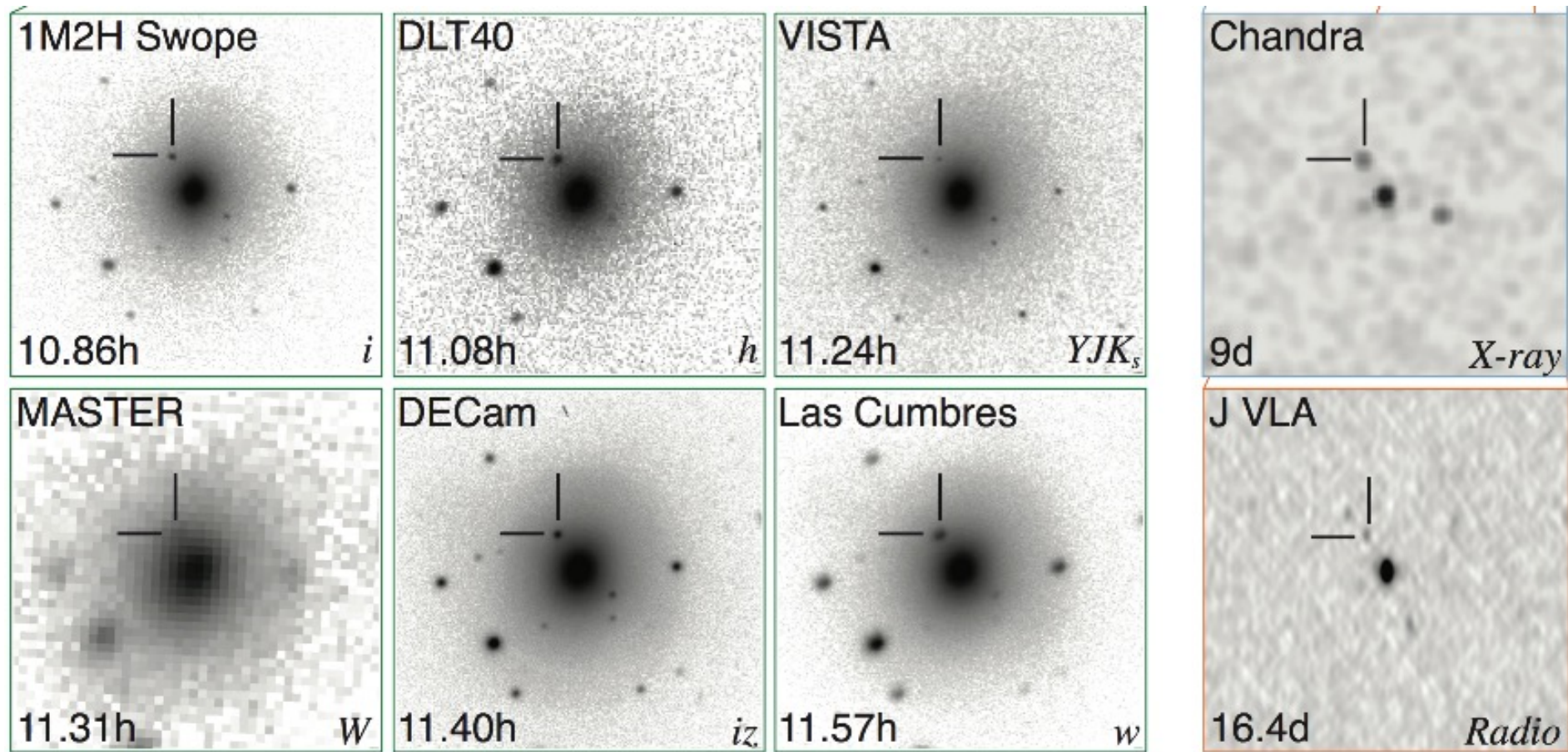


Swope +10.9 h



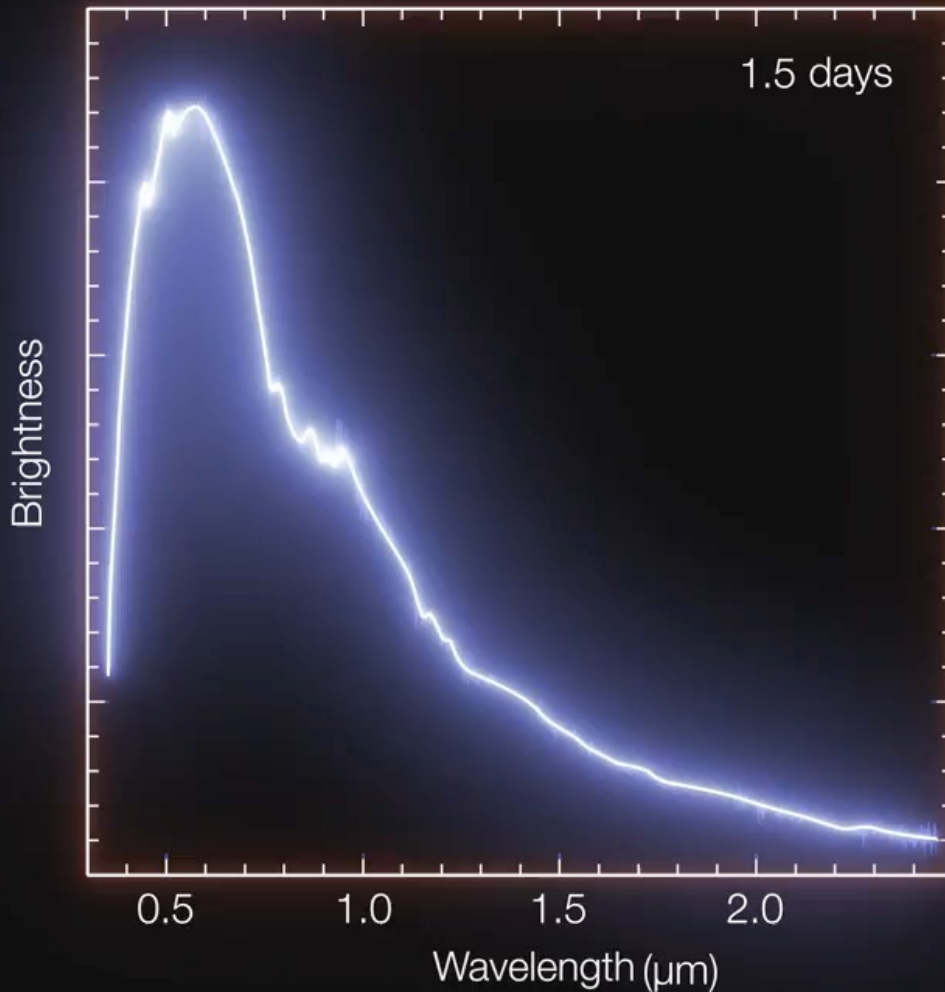
DLT40 -20.5 d





Shown here are 8 images of the aftermath of the BNS merger (designated SSS17a/AT2017gfo). On the left are six optical images taken between 10 and 12 hours after the merger by different telescopes. On the right are images constructed from x-ray and radio observations. The x-ray image was taken 9 days after the merger by NASA's [Chandra X-ray Observatory](#). 16 days after the merger NRAO's [Jansky Very Large Array \(VLA\)](#) captured the radio image. In all 8 images the galaxy NGC 4993 is seen in the middle and SSS17a/AT2017gfo is marked by two lines.

Brightness of the kilonova



For the first time, it was observed an ultraviolet, optical, and infrared transient (known as a kilonova), due to the radioactive decay of heavy elements formed by neutron capture.

This observation firmly connects kilonovae with the BNS merger, providing evidence supporting the idea that kilonovae result from the radioactive decay of the heavy elements formed by neutron capture during a BNS merger.

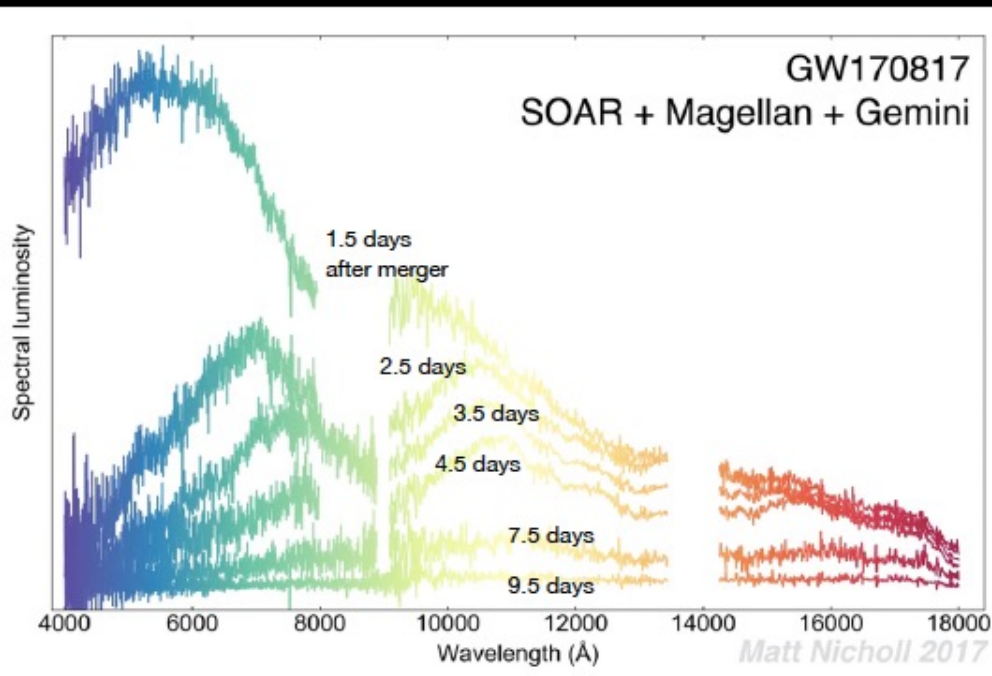
Kilonova

SSS17a

August 17, 2017

August 21, 2017

Swope & Magellan Telescopes



Element Origins

Jennifer Johnson/SDSS, CC BY

1 H																	2 He																	
3 Li	4 Be																	5 B	6 C	7 N	8 O	9 F	10 Ne											
11 Na	12 Mg																	13 Al	14 Si	15 P	16 S	17 Cl	18 Ar											
19 K	20 Ca	21 Sc	22 Ti	23 V	24 Cr	25 Mn	26 Fe	27 Co	28 Ni	29 Cu	30 Zn	31 Ga	32 Ge	33 As	34 Se	35 Br	36 Kr																	
37 Rb	38 Sr	39 Y	40 Zr	41 Nb	42 Mo	43 Tc	44 Ru	45 Rh	46 Pd	47 Ag	48 Cd	49 In	50 Sn	51 Sb	52 Te	53 I	54 Xe																	
55 Cs	56 Ba			72 Hf	73 Ta	74 W	75 Re	76 Os	77 Ir	78 Pt	79 Au	80 Hg	81 Tl	82 Pb	83 Bi	84 Po	85 At	86 Rn																
87 Fr	88 Ra																																	
																		57 La	58 Ce	59 Pr	60 Nd	61 Pm	62 Sm	63 Eu	64 Gd	65 Tb	66 Dy	67 Ho	68 Er	69 Tm	70 Yb	71 Lu		
																		89 Ac	90 Th	91 Pa	92 U													

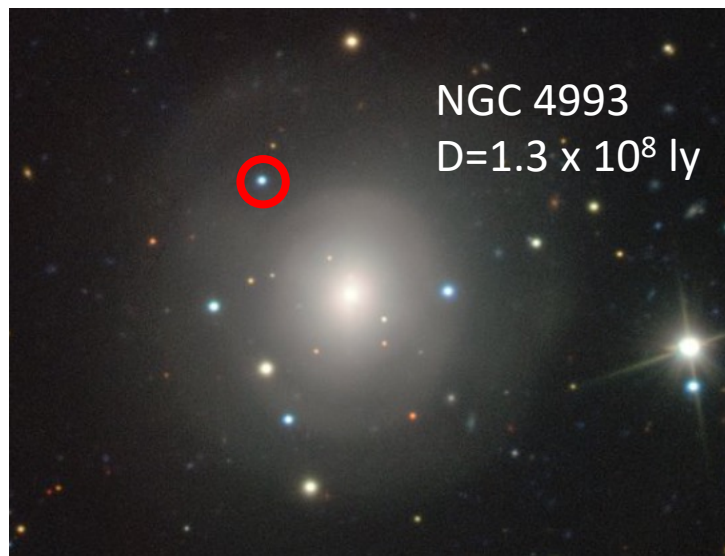
Merging Neutron Stars
Dying Low Mass Stars

Exploding Massive Stars
Exploding White Dwarfs

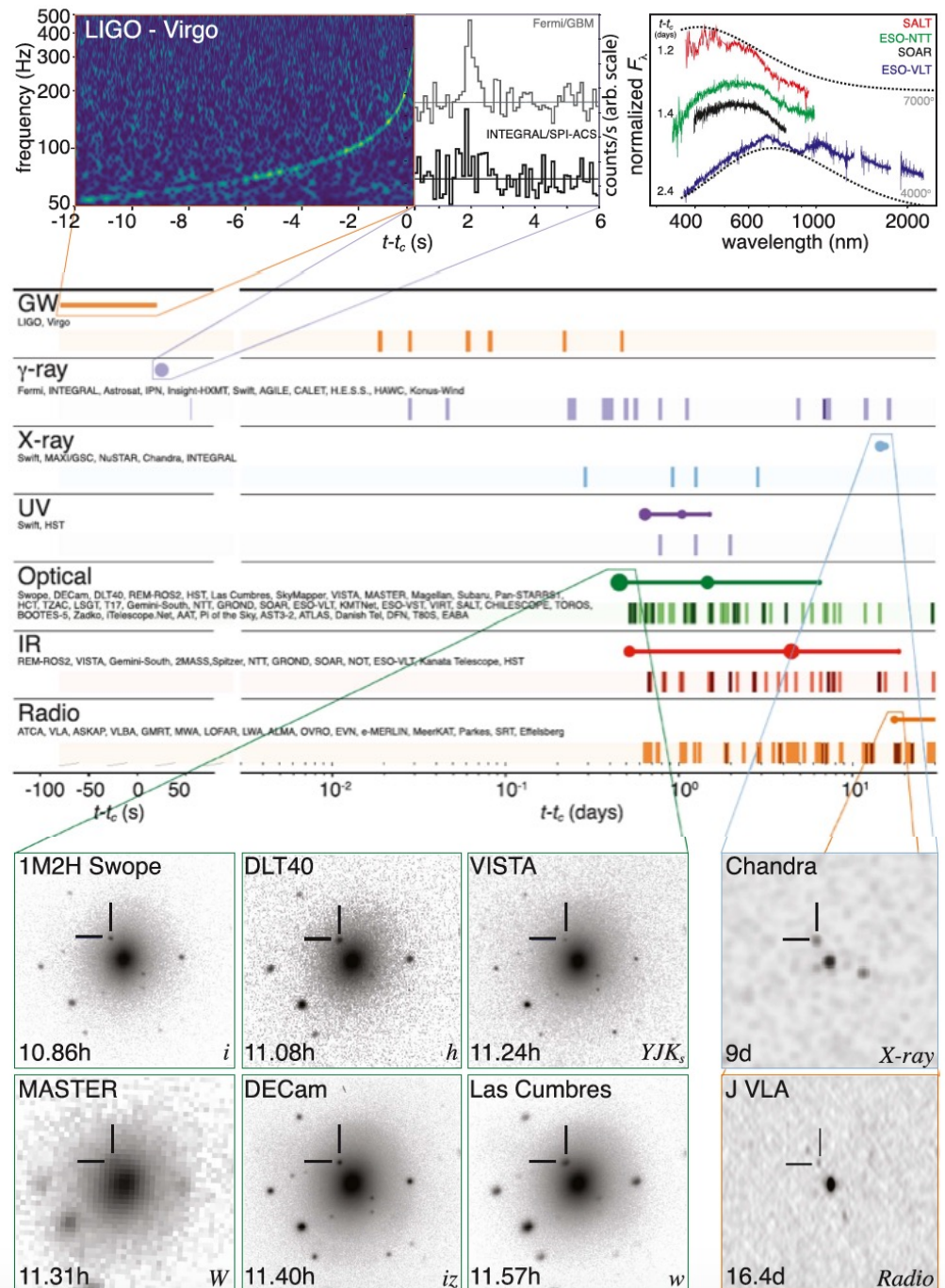
Big Bang
Cosmic Ray Fission



Observations Across the Electromagnetic Spectrum

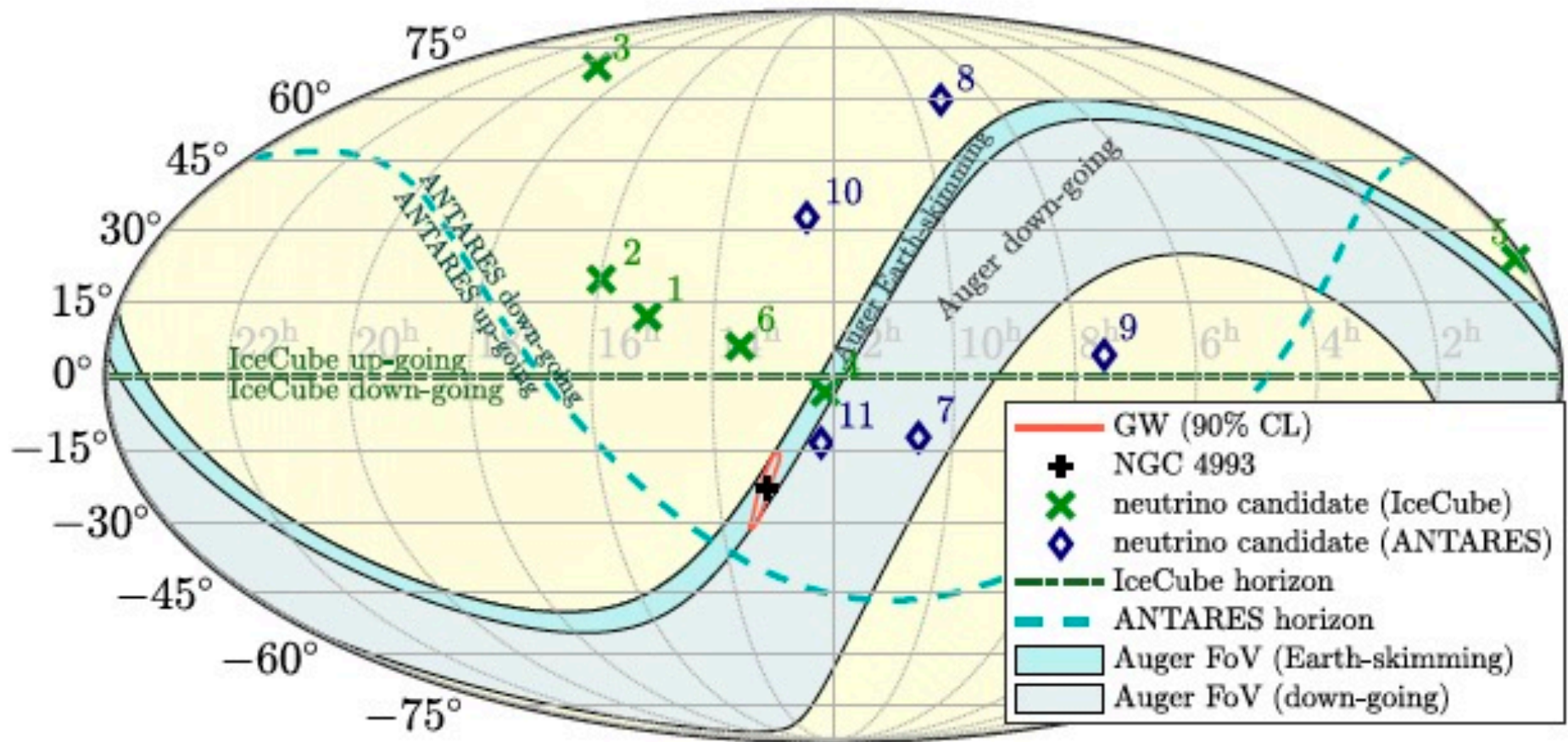


Credit: European Southern Observatory
Very Large Telescope



Abbott, et al. ,LIGO Scientific Collaboration and Virgo
Collaboration, "Multi-messenger Observations of a
Binary Neutron Star Merger" Astrophys. J. Lett.,
848:L12, (2017)

Search for neutrinos in coincidence with the BNS merger



Speed of gravitational waves

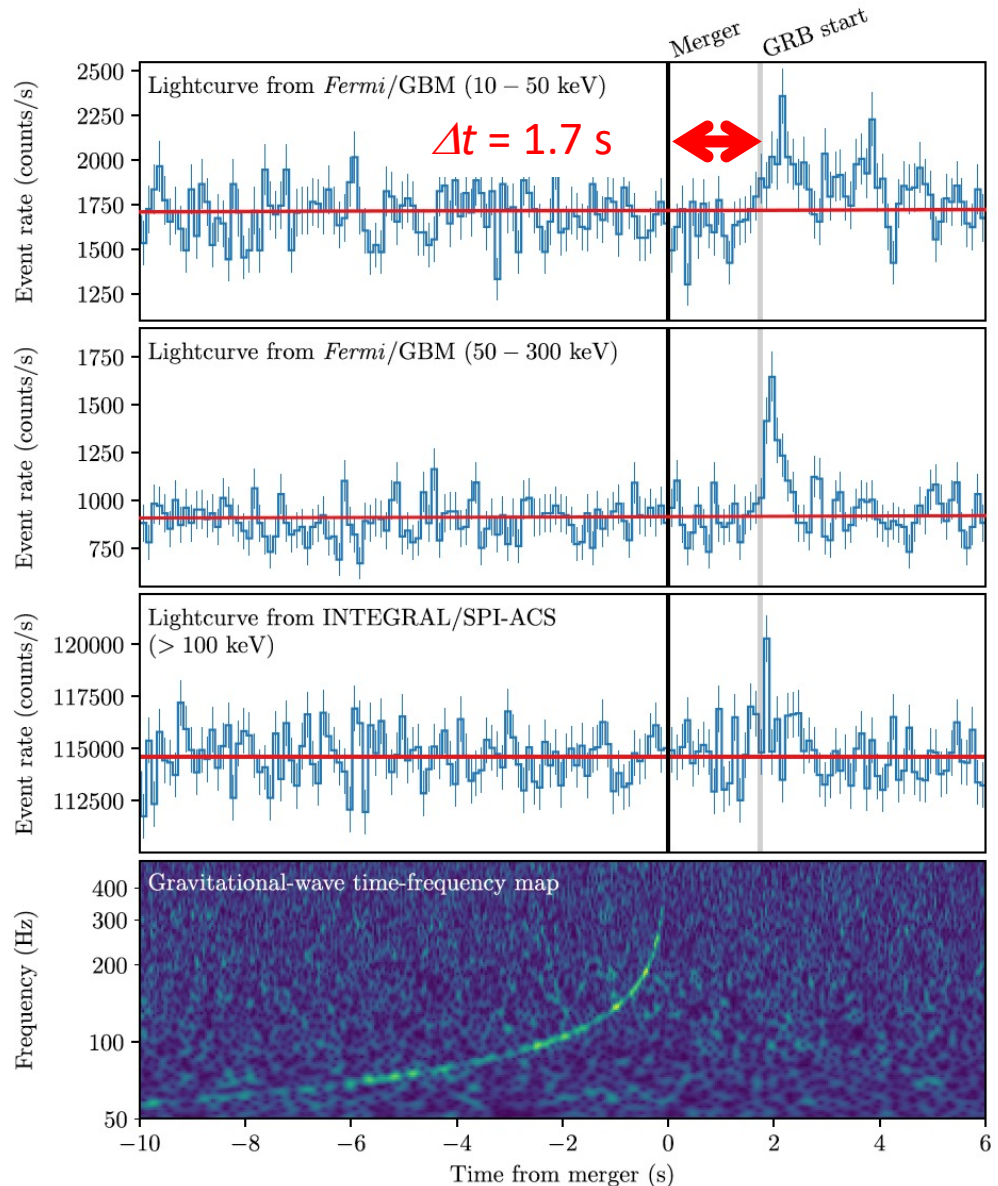
- GW170817 provides a stringent test of the speed of gravitational waves

$$\frac{v_{GW} - c}{c} \approx \frac{c\Delta t}{D}$$

- $\Delta t = 1.74 \pm 0.05$ s
- $D \approx 26$ Mpc
 - Conservative limit – use 90% confidence level lower limit on GW source from parameter estimation

$$-3 \times 10^{-15} \leq \frac{v_{GW} - c}{c} \leq +7 \times 10^{-16}$$

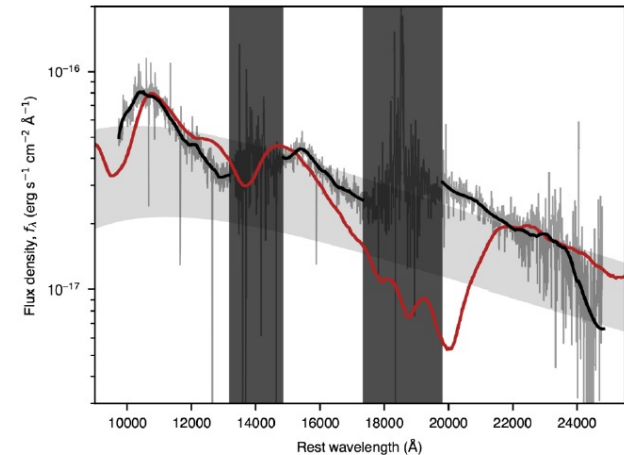
- GW170814 also puts limits on violations of Lorentz Invariance and Equivalence Principle



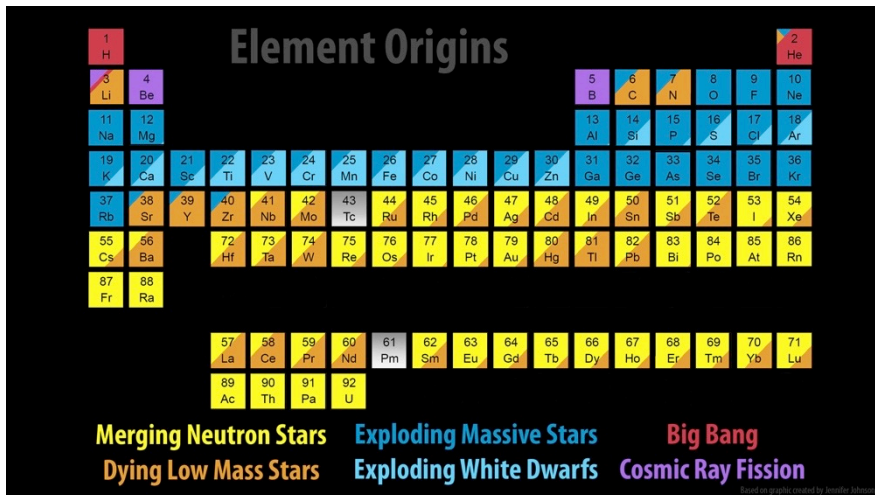
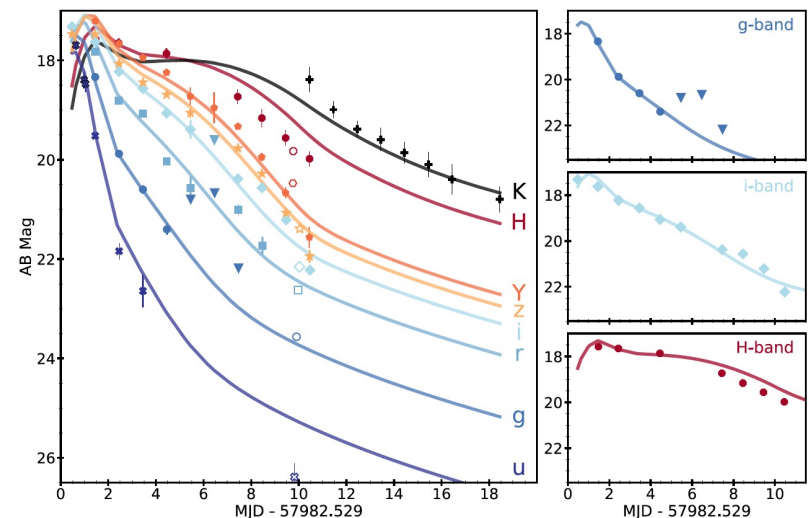
Binary Neutron Star Mergers Produce Kilonovae

- Electromagnetic follow-up of GW170817 provides strong evidence for kilonova model
 - kilonova - isotropic thermal emission produced by radioactive decay of rapid neutron capture ('r-process') elements synthesized in the merger ejecta
- Spectra taken over 2 week period across all electromagnetic bands consistent with kilonova models
 - “Blue” early emission dominated by Fe-group and light r-process formation; later “red” emission dominated by heavy element (lanthanide) formation
- Recent radio data prefers ‘cocoon’ model to classical short-hard GRB production!

Kasliwal et al. 2017,
Science, DOI: <https://doi.org/10.1126/science.aap9455>



Cowperthwaite, et al. 2017,
Ap. J. Lett. DOI: <https://doi.org/10.3847/2041-8213/aa8fc7>

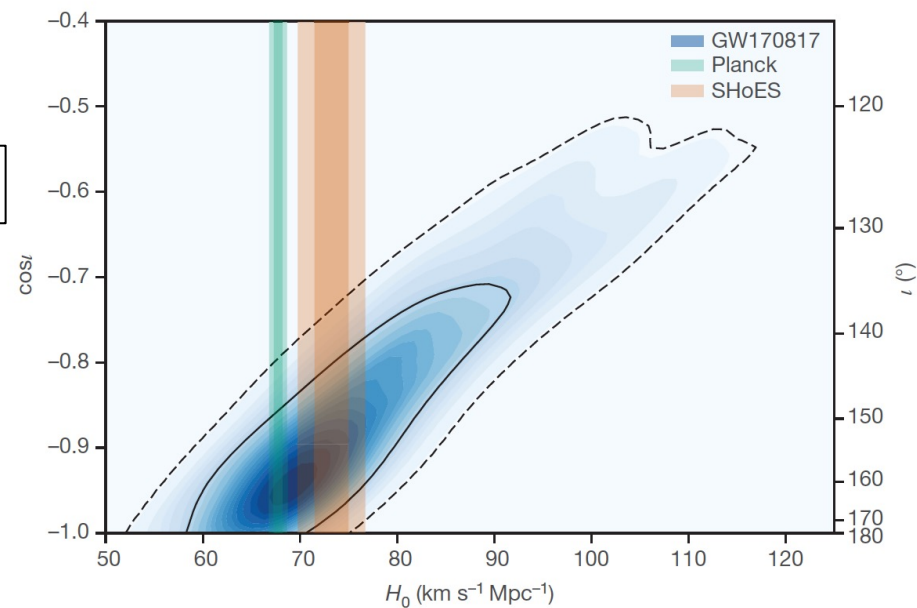
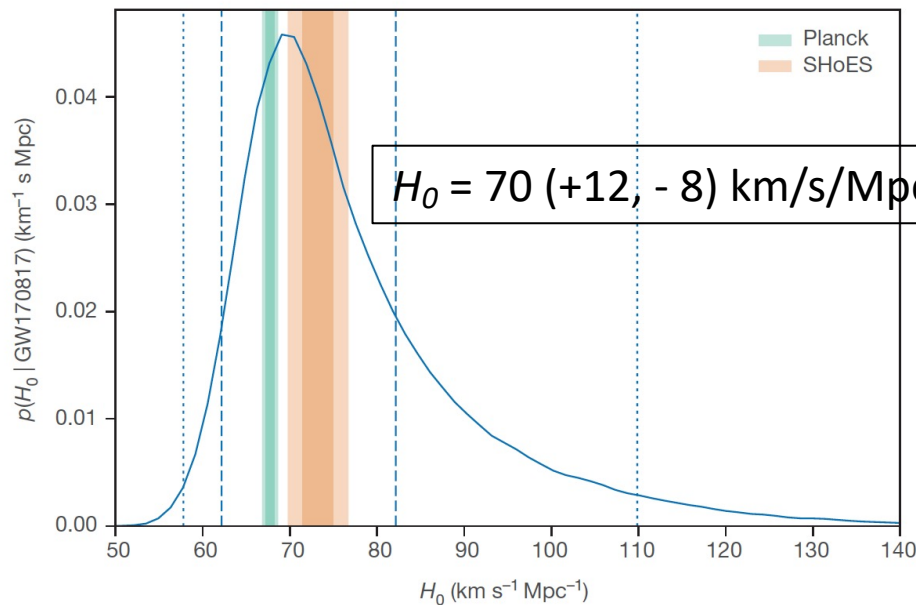


A gravitational-wave standard siren measurement of the Hubble constant

- Gravitational waves are ‘standard sirens’, providing absolute measure of luminosity distance d_L
- can be used to determine H_0 directly if red shift is known:

$$c z = H_0 d_L$$

- ... without the need for a cosmic distance ladder!



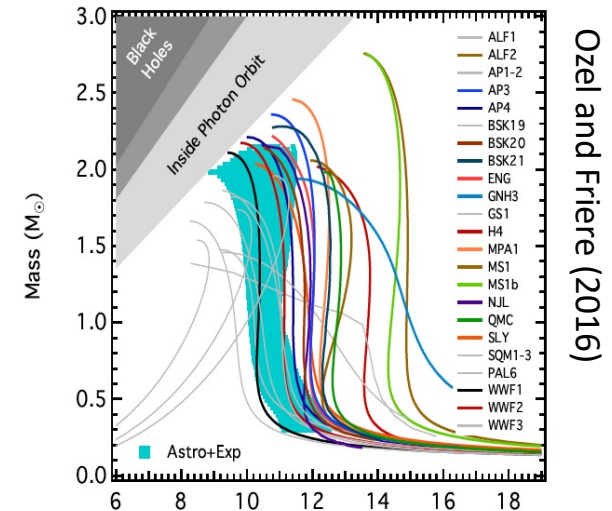
Abbott, et al., LIGO-Virgo Collaboration, 1M2H, DeCAM GW-EM & DES, DLT40, Las Cumbres Observatory, VINRO UGE, MASTER Collaborations, A gravitational-wave standard siren measurement of the Hubble constant", [Nature 551, 85–88 \(2017\)](#).

Constraining the Neutron Star Equation of State with GW170817

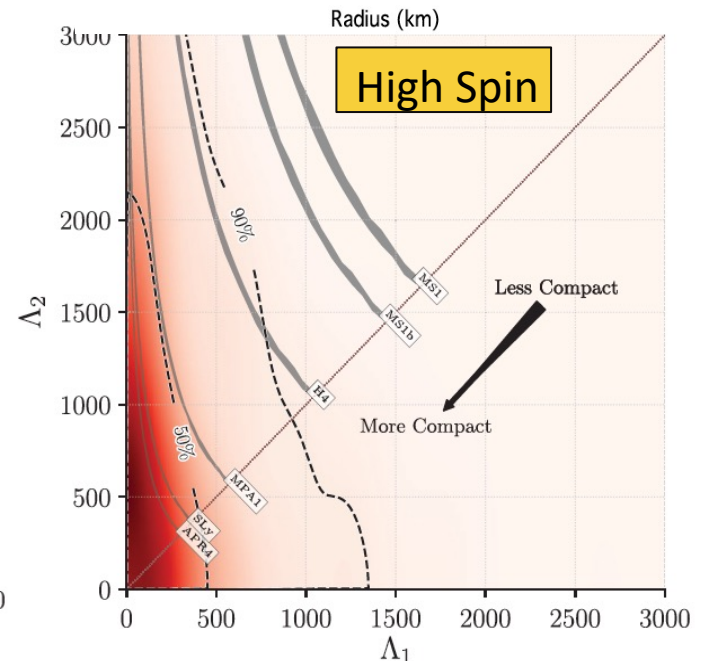
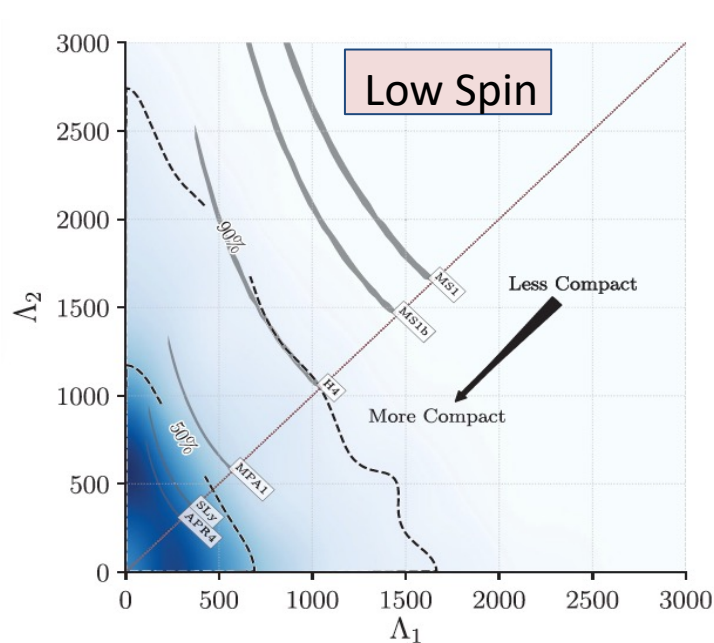
- Gravitational waveforms contain information about NS tidal deformations → allows us to constrain NS equations of state (EOS)
- Tidal deformability parameter:

$$\Lambda = \frac{2}{3}k_2 \left(\frac{R}{M} \right)^5$$

- GW170817 data consistent with softer EOS → more compact NS



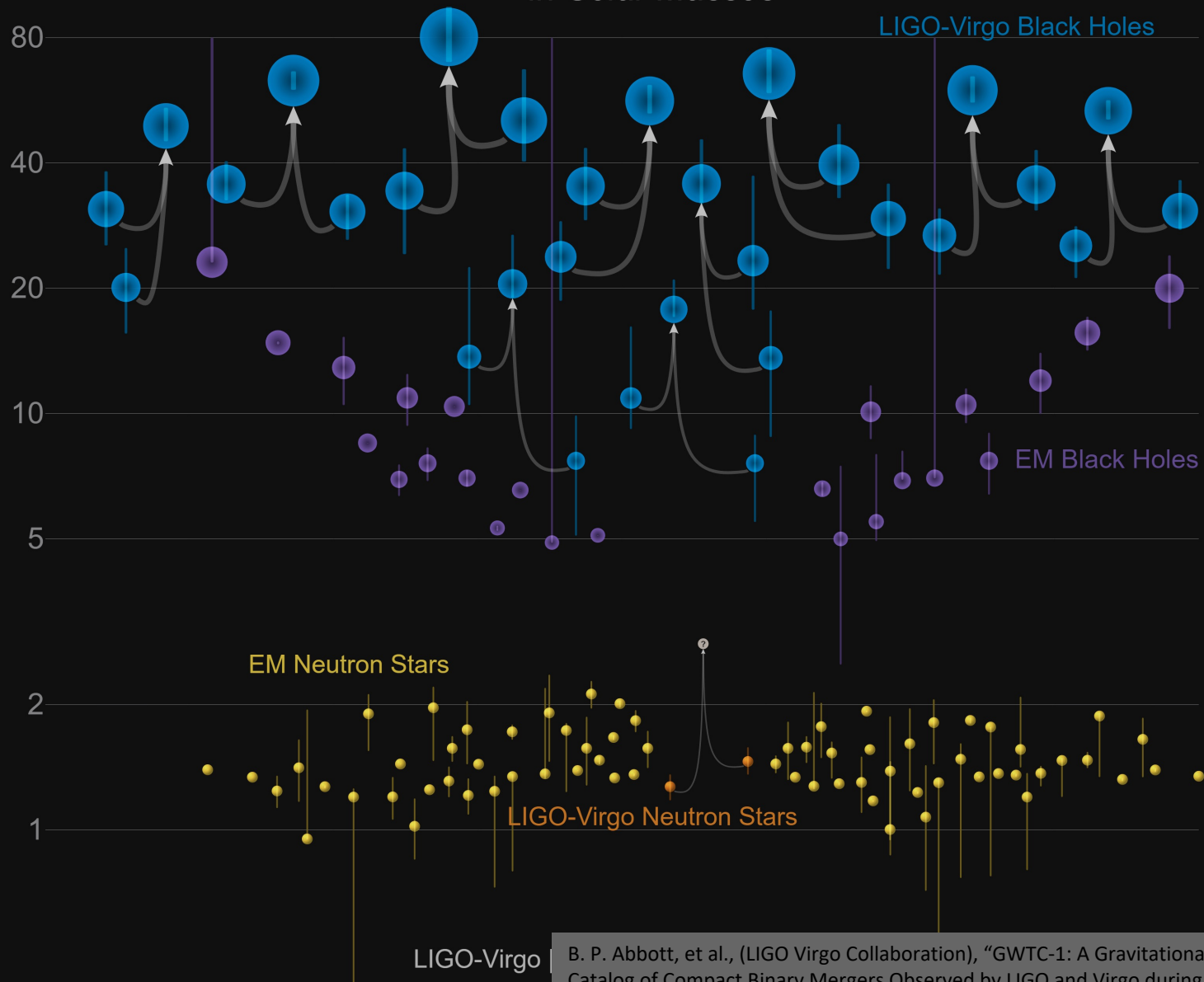
Ozel and Friere (2016)



Abbott, et al. ,LIGO Scientific Collaboration and Virgo Collaboration, "GW170817: Observation of Gravitational Waves from a Binary Neutron Star Inspiral" *Phys. Rev. Lett.* 161101 (2017)

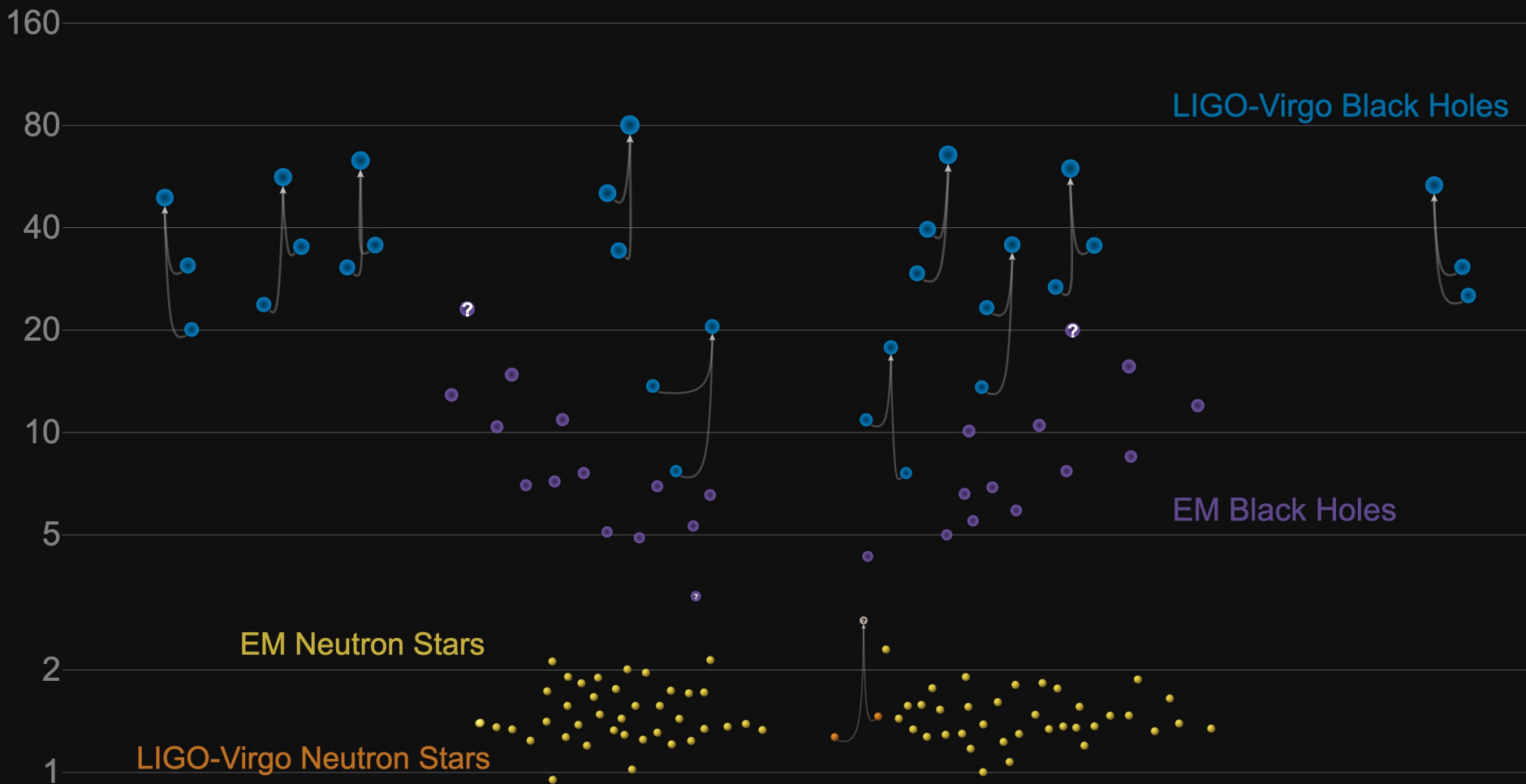
Masses in the Stellar Graveyard

in Solar Masses



B. P. Abbott, et al., (LIGO Virgo Collaboration), "GWTC-1: A Gravitational-Wave Transient Catalog of Compact Binary Mergers Observed by LIGO and Virgo during the First and Second Observing Runs", <https://arxiv.org/abs/1811.12907>

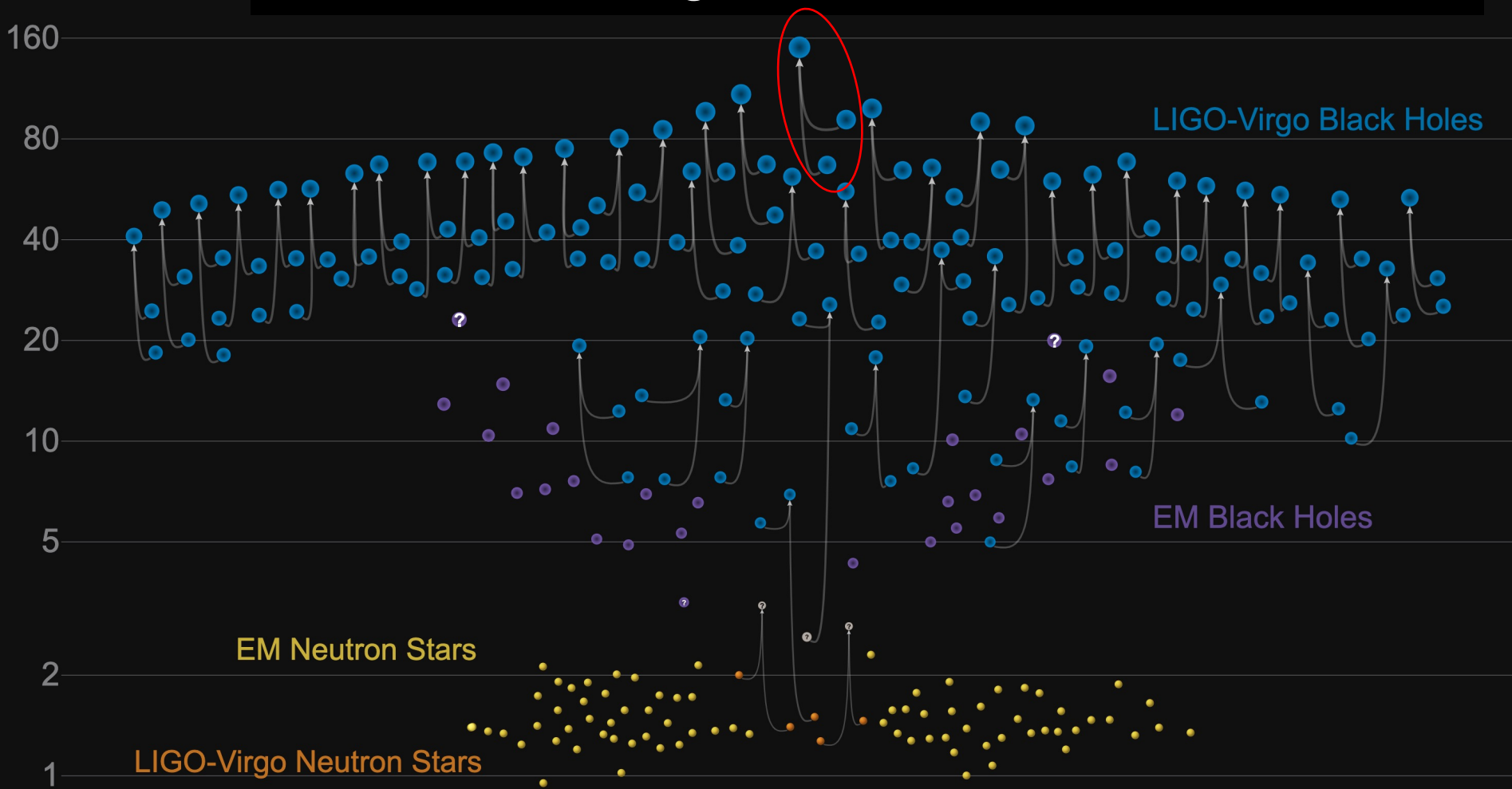
Detected Events in the First Two LIGO-Virgo Observing Runs



GWTC-2 plot v1.0

LIGO-Virgo | Frank Elavsky, Aaron Geller | Northwestern

Detected Events in the First Two LIGO-Virgo Observing Runs and the O3a Run



GWTC-2 plot v1.0

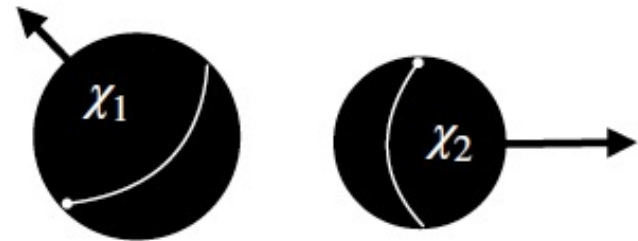
LIGO-Virgo | Frank Elavsky, Aaron Geller | Northwestern

Gravitational waves encode source properties, like ...

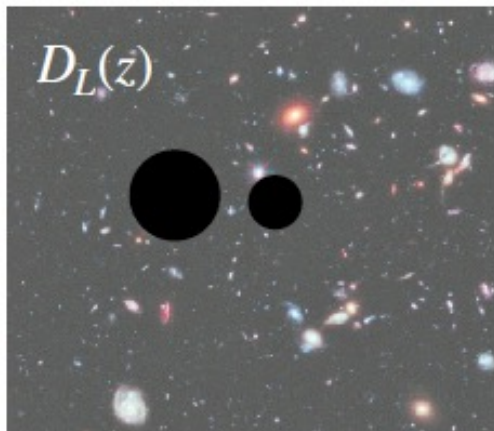
How *big* is each black hole or neutron star?



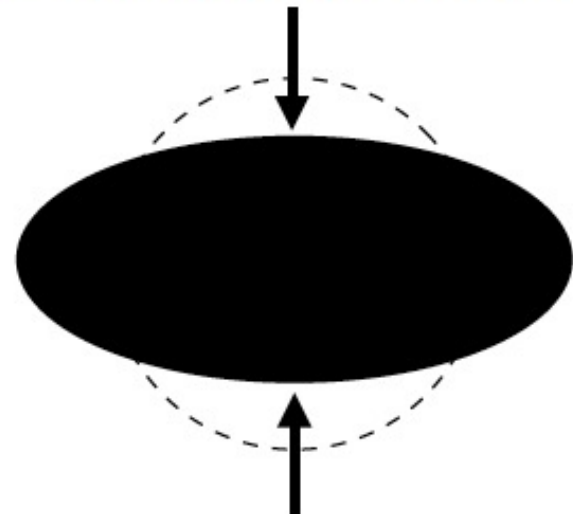
How fast are they *spinning*?



Where and when did they merge?



How squishy are neutron stars?



GRAVITATIONAL WAVE **MERGER** DETECTIONS

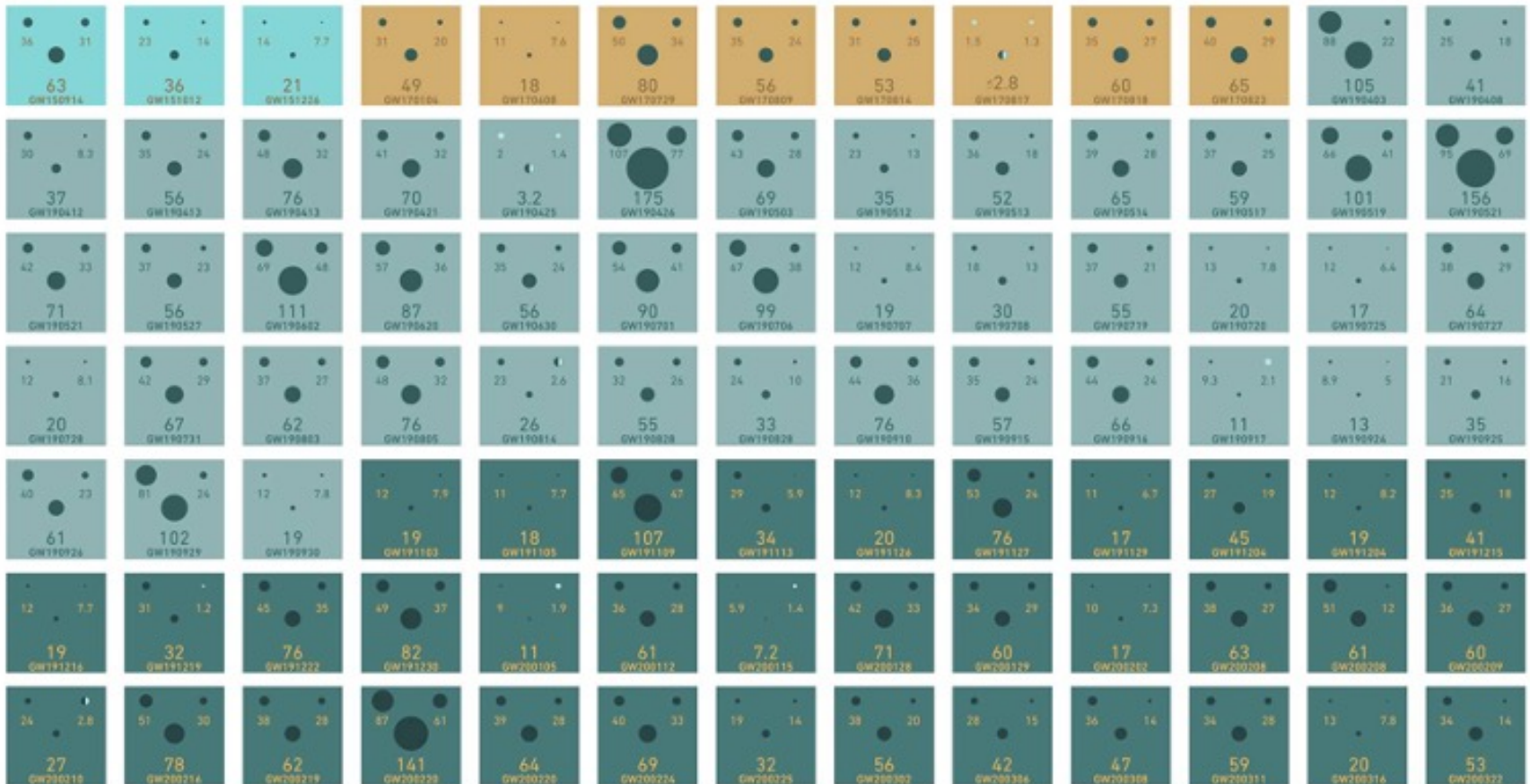
→ SINCE 2015

SERVING IN

01 2015-2016

02 2016-2017

03a+b 2019-2020



Y

BLACK HOLE
BINARY MASS
FINAL MASS

→ 31
→ 32

NEUTRON STAR
(SHOWN AT X10 SCALE)
● UNCERTAIN OBJECT

SECONDARY MASS
DATE

UNITS ARE SOLAR MASSES
1 SOLAR MASS = 1.989×10^{30} kg

Note that the mass estimates shown here do not include uncertainties, which is why the final mass is sometimes larger than the sum of the primary and secondary masses. In actuality, the final mass is smaller than the primary plus the secondary mass.

The events listed here pass one of two thresholds for detection. They either have a probability of being astrophysical of at least 50%, or they pass a false alarm rate threshold of less than 1 per 3 years.



GRAVITATIONAL WAVE **MERGER** DETECTIONS

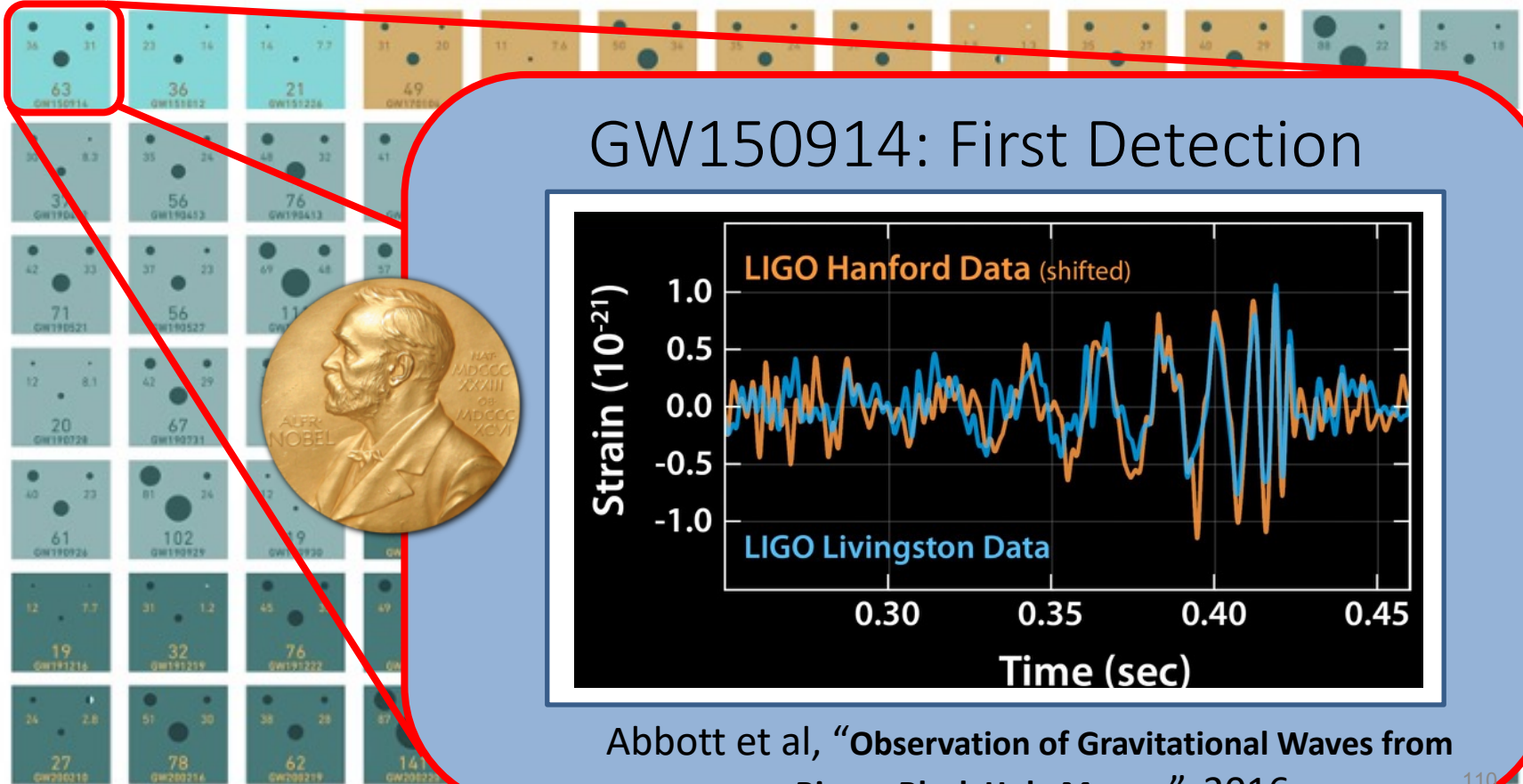
→ SINCE 2015

SERVING IN

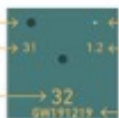
01 2015-2016

02 2016-2017

03a+b 2019-2020



BLACK HOLE
BINARY MASS
FINAL MASS



NEUTRON STAR
(SHOWN AT X10 SCALE)
● UNCERTAIN OBJECT

SECONDARY MASS
DATE

UNITS ARE SOLAR MASSES
1 SOLAR MASS = 1.989×10^{30} kg

Note that the mass estimates shown here do not include uncertainties, which is why the final mass is sometimes larger than the sum of the primary and secondary masses. In actuality, the final mass is smaller than the primary plus the secondary mass.

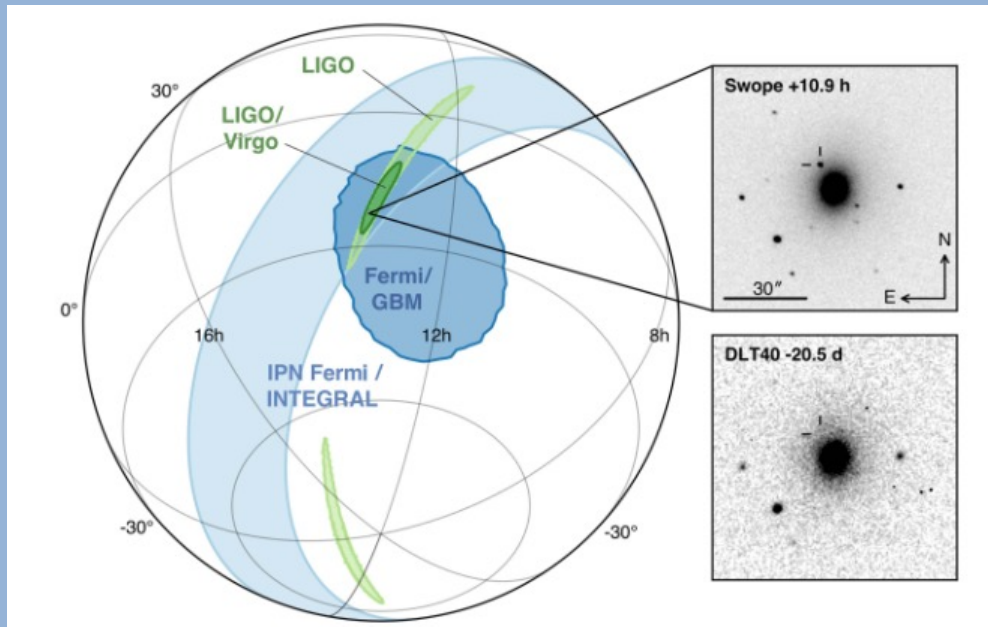
The events listed here pass one of two thresholds for detection. They either have a probability of being astrophysical of at least 50%, or they pass a false alarm rate threshold of less than 1 per 3 years.



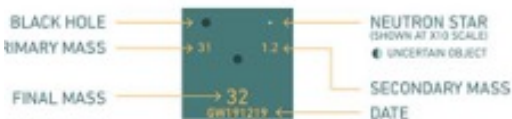
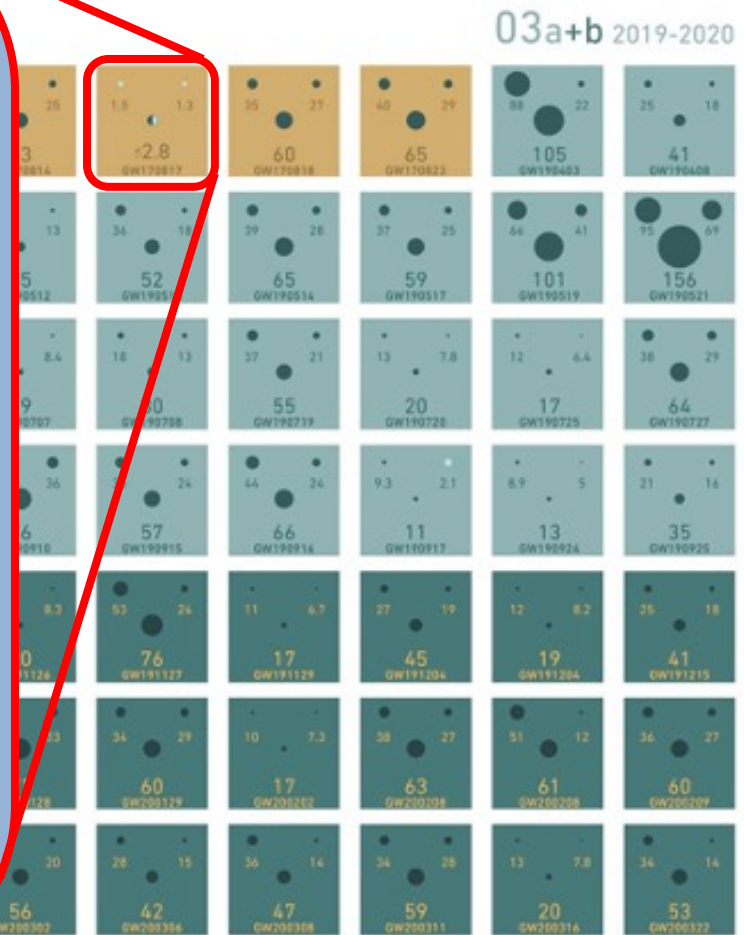
GRAVITATIONAL WAVE **MERGER** DETECTIONS

→ SINCE 2015

GW170817: Neutron Stars and Multi-messenger Observation



From Abbott et al, “Multi-Messenger Observations of a Binary Neutron Star Merger”, 2017



UNITS ARE SOLAR MASSES
1 SOLAR MASS = $1.989 \times 10^{30} \text{ kg}$

Note that the mass estimates shown here do not include uncertainties, which is why the final mass is sometimes larger than the sum of the primary and secondary masses. In actuality, the final mass is smaller than the primary plus the secondary mass.

The events listed here pass one of two thresholds for detection. They either have a probability of being astrophysical of at least 50%, or they pass a false alarm rate threshold of less than 1 per 3 years.



GRAVITATIONAL WAVE **MERGER** DETECTIONS

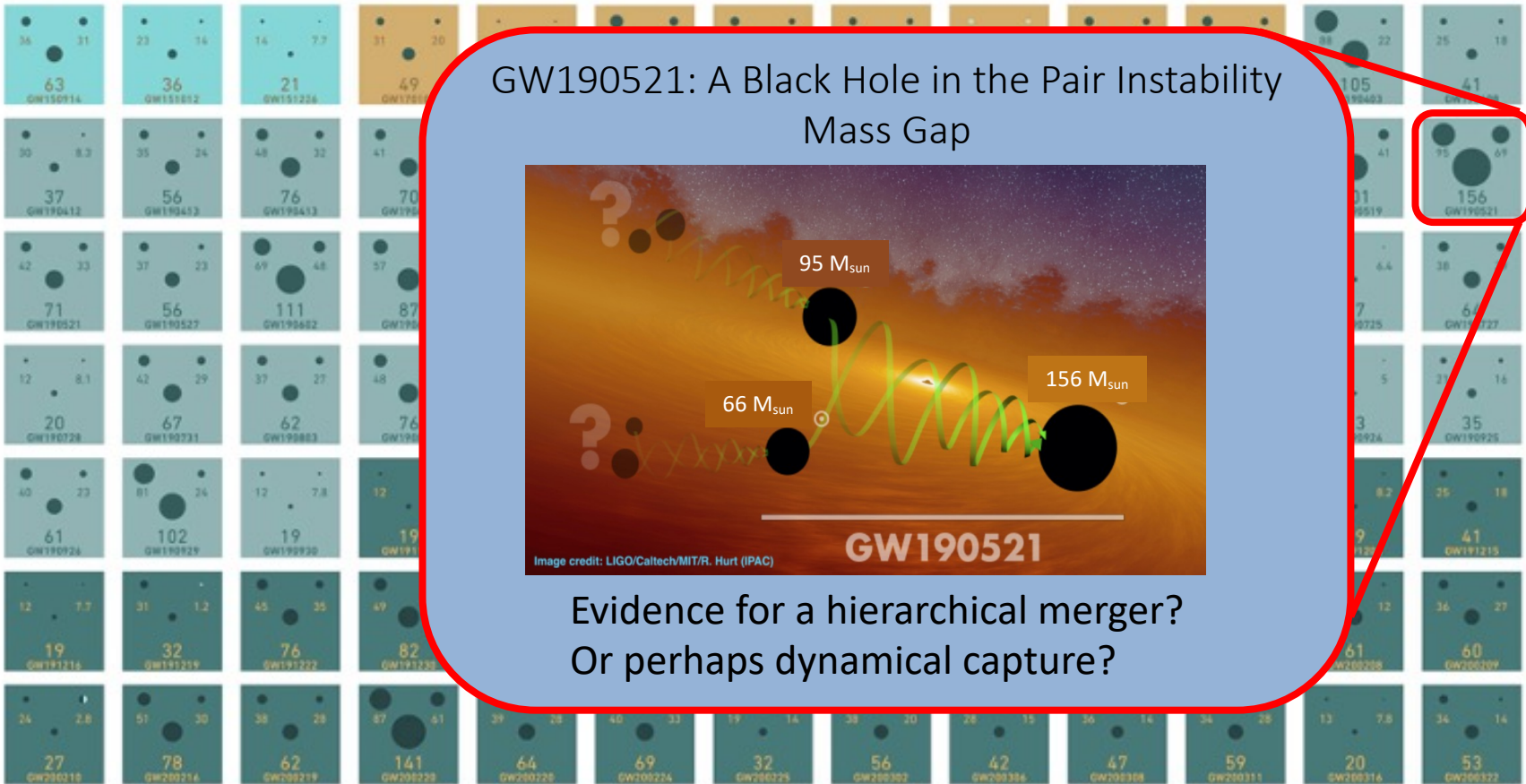
→ SINCE 2015

SERVING IN

01 2015-2016

02 2016-2017

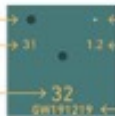
03a+b 2019-2020



BLACK HOLE

BINARY MASS

FINAL MASS



NEUTRON STAR

(SHOWN AT X10 SCALE)

● UNCERTAIN OBJECT

SECONDARY MASS

DATE

UNITS ARE SOLAR MASSES
1 SOLAR MASS = $1.989 \times 10^{30} \text{ kg}$

Note that the mass estimates shown here do not include uncertainties, which is why the final mass is sometimes larger than the sum of the primary and secondary masses. In actuality, the final mass is smaller than the primary plus the secondary mass.

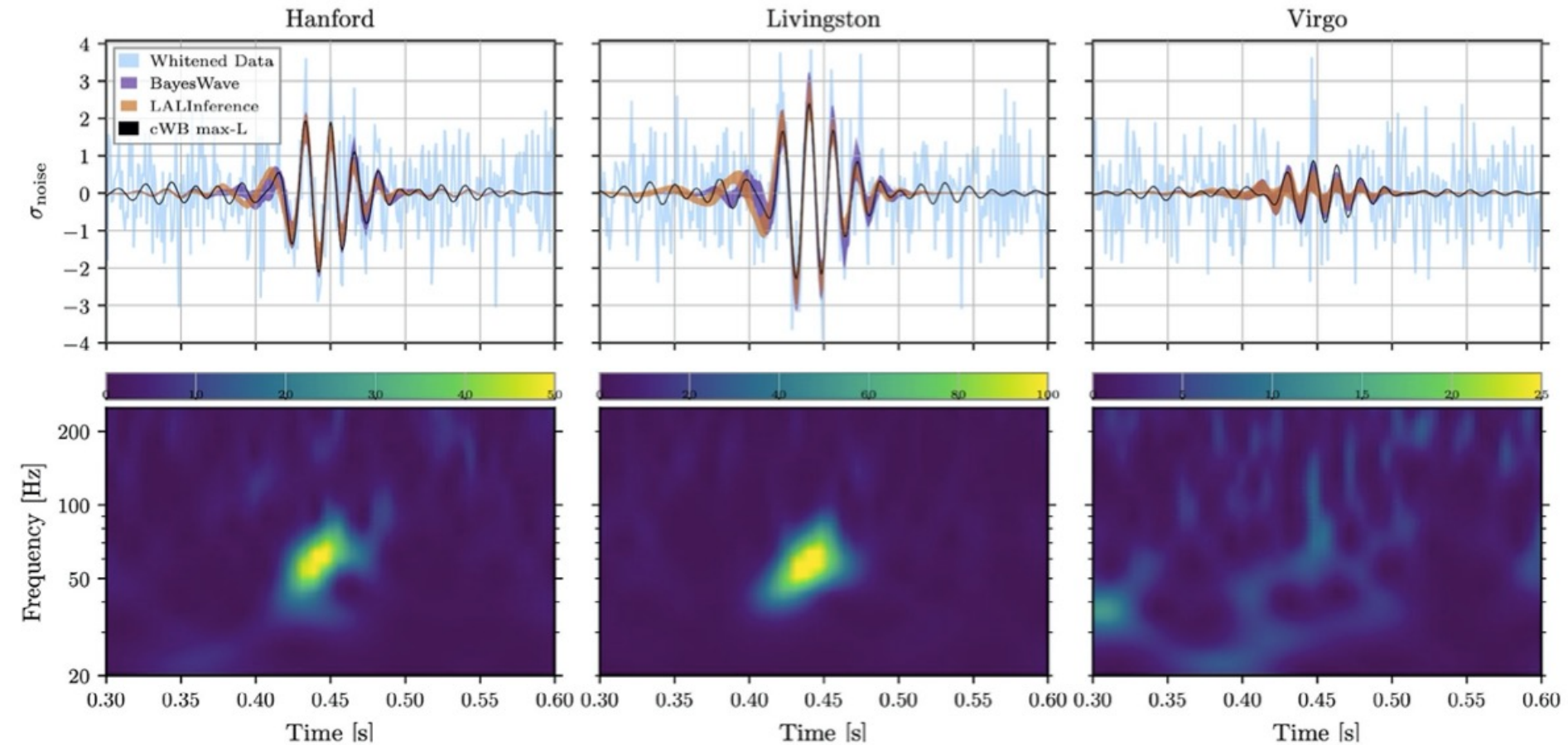
The events listed here pass one of two thresholds for detection. They either have a probability of being astrophysical of at least 50%, or they pass a false alarm rate threshold of less than 1 per 3 years.



Slide: S. Fairhurst

The Most Massive & Distant Black Hole Merger Yet: GW190521

(May 21, 2019)



The signal was shorter in duration (0.1 s), and peaked at lower frequency than any other binary black hole merger observed to date.

The time interval that the signal spends in the sensitivity band is inversely proportional to the total mass of the binary system.

The frequency of the merger is also inversely proportional to the binary's total mass.

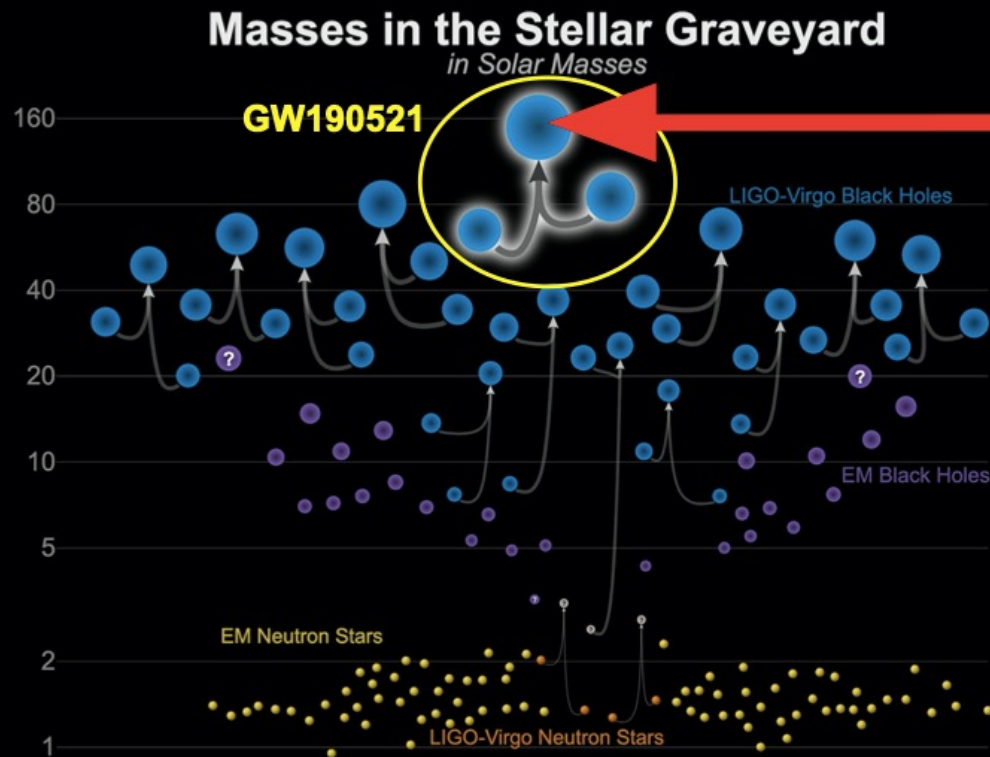
GW190521 parameters

- Most massive observation to date
- Most distant
- Pair-instability supernova mass gap, $65\text{-}120 M_{\odot}$
- Intermediate Mass Black Hole
- Important astrophysical implications
- Orbital precession

TABLE I. Parameters of GW190521 according to the NRSur7dq4 waveform model. We quote median values with 90% credible intervals that include statistical errors.

Parameter	
Primary mass	$85^{+21}_{-14} M_{\odot}$
Secondary mass	$66^{+17}_{-18} M_{\odot}$
Primary spin magnitude	$0.69^{+0.27}_{-0.62}$
Secondary spin magnitude	$0.73^{+0.24}_{-0.64}$
Total mass	$150^{+29}_{-17} M_{\odot}$
Mass ratio ($m_2/m_1 \leq 1$)	$0.79^{+0.19}_{-0.29}$
Effective inspiral spin parameter (χ_{eff})	$0.08^{+0.27}_{-0.36}$
Effective precession spin parameter (χ_p)	$0.68^{+0.25}_{-0.37}$
Luminosity Distance	$5.3^{+2.4}_{-2.6} \text{ Gpc}$
Redshift	$0.82^{+0.28}_{-0.34}$
Final mass	$142^{+28}_{-16} M_{\odot}$
Final spin	$0.72^{+0.09}_{-0.12}$
P ($m_1 < 65 M_{\odot}$)	0.32%
\log_{10} Bayes factor for orbital precession	$1.06^{+0.06}_{-0.06}$
\log_{10} Bayes factor for nonzero spins	$0.92^{+0.06}_{-0.06}$
\log_{10} Bayes factor for higher harmonics	$-0.38^{+0.06}_{-0.06}$

The most massive black hole ever observed with gravitational waves

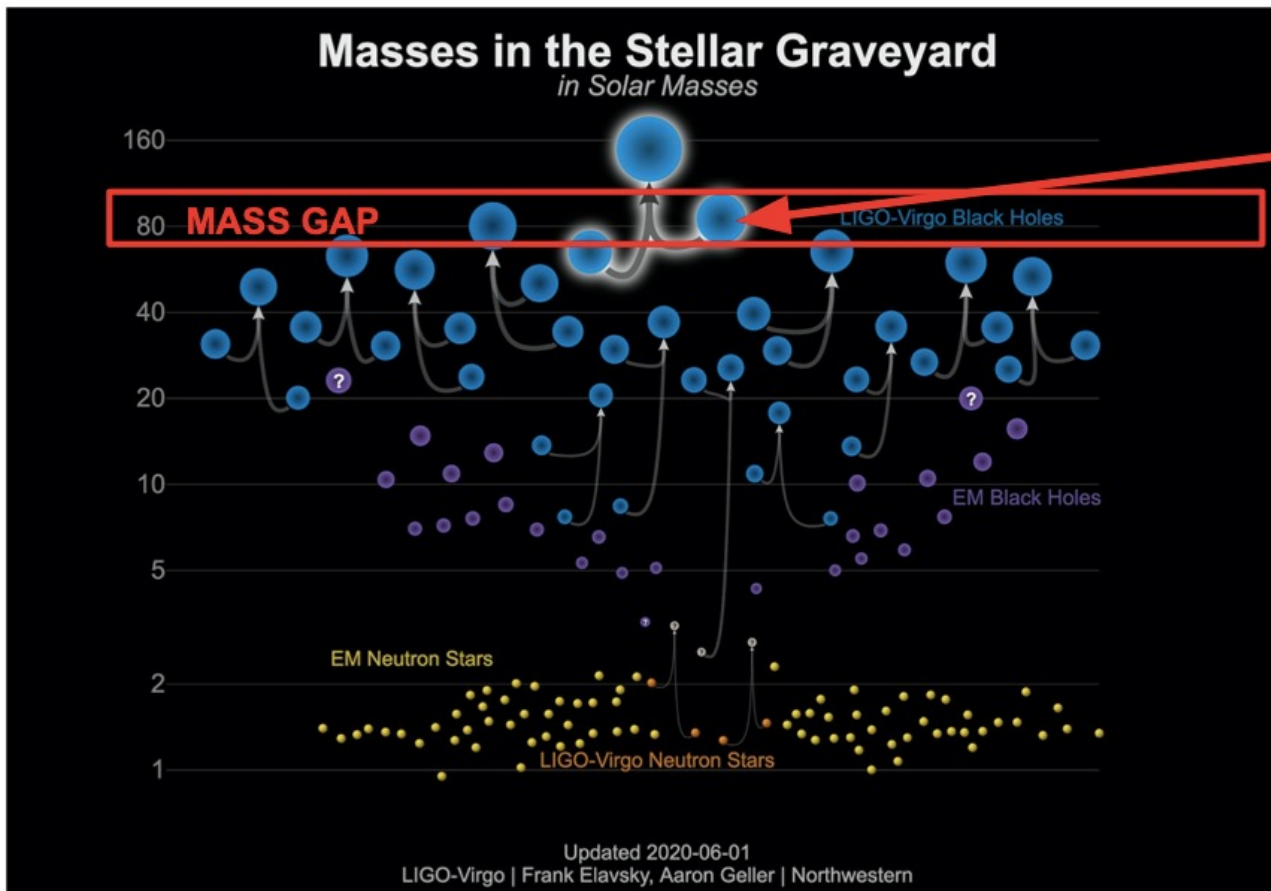


Updated 2020-06-01
LIGO-Virgo | Frank Elavsky, Aaron Geller | Northwestern

The final black hole is

- the most massive black hole ever observed with gravitational waves
- the first evidence of a black hole in the 100 - 1000 solar mass range
- an intermediate-mass black hole: the missing link between stellar-mass and supermassive black holes

The first black hole in the pair-instability mass gap



- One of the two merging black holes has mass 85 solar masses: it cannot form from stellar collapse
- Very massive stars (He core $\sim 30 - 135$ solar masses) undergo (PULSATONAL) PAIR INSTABILITY
- Expected gap in the black hole mass spectrum between ~ 65 and ~ 120 solar masses

GW190521 crashes the party because the mass of larger black hole that merged (the ‘primary’ black hole) sits squarely in the interval where stellar collapse is not expected to directly produce black holes – and, moreover, it produced a post-merger remnant black hole that can be classified as an intermediate mass black hole.

Challenge for the models of black hole formation

In dense star clusters and galactic nuclei, black holes can have close encounters with other black holes

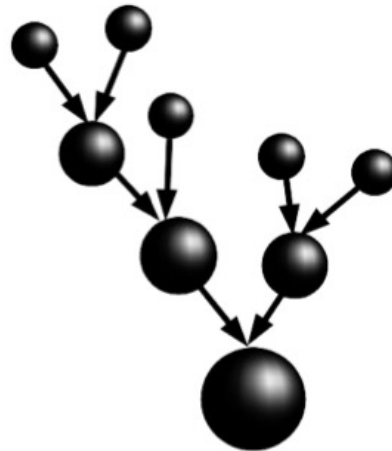


credit: NASA / ESA / Hubble

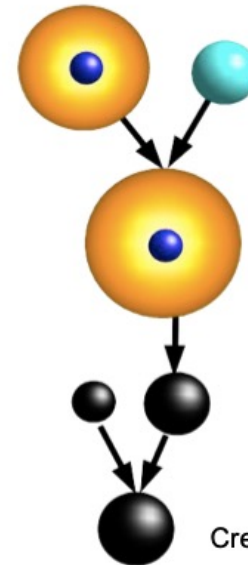


credit: NASA, ESA, F. Paresce, R. O'Connell

Hierarchical mergers

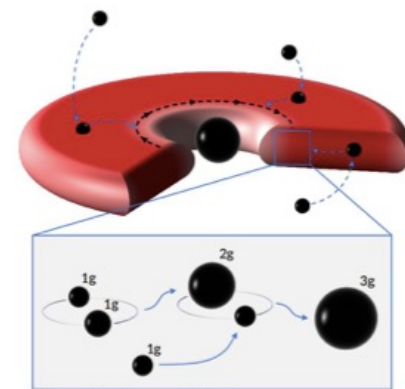


Stellar mergers



Credit: Ugo N. Di Carlo

AGN disks



Credit: Imre Bartos

...or even more exotic scenarios

This multiple merger scenario requires that black holes form in special environments where there are enough other black holes nearby for multiple merger events to occur. Astronomers have proposed dense clusters of stars or the disks of active galactic nuclei as possible examples of such special environments.

The Most Massive & Distant Black Hole Merger Yet: GW190521

(May 21, 2019)

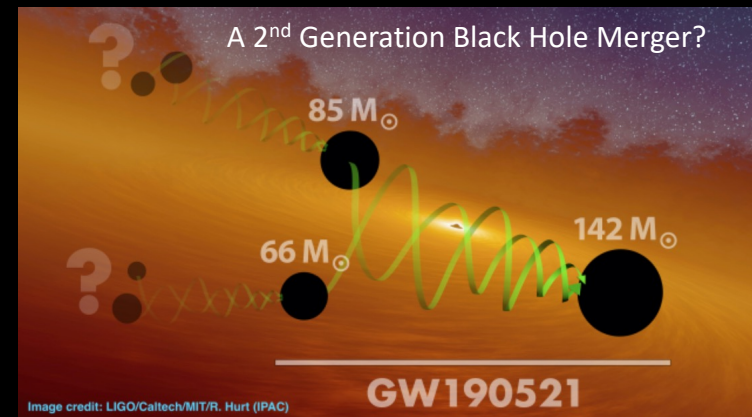
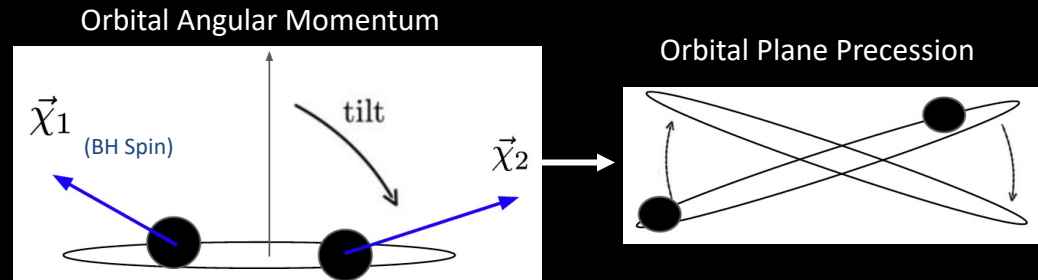
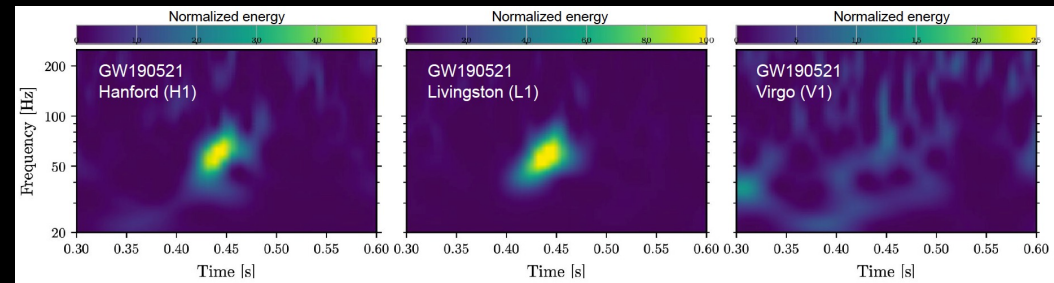
The furthest GW event ever recorded: ~ 7 Gyr distant

At least one of the progenitor black holes ($85 M_{\text{sun}}$) lies in the pair instability supernova gap

Strong evidence for spin precession; both progenitor black holes were spinning

Evidence that GW190521 might be a 2nd generation merger!!

The final black hole mass is $145 M_{\text{sun}}$ is the first ever observation of an intermediate mass black hole



Abbott, et al., "GW190521: A Binary Black Hole Merger with a Total Mass of $150 M_{\text{sun}}$ ", [Phys. Rev. Lett. 125, 101102 \(2020\)](#).

Abbott, et al., "Properties and Astrophysical Implications of the $150 M_{\text{sun}}$ Binary Black Hole Merger GW190521", [Ap. J. Lett. 900, L13 \(2020\)](#).

Image credit: LIGO/Caltech/MIT/R. Hurt (IPAC)

A Possible Electromagnetic Counterpart to GW190521

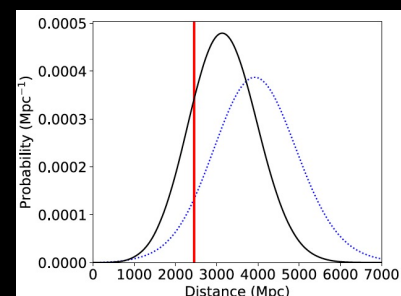
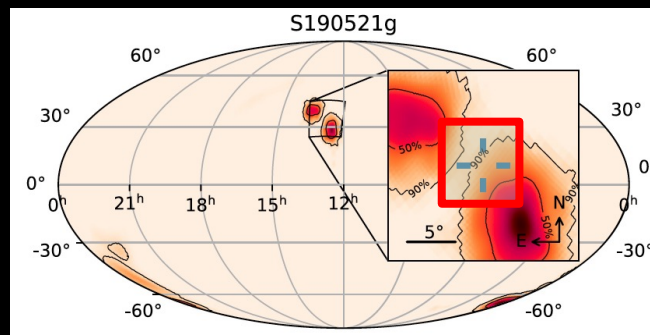
Zwicky Transient Facility surveyed 48% of the LIGO-Virgo 90% error box for GW190521

An electromagnetic flare in the visible was found within the initial 90% LIGO-Virgo contour beginning ~ 25 days after GW190521, lasting for ~ 100 days

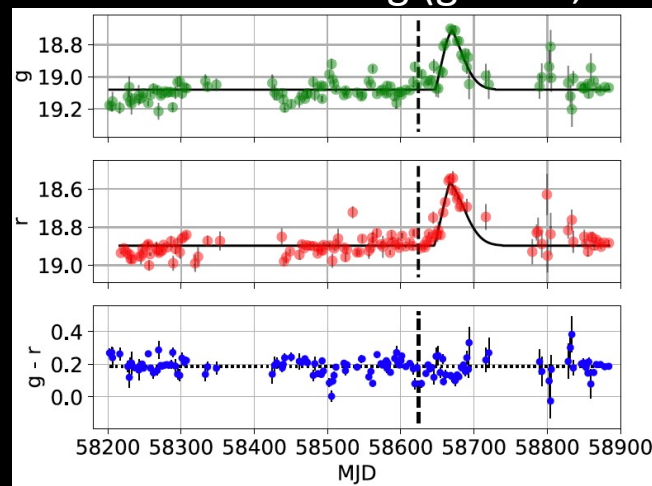
Consistent with LIGO-Virgo initial distance estimates

But less consistent with updated maps

The EM flare is consistent with emission from gas in the accretion disk of an active galactic nucleus (AGN) excited by the 'kicked' black hole passing through the AGN disk

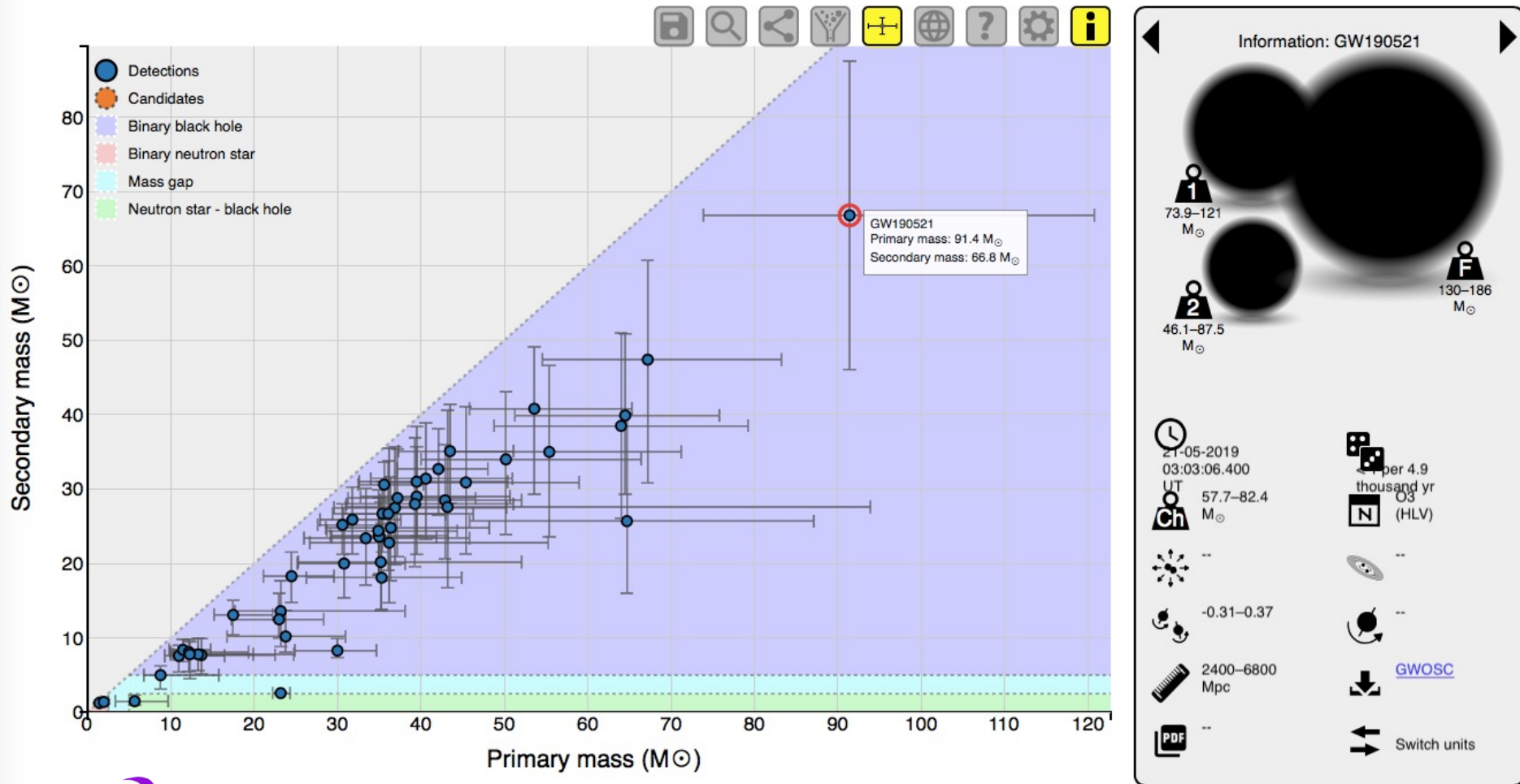


EM Flare from S190521g (g-band, r-band)



Interactive Catalogue of Binary Black Holes

LIGO-Virgo Compact Binary Catalogue



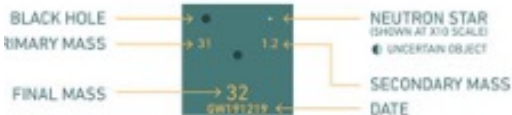
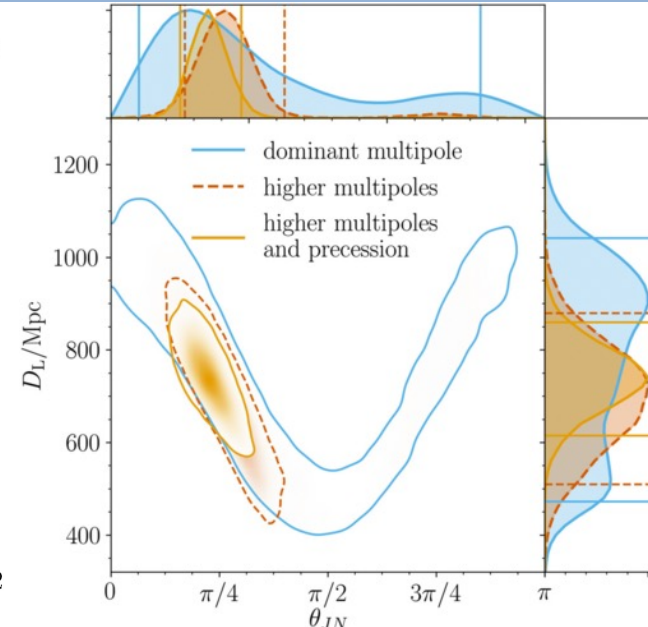
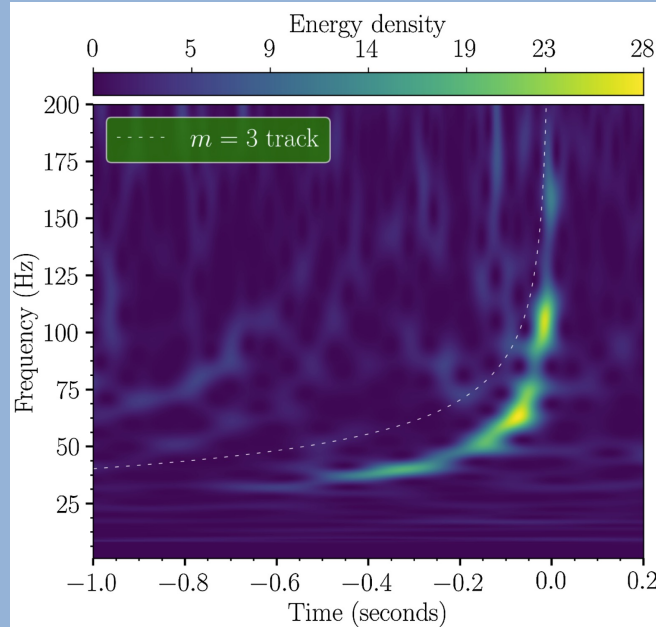
GRAVITATIONAL WAVE **MERGER** DETECTIONS

→ SINCE 2015

SERVING IN 01 2015-2016

2019-2020

GW190412: Unequal mass binary



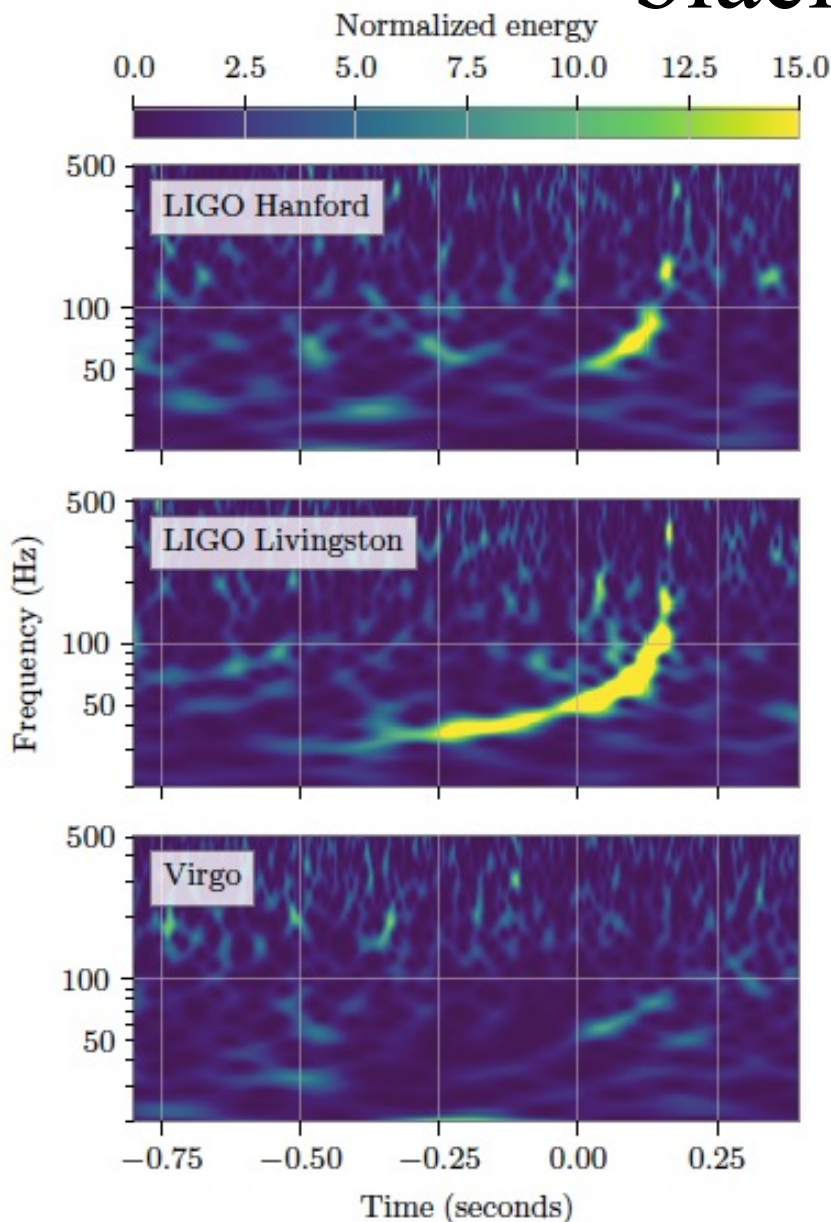
UNITS ARE SOLAR MASSES
1 SOLAR MASS = $1.989 \times 10^{30}\text{kg}$

Note that the mass estimates shown here do not include uncertainties, which is why the final mass is sometimes larger than the sum of the primary and secondary masses. In actuality, the final mass is smaller than the primary plus the secondary mass.

The events listed here pass one of two thresholds for detection. They either have a probability of being astrophysical of at least 50%, or they pass a false alarm-rate threshold of less than 1 per 3 years.



GW190412: the first unequal-mass black hole merger



- One black hole in the system is more than 3 times heavier than the other: $30 M_{\odot} + 8 M_{\odot}$.
- This asymmetry in masses modifies the gravitational-wave signal in such a way that we can better measure other parameters, such as the distance and inclination of the system, the spin of the heavier black hole, and the amount that the system is precessing.
- Due to the unequal masses of GW190412 we can for the first time put strong constraints on the spin of the larger black hole, which we find to be spinning at about 40% of the maximal spin allowed by general relativity.

GRAVITATIONAL WAVE **MERGER** DETECTIONS

→ SINCE 2015

SERVING IN

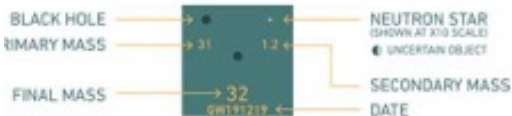
01 2015-2016

02 2016-2017

03a+b 2019-2020



Y



UNITS ARE SOLAR MASSES
1 SOLAR MASS = 1.989×10^{30} kg

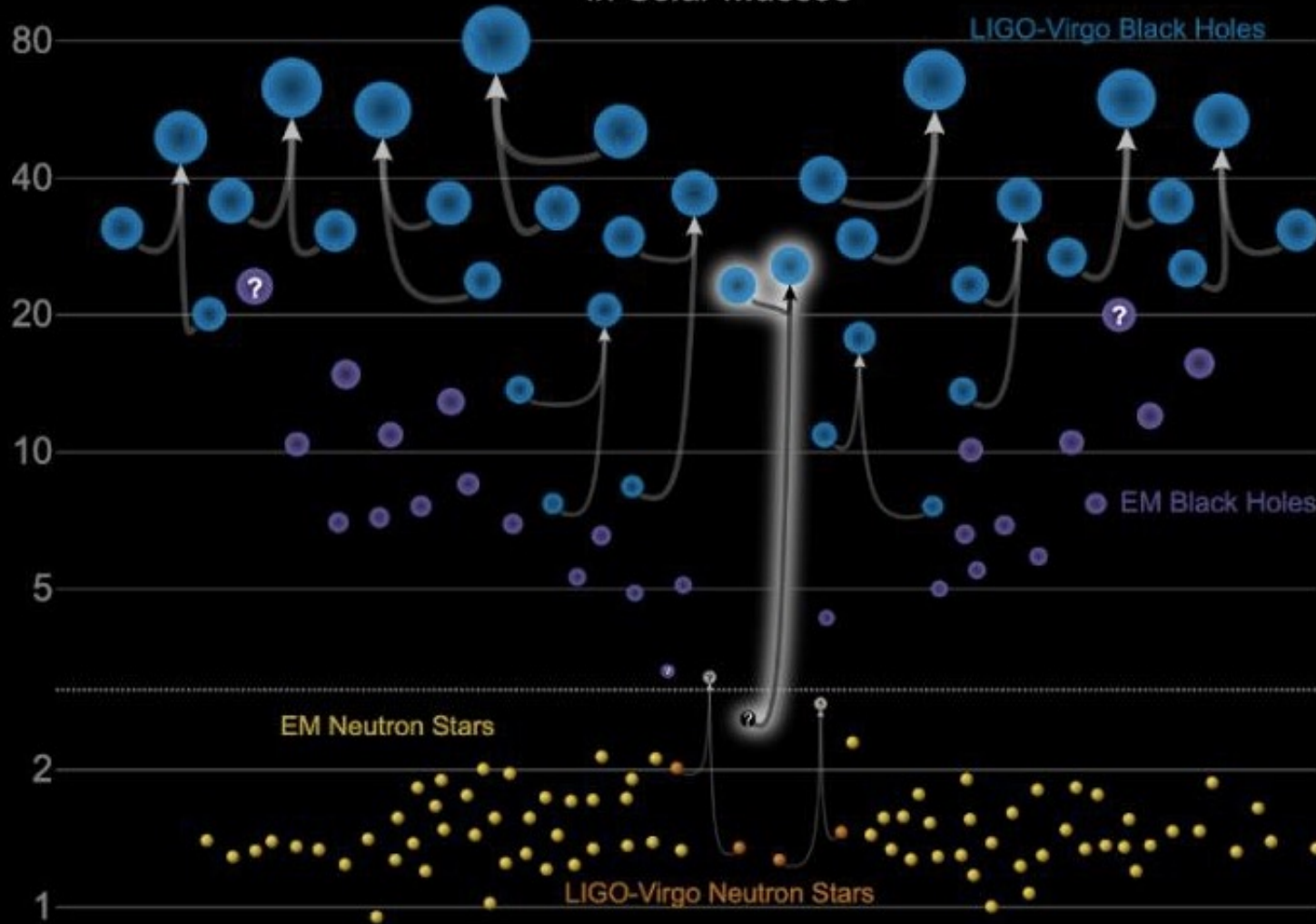
Note that the mass estimates shown here do not include uncertainties, which is why the final mass is sometimes larger than the sum of the primary and secondary masses. In actuality, the final mass is smaller than the primary plus the secondary mass.

The events listed here pass one of two thresholds for detection. They either have a probability of being astrophysical of at least 50%, or they pass a false alarm rate threshold of less than 1 per 3 years.



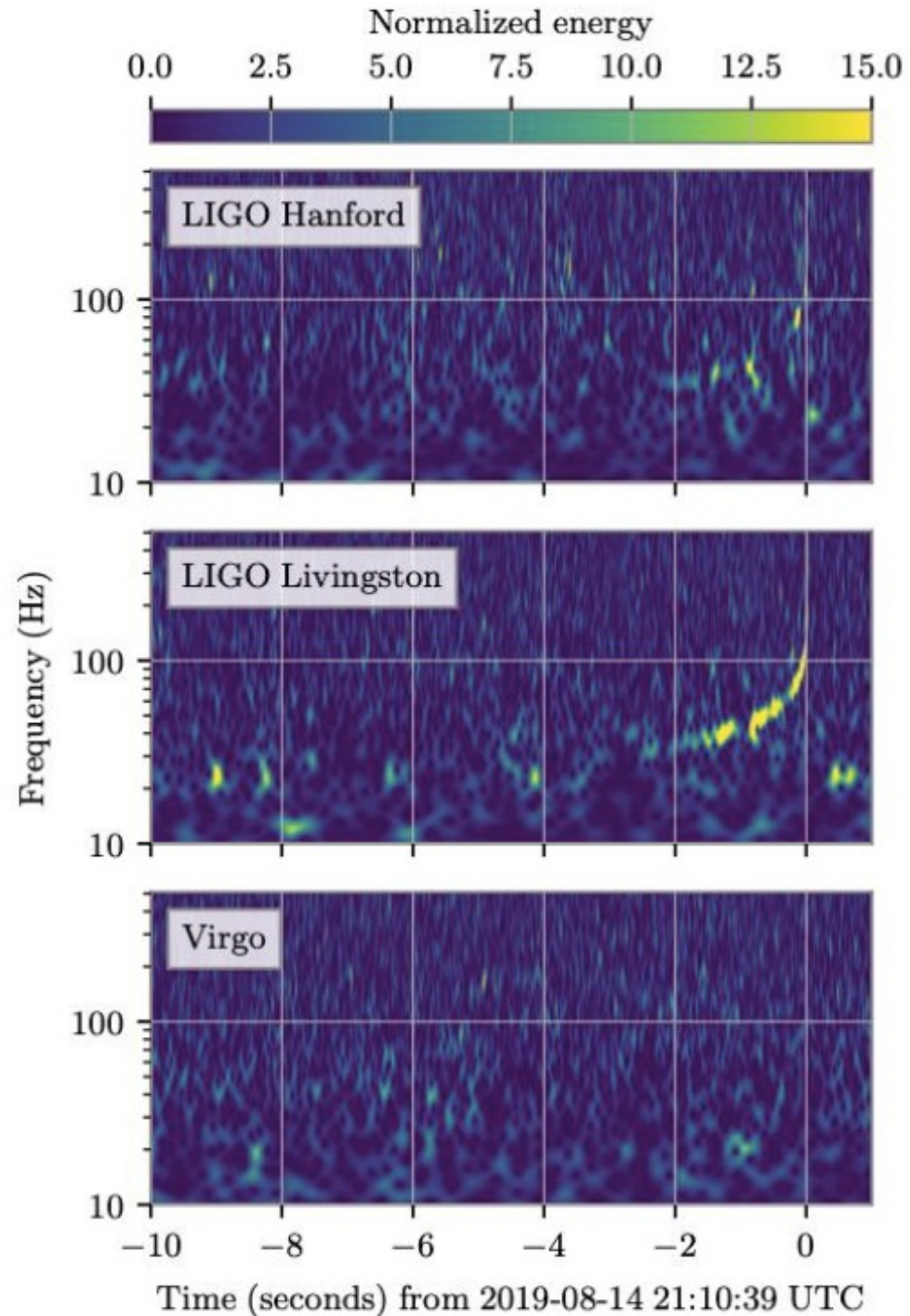
GW190814

Masses in the Stellar Graveyard *in Solar Masses*



GW190814

- Exactly two years after the first triple coincidence event, the extremely loud event GW190814 was produced by the merger of a black hole and an undetermined object.
- The most asymmetric system observed (the heavier compact object is about nine times more massive than its companion), $23 M_{\odot} + \sim 3 M_{\odot}$.
- The second mass is either the lightest black hole or the heaviest neutron star ever discovered in a system of two compact objects.



Mystery Merger: GW190814

(Aug 14, 2018)

The secondary mass of $2.6 M_{\text{sun}}$ lies in a 'mass gap';

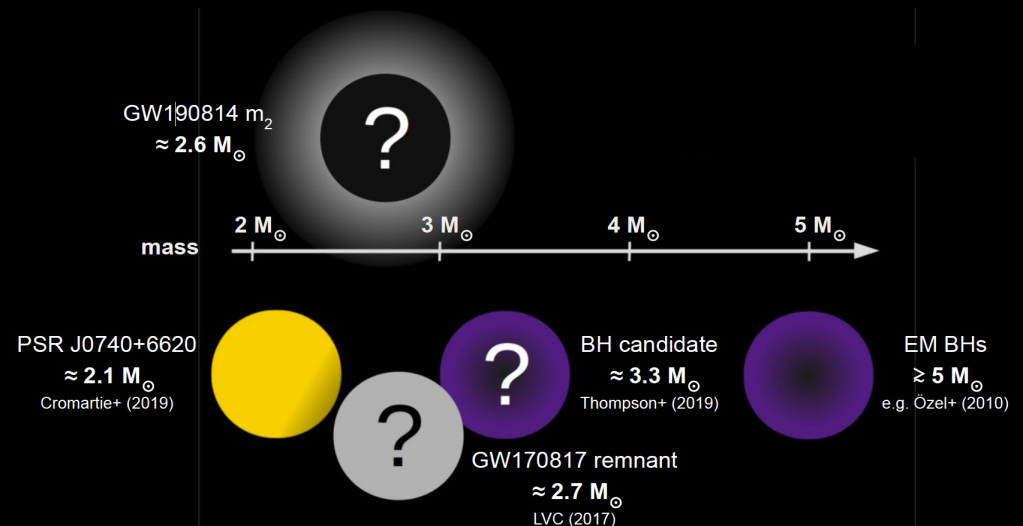
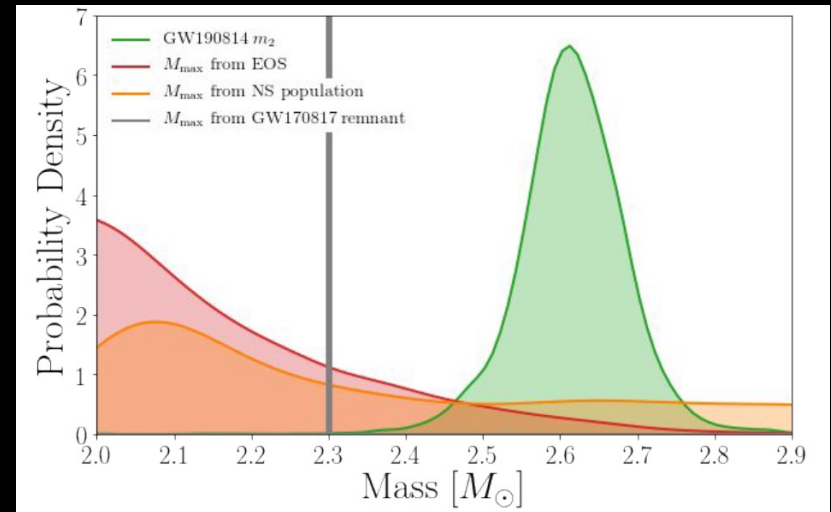
It's greater than estimates of the maximum possible NS mass and less than masses of the lightest black holes ever observed

Mass of this object comparable to the final merger product in GW170817, which was more likely a black hole.

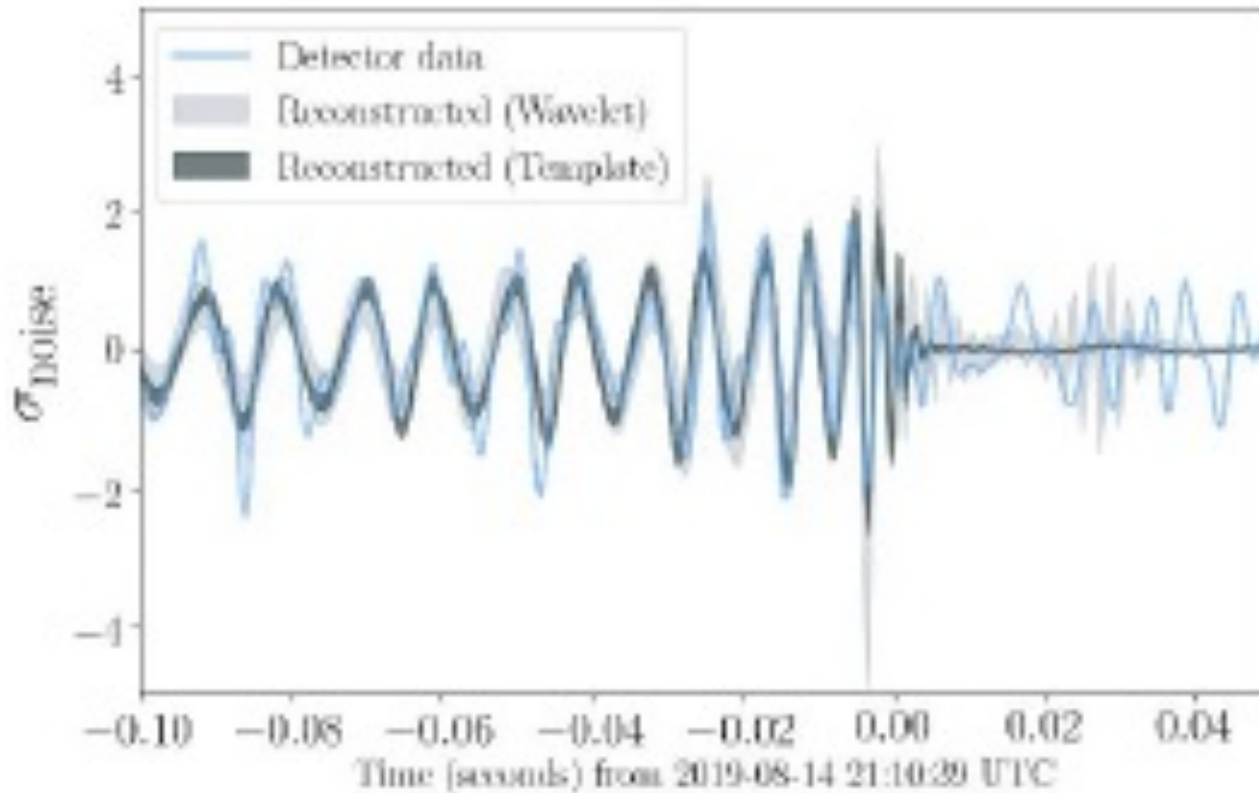
How did this system form? This detection challenges existing binary formation scenarios

young dense star clusters and disks around active galactic nuclei are slightly favored, but many other possibilities

Many follow up observations by electromagnetic observatories, but no confirmed counterpart found



GW190814



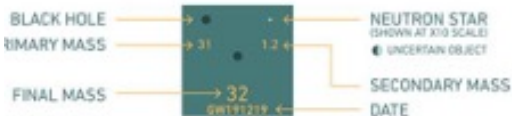
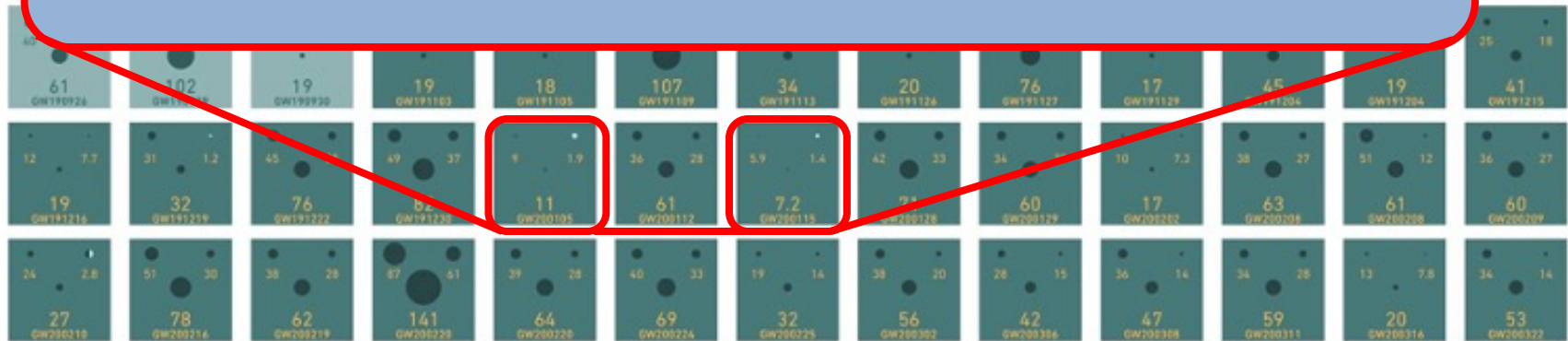
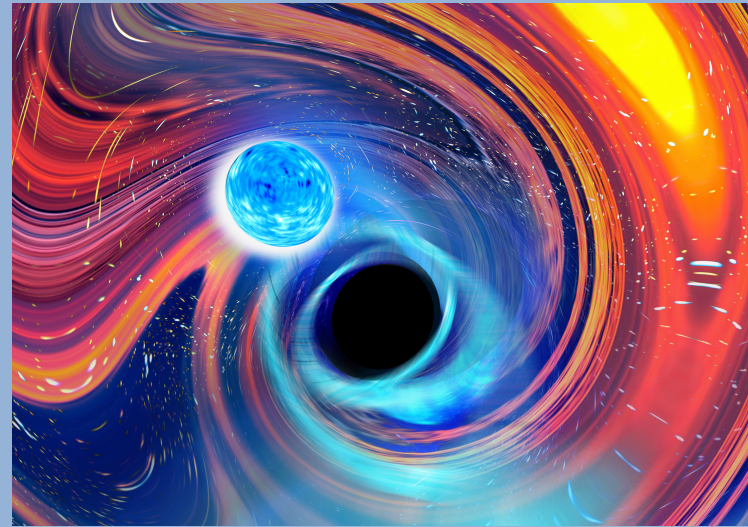
- For a system as massive and asymmetric as GW190814, the tidal imprint is too small to measure. In this case, our attempt to measure tides does not tell us whether GW190814 was caused by the merger of a black hole and a neutron star, as opposed to two black holes.
- Theoretical models for neutron-star matter, as well as observations of the population of neutron stars with electromagnetic astronomy, allow us to estimate the maximum mass that a neutron star can attain. These predictions suggest that the lighter compact object is probably too heavy to be a neutron star, and is therefore more likely to be a black hole.
- We can't rule out the possibility that GW190814 contains an especially heavy neutron star.

GRAVITATIONAL WAVE **MERGER** DETECTIONS

→ SINCE 2015

GW200105 and GW200115: Observation of Neutron Star Black Hole Mergers

First unambiguous observations
of NS-BH system



UNITS ARE SOLAR MASSES
1 SOLAR MASS = 1.989×10^{30} kg

Note that the mass estimates shown here do not include uncertainties, which is why the final mass is sometimes larger than the sum of the primary and secondary masses. In actuality, the final mass is smaller than the primary plus the secondary mass.

The events listed here pass one of two thresholds for detection. They either have a probability of being astrophysical of at least 50%, or they pass a false alarm rate threshold of less than 1 per 3 years.

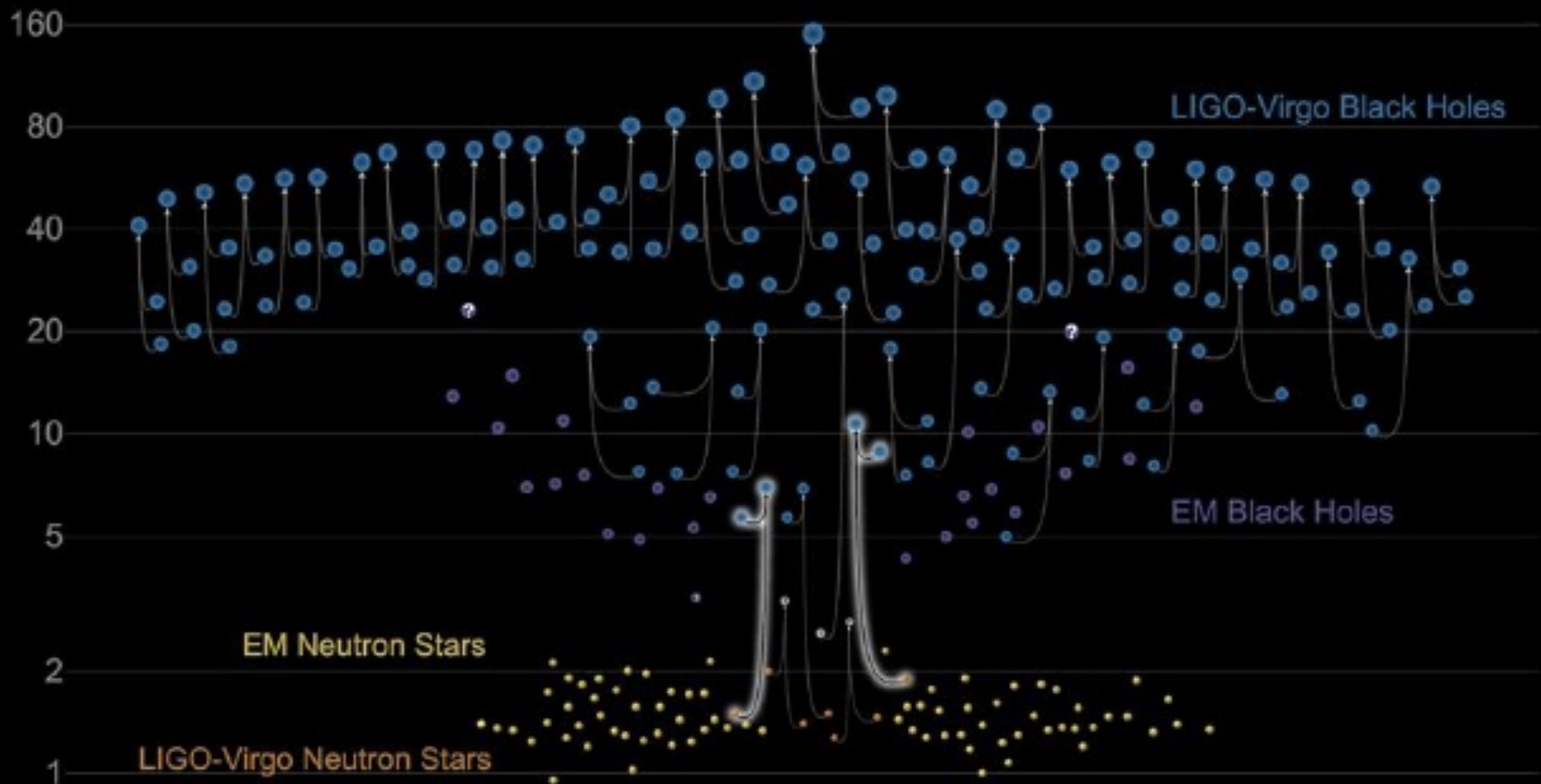


Neutron star – Black hole Binaries:

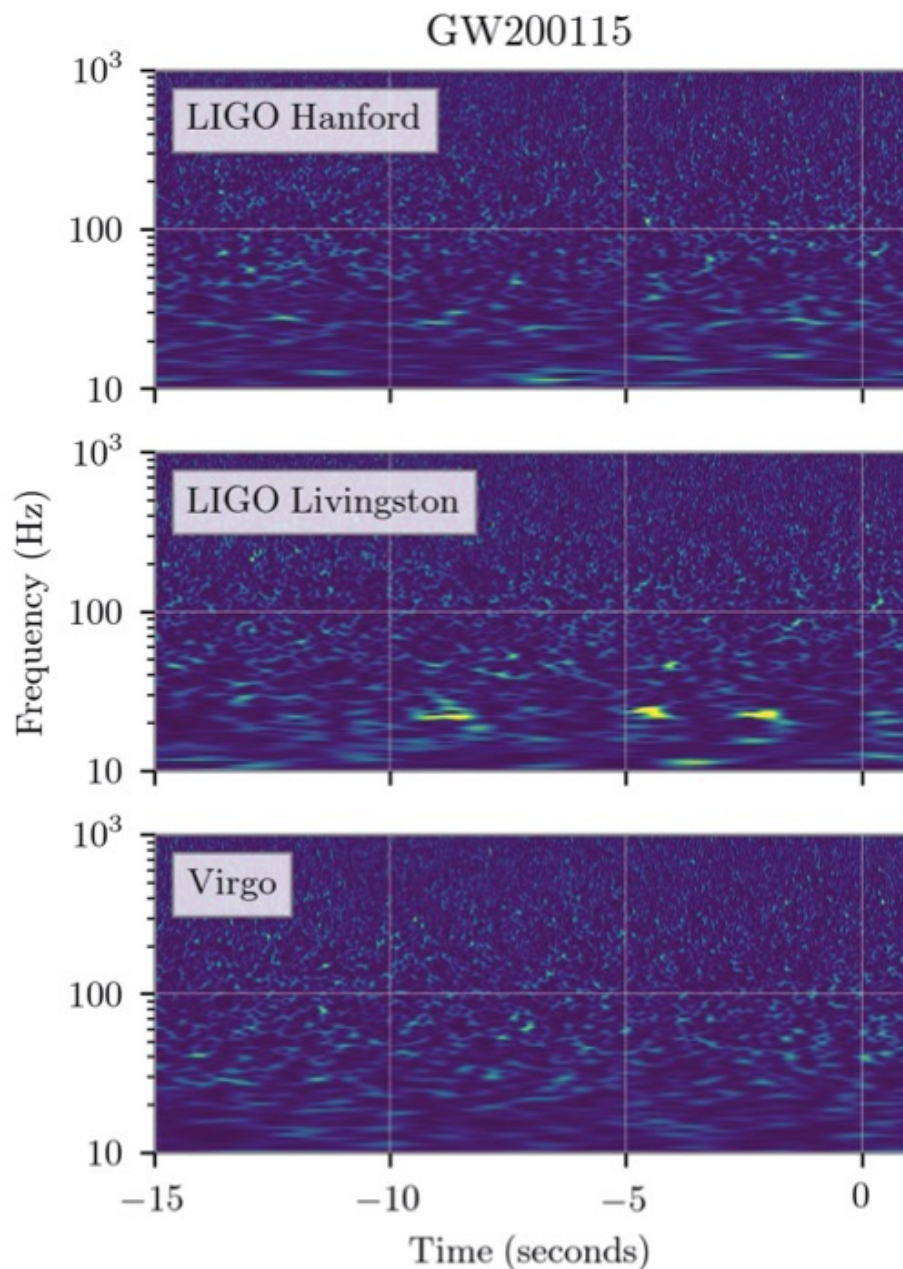
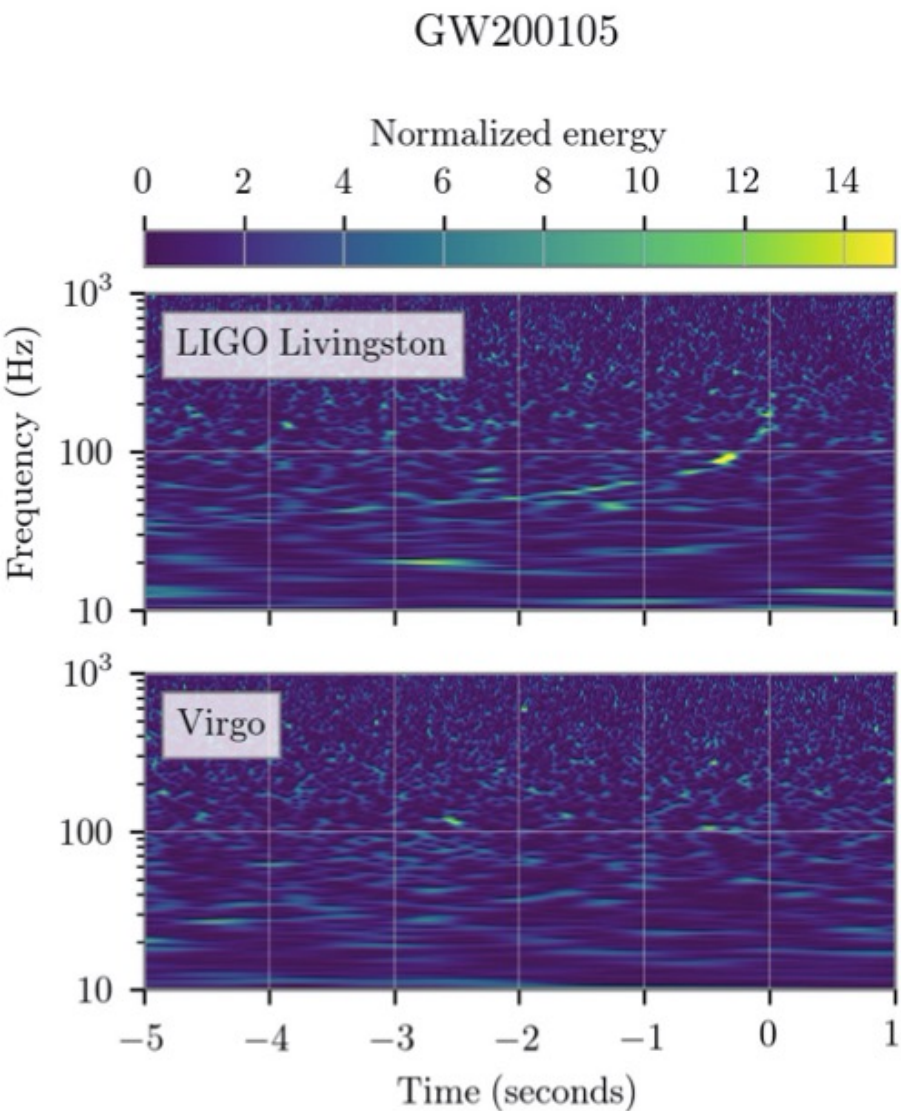
GW200105 and GW200115

Masses in the Stellar Graveyard

in Solar Masses

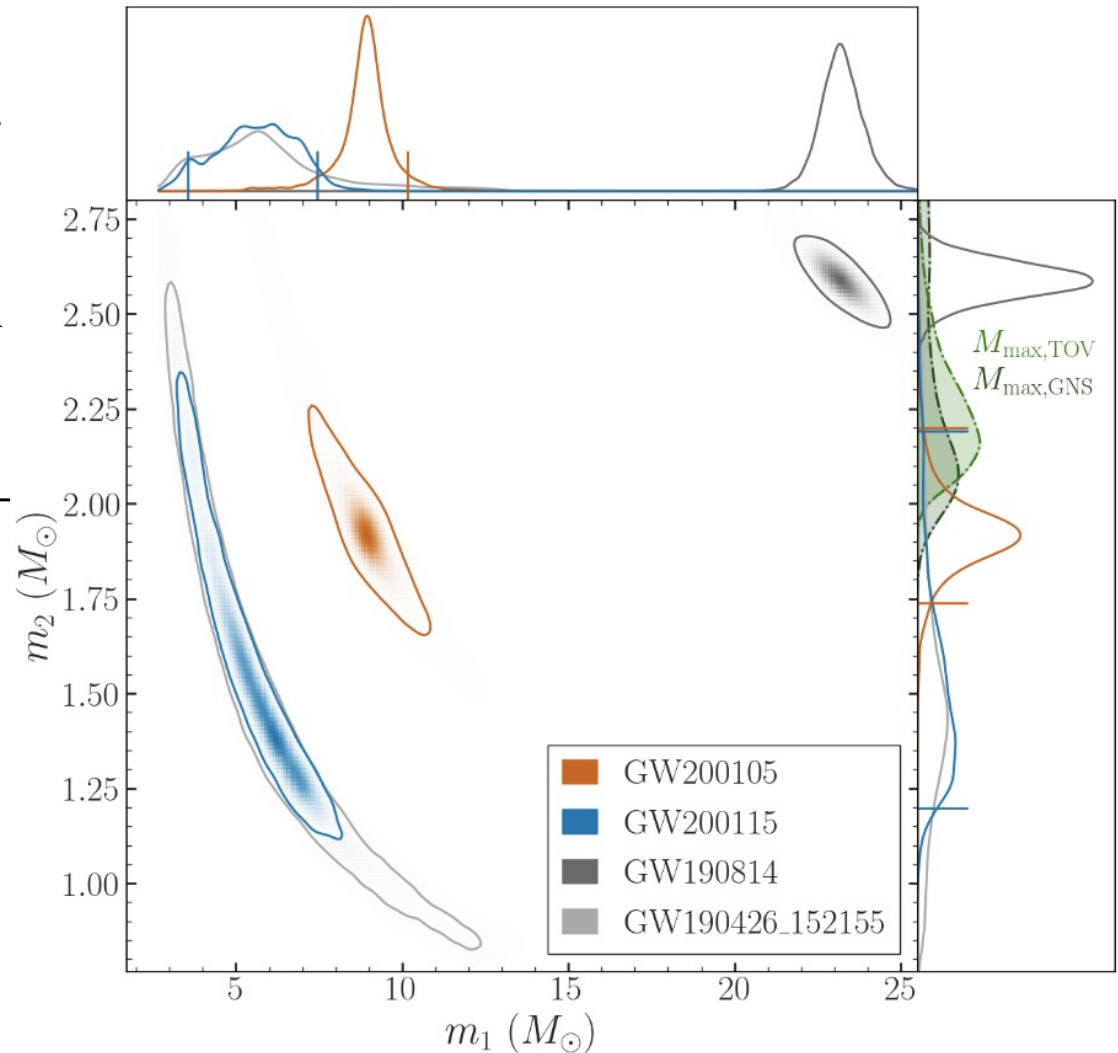


Neutron star – Black hole Binaries

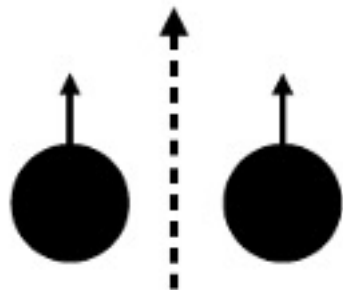


Neutron star – Black hole Binaries

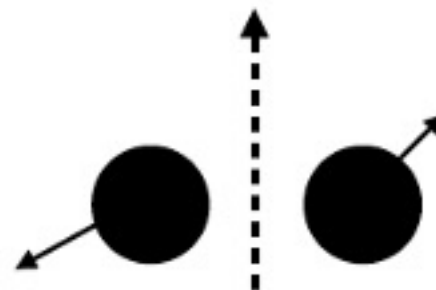
- GW200105: $8.9 M_{\odot} + 1.9 M_{\odot}$, their merger happened 800 million years ago.
- GW200115: $5.7 M_{\odot} + 1.5 M_{\odot}$, their merger happened nearly 1 billion years ago.



Neutron star – Black hole Binaries: how did they form?



- **Isolated binary evolution:** two stars orbiting each other explode in supernova explosion leaving behind a black hole and a neutron star.
- The spin directions of the BH tend to align with the binary orbit, we expect the neutron star to orbit in the equatorial plane of the black hole.



- **Dynamical interaction:** the neutron star and the black hole formed separately in unrelated supernova explosions and afterwards find each other.
- No prefer direction of the spin, and so the neutron star orbit could have any orientation relative to the black hole's equatorial plane.

GW200105 and GW200115

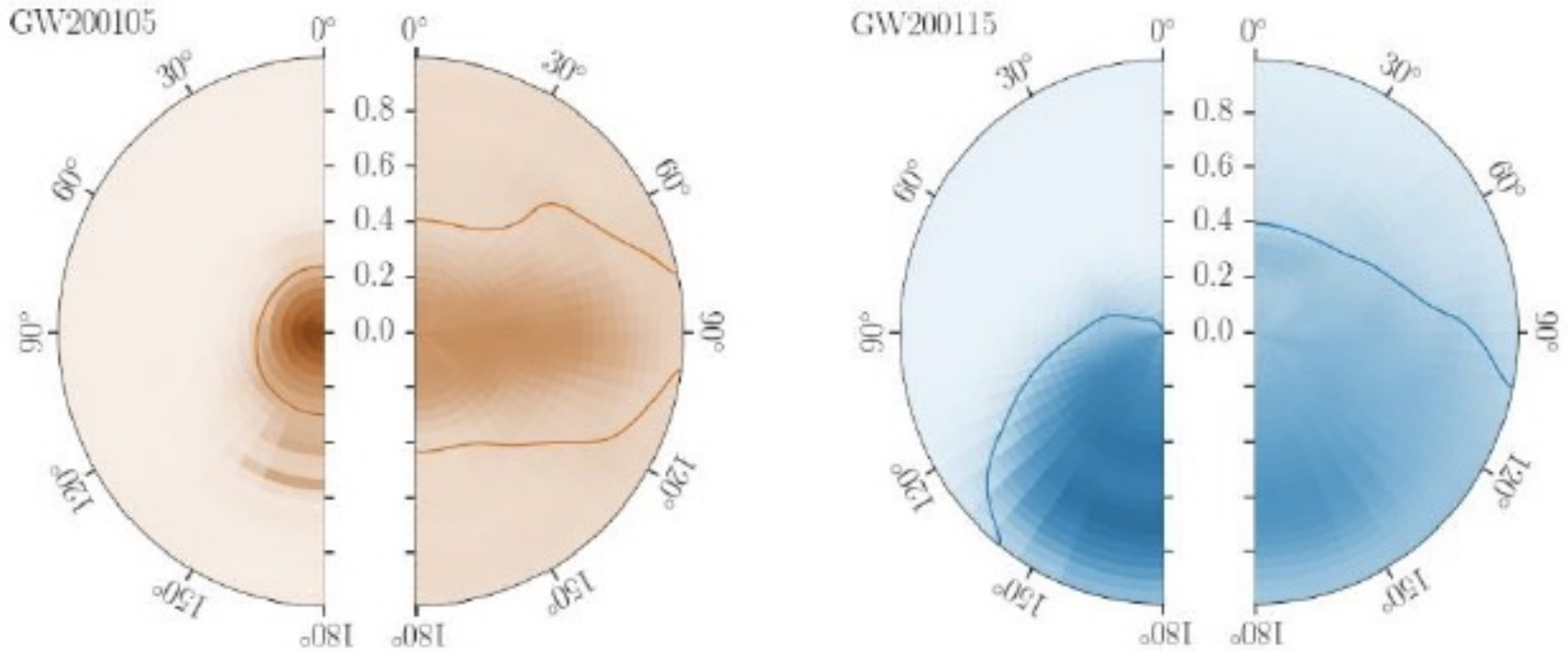
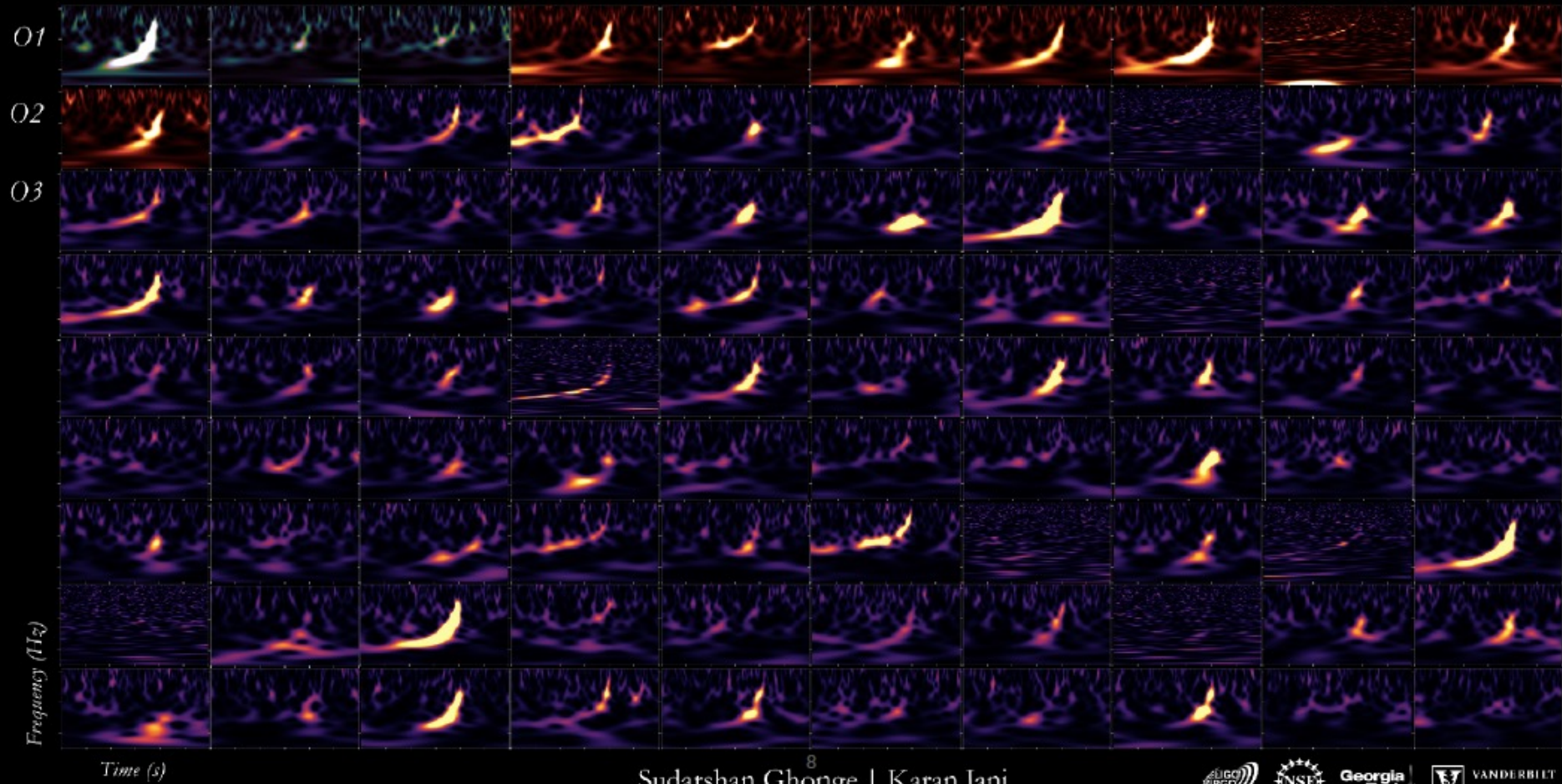


Figure 3: The inferred spin magnitude and direction of the black holes (left half-disks) and neutron stars (right half-disks) of GW200105 and GW200115. The radius of the disk indicates the spin magnitude, and range between 0 (no spin) to 1 (maximum rotation rate of black holes). The spin direction is shown as an angle, which ranges from 0° (objects spin in the same direction as the orbit of the binary) to 180° (objects spin in the opposite direction of the orbit of the binary). Shading indicates probable values of spin magnitude and direction. The left-most hemisphere has shading that peaks near the centre, indicating that GW200105's black hole has a spin that is likely small. The second to right hemisphere's shading extends downward, indicating that GW200115's black hole may be spinning in a direction opposite to the orbital motion.

Gravitational-Wave Transient Catalog

Detections from 2015-2020 of compact binaries with black holes & neutron stars



Sudarshan Ghonge | Karan Jani



Georgia Tech

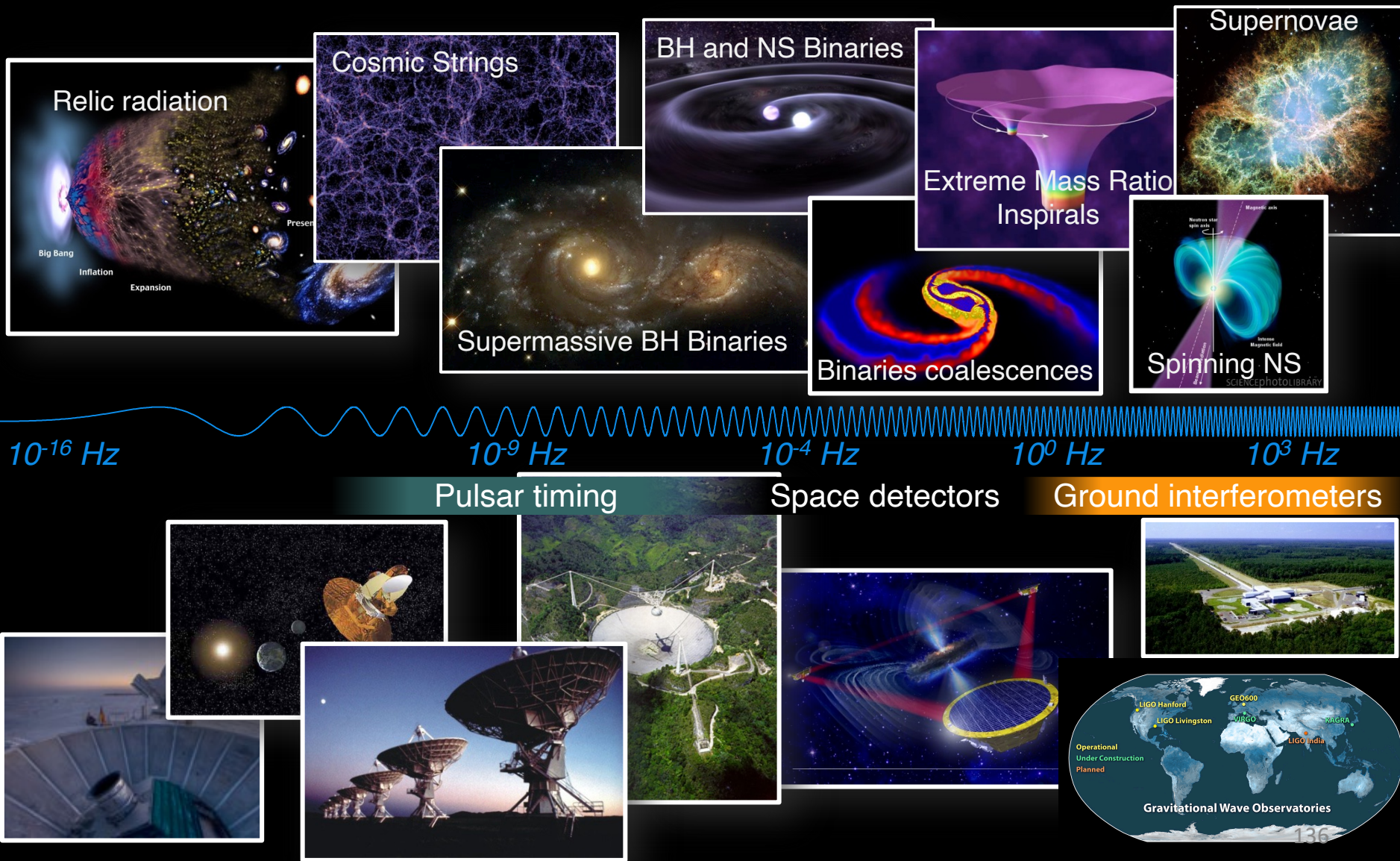
VANDERBILT UNIVERSITY



Scientific Achievements

- Direct observation of a gravitational wave signal (The LIGO Scientific Collaboration, the Virgo Collaboration, Abbott, et al., 2016).
- Evidence for the existence of black holes
- Observation of electromagnetic and gravitational wave signature from the merger of binary neutron stars: start of multi-messenger astronomy (The LIGO Scientific Collaboration, the Virgo Collaboration, Abbott, et al., 2017).
- Multiple observations are providing insights on the population properties of binary black-holes and also illuminating on their formation channels (The LIGO Scientific Collaboration, the Virgo Collaboration, Abbott, et al., 2021).
- A new way to test general relativity in the strong field limit and a new way to probe the cosmological history of the universe (The LIGO Scientific Collaboration et al., 2020).

The Gravitational Wave Spectrum





Also available as a
Web App



Chirp

Keep track of the
latest gravitational
wave alerts.

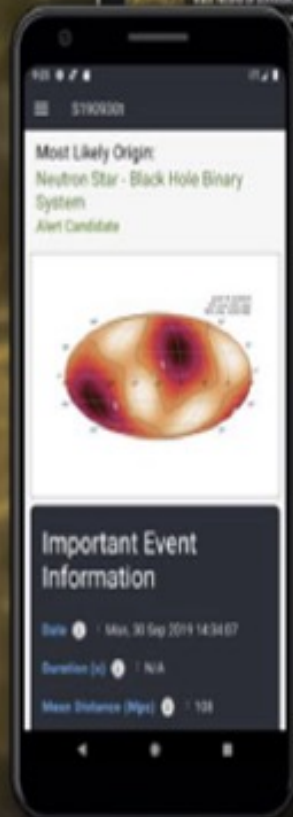


GET IT ON
Google Play



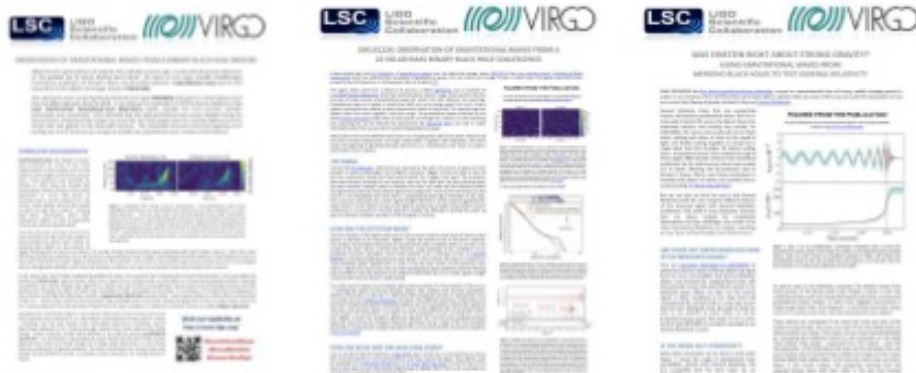
Download on the
App Store

LASER LABS



You can find lots more resources at

www.gw-openscience.org



Visit our websites

www.ligo.org

www.virgo-gw.eu

gwcenter.icrr.u-tokyo.ac.jp/en/



Bibliography

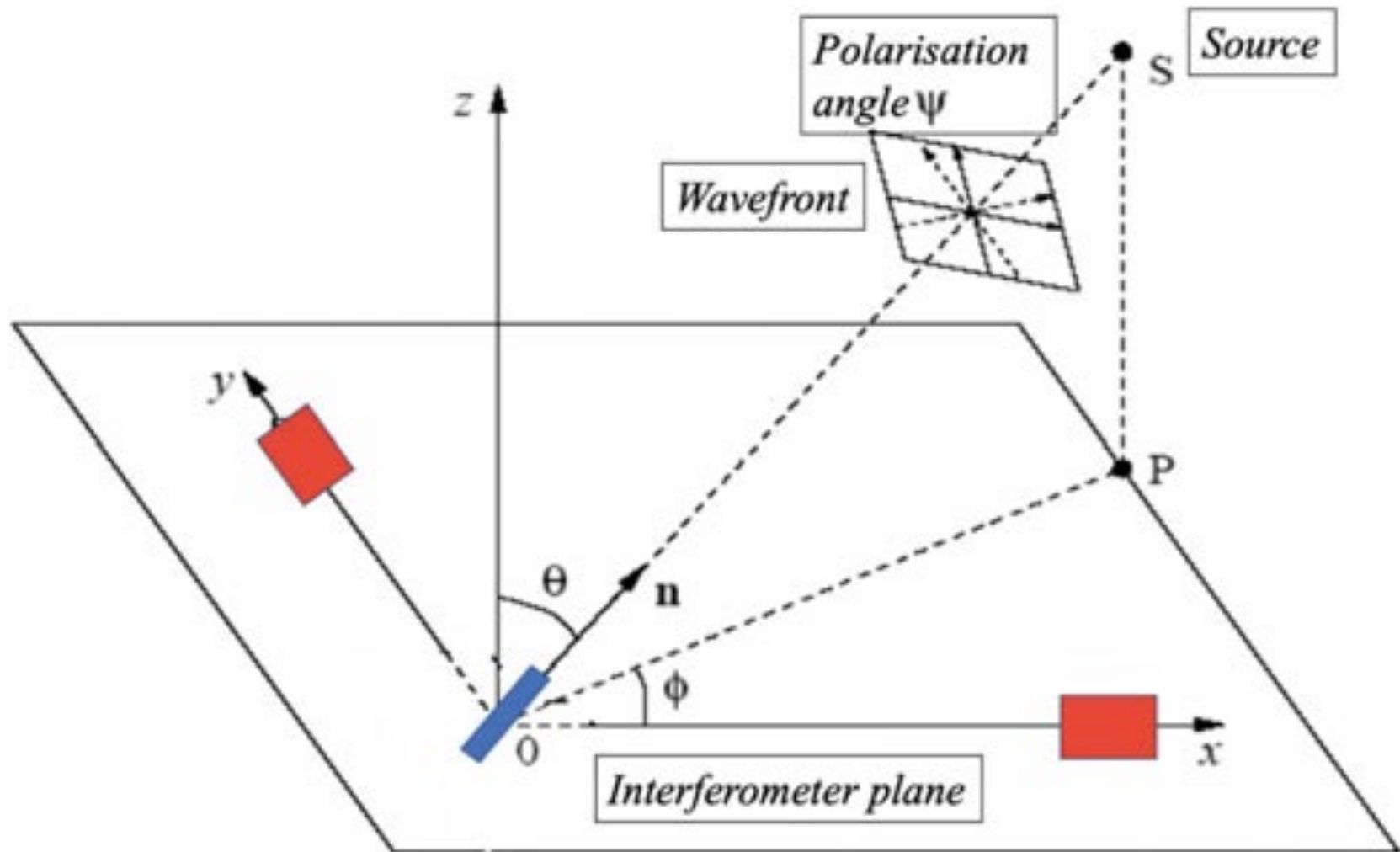
- B.P. Abbott et al, Phys.Rev.Lett. 116 (2016) no.24, 241102
- B.P. Abbott et al, Astrophys.J. 818 no.2, L22, 2016.
- B.P. Abbott et al, Phys.Rev.Lett. 116 no.22, 221101, 2016.
- B.P. Abbott et al, Phys. Rev. D 93, 122010, 2016.
- B.P. Abbott et al, The Astrophysical Journal Letters, Volume 826, Number 1 2016.
- B.P. Abbott et al, Phys.Rev.Lett. 116 (2016) no.24, 241103.
- B.P. Abbott et al, Phys.Rev. X6 (2016) no.4, 041015.
- B.P. Abbott et al, Astrophys.J. 832 (2016) no.2, L21.
- B.P. Abbott et al, Astrophys.J. 841 (2017) no.2, 89.
- A.Albert et al, Phys.Rev. D96 (2017) no.2, 022005.
- B.P. Abbott et al, Phys.Rev.Lett. 118 (2017) no.22, 221101.
- B.P. Abbott et al, Phys.Rev.Lett. 119 (2017) no.14, 141101.
- B.P. Abbott et al, Phys.Rev.Lett. 119 (2017) no.16, 161101.
- B.P. Abbott et al, Astrophys.J. 848 (2017) no.2, L12.

Bibliography

- B.P. Abbott et al, *Astrophys.J.* 848 (2017) no.2, L13.
- A.Albert et al, *Phys.Rev.* D96 (2017) no.2, 022005.
- B.P. Abbott et al, *Nature* 551 (2017) no.7678, 85-88.
- B.P. Abbott et al, *Astrophys.J.* 850 (2017) no.2, L39.
- A.Albert et al, *Astrophys.J.* 850 (2017) no.2, L35.
- B.P. Abbott et al, *Astrophys.J.* 851 (2017) no.2, L35.
- B.P. Abbott et al, *Astrophys.J.* 851 (2017) no.1, L16
- B.P. Abbott et al, *Phys.Rev.Lett.* 121 (2018) no.16, 161101
- B.P. Abbott et al, *Phys.Rev.* X9 (2019) no.1, 011001.
- B.P. Abbott et al, *Astrophys.J.* 871 (2019) no.1, 90.
- B.P. Abbott et al, *Phys.Rev.* X9 (2019) no.3, 031040.
- B.P. Abbott et al, *Astrophys.J.* 882 (2019) no.2, L24.
- B.P. Abbott et al, *Physical Review D*, 2020, 102(4), 043015.
- B.P. Abbott et al, *Physical review letters*, 2020, 125(10).
- R. Abbott et al, *Astrophys.J.Lett.* 913 (2021) 1, L7.
- R. Abbott et al, *Phys.Rev.X* 11 (2021) 021053.
- R. Abbott et al, *Astrophys.J.Lett.* 915 (2021) 1, L5.
- R. Abbott et al, *Astrophys.J.Lett.* 941 (2022) 2, L30

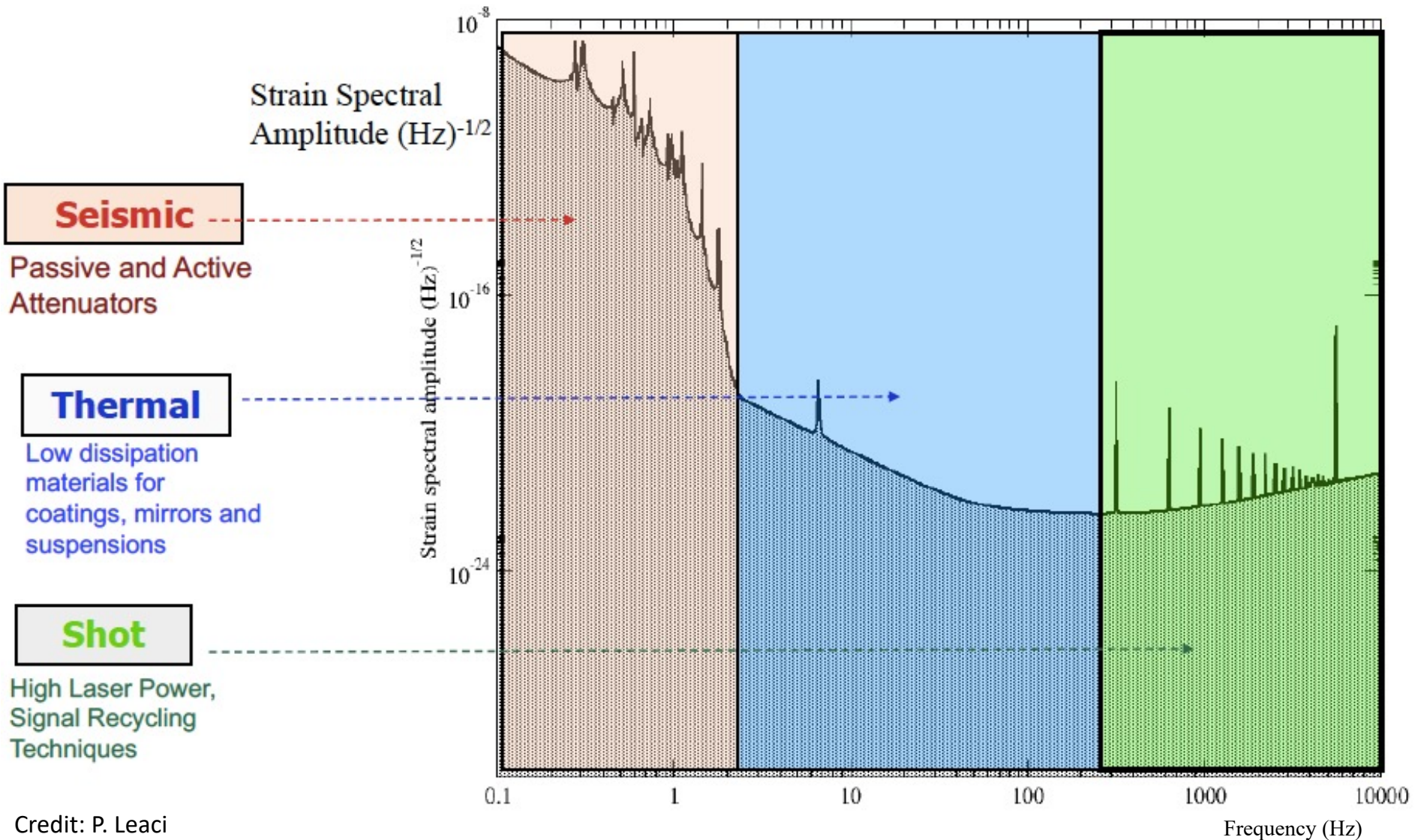


Overflow slides



The coordinate systems used to compute the GW antenna pattern of a Michelson interferometer: the origin is set at the beamsplitter, the arms lie along the x and y axes, the source is identified by two polar angles θ and ϕ

Interferometer Intrinsic Noise Spectrum

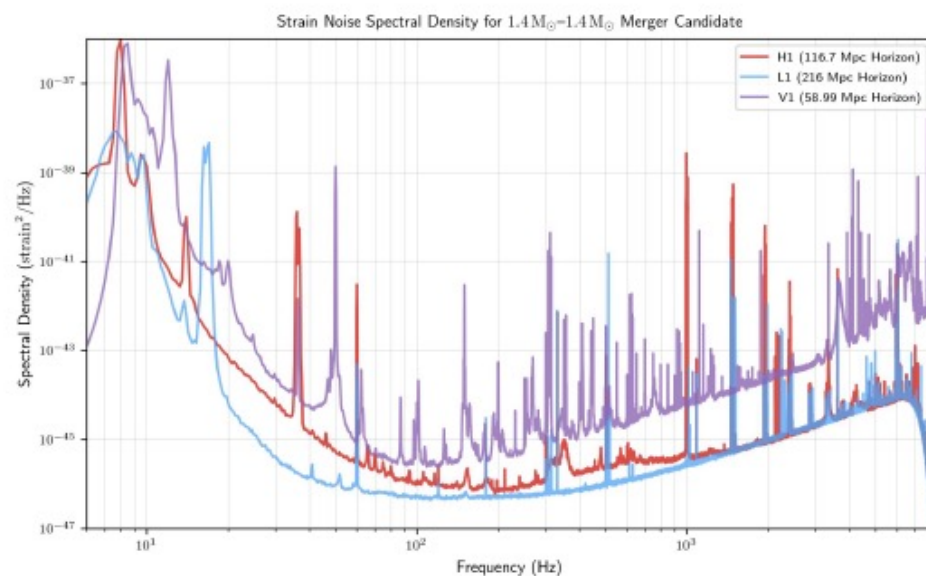


Revisiting our assumptions

In reality, LIGO data is not well-modeled.

- **non-stationary** over short and long time-scales
- **non-Gaussian**

The only characterization of the LIGO noise is from observations.



LIGO and Virgo PSD for O3.

The PSD shows a **measure of the sensitivity** and how the **noise varies over frequency** bins.



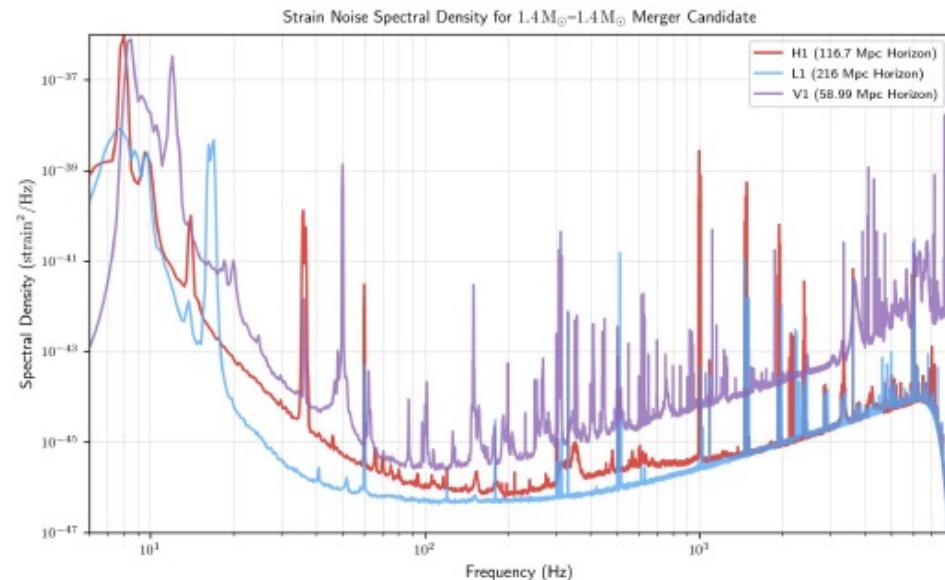
Revisiting our assumptions – colored noise

LIGO noise is not **white** - the power is not distributed evenly across frequencies.

whitened template
and data

$$\rho(t) = \int_{-\infty}^{+\infty} d\tau \hat{h}(\tau) \hat{d}(t + \tau)$$

$$\hat{d}(\tau) = \int_{-\infty}^{+\infty} df \frac{\tilde{d}(f)}{\sqrt{S_n(|f|)}} \exp 2\pi i f \tau$$



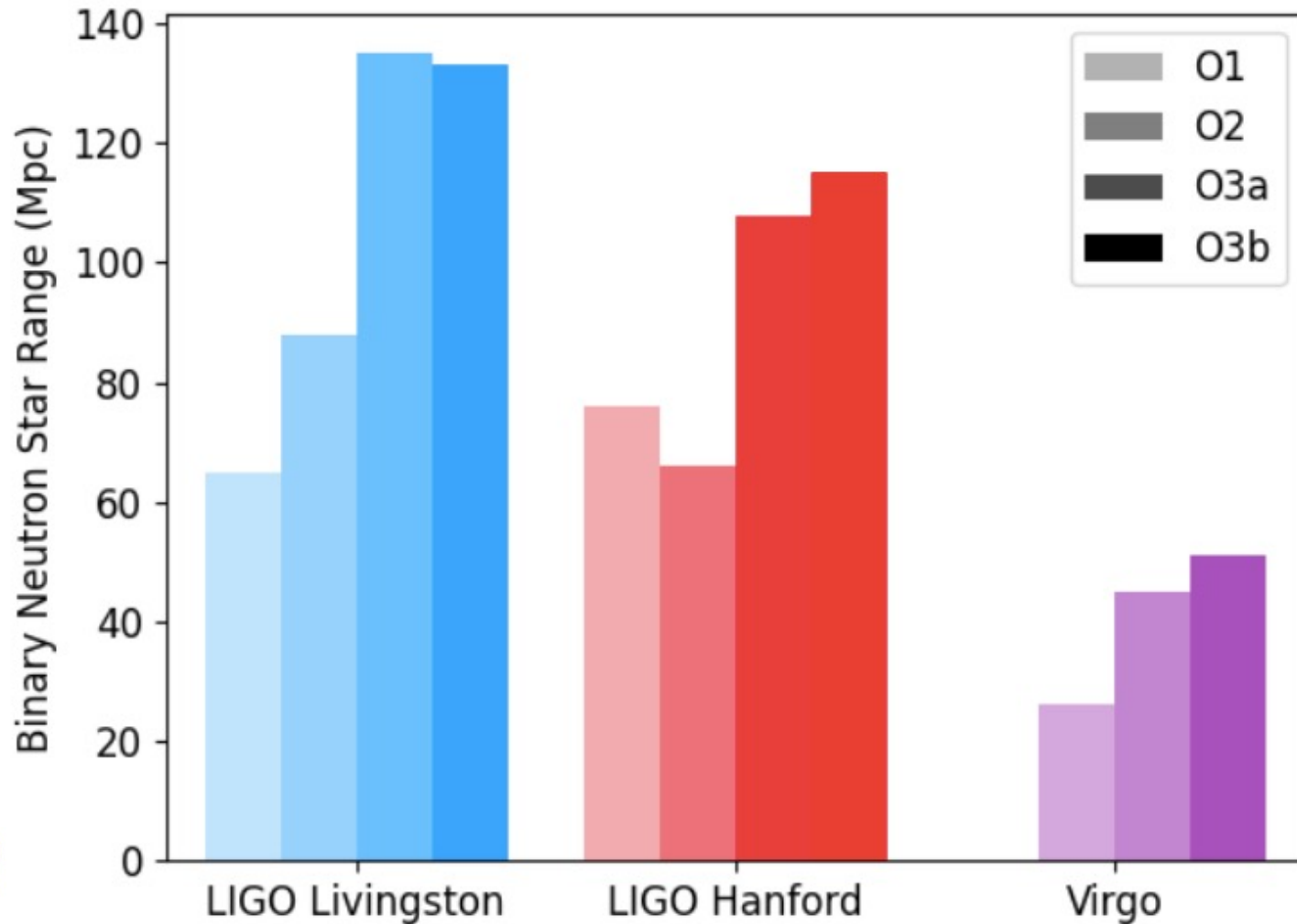
LIGO and Virgo PSD for O3.

The **PSD varies across frequency** bins, so the data needs to be whitened before filtering, essentially scaled by the PSD in frequency space.

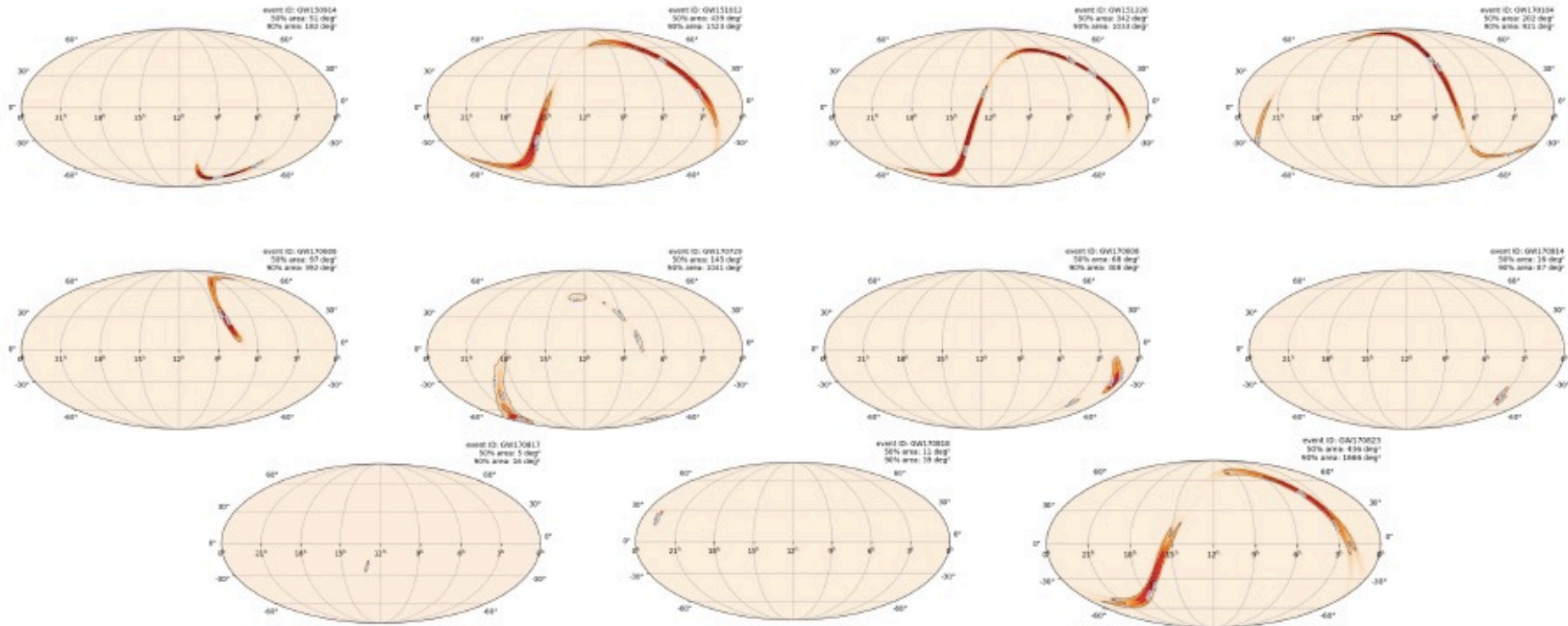
Gravitational Wave Transients Catalog

- GWTC-1: 11 confirmed events (10 BBHs, 1BNS), O1+O2
 - GWTC-2: 39 confirmed events, O3a
 - GWTC-2.1: 8 new events in O3a and reclassified 3 candidates in GWTC-2-> 55 total events
 - GWTC-3: 35 events in O3b
-
- O1 from 12th September 2015 to 19th January 2016
 - O2 from 30th November 2016 to 25th August 2017
 - O3a from April 1st to October 1st, 2019
 - O3b from November 2019 to March 2020

Detector Sensitivity

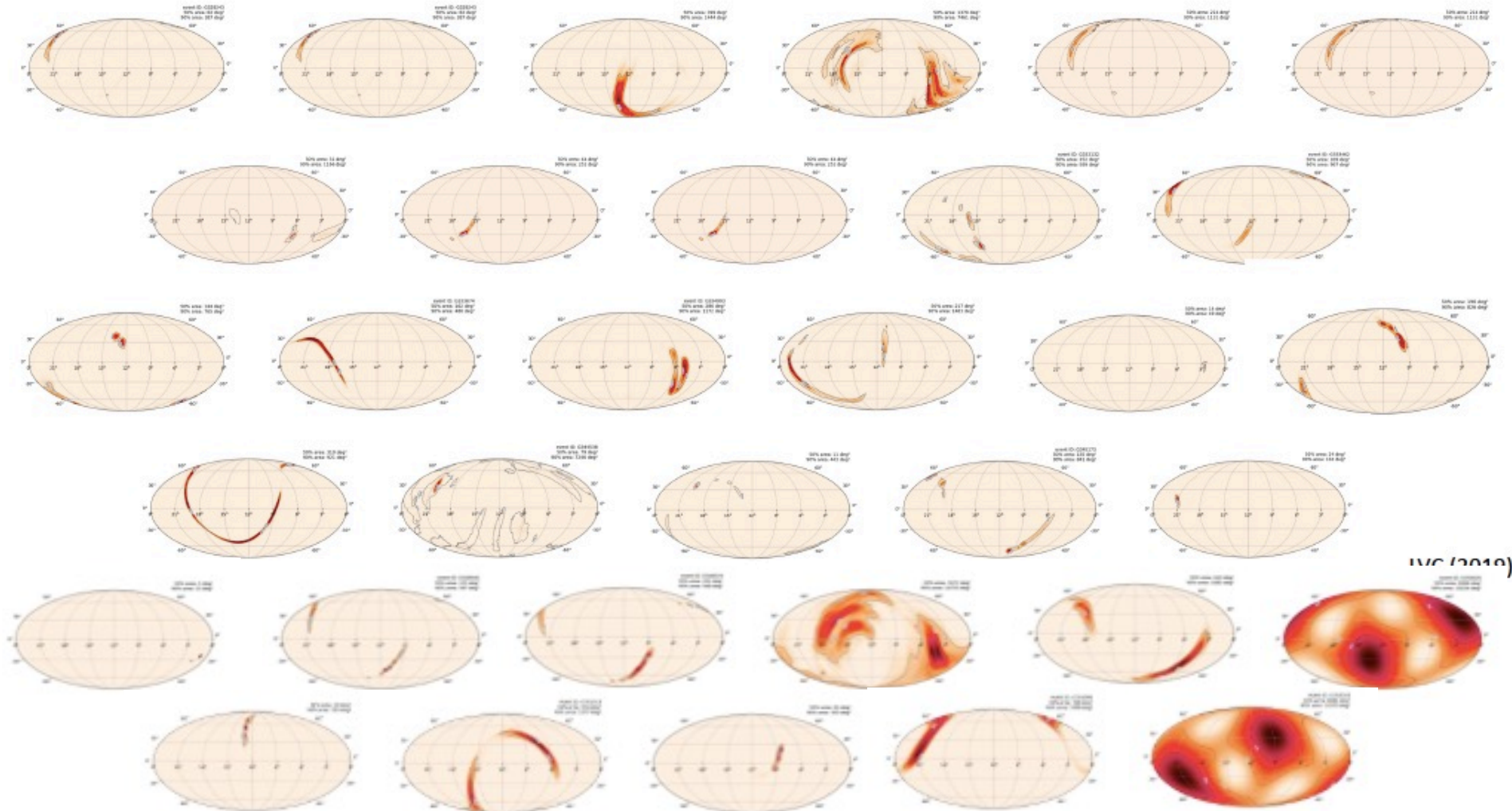


LVC observations after O1-O2: 11 detections (10 BBH + 1BNS)





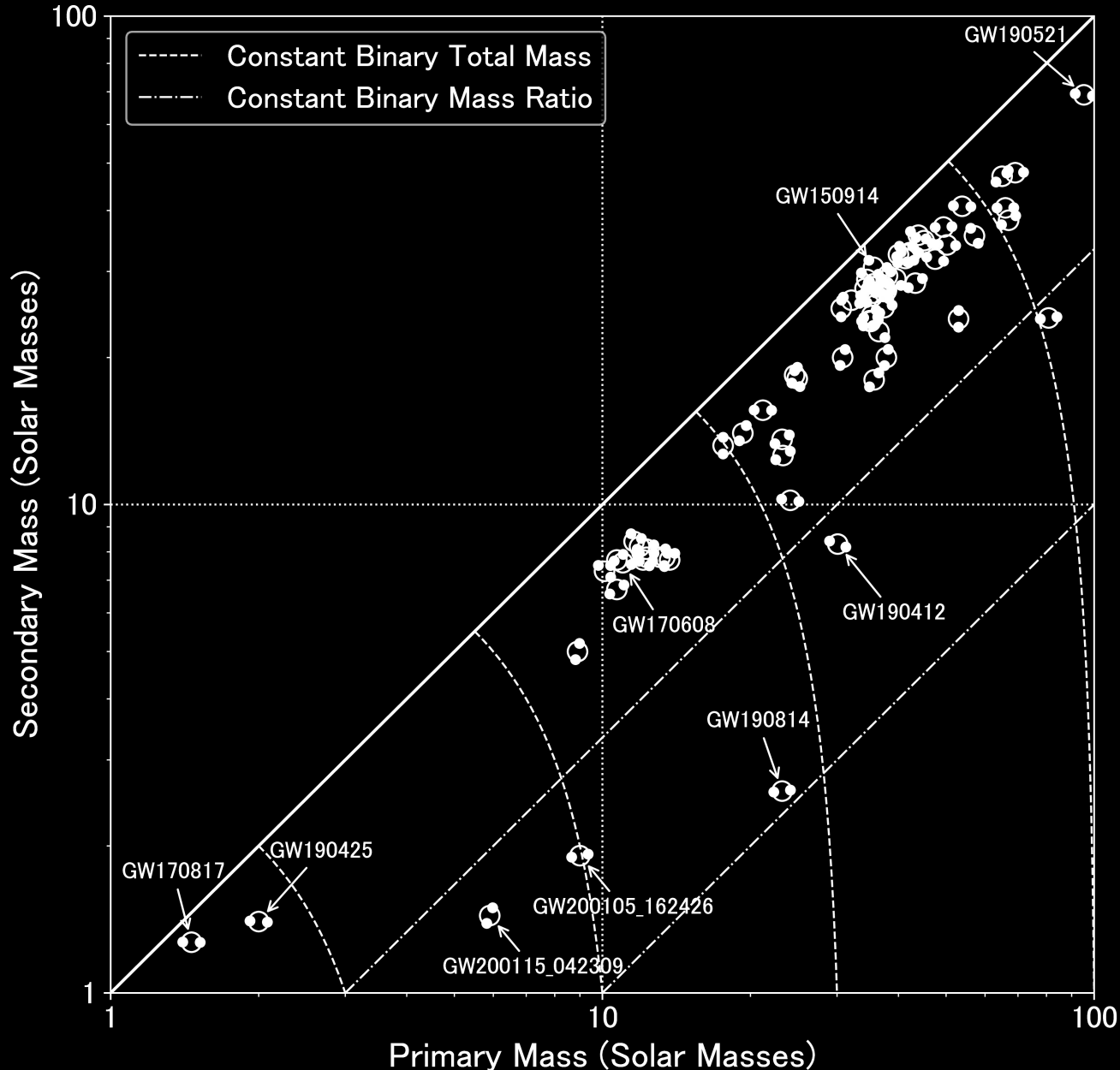
LVC candidates (so far) in O3 – since April 2019 – 33 Candidates



LVC (2019)

The population properties

We use a set of 74 compact binary mergers identified in LIGO-Virgo data up to the end of the third observing run including 70 binary black hole (BBH) events, two binary neutron stars (BNS), and two neutron-star black hole (NSBH) mergers.



The population properties of black holes and neutron stars

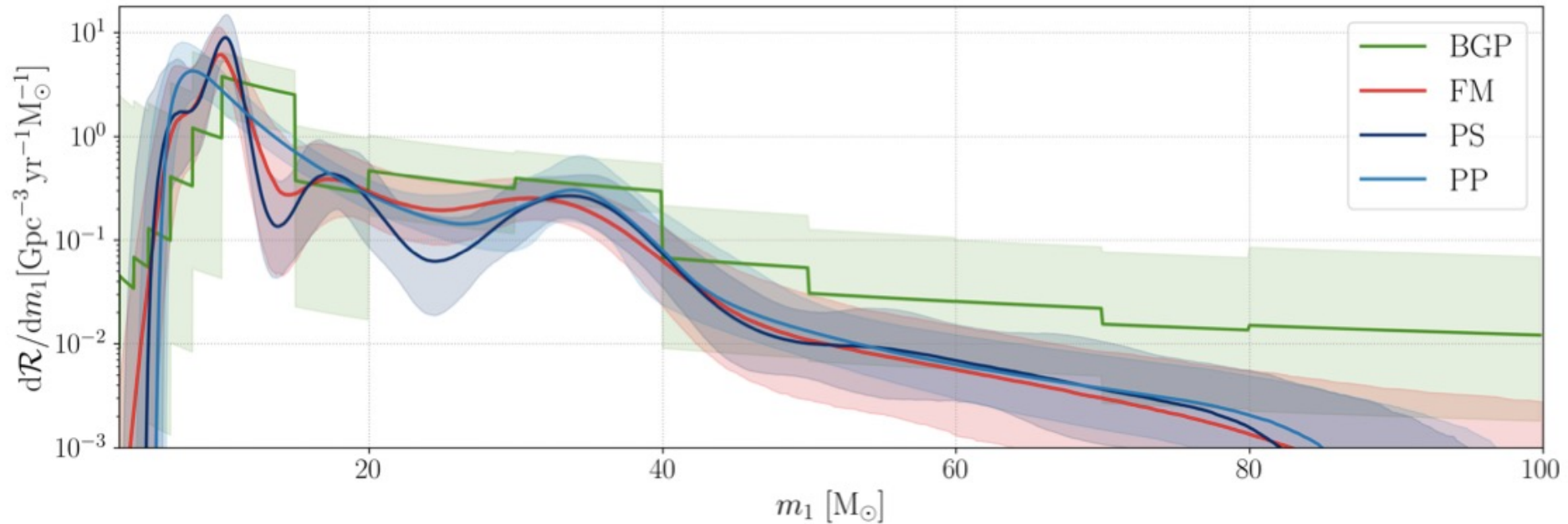


FIG. 11. The differential merger rate for the primary mass predicted using three non-parametric models compared to the fiducial PP model. Solid curves are the medians and the colored bands are the 90% credible intervals.

- We can identify two new bumps in the distribution of the more massive black hole in each binary (also called the primary) at around 10 and 18 M_{\odot} , in addition to the previously-identified peak at about 35 M_{\odot} .
- While isolated binary evolution models can explain the clustering of sources in the 8-10 M_{\odot} range, the origins of the additional peaks are not yet understood. Similarly to the lower mass gap, we are unable to confidently identify the presence of an upper mass gap for binary black holes.

